

IRRIGATION ENGINEERING CENTER PROJECT
IN
THE KINGDOM OF THAILAND
RESEARCH REPORT
ON
DESIGN AND ANALYSIS SYSTEM
OF
SOFT CLAY FOUNDATION

MARCH 1990

JAPAN INTERNATIONAL COOPERATION AGENCY

JICA LIBRARY



1081842(5)

21077

No.

IRRIGATION ENGINEERING CENTER PROJECT
IN
THE KINGDOM OF THAILAND
RESEARCH REPORT
ON
DESIGN AND ANALYSIS SYSTEM
OF
SOFT CLAY FOUNDATION

MARCH 1990

JAPAN INTERNATIONAL COOPERATION AGENCY

A D T
JR
89 — 75



P r e f a c e

Large lower plain of big river basin in South East Asia are not only main rice-producing districts of its countries but also fields of industrial and economical activities and people living purpose.

To stabilize food productions, such as rice, agricultural water-use facilities were constructed. In these districts these facilities are very important for both food productions and social infrastructures and so planning, design and construction of these facilities are needed.

However, these districts of South East Asia generally consists of very soft soil foundation and thus it is difficult to apply the usual analysis method to design and construction of such foundations.

Actually, we can see that many agricultural facilities have already disordered caused by differential settlements and slope failures. Hence, many facilities have lost their functions.

One of the main activity of Irrigation Engineering Center is the establishment of planning method and design criteria and setting up the technical calculation systems.

This research of very soft soil Foundation Analysis system is one of the above mentioned activities of Irrigation Engineering Center Project and this system has been developed and prepared by Japanese Institute of Irrigation and Drainage, JIID.

If it is possible to systemize the procedure of planning and design of agricultural water-use facilities using above, very soft soil foundation analysis system like the one mentioned above, in future, we can contribute to improve agricultural water-use facilities and the food production in South East Asia will be stabilize.

Lastly, we take this opportunity to express our deep gratitude to all those concerned with us in short term basis us. and made close cooperation and assistance and experts The Japanese working in Irrigation Engineering Center, IEC of Thailand.

March 1990

Nobuyoshi SAKINO

Director
Agricultural Development
Cooperation Development,
Japan International,
Cooperation Agency, JICA

Table of Contents

1. Outline of This Research Work	
1-1 Background of The Carriedout Research Work.....	p 1-1
1-2 Purpose of The Carriedout Research Work	p 1-1
2. Outline of Components of Soft Soil Foundation Analysis System.....	P 2-1
2-1 Monitoring System.....	P 2-1
2-2 F.E.M. Analysis System.....	P 2-3
2-3 Slope Stability Analysis System.....	P 2-4
3. Monitoring System.....	P 3-1
3-1 Objectives.....	P 3-1
3-2 System Components of the Monitoring System.....	P 3-2
3-3 Procedure for Plotting Graphs in the Monitoring System.....	P 3-16
3-4 Plan of Slope Behaviour Observation System at the Testing Site.....	P 3-21
3-5 Operation Manual for the Monitoring System.....	P 3-28
4. F.E.M. Analysis System.....	P 4-1
4-1 Objectives and Analysis Method.....	P 4-1
4-2 Procedure of Analysis.....	P 4-3
4-3 Determination of Parameters for Analysis.....	P 4-4
4-4 Procedure of Analysis Model Preparation.....	P 4-22
4-5 Graphic Output of the Results of Analysis.....	P 4-30
4-6 Operation Manual for the F.E.M. Analysis System.....	P 4-33
5. Slope Stability Analysis System.....	P 5-1
5-1 Objectives and Analysis Method.....	P 5-1
5-2 Determination of Design Parameters.....	P 5-3
5-3. Operation Manual for the Slope Stability Analysis Systems.....	P 5-27

1. Outline of this research work.

1-1. Background of the carried out research work.

Irrigation Engineering Center Project is a project aims to develop appropriate technology to be applied to planning, designs and construction of irrigation and drainage facilities and to transfer of knowledge to encourage engineers in Thailand who have constructed many agricultural pump stations and irrigation facilities to change the yield of large chaopraya plain.

However, soils at which these irrigation facilities were constructed are very soft clay named Bangkok Clay, and so differential settlement of facilities foundation and slip failures of slopes occurred. Functions of these facilities even stopped sometimes.

Royal Irrigation Department has the conventional analysis programs for design of agricultural water-use facilities but these programs are not enough to simulate foundation behaviours of Bangkok Clay, accurately.

Therefore, it is necessary to estimate material properties of Bangkok Clay accurately, and to observe and simulate behaviours of soft clay foundations before constructions of any new agricultural facilities.

Japan International Cooperation Agency has promoted the model infrastructure improvement project aiming at construction of testing canal facilities and modification and preparation of programs which has installed in Royal Irrigation Department, RID. The purpose of this research work is setting up the soft soil foundation analysis system while taking account the aims of the Irrigation Engineering Center Project.

1-2 Purpose of The Carriedout Research Work

The purposes of the Soft Soil Foundation Analysis System are as follows

- 1) To observe and examine behaviour of slopes which consist of 4 sections through investigation of construction condition of the testing canal facility which is constructed on the soft soil foundation.
- 2) To obtain the actual stress and deformation behaviour of Bangkok Clay.
- 3) To examine effectiveness of the countermeasures against the soft soil foundation of Bangkok Clay and finally
- 4) To study a practical design method for excavated canals on the soft soil foundations using judgements reached after taking everything mentioned above into consideration.

This system is composed of three systems, namely, the Monitoring System, the Finite Element Method Analysis System and the Slope Stability Analysis System. Each system has the following functions and features, and if these functions are fulfilled systematically as shown in Fig 1-1, these systems will be very useful for grasping fully the behaviour of Bangkok Clay foundation.

1) Monitoring System

Using this system, not only gathering and recording the actual measured data, but slope failure prediction will be tried using the actual measured data. For this purpose, this system employs the graph plotting function of Kurihara's method and Saito's two methods.

2) F.E.M. Analysis System

In order to examine soft clay behaviour, it is necessary to use a stress-strain model which can express creep or relaxation behaviour etc. where passage of time is taken into consideration in addition to elasto-plasticity. Consequently, this system adopted the Sekiguchi-Ohta model which can express passage of time and has produced satisfactory results. Besides, this system can simultaneously express pore water flow coupled with soil deformation. We can therefore take water level fluctuation into account. Since this system

can simulate the actual construction plan, we will be able to predict the excavated slope behaviour which will be very similar to the actual behaviour.

3) Slope Stability Analysis System

The slope stability analysis program, which is intended to be able to evaluate clay properties similar to that of actual conditions as much as possible, has been set up using rate of strength decrease by excavation and Bjerrum's coefficient about the excavated slope on the soft soil foundation.

This system enables us to carry out excavated soft soil slope stability analysis which cannot be analyzed by normal slope stability analysis.

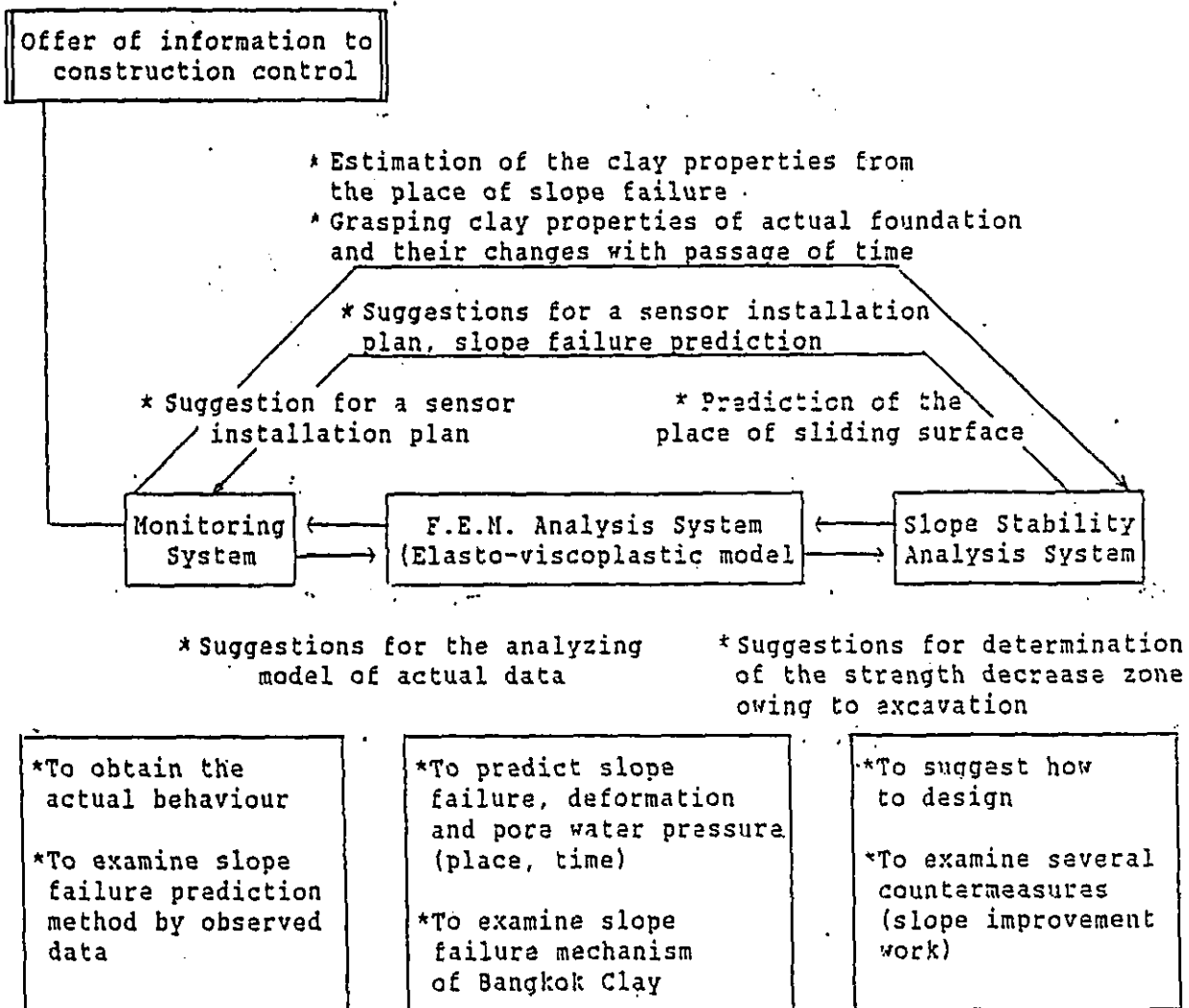


Fig.1-1 Function and relationship of each system in the Soft Soil Foundation Analysis System

2. Outline of components of the Soft Soil Foundation Analysis System

2-1 Monitoring System

(1) Hardware of the Monitoring System

Hardware of the Monitoring System will be set up at two places, that is, the room for investigation at the testing site and the computer room in IEC.

1) Hardware system in the room for investigation at the testing site

(in the case of auto-measured sensors)

At the testing site, several kinds of measured data will be gathered by Data Logger (TDS-301) and these data will be written on floppy disks by Micro Disk Memory (RM-351)

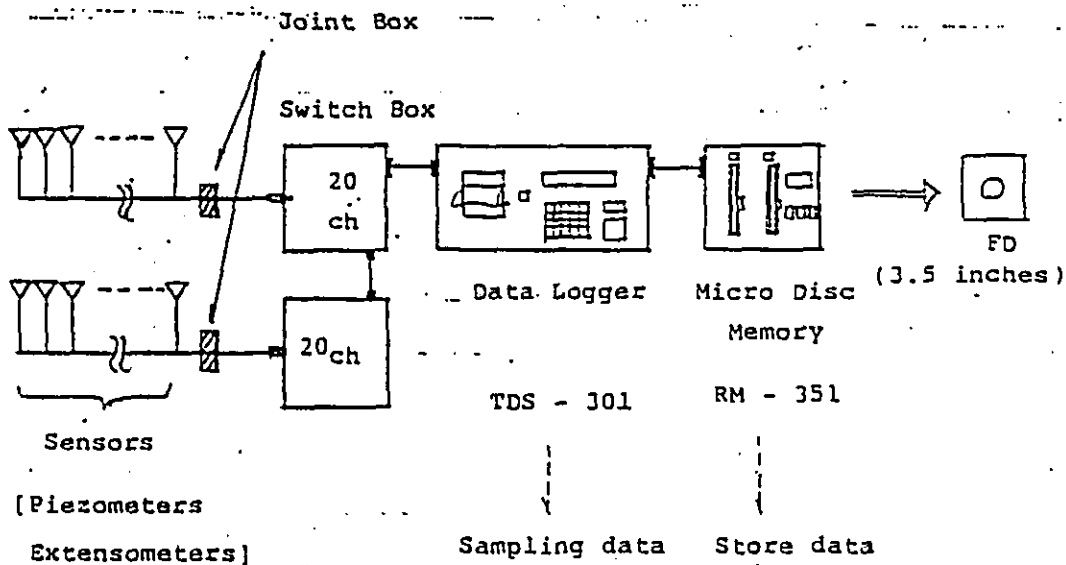


Fig.2-1 Hardware system in the Monitoring System at the testing site

2) Hardware system in IEC computer room

The measured data which will have been written on 3.5 inch floppy disks at the testing site will be sent to the IEC computer room. Then, these data will be transferred to the public file area in the VAX-System (VAX3350 or 750) after these data format are converted by personal computer (APC/IV). After that, historical graphs, analyzing graphs of each sensor and slope stability control graphs will be plotted by terminal equipment (VT241) of the VAX-System and XY plotter (C1077)

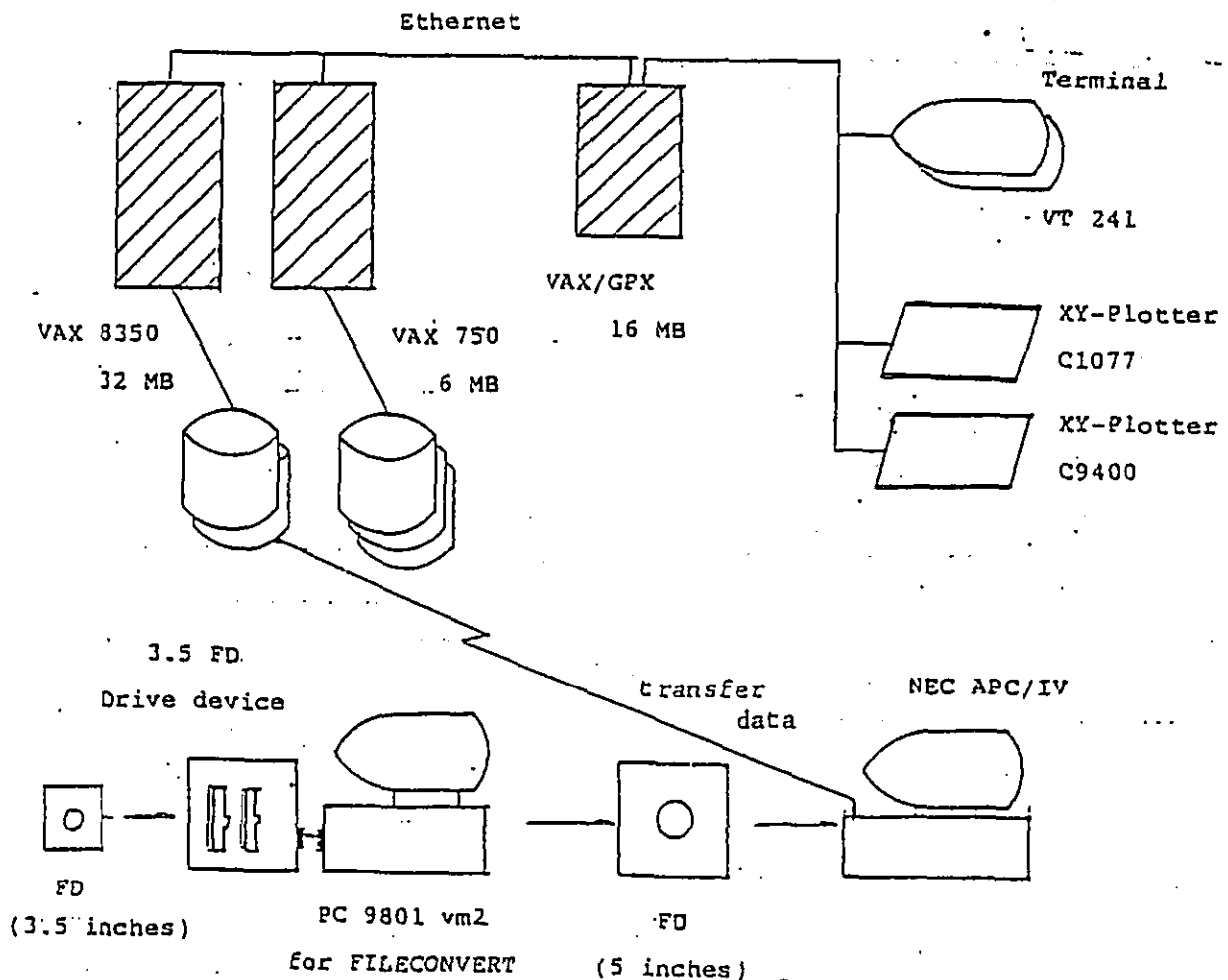


Fig. 2-2 Hardware System in IEC computer room

(2) Software in the Monitoring System

Software in the Monitoring System are graph-plotting programs after processing data measured by each sensor, and these are composed of three (3) kinds of graph-plotting system as follows

- a) Historical graph plotting system for measured data
- b) Analysis graph plotting system for measured data
- c) Slope failure prediction and construction control graphs

Using system a), we can follow up the slope behaviour with time in correspondance with the excavation stage and we can grasp its general tendencies, and using system b), we can observe displacement on the slope surface and in the ground and pore water pressure in the foundation concentrating on the places we should pay attention to, and we can observe each kind of correlative behaviour.

Furthermore, using system c), we can propose several kinds of slope failure control graphs (e.g. displacement ratio; creep strain ratio) for prediction of excavated slope failure, and we can examine these graphs for their validity.

For details of software, please refer to Chapter 3.

2-2 F.E.M. Analysis System

(1) Hardware for the F.E.M. Analysis System.

All of the hardware for the F.E.M. Analysis System are components of the VAX-System in the IEC computer room, and using them, calculation and plotting graphs can be carried out. Equipment to be used are as follows.

- ① VAX-8350
- ② VT-241 (Terminal equipment)
and
- ③ XY plotter (CalComp)

(2) Software for the F.E.M. Analysis System

Software for the F.E.M. Analysis System are composed of the following 2 groups of software.

- a) Elasto-viscoplastic model analysis programs
(Sekiguchi-Ohtas' model)

b) Diagrams drawing program series for the results of Analysis

- ① Displacement diagrams
- ② Principal stress diagrams
- ③ Pore water pressure contour diagrams etc.

Using analysis program a), the actual phenomena can be examined taking construction conditions (passage of time, depth of excavation) into account, and we can predict behaviour such as displacement of the excavated slope and pore water pressure.

And using program series b), we can get diagrams of the results of simulation for slope behaviour prediction using program a), and slope behaviour as time passes at the excavation stage can be visualized.

For details, please refer to Chapter 4.

2-3 Slope Stability Analysis System.

(1) Hardware for the Slope Stability Analysis System.

Slope stability analysis can be carried out by the Vax-System in the IEC computer room.

(2) Software for the Slope Stability Analysis System

This system is composed of the following 2 programs.

a) Modified slope stability analysis program

b) Diagram drawing program for the results of slope stability analysis

The modified slope stability analysis program can be applied not only to non-treatment excavated slopes but to improved composite ground slopes. As a matter of course, this program can also be applied to fill dams.

Regarding the evaluation of strength of soft soil foundation, this program takes rate of strength decrease by excavation and Bjerrum's coefficient into consideration. And concerning the Sand or Gravel Compaction Pile Method, this program can also take strength increase which is caused by consolidation into consideration. On the determination of total strength of the composite ground, the replacement ratio of soft clay foundation with pile materials is adopted.

For details, please refer to Chapter 5

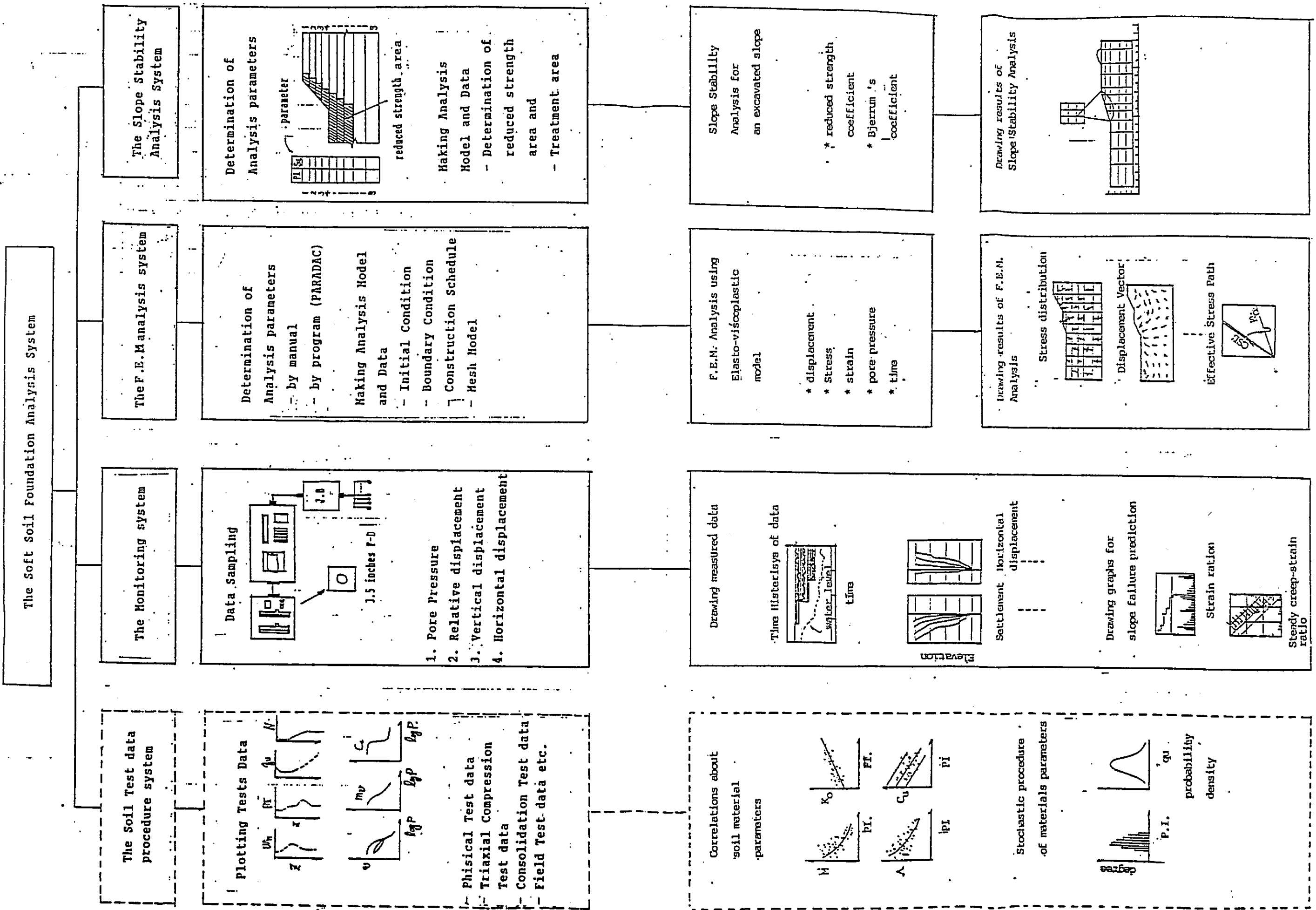


Fig. 2-3 Schematic Outline of the Soft Soil Foundation Analysis System

3. Monitoring System

3-1 Objectives

The purposes of the Monitoring System are as follows,

- 1) To obtain the actual behaviour data of the excavated testing canal facilities on the soft soil foundation.

We can obtain time historical data of pore water pressure and displacement and the position of the slope failure surface.

- 2) To apply the actual behaviour data of the excavated testing facilities to the other systems.

① Applicability of the Sekiguchi-Ohta Model which is used in F.E.M. Analysis can be verified and the failure mechanism of Bangkok Clay can be examined using actual behaviour data of the excavated testing canal facilities.

② The Slope Stability Analysis Method can be verified by estimating the shear strength of soft soil from the place of sliding surface obtained by the monitoring.

3-2 System components of the Monitoring System

(1) Components of the Monitoring System at the project site

1) Hardware components

① Installation plan of measuring instruments

The name and the number of measuring instruments are shown in Table 3-1. And Fig. 3-2 shows the installation plan for measuring instruments in a plane figure.

Figs. 3-3, 3-4 and Table 3-2 show installation plans (horizontal distance and depth) for every cross section except the one which will be improved by soil cement columns.

This installation plan for the measuring instruments was determined with reference to the results of F.E.M. analysis at the detailed design stage in which the construction plan was taken into consideration, especially the relation between the volume of excavation and time. For details, please refer to Appendix 3-1.

The installation plan for the extensometer was changed so they were installed more around the top of slope as shown in Figs. 3-3 and 3-4. The reason for the change is that installation work for extensometers deeper than the middle of slope seems to be difficult when considering the construction condition of the site and the weakness of the soft clay foundation. Consequently, it is considered better to measure mainly the extension of the ground surface around the top of slope than to measure the deformation of the slope surface by extensometers.

Table 3-1 NUMBER OF MEASURING INSTRUMENTS

Installation Plan

Section Instrument		①	②	③	④	Remarks
		non-treat- ment 1:4	non treat- ment 1:6	Soil Cement Columns	Sand Com- paction piles	
Inclinometers	X	3 x 5	2 x 5	-	2 x 5	location X sensor
Settlement gauges	O	3 x 5	2 x 5	-	2 x 5	location X sensor
Piezometers	□	2 x 3	2 x 3	—	2 x 3	location X sensor
Extensometers	T	1 x 6	—	—	—	location X sensor
Displacement Piles	•	31	23	23	27	Files

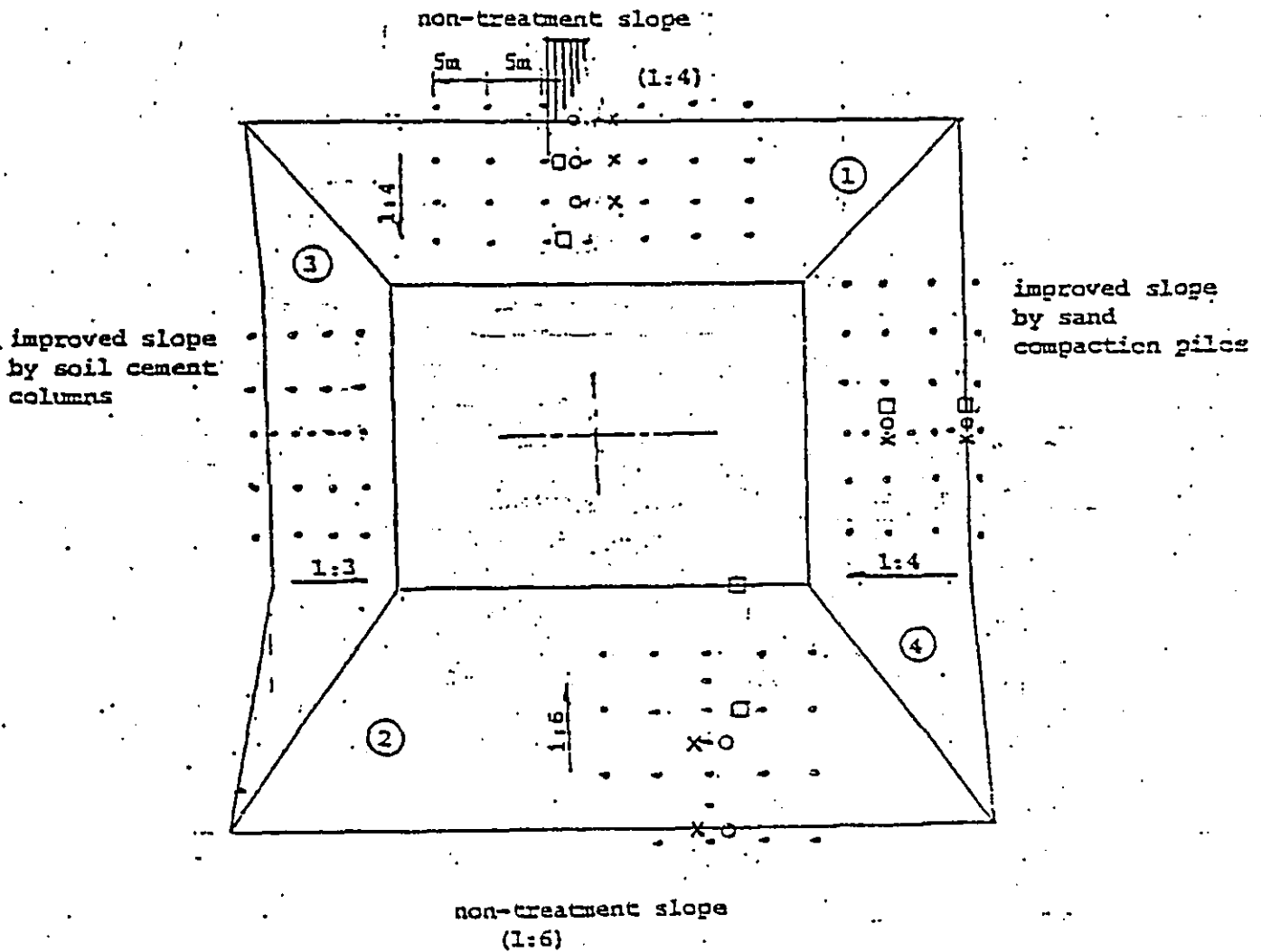


Fig.3-2 PLAN OF MEASURING INSTRUMENTS

INSTALLATION PLAN FOR THE INSTRUMENTS

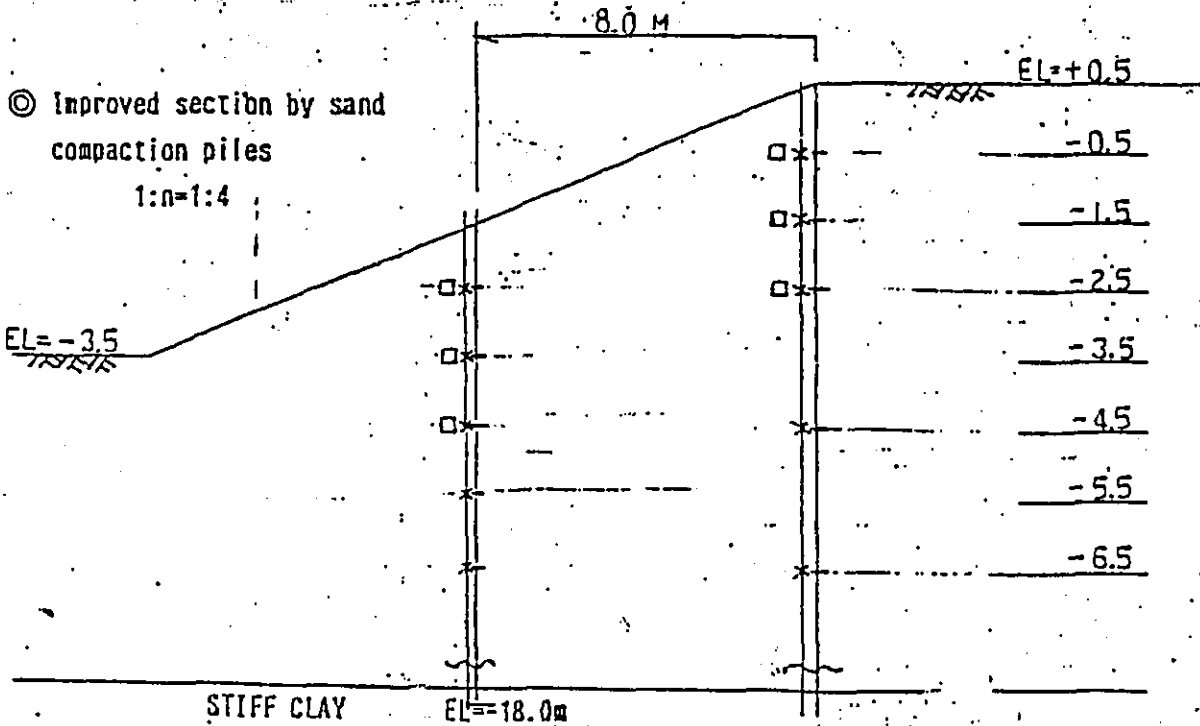
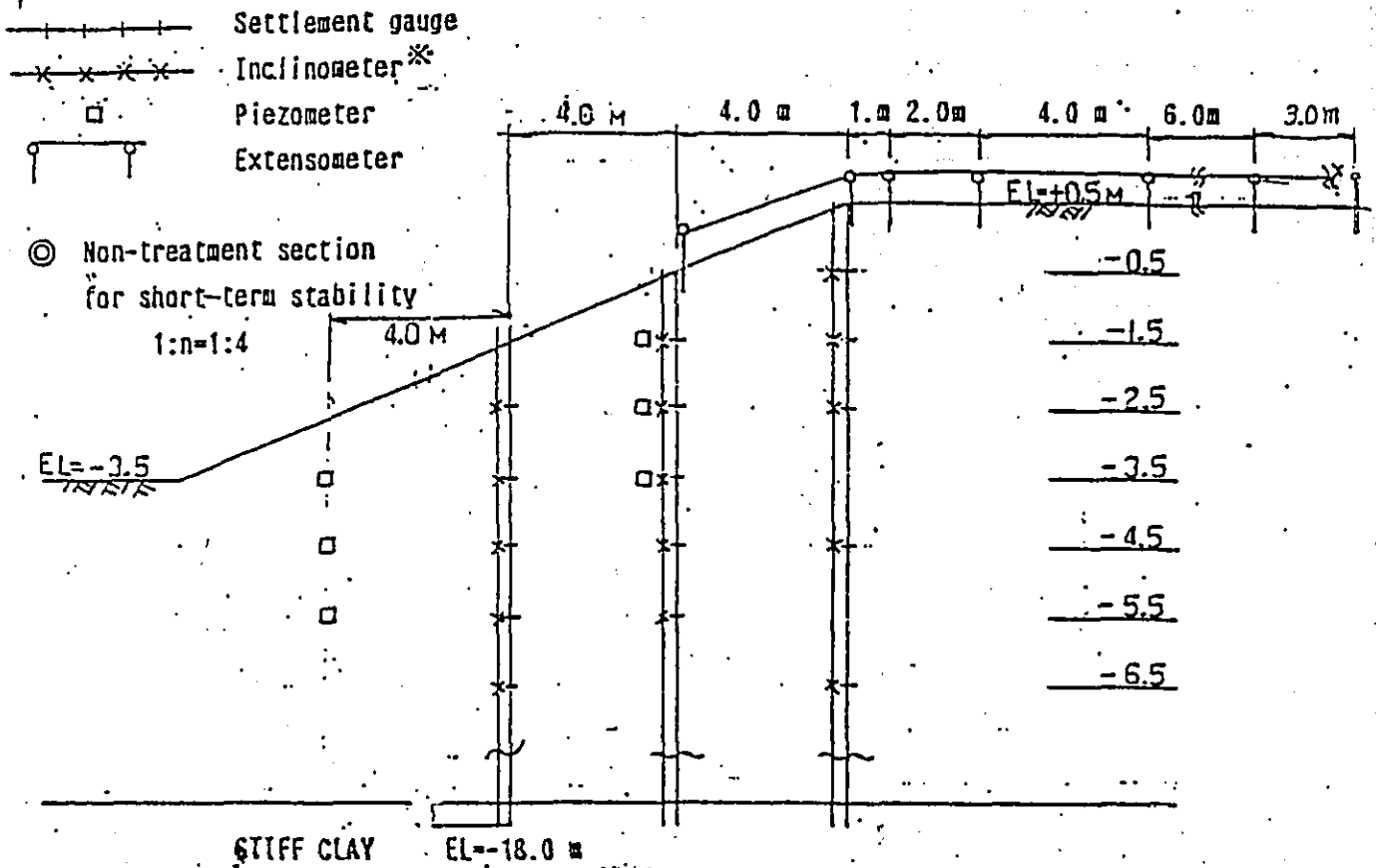
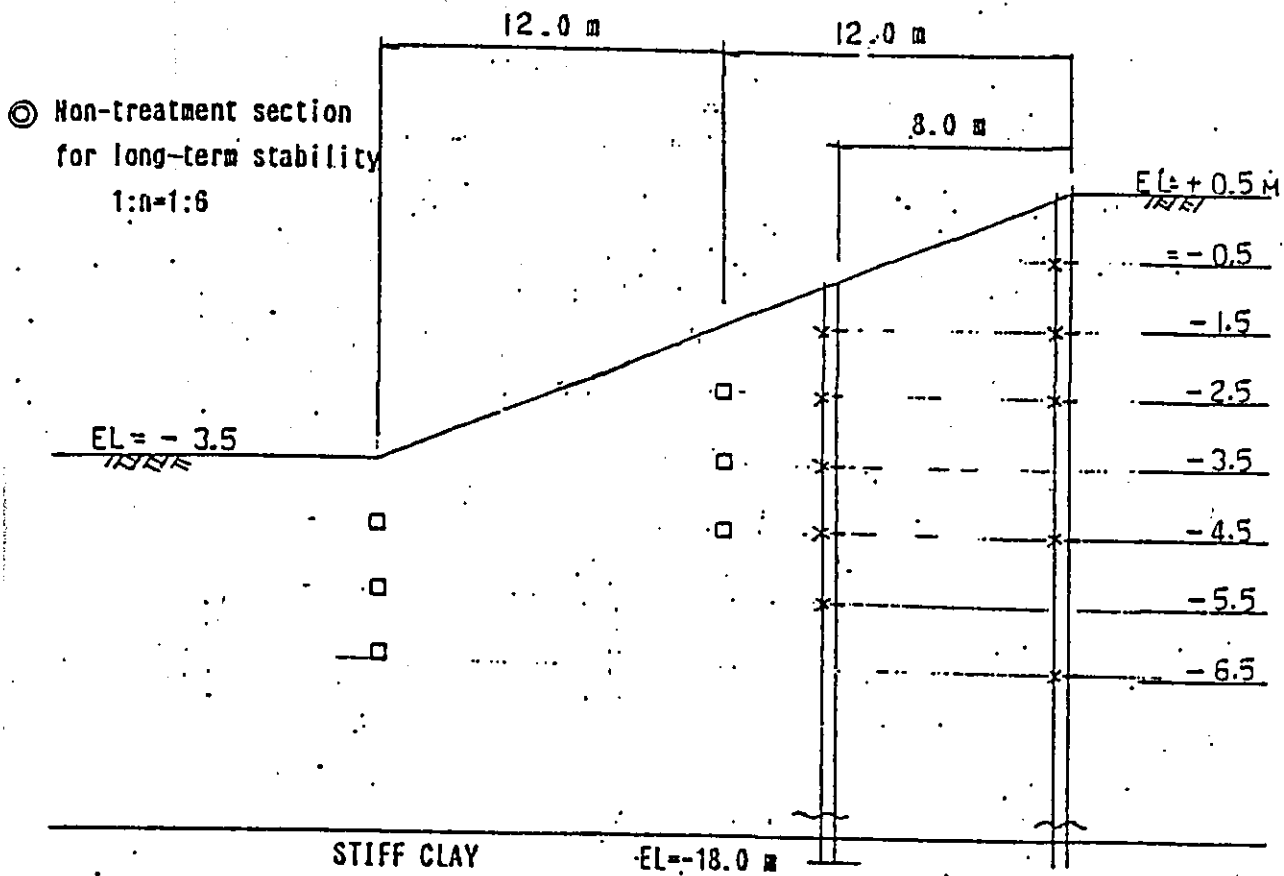


Fig.3-3 Arrangement of measuring instruments on each slope (1)



* 1) Regarding the Inclinator, this symbol (-x-) shows the measurement and reading point.

Arrangement of Extensometer is as follows:

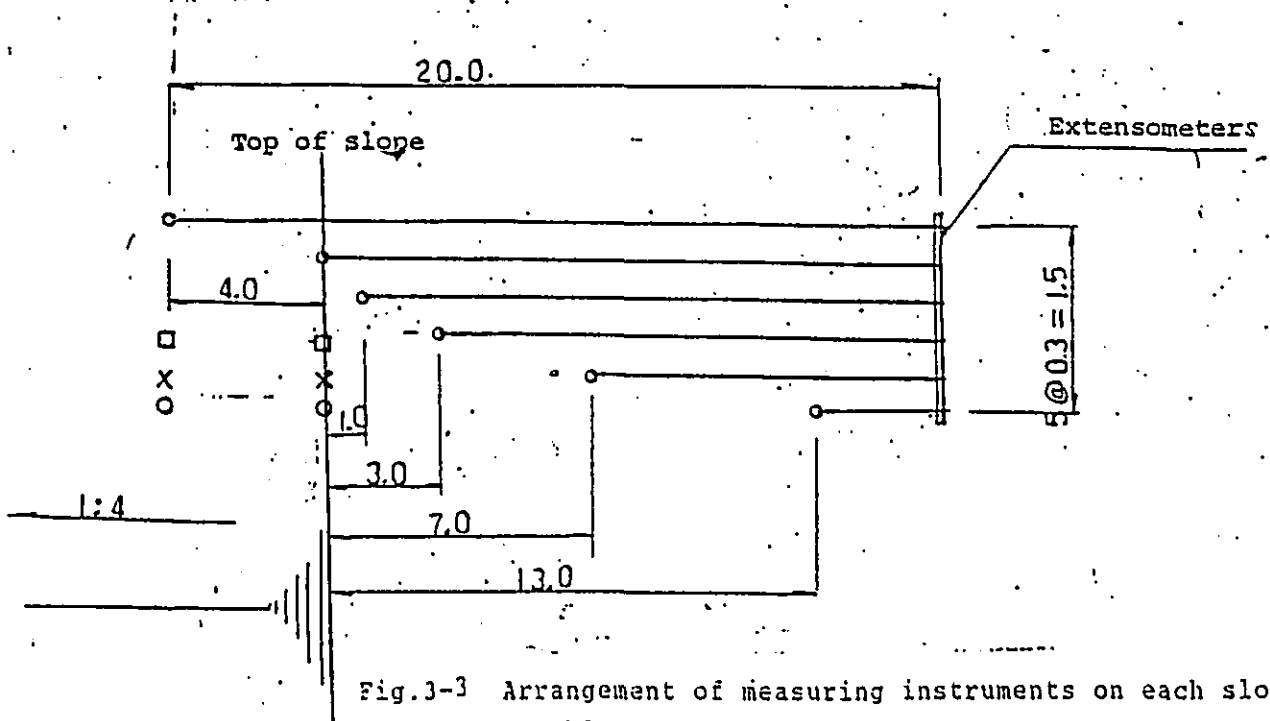


Fig.3-3 Arrangement of measuring instruments on each slope

Table 3-2 Quantities and Numbering of the Instruments.

Name of Instrument	Installation place	Non treatment slope for short-term stability (1:4)					Improved slope by sand compaction piles (1:4)			Non treatment slope for long-term stability (1:6)											
		0 m	4 m	8 m	12 m	16 m	0 m	8 m	12 m	16 m	24 m										
Piezometer	Distance from top of slope	I	II	III	IV																
	Elevation																				
		-0.5																			
		-1.5	○																		
		-2.5	○	○																	
		-3.5	○	○	○																
Settlement gauge																					
		-0.5	○																		
		-1.5	○	○																	
		-2.5	○	○	○																
		-3.5		○	○																
		-4.5	○	○	○																
Recording and reading point of inclinometer																					
		-0.5	○																		
		-1.5	○	○																	
		-2.5	○	○	○																
		-3.5		○	○																
		-4.5	○	○	○																
	-5.5		○	○																	
	-6.5	○																			

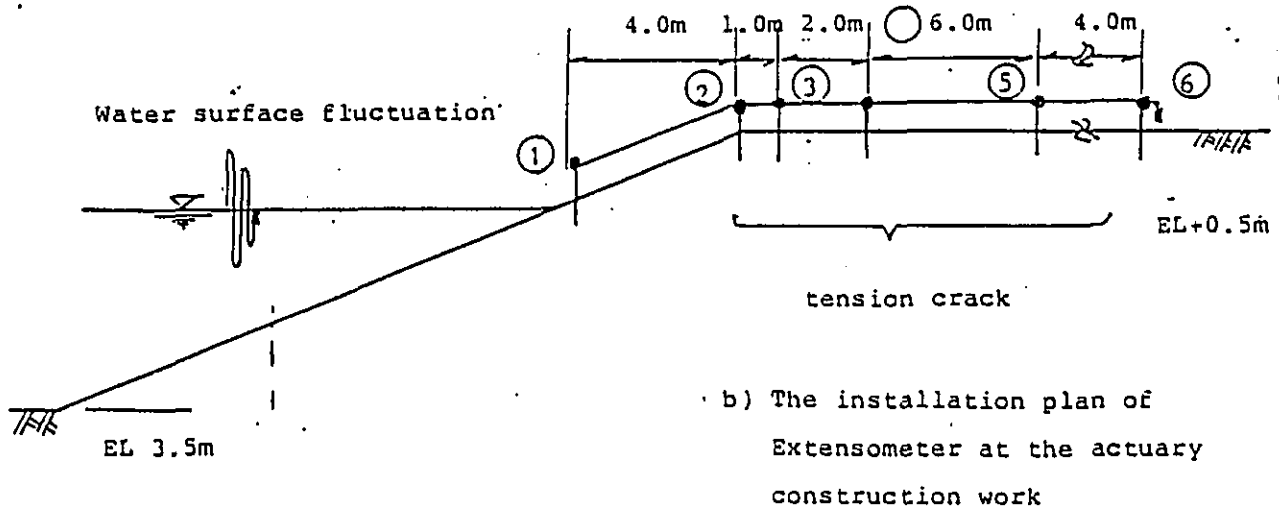
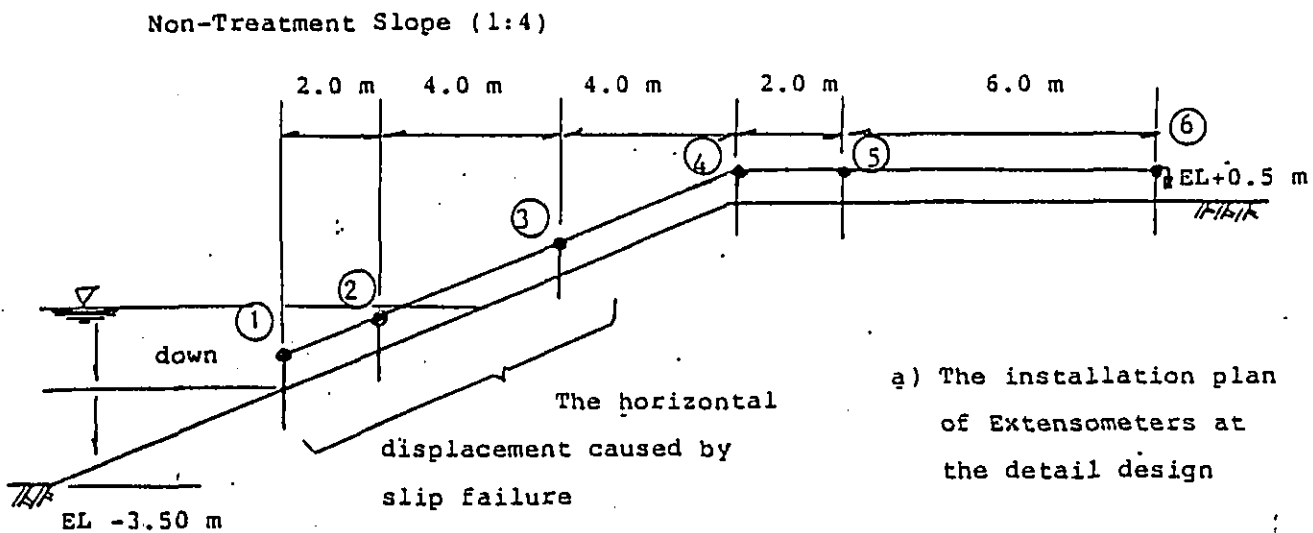


Fig. 3-4 Modification of the installation plan of Extensometers

② Components of monitoring equipment

Analog data (voltage) obtained from measuring instruments will be converted into physical quantities such as displacement and pore water pressure after data transfer and analog-digital conversion using monitoring equipment as in Fig 3-5.

i) In the case of auto-measuring sensors (extensometers, piezometers)

Data sampling will be done by Data Logger (TDS - 351) and the data will be recorded on floppy disks (3.5 inches) by Micro Disk Memory.

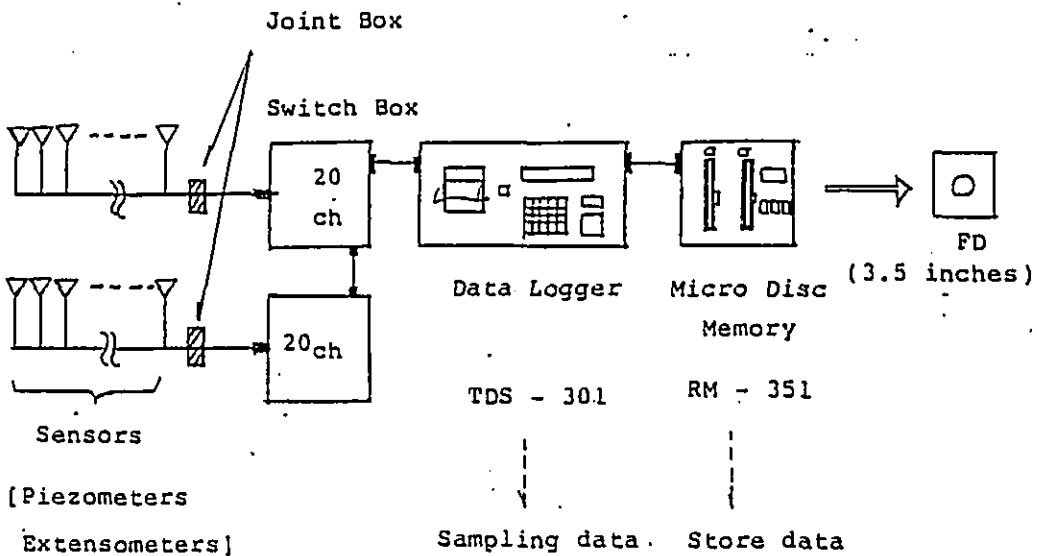


Fig. 3-5 Hardware of monitoring system at the site

ii) In the case of manual-measuring sensors

Data obtained from inclinometers will be converted into physical quantities and will be recorded on floppy disks by Geollogger.

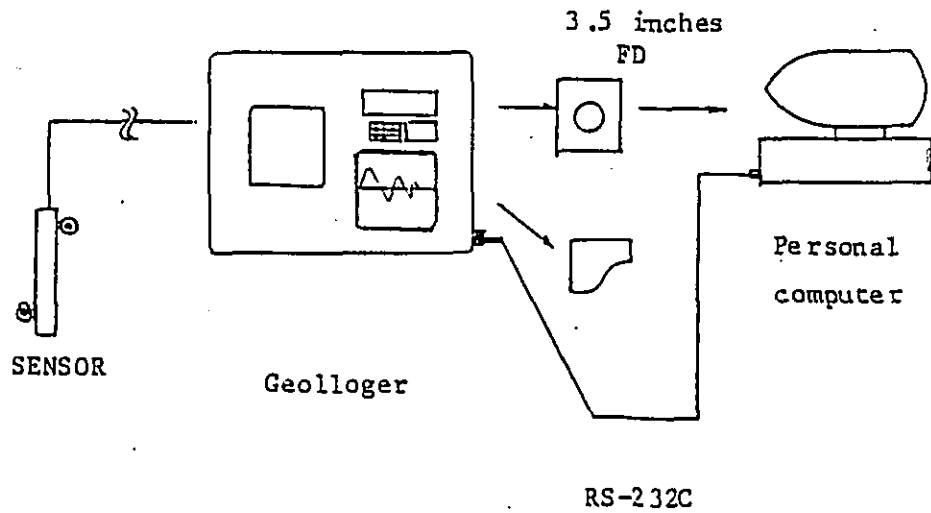


Fig. 3-6 Components of equipment used with inclinometers

(2) Computer system for the Monitoring System in IEC

1) Hardware

Data obtained at the testing site will be transferred into public disk files of the Vax-System after being converted from NEC to IBM data format using PC 9801 Vm2 and APC/IV as shown in Fig. 3-7. After that, these sampling data will be calculated and plotted in graphs.

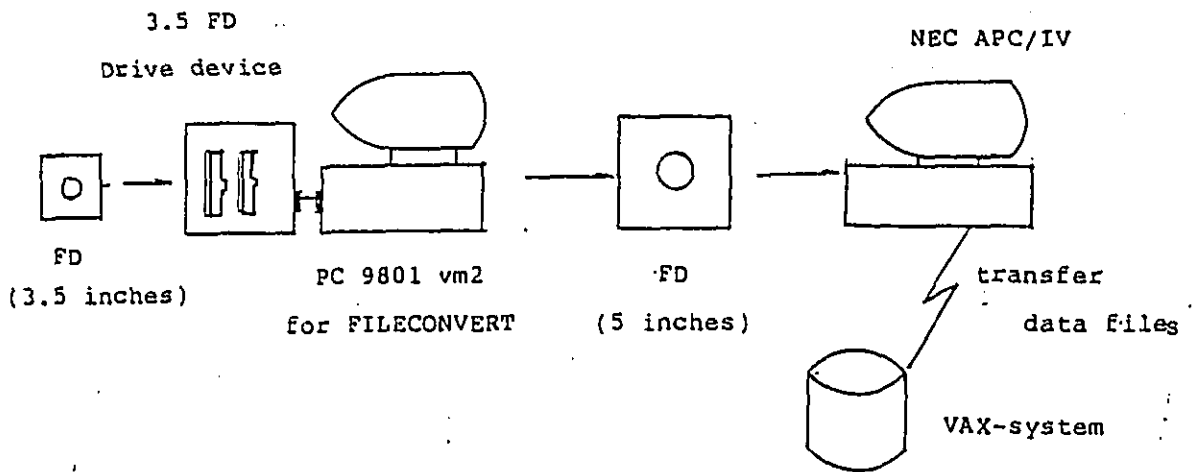


Fig. 3-7 Hardware (1)
(data read path into personal computer)

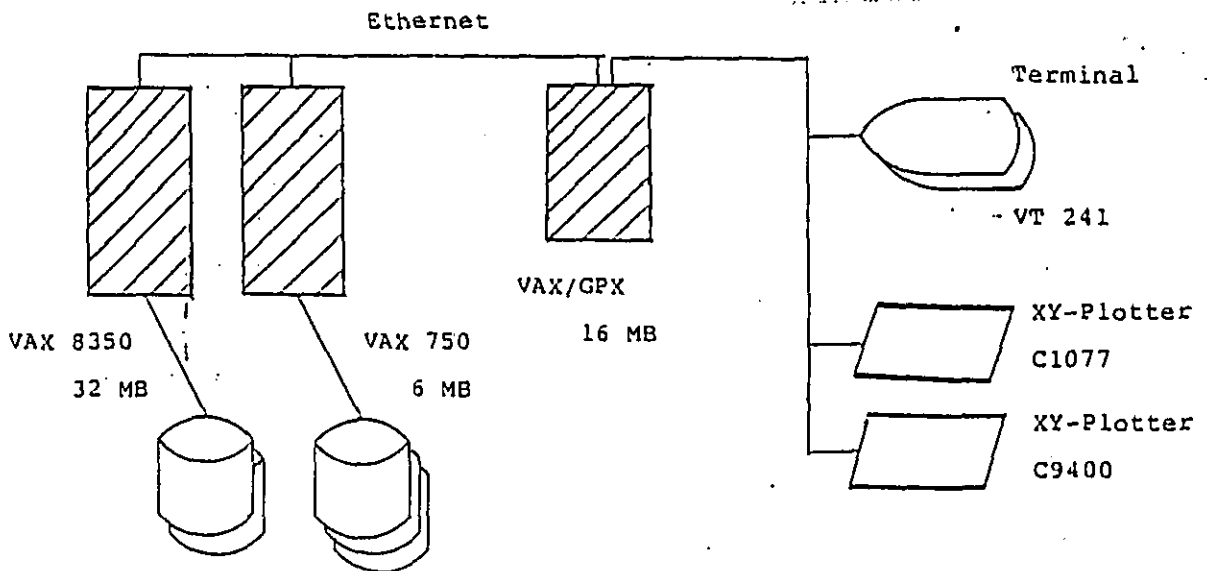


Fig. 3-8 Hardware (2)
(graphic system in the VAX-SYSTEM)

2) Software

(Data transfer and drawing system)

① Outline of software

Software, the processes of which are a) reading measured data by personal computer, b) data transfer to the VAX-System and c) plotting graphs from measured data by the VAX-System, are as follows:

- a) Software for conversion from N88 - BASIC to MS-DOS
..... FILECONVERTER (NEC)
- b) Sequential master file making program for data transferred into the
VAX-system..... S82 MS1. FOR.
- c) Data check program for data master file S82 MS2. FOR.
- d) SORT/MERGE Program for several kinds of master file
- e) Graph program for measured data S82 MS3. FOR.

② Type and significance of plotted graphs in the Monitoring System

Arranging data and plotting are performed by program S82 MS3. FOR. and 9 kinds of graphs can be drawn. These graphs can roughly be divided into three, namely, time historical graphs, data analysis graphs and graphs for slope failure prediction and construction control.

Examples of each kind follow:

i) Time historical graphs

Changes of data obtained by measuring instruments will be plotted as historical axis. These graphs should be prepared for each sensor.

These historical graphs will make the following possible.

- a) To know the general tendency of data which are measured at the testing site everyday.
- b) To examine the presence of sudden changes and to discover the critical condition of slope stability.

THAILAND MODEL INFRA
MONITORING SYSTEM

NO. 256-031 31 CH INCLINOMETER EL. 10.800
 NO. 256-033 33 CH EXTENSOMETER EL. 9.800
 NO. 256-015 15 CH PORE PRESSURE G. EL. 9.800
 NO. 256-017 37 CH SURFACE EXTENS. EL. 8.800

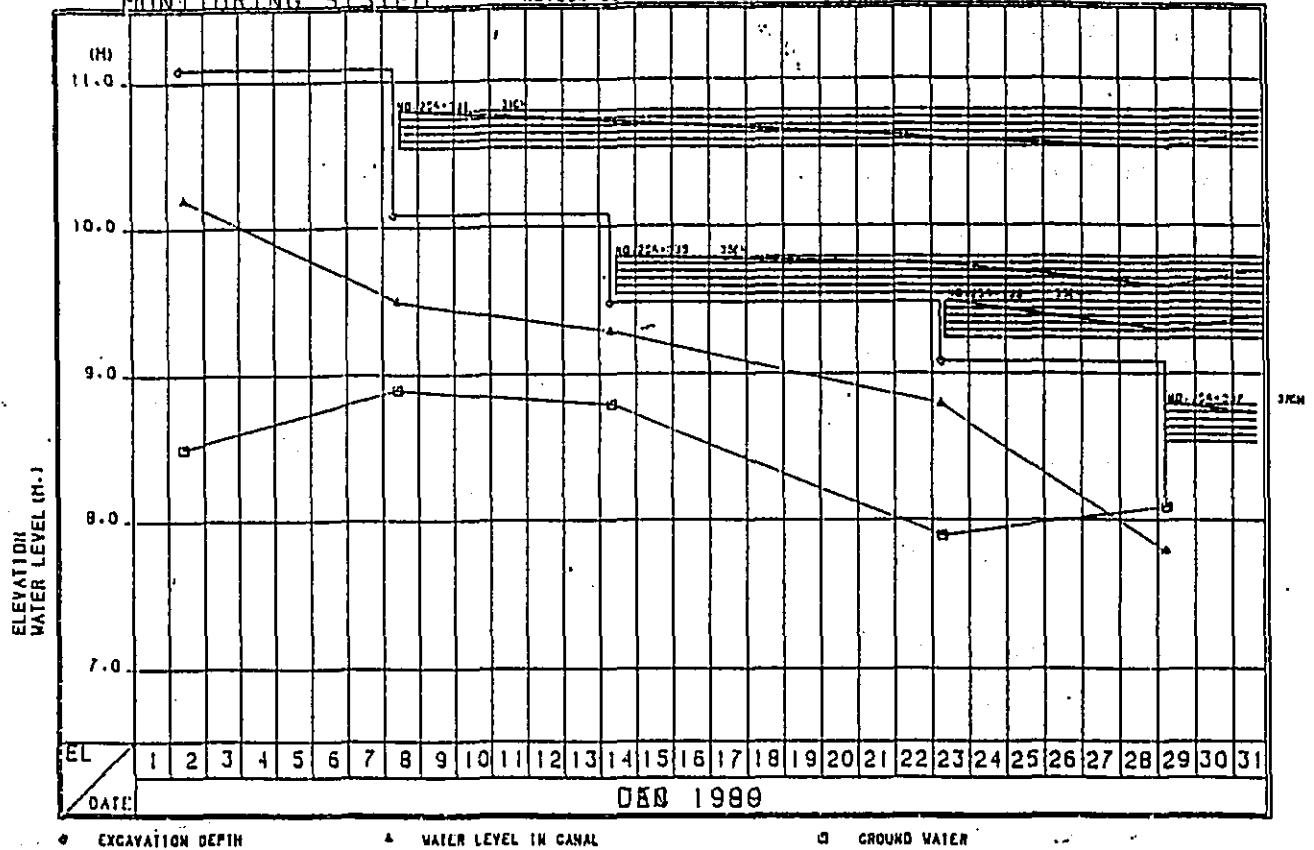


Fig. 3-9 Example of historical graph

ii) Analysis graphs

For analysis, the following graphs can be drawn.

- Vertical distribution of horizontal displacement (from data by inclinometers).
- Vertical distribution of vertical displacement (from data by settlement gauges).
- Behaviour of horizontal displacement obtained by each inclinometer
 - Comparison with prediction by F.E.M. analysis.
- Behaviour of vertical displacement obtained by each settlement gauge
 - Comparison with prediction by F.E.M. analysis.
- Behaviour of relative displacement of ground surface at every section between sensors (from data by extensometers).

Graphs of a) and b) mentioned above will enable us to grasp horizontal and vertical displacement of the insides of the slope with time. Accordingly, sliding surface in the ground and displacement of clod can roughly be estimated.

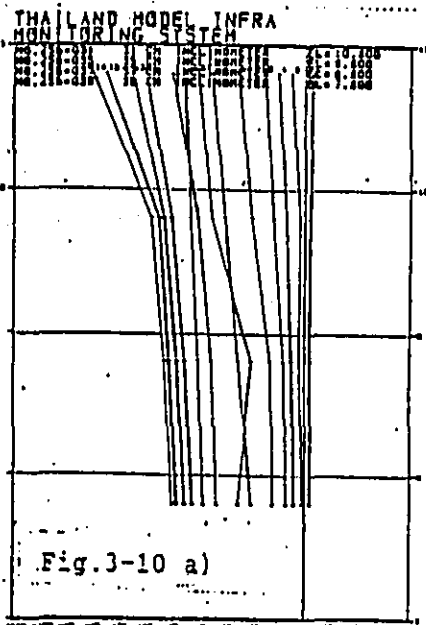


Fig.3-10 a)

Lateral Flow at a cross section

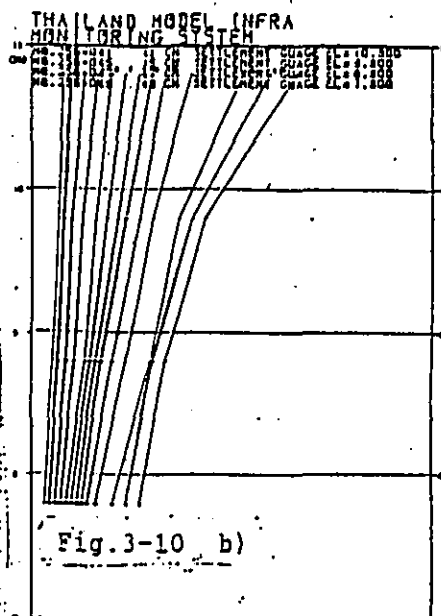


Fig.3-10 b)

Vertical Displacement at a cross section.

Graphs of c) and d) will enable us to trace displacement where the sensors are in the ground taking time into consideration. Comparing horizontal and vertical displacement of Nodal Points obtained by F.E.M. analysis with those of actual data obtained by sensors, displacement condition in the ground can be verified.

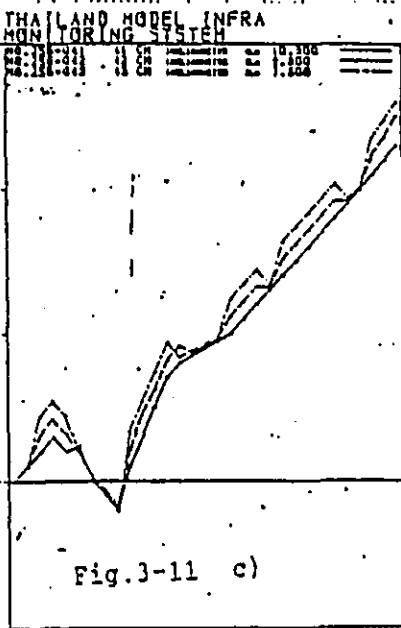


Fig.3-11 c)

Lateral Flow at each measuring point

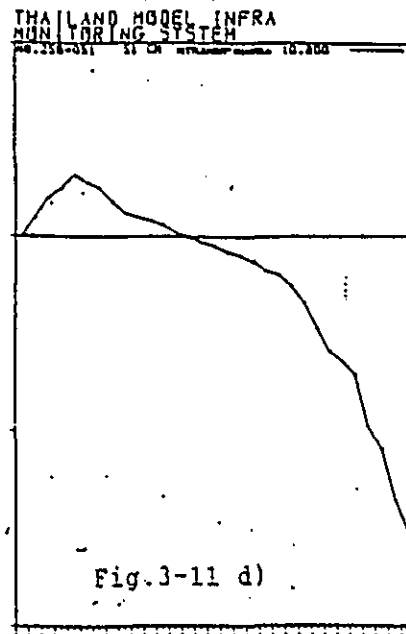
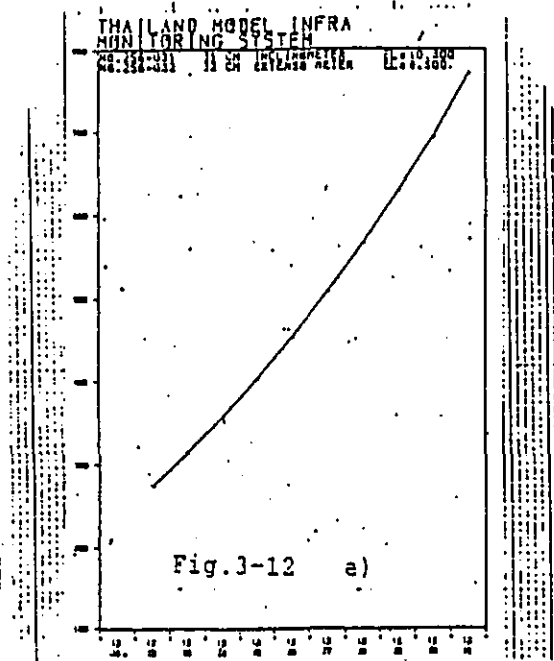


Fig.3-11 d)

Vertical Displacement at each measuring point.

Graphs of e) will enable us to grasp the elastic behaviour of every section on the excavated slope surface and around the top of the slope. This figure, furthermore, will enable us to predict the sliding surface on the ground.



Relative Displacement
at the slope surface

iii) Graphs for slope failure prediction and construction control

Strain and strain ratios will be calculated from data obtained by extensometers, and strain ratios shall be used as indices for warning against slope failure and for time prediction of failure.

There are three kinds of these graphs, and they are as follows:

a) Historical graphs of strain ratios

These graphs show strain ratios with time as a bar graph. If the warning strain ratios against slope failure are set in several steps and if countermeasures are ready to be conducted in accordance with these warning, then these are applicable to construction control.

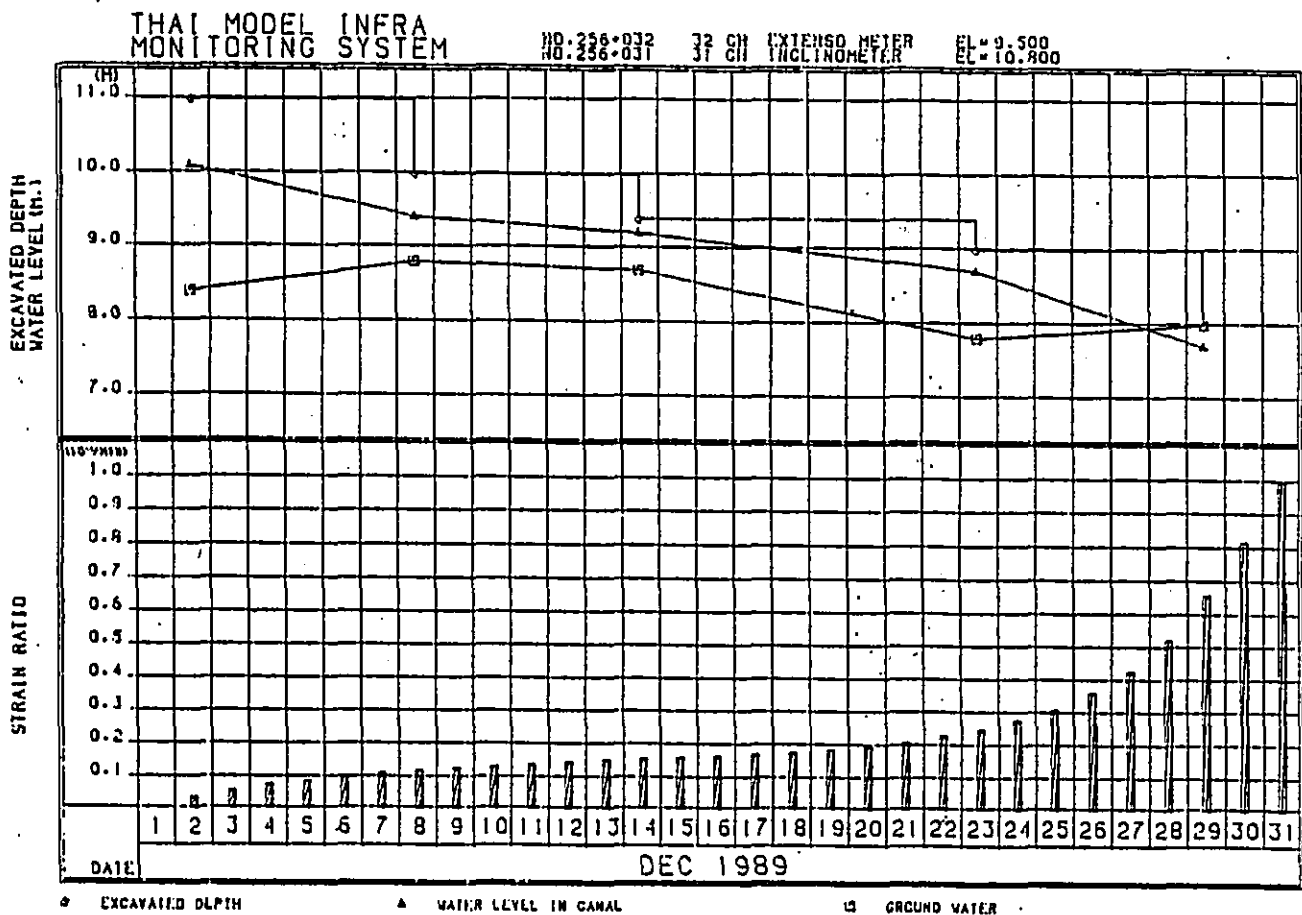


Fig. 3-13 Example of historical graph of strain ratios

b) Historical graphs of steady creep-strain ratios

(Saito's method (1))

c) Historical graphs of tertiary creep-strain ratios

(Saito's method (2))

The graphs b) and c) were proposed by Dr. Saito in 1965 and have had a lot of positive results in the time prediction of slope failures.

The advantage of these graphs b) and c) is the width of applicability, that is, these methods encompass almost all kinds of slope failure and have almost no relation to the soil properties of the slope. For an explanation of the theoretical and experimental background to Saito's methods, please refer to Appendix 4-2.

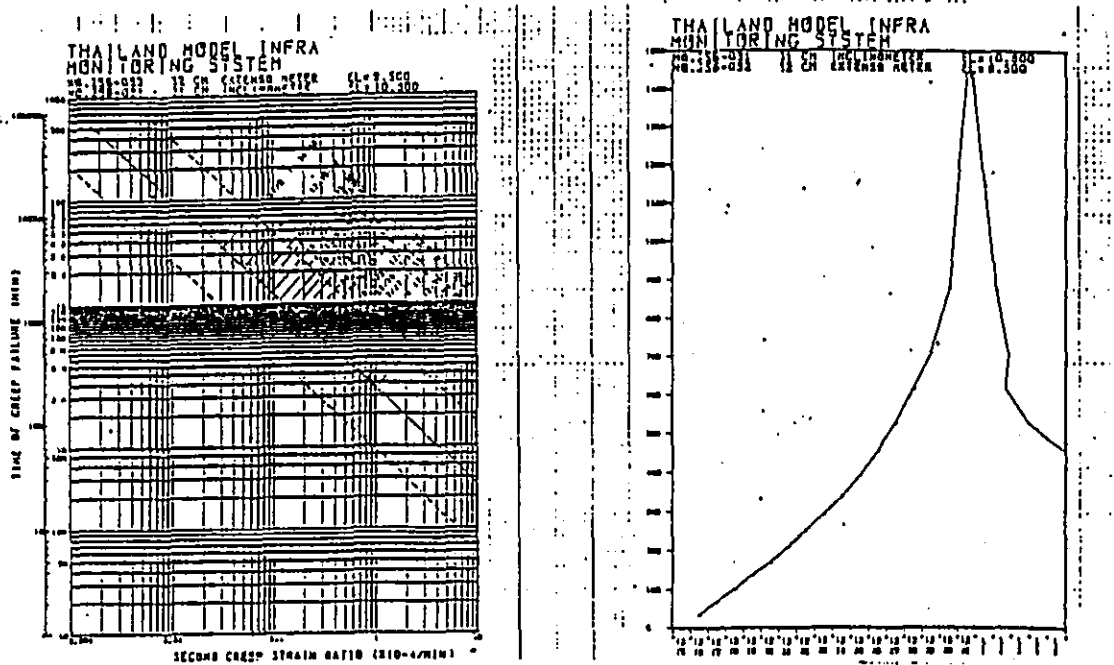


Fig. 3-14 Examples of historical graphs for slope failure prediction and construction control

b. steady creep-strain ratios c. tertiary creep-strain ratios

3-3 Procedure for plotting graphs in the Monitoring System

(1) Flowchart of plotting graphs

Fig 3-15 shows the series in the procedure for plotting graphs from data.

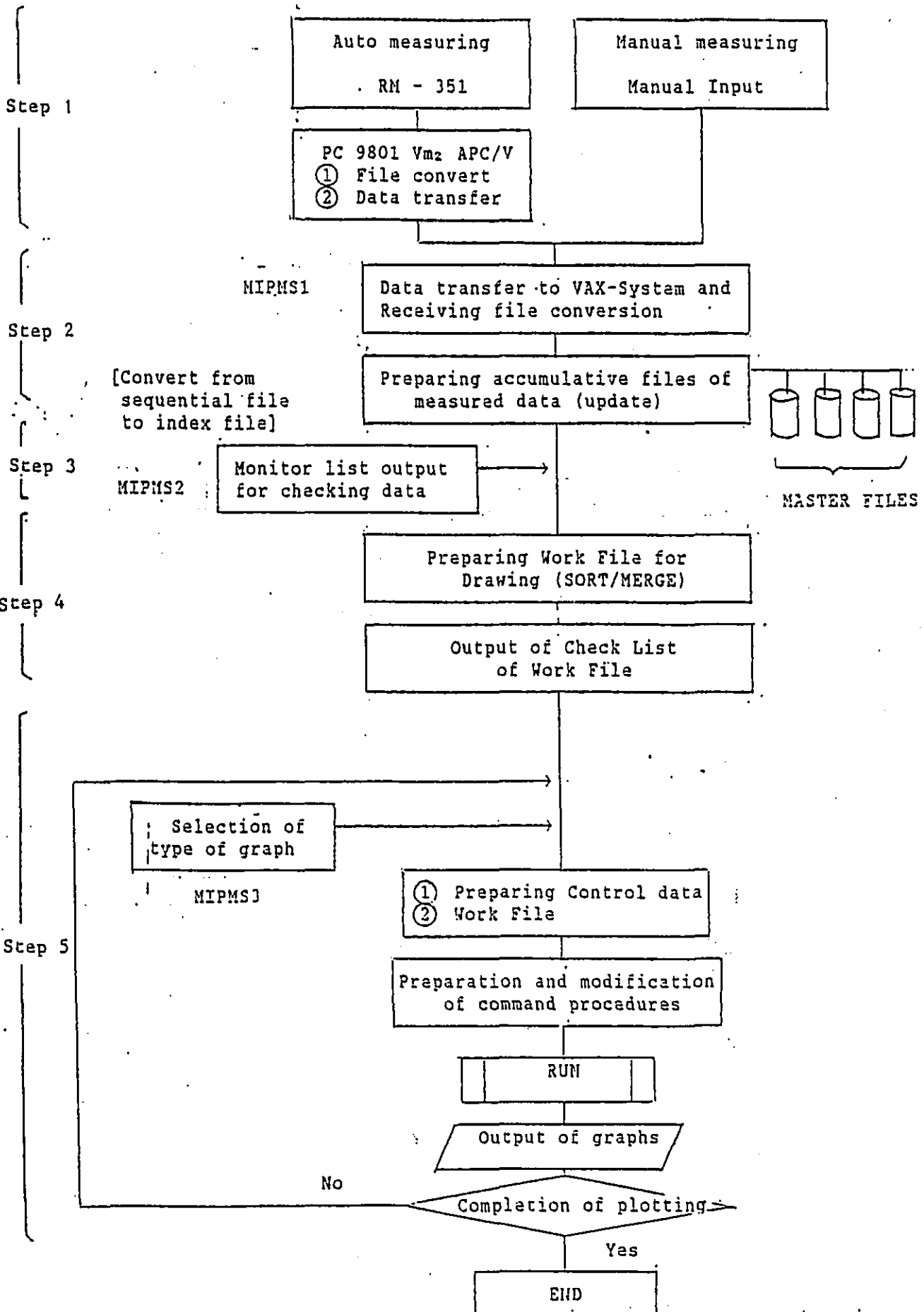


Fig 3-15 Flowchart of plotting process

(2) Explanation of plotting procedure

According to the flowchart for plotting graphs illustrated above, this section explains the procedure for plotting graphs in the Monitoring System.

Step 1 Data reading of auto-measured data into APC/IV and file conversion

Recorded data in the Micro Disk Memory at the testing site is in N 88 - Basic format, and this format cannot be read by personal computer APC/IV which is the terminal equipment of VAX-8350. Consequently, the following file conversion into MS-DOS format is necessary

- ① To initialize a 5 inch floppy disk in IBM MS-DOS format.
- ② To activate PC 9801 Vm2 by N88-BASIC.
- ③ To insert a 3.5 inch floppy disk (sequential file) into the external floppy disk drive and to read the data file and to print out the data.
- To activate PC 9801Vm2 by MS-DOS again and to activate "FILECONVERTER".
- ④ To convert data file format from N88 Basic to MS-DOS format by "FILECONVERTER" and to print out the list for checking.
- ⑤ To transfer data files (MS-DOS IBM), whose format is converted by personal computer PC9801Vm2, from NEC APC/IV to public magnetic file of the VAX-System.

(For details of file conversion and disk area, please refer to the operation manual)

Step 2 Data transfer of sampling data into the VAX-System and preparation of measured data master file

To transfer a data file using APC/IV which has a virtual emulator of VAX-VT240 and to prepare an Auto-measured Data Master File after conversion of receiving file format using program S82MS1.

At this step, the other three files, which are the Manually-measured Data Master File, the Measuring Instruments Master File and the Construction Data Master File are simultaneously prepared.

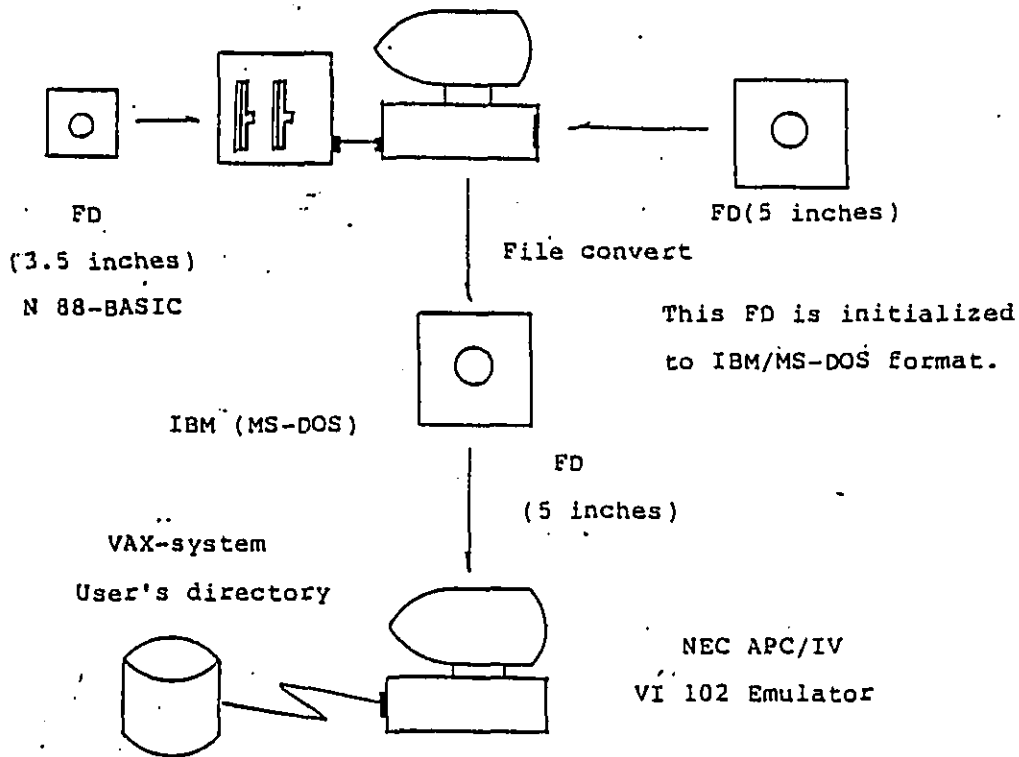


Fig. 3-16 File convert of sampling data file and transfer data file to VAX-system

Auto-measured data master File (ADMST)	Manually-measured data master file (MDMST)	Sensor data master file (SKMST)	Construction data master file (CKMST)
--	--	---------------------------------	---------------------------------------

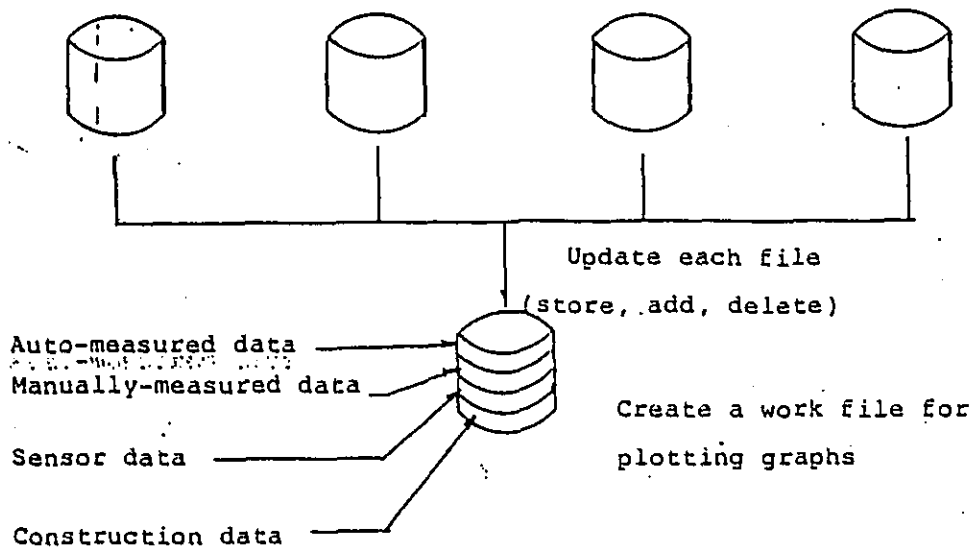


Fig. 3-17 Components of Master Files

Step 3 Monitor list output for data check

At this step, the program S82MS2 carries out matching between the Measured Data Master Files and the Measuring Instruments Master File and checks the data, double data reading and lack of data.

Step 4 Preparation of work file for plotting graphs

A data work file is prepared for plotting graphs from 4 kinds of data master files which are prepared at step 2 by SORT/MERGE function.

Step 5 Execution of plotting graphs

In order to execute plotting by program S82MS3. FOR., control data are prepared.

These data are for selections of type of graph plotting, the date, and the names of sensors. Graphs selected are output on a XY plotter by S82M3 using the control data file and the Work File prepared before. If several graphs are needed, control data shall be changed again.

3-4 Plan of slope behaviour observation system at the testing site

The way in which the slope observation system in the Monitoring System is operated can be divided into two (2), namely, an observation system as operated during normal times and in that of an emergency, according to the construction condition of the testing site and slope behaviour.

(1) Observation system as operated during normal times in the case that the excavated slope is stable.

1) Frequency of observation

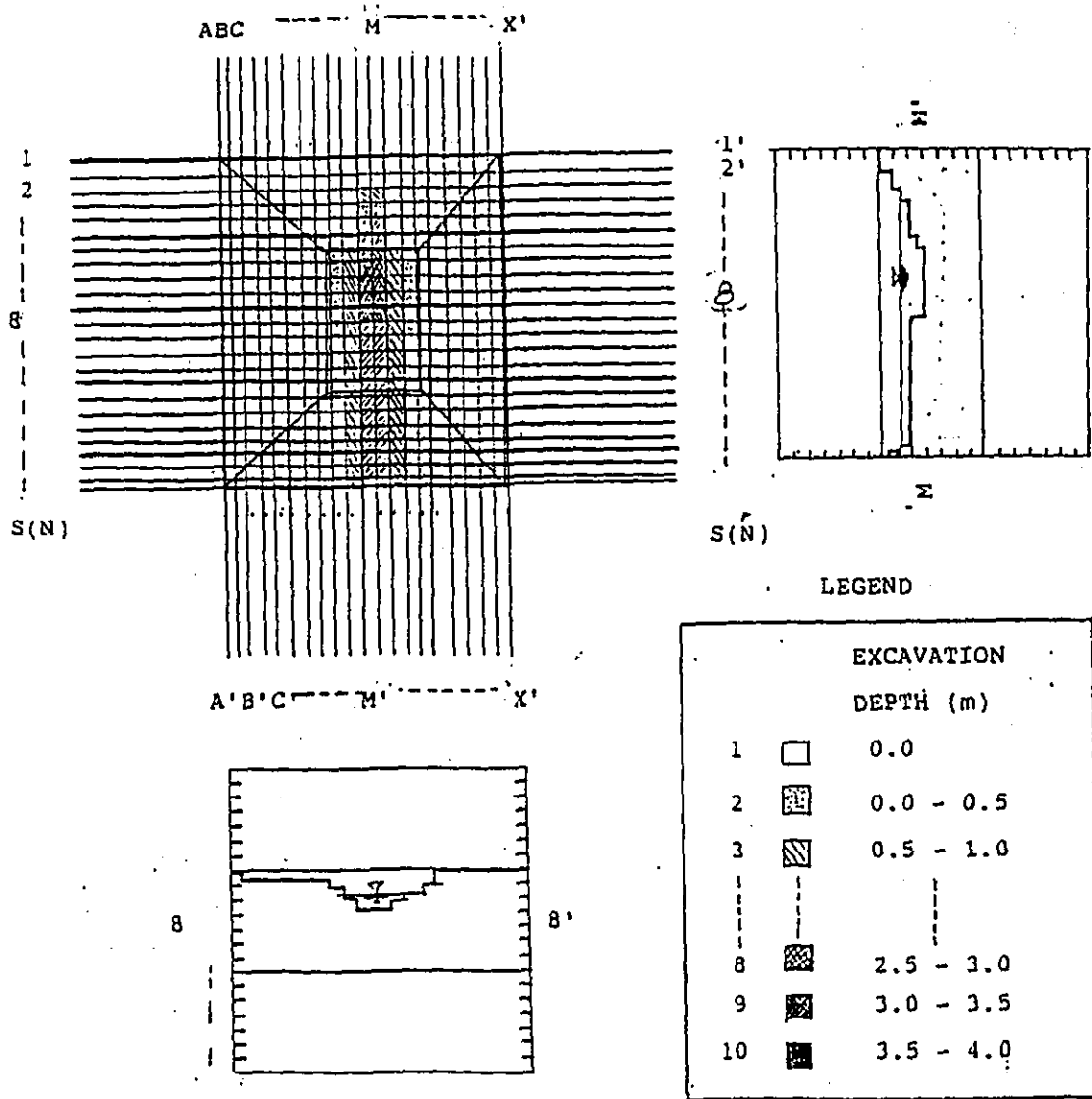
At the beginning of excavation, it is considered that there isn't much large deformation. Consequently, if we take measurements from sensors at scheduled times 3 times a day in the auto-measuring system and 1 time a day or 1 time every 2 days in the manually-measured system, observation frequency will be enough (refer to Table 3-3).

Data obtained at the testing site should be transferred to the VAX-System in IEC at a frequency of about 1 time per week and several kinds of graphs should be plotted by the drawing system in the Monitoring System.

2) Diagrams of the excavation situation

In order to grasp the rough configuration of each section at each excavation stage taking the passage of time into account, I would like to propose making plane and cross sectional diagrams of the excavation situation.

Fig.3-18 shows an example of these kinds of diagrams and they are not only useful for construction control, but also give useful information about nfiguration data and construction data e.g. time, water level in the testing canal, boundary condition of seepage to the F.E.M. analysis model which is linked with the Monitoring system. For these details, please refer to "4-3 Procedure of Analysis Model Preparation".



- ① Information for construction control
- ② Information for the boundary conditions of F.E.M. Analysis model (e.g. time, water level, etc)

Fig. 3-18 Diagrams of the excavation situation

3) Plotting control graphs of slope failure at the testing site.

There is a possibility that the advancement of the slope failure will be found late under the weekly periodical data processing in VAX-System. I, therefore, would like to propose that control graphs mentioned below should be plotted everyday by hand at the testing site for daily control of slope failure.

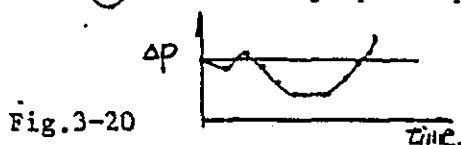
① Bar graph of strain ratio



To trace extension and strain on the slope surface.

To calculate strain ratio from extensometer data.

② Historical graph of pore water pressure



Auto measured piezometers data and the water level in the testing canal.

In graphs ① and ② above or in graphs plotted by the Monitoring System, if the strain ratios rapidly increase and exceed the strain ratio warning value*, or if pore water pressure increases in comparison with the water level in the canal, it is surmised that sliding is proceeding inside the slope. In this case, the observation system should be changed to the emergency system as described in the following section.

*1. The strain ratio warning value

The strain ratio warning value should be determined on the basis of precedent data of excavated slope failure and the results of F.E.M. analysis and two (2) warning values should be determined in correspondence with the following two (2) stages.

- a) The beginning stage at which there is little distribution of sliding zones inside the slope.
- b) The stage at which distribution of sliding zones spreads quite widely and slope failure will occur soon.

When the strain ratio reaches the first warning value, the observation system should be changed to the emergency observation system to increase the frequency of observation.

(2) Observation system in emergency

When out of the ordinary slope behaviour is found in the control graphs for slope failure in the ordinary observation system, the observation system should be changed to emergency observation system.

1) Frequency of observation

Frequency of observation should be changed, in the case of auto-measuring instruments, from 3 times/day to 6 times/day, and in the case of manually-measured instruments, to more often than 1 time/day at least.

Deformation on the slope surface and around the top of slope etc. should be recorded by visual observation and/or camera everyday.

2) Plotting control graphs for slope failure

In the emergency observation system, not only continue to plot bar graphs of strain ratio and historical graphs of pore water pressure in the normal observation system, but the following control graphs should also be plotted at the testing site.

① Historical graph of steady creep-strain ratio

(Saito's method (1))

② Historical graph of tertiary creep-strain ratio

(Saito's method (2))

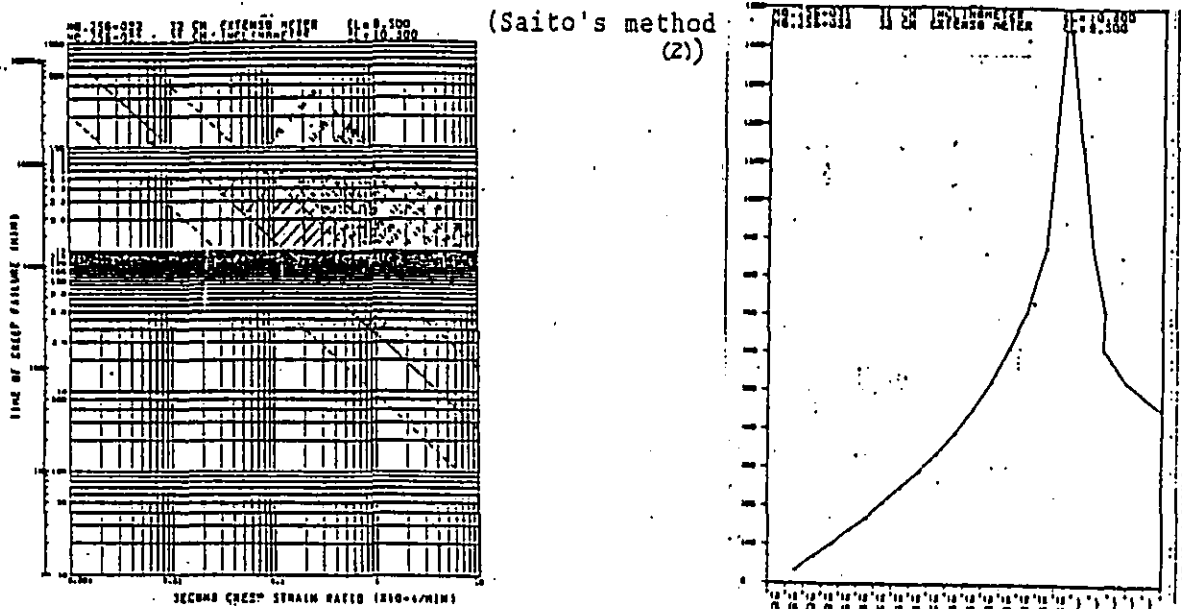


Fig.3 Steady creep-strain ratio

Tertiary creep-strain ratio

Using these graphs, examination of time prediction of slope failure should be started. Regarding the interpretation and plotting method of these graphs, please refer to Appendix 3.

I would like to propose that plotting these graphs should be carried out by XY plotter on demand because they can be plotted by the Monitoring System.

3) Verification of the result of plotted graphs

In the case that the following phenomena occur in the plotted graphs, investigation of the phenomena should be carried out at the testing site, and the phenomena should be verified by the results of F.E.M. analysis.

① Slope surface behaviour

- | | |
|---|---------------|
| i) Relative displacement graph — Rapid increase in of the slope surface relative displacement | } At the site |
| ii) Historical graph of strain — Rapid increase ratios (Kurihara's method) in strain ratio | |
| iii) Historical graph of steady — Time prediction creep-strain ratios of slope failure | |
| iv) Historical graph of tertiary — Time prediction creep-strain ratios of slope failure | |
- a) Deformation of the slope surface

b) Extension around the top of the slope

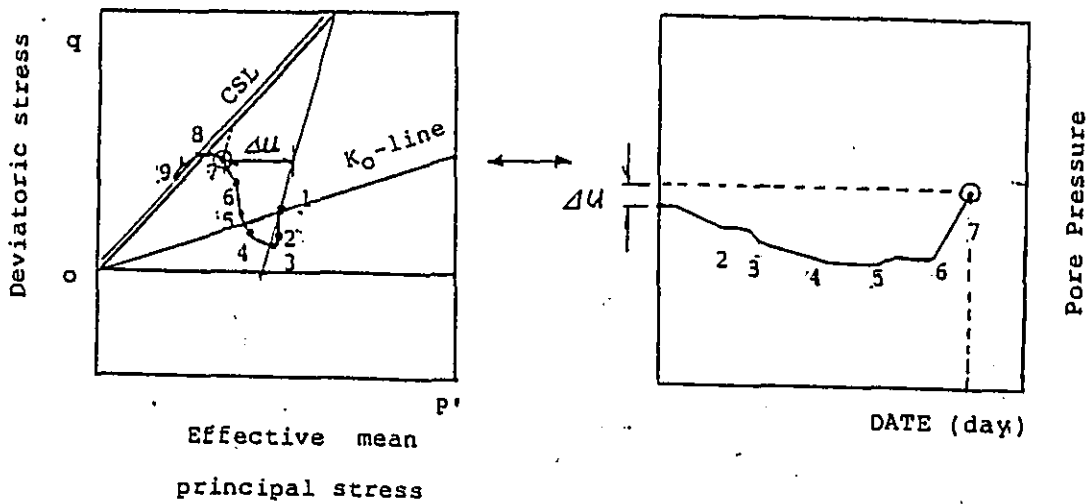
Presence of cracks

② Underground displacement behaviour and pore water pressure behaviour

- | | |
|--|--|
| i) Distribution graph of — Place where vertical underground vertical displacement rapidly increases under the ground (Settlement gauge) | } To verify the place of failure zone by the results of F.E.M. analysis and to examine the presence of slope failure synthetically |
| ii) Distribution graph of — Place where horizontal underground horizontal displacement rapidly increases under the ground (Inclinometer) | |
| iii) Historical graph of — Place where pore water pore water pressure rapidly increases | |

③ Prediction of stress distribution under the ground by effective stress path
 Plotting the effective path of the elements in F.E.M. analysis model which correspond with the place where the value in graphs mentioned in 2 is out of the ordinary, we can grasp how close the effective pass is approaching to the critical state line at the analyzing stage which corresponds with the time of investigation.

The method as shown in Fig.3-23 enables us to compare the stress distribution under the ground with the actual pore water pressure data.



The effective stress path of the element in F.E.M. Analysis Model

The hysteresis of pore pressure at a point under ground foundation is measured by an open piezometer.

Fig. 3-23 Prediction of a pore pressure behavior and a failure of a soil element

4) Countermeasures

After plotting graphs, the construction control supervisor and the contractor should judge the slope behaviour and should propose countermeasures as follows to the Advisory Committee and/or the Implementation and Coordination Working Committee.

- ① Rise of water level in the canal
- ② Modification of excavation order
- ③ Modification of excavation method
- ④ Observation system in future

The Advisory Committee and/or the Implementation and Coordination Working Committee which have received these proposals should decide on the countermeasures, and instruct the construction control supervisor and the contractor to carry out the countermeasures.

3-5 OPERATION MANUAL
FOR
THE MONITORING SYSTEM

3-5 Operation manual for the Monitoring System

(1) Procedure for plotting graphs in Monitoring System

The following Fig. 3-16 illustrates the execution process of the Monitoring system from reading measured data at the site to plotting several kinds of graphs.

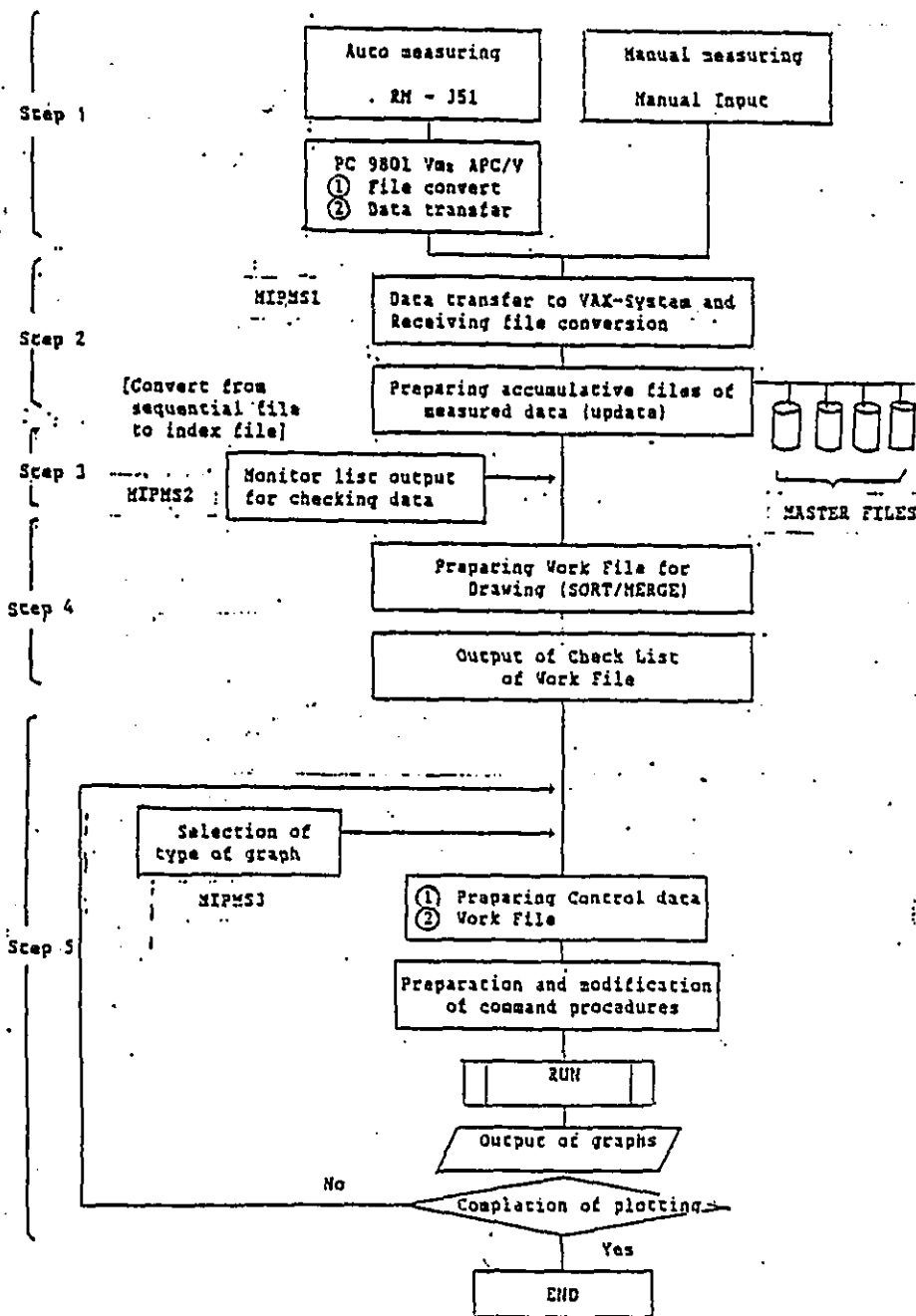


Fig. 3-25 Flowchart of plotting process

In conformity with Fig. 3-16, the next section explains operation procedures at each step, the function of each program and preparation of input data.

(2) Explanation of operation procedures at each step

1) Step 1 Data format conversion of auto-measured data and transfer of the data to VAX system.

The operating procedures are as follows.

- 1) Initialize a 5 inch floppy disk by APC/4 in MS-DOS format of IBM type.
- 2) Activate personal computer NEC 9801 using N88-BASIC (DISK-BASIC) and external floppy disk drive (for PC 9801 and for 3.5 inch F.D.).
- 3) Insert 3.5 inch floppy disk on which measured data was written by Micro Disk Memory (RM-351) into NO. 1 of external floppy disc drive.

Remarks : Drive number on screen of personal computer

In the case of N88-BASIC 3:

In the case of MS-DOS C:

```
Disk version
How many files(0-15)?
NEC N88 BASIC(86) version 4.0
Copyright (C) 1983 by NEC Corporation / Microsoft Corp.
500564 Bytes free
OK
```

Fig. 3-26 Screen

4) To check the contents of the 3.5 inch floppy disk

- ① Display the filename written on the 3.5 inch floppy disk.

FILES 3 : R

```
FILES 3:
DAT001* 1 DAT002* 1 DAT003* 1 DAT004* 1
DAT006* 1 DAT007* 1 DAT008* 1 DAT009* 1
DAT011* 1 DAT012* 1 DAT013* 1 DAT014* 1
DAT016* 1 DAT017* 1 DAT018* 1 DAT019* 1
DAT021* 1 DAT022* 1 DAT023* 1 DAT024* 1
DAT026* 1 DAT027* 1 DAT028* 1 DAT029* 1
DAT031* 1 DAT032* 1 DAT033* 1 DAT034* 1
DAT036* 1 DAT037* 1 DAT038* 1 DAT039* 1
DAT041* 1 DAT042* 1 DAT043* 1 DAT044* 1
DAT046* 1 DAT047* 1 DAT048* 1 DAT049* 1
DAT051* 1 DAT052* 1 DAT053* 1 DAT054* 1
DAT056* 1 DAT057* 1 DAT058* 1 DAT059* 1
DAT061* 1 DAT062* 1 DAT063* 1 DAT064* 1
DAT066* 1 DAT067* 1 DAT068* 1 DAT069* 1
DAT071* 1 DAT072* 1 DAT073* 1 DAT074* 1
DAT076* 1 DAT077* 1 DAT078* 1 DAT079* 1
DAT081* 1 DAT082* 1 DAT083* 1 DAT084* 1
DAT086* 1 DAT087* 1 DAT088* 1 DAT089* 1
DAT091* 1 DAT092* 1 DAT093* 1 DAT094* 1
DAT096* 1 DAT097* 1 DAT098* 1 DAT099* 1
```

Fig. 3-27 Screen

- ② Load necessary data files one by one and check the contents on the screen.

(To compare with data recorded on mini printer's paper by Data Logger)

```
LOAD " 3 : DAT 001 (R)
file name
LIST (R)
```

```
11827 03.23 007:35:00 000+000076010+000079011+000078012+000
*****021*****022*****023*****024*****025*****026**
```

```
11827 03.23 007:35:00 000+000076010+000079011+000078012+000
*****021*****022*****023*****024*****025*****026**
```

```
A>
A>
A>B:
B>DIR
```

Fig. 3-28 Screen

5) To activate MS-DOS (NEC) in PC-9801 Vm2

- ① Insert MS-DOS system disk (NEC 9801, MS-DOS #1) into disk drive No. A and press the RESET key.
- ② After the following screen menu is displayed, select No. 9 menu to activate MS-DOS.

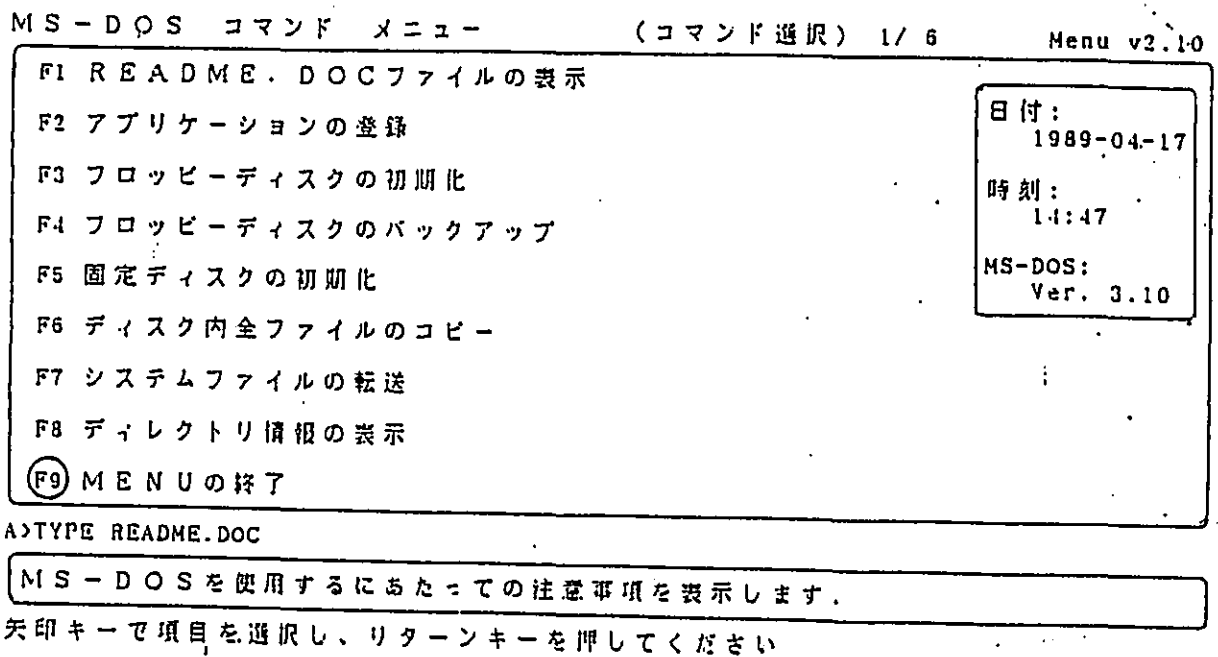


Fig. 3-29 Screen menu (MS-DOS)

6) To load "FILECONVERTER".

- ① Insert the "FILECONVERTER" (MS-DOS #2) floppy disk into disk drive No. B and activate the "FILECONVERTER" by the following command.

```
A > B :  
B > DIR          (----- (To confirm that  
B > FILECONV     FILECONVERTER is in)
```

The screen is displayed as follows:

```
B>DIR  
ドライブ B: のディスクのボリュームラベルはありません。  
ディレクトリは B:¥  
  
EXE2BIN  EXE      2880  87-10-23  0:00  
LIB      EXE     24138  87-10-23  0:00  
LINK     EXE     41114  87-10-23  0:00  
MAKE     EXE     18675  87-10-23  0:00  
MAPSYM   EXE     51904  87-10-23  0:00  
FILECONV EXE     32432  87-10-23  0:00  
NECDIC   SYS     520192  87-10-23  0:00  
      7 個のファイルがあります。  
      556032 バイトが使用可能です。  
  
B>  
  
C1      CU      CA      SI      SU      VOID  NWL      INS      REP      Z
```

Fig. 3-30 Screen

- ② Select the direction of conversion. The direction of data format conversion is from N88 to MS - DOS, and hence select "1/N88-MS-DOS" and press the RETURN key.

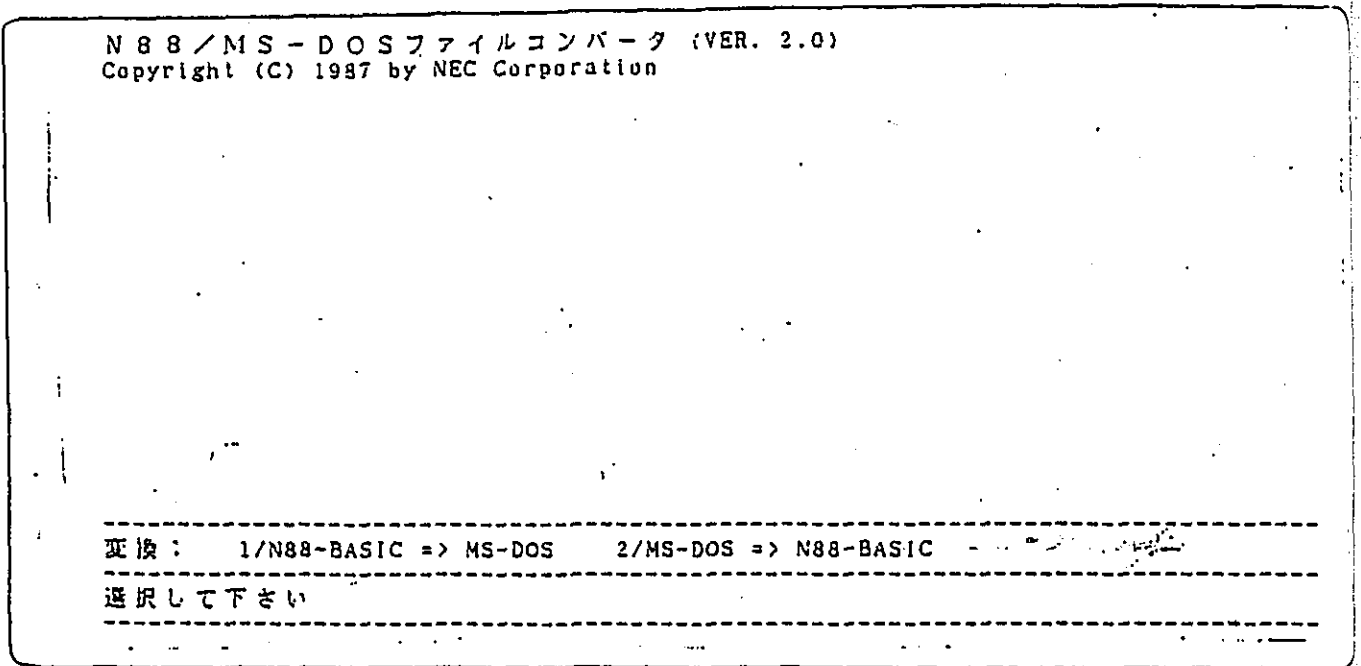


Fig. 3-31 Screen

- ③ Convert the data file format file by file. Select conversion "1/File " and press the RETURN key.

- ④ Key in floppy disc drive No. in which there is a 3.5 inch floppy disk formatted in N88-BASIC.

C : (R) ↘

- ⑤ Key in floppy disc drive No. in which there is a floppy disc to be formatted in MS-DOS

B : (R) ↘

- ⑥ Select the name of the data file written in N88-BASIC format which the user wants converted into MS-DOS.

DAT 001

```

----- [ N 8 8 - B A S I C   D i r e c t o r y ] -----
DAT001 *   DAT002 *   DAT003 *   DAT004 *   DAT005 *
DAT006 *   DAT007 *   DAT008 *   DAT009 *   DAT010 *
DAT011 *   DAT012 *   DAT013 *   DAT014 *   DAT015 *
DAT016 *   DAT017 *   DAT018 *   DAT019 *   DAT020 *
DAT021 *   DAT022 *   DAT023 *   DAT024 *   DAT025 *
DAT026 *   DAT027 *   DAT028 *   DAT029 *   DAT030 *
DAT031 *   DAT032 *   DAT033 *   DAT034 *   DAT035 *
DAT036 *   DAT037 *   DAT038 *   DAT039 *   DAT040 *
DAT041 *   DAT042 *   DAT043 *   DAT044 *   DAT045 *
DAT046 *   DAT047 *   DAT048 *   DAT049 *   DAT050 *
DAT051 *   DAT052 *   DAT053 *   DAT054 *   DAT055 *
DAT056 *   DAT057 *   DAT058 *   DAT059 *   DAT060 *
DAT061 *   DAT062 *   DAT063 *   DAT064 *   DAT065 *
DAT066 *   DAT067 *   DAT068 *   DAT069 *   DAT070 *
DAT071 *   DAT072 *   DAT073 *   DAT074 *   DAT075 *
DAT076 *   DAT077 *   DAT078 *   DAT079 *   DAT080 *
DAT081 *   DAT082 *   DAT083 *   DAT084 *   DAT085 *
DAT086 *   DAT087 *   DAT088 *   DAT089 *   DAT090 *
-----
N 8 8 - B A S I C のファイル名は  DAT001
-----
選択して下さい
-----

----- [ N 8 8 - B A S I C   =>   M S - D O S ] -----
DAT100   =>

```

Fig. 3-32. Screen

- ⑦ Key in the name of the data file to be converted to MS-DOS format.

DAT 001

```
-----  
MS-DOSのファイル名は  
ファイル名を入力して下さい  
-----  
[ N88-BASIC => MS-DOS ]  
DAT100 => DAT001
```

Fig. 3-33 Screen

- ⑧ Create a sequential file-not a random file.
Select "2 /NO" and press the RETURN key.

```
-----  
ランダムデータファイルですか      1/YES      2/NO  
選択して下さい  
-----  
[ N88-BASIC => MS-DOS ]  
DAT100 => DAT001
```

Fig. 3-34 Screen

- ⑨ Since conversion of JIS code in Japanese is not necessary, select "2 /NO" and press the RETURN key.

```
-----  
日本語 J I S コードの 変換は      1/YES   2/NO  
-----  
選択して下さい  
-----  
[ N88-BASIC => MS-DOS ]  
DAT003      =>  DAT003
```

Fig. 3-35 Screen

- ⑩ Select "1/Yes" in order to check parameters and press the RETURN key

```
-----  
パラメータを確認して下さい      1/YES   2/NO  
-----  
選択して下さい  
-----  
[ N88-BASIC => MS-DOS ]  
DAT100      =>  DAT001
```

Fig. 3-36 Screen

- ⑪ The display asks whether another file conversion must be carried out or not. If not, select "2/NO" and press the RETURN key.

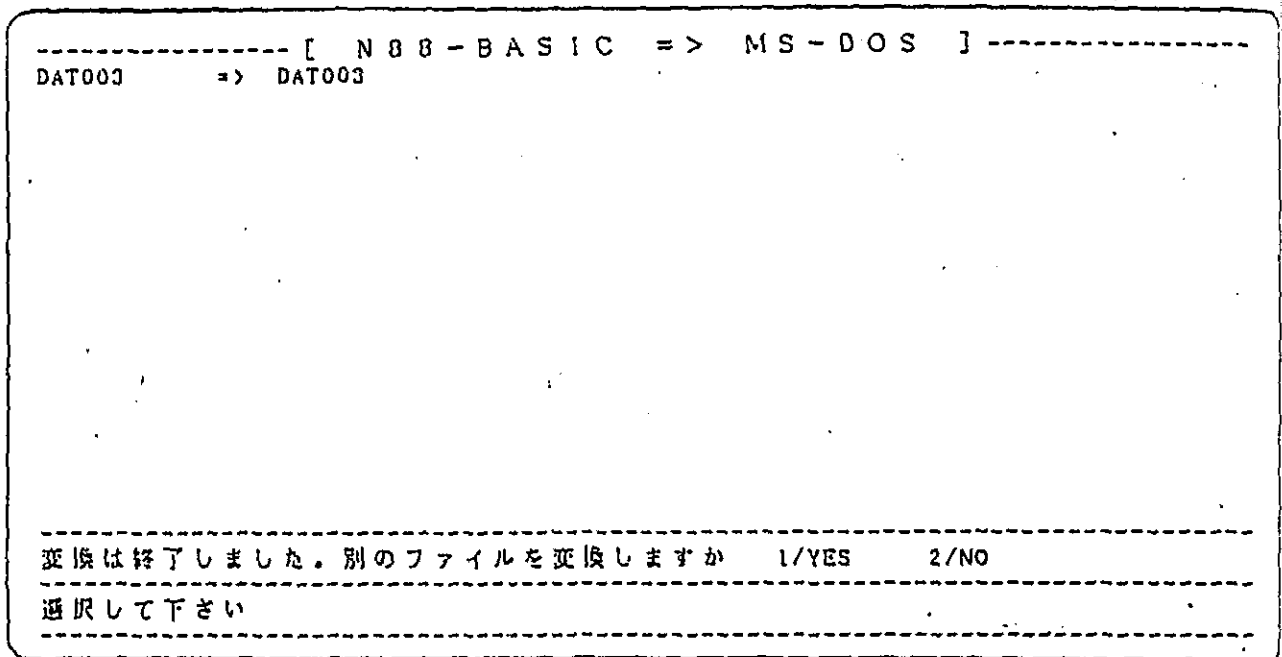


Fig. 3-37 Screen

- ⑫ File conversion is completed.
Press any key

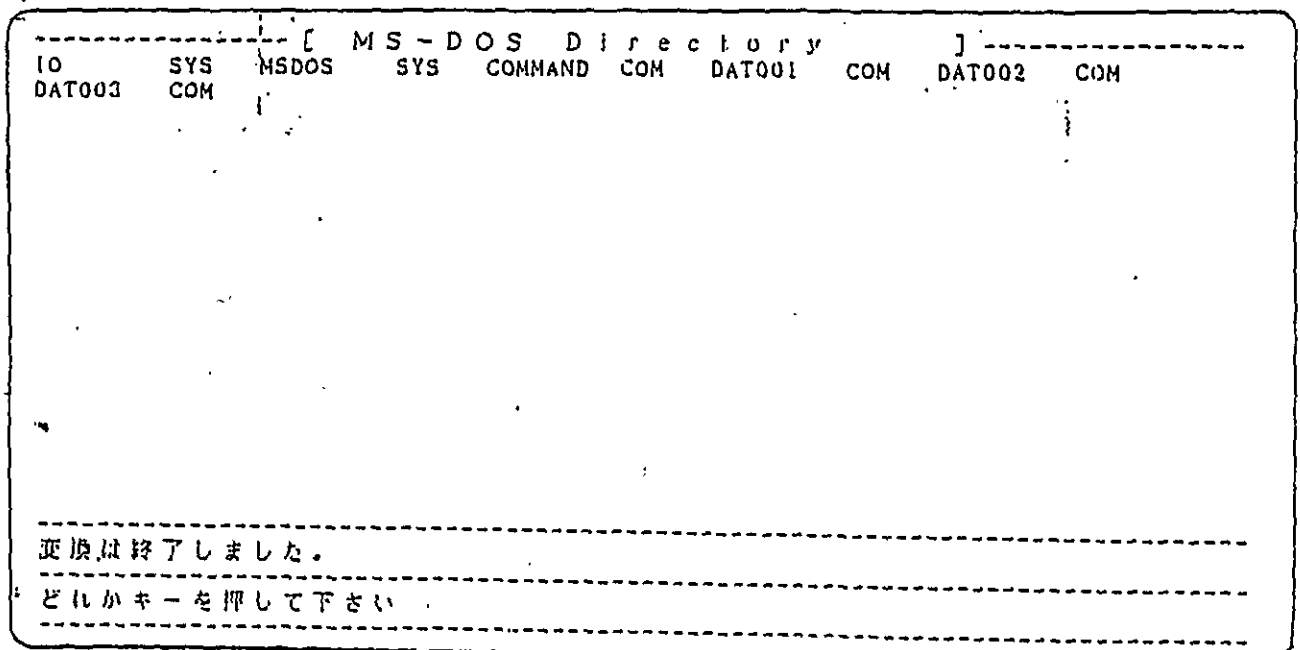


Fig. 3-38 Screen

- ⑬ Display and check the contents of a file which has been converted to 5 inch floppy disk on the screen in MS-DOS

- i) B > DIR R
- ii) B > TYPE DATA 001.COM R
- iii) COPY

```
B>^C
B>TYPE DAT001.COM
03.27
-09:00:00
000+000102
010+000327
011+000318
012+000344
013+000205
014+000328
015+000326
016+000311
017+000165
018+000141
019+000138
020*****
021*****
022*****
023*****
024*****
0^C
```

Fig. 3-39 Screen

- ⑭ Insert the 5 inch floppy disk which was converted to MS-DOS format by NEC PC301 Vm2 into the internal disk drive of NEC APC/IV, and check the contents of the data file.

- i) Activate MS-DOS in APC/IV

- ii) Insert the 5 inch data file floppy disk into disk drive B, key in the following command procedure and the contents of the file will be displayed for checking.

2]. Step 2

- 1) To transfer the data file on the 5 inch floppy disk into user's directory of the VAX-System and prepare the Measured Data Master File using APC/IV.

- ① Display virtual emulator on the screen VT 102

```
A > KERMIT
```

```
.KERMIT-MS > CONNECT
```

- ② Key in the following command to transfer data file into user's directory

```
KERMIT-MS > SEND A: FILENAME [VAXFILE NAME]
```

- 2) Display the transferred data on the terminal display VT 240 of the VAX-System for checking the contents of the data file.

```
$ ED DAT001.COM
```

DATA FILE NAME IN VAX

- 3) Data format of the data files which have been transferred to the user's directory in the VAX-System have to be converted by users and create or update the Auto-Measured Data Master File. For conversion and update, the program "S32 MS1.FOR." is used. This program shall be run after modification of the following command procedure "MONI1.COM" using edit function

- i) \$ ED MONI 1.COM R

- ii) Key in the following and run the program

- a) MONI 1.COM R

- iii) The contents of the Auto-Measured Data Master File (ADMST) which has been updated will be output as shown in Fig. 3 by Line Printer. And, hence, these contents should be checked.

- iv) Update the other three master files, namely, the Manually measured Data Master File, the Construction Data Master File and the Measuring Instruments Master File..

① How to create or to update the Manually-Measured Data Master File (MDMST)

At the merge application of the data file, the edit function of the terminal display VT240 is used in the VAX-System and the data file is created or updated. The data format of this file is the same as that of the Auto-measured Data Master File.

Data Records Type

Table 3-4

Variable	type	Content
MY	I2	time (year)
MM	I2	time (month)
MD	I2	time (day)
NT	I2	time (hour)
NM	I2	time (minute)
NS	I2	time (second)
MR	I3	the number of the record
SEQ	I3	the number of the channel
AS	S	symbol of
DIM (I, J)	I6	the value of measuring data

② Preparation of the Construction Data Master File (CKMST)

Process of creation or update of construction data master file is the same as that of the Manually-Measured Data Master File, whereas the data record format of this master file is as follows.

Data record type (free format)

Table 3-5

Variable	type	Content
MY (I)	I2	time (year)
MM (I)	I2	time (month)
MD (I)	I2	time (day)
SFJ	F12.3	the depth of the excavation at A point
SFE	F12.3	the depth of the excavation at B point
SEK	F12.3	the depth of the excavation at C point
SW	F12.3	the water level of testing canal
ST	F12.3	the ground water level
SF	I	DUMMY

③ Creation, or update of the Measuring Instruments Data Master File (SKMST)

Creation, or update of the Measuring Instruments Data Master File is the same as those of MDMST and CKMST mentioned above. The data record format of this master file is as follows

Data record type (free format)

Table 3-6

Variable	type	Content
KCH	I3	the number of the channel of the datalogger
KCD	I2	the code of the sensor
EHEM	F12.5	the coefficient of the calibration
ESYO	F12.5	the initialized value of the sensor
ESET	A16	the position of the installed sensor
EEL	F12.5	the elevation of the installed sensor
MY	I2	time (year)
MM	I2	time (month)
MD	I2	time (day)
KSIO	I	the working state of the sensor
		0 non-store the data
		1 store the data

Note: In the following table, the code numbers (KCD two-digit integer number) designate the type of measuring instruments.

Table 3-7 Sensor Coad Table

Coad	Sensor name
01	Inclinometer
02	Extensometer
03	Piezometer
04	Settlement Gauge
05	Survey pile
06 - 10	Dummy
11	Water level in Canal
12	Ground water level

3] Step 3 Output of monitor list for checking the measured data

Match two measured data master files (ADMST,MDMST) against the Measuring Instruments Data File (SKMST) in order to check the date, double data reading and lack of measured data using the program "S32MS2.FOR".

This program can be run by command procedure "MONI2.COM" as shown in Fig 3 - 39

```

-----
S!FOR/LIS/DEBUG/NOOP S32MS2
S!LINK/DEBUG S32MS2
S ASSIGN S32MS2.J.DAT FOR005
S ASSIGN S32MS2.J.DUT FOR005
-----
S! ASSIGN S32MS2.J.DAT FOR030
S ASSIGN SYS$COMMAND SYS$INPUT
S! ASSIGN SYS$COMMAND SYS$INPUT
S RUN S32MS2
S! PRINT S32MS2.J.CUT
-----

```

Fig. 3-39 Command Procedure

4) Step 4 Creation of the Work File for plotting graphs

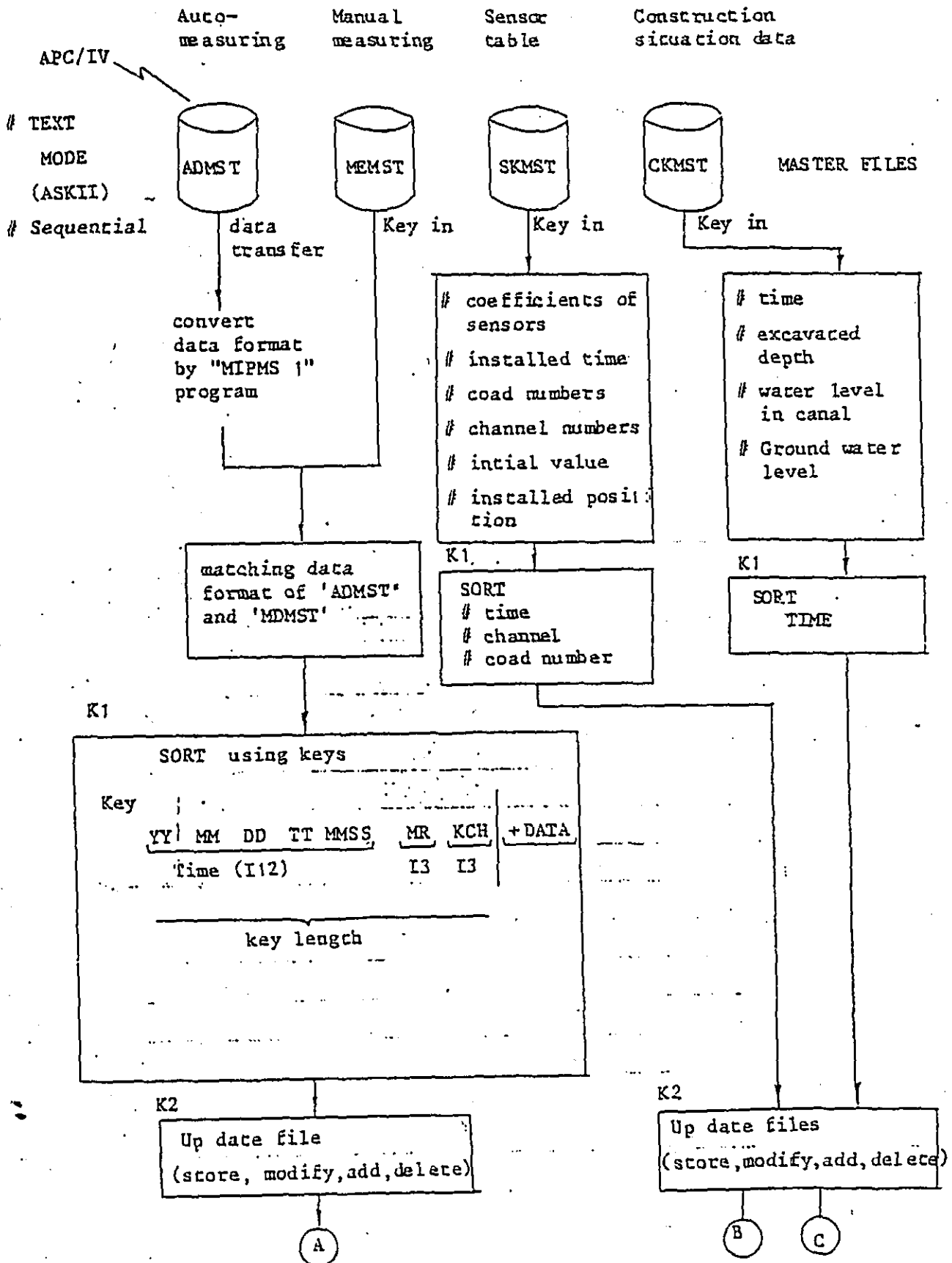


Fig. 3-40 Making the work file for drawing (1)

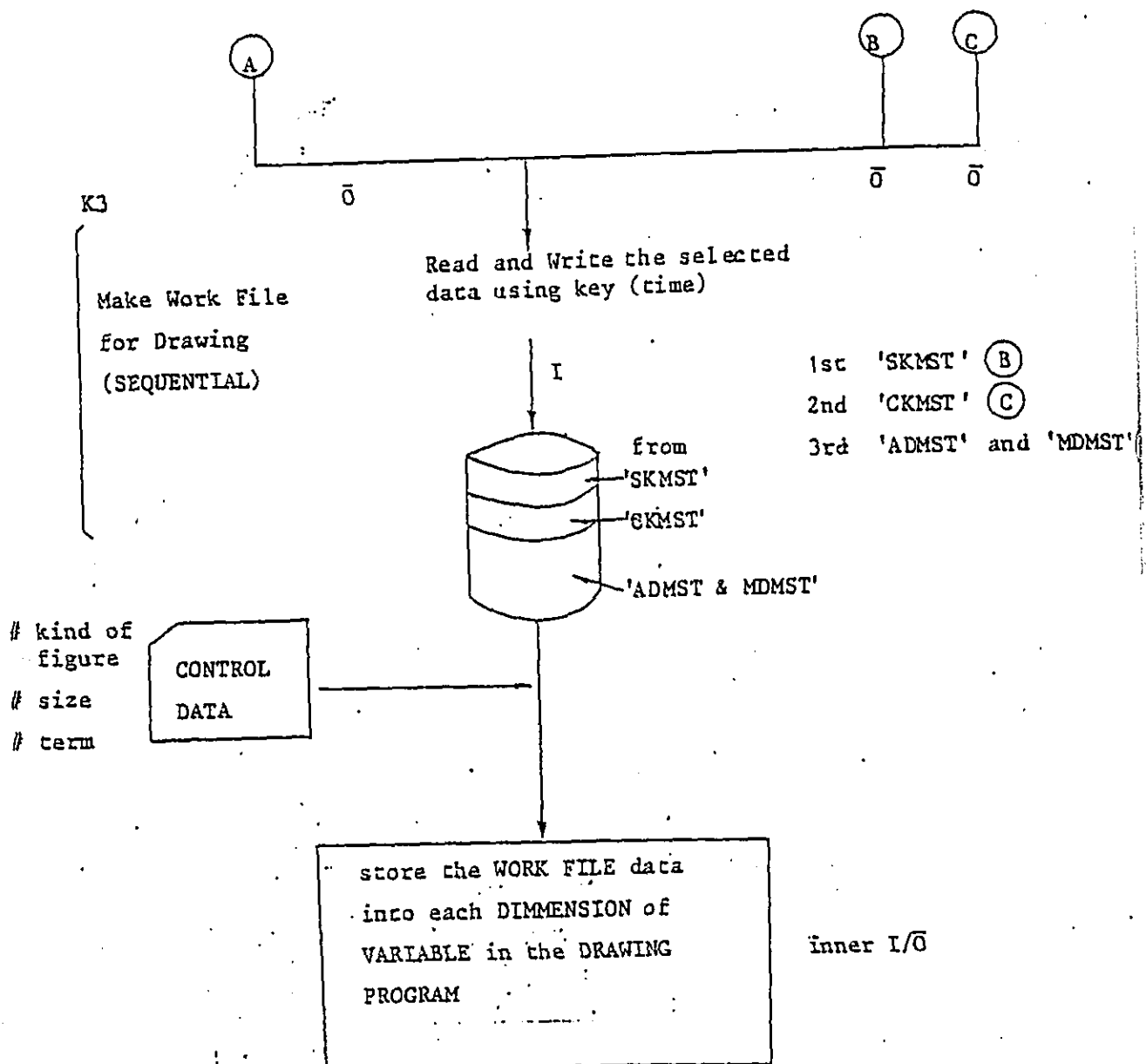


Fig.3-40 Making the work file for drawing (2)

Problems

- * 1 How to sort
- * 2 How to update
- * 3 How to make WORK FILE

- ① Combine four master files which have been prepared in step 2 into one Work File by SORT/MERGE application and plot graphs by this Work File.
- ② Output check list of the Work File for checking data.

5) Step 5 Execution of plotting graphs

At this step, several kinds of graphs are plotted using the graph plotting program \$82MS3.FOR. For this purpose, control data other than the Work File for plotting mentioned above is needed. The following Fig.3 - shows necessary data files for plotting graphs.

- ① The Work File for plotting graphs has already been prepared.
- ② To prepare control data records

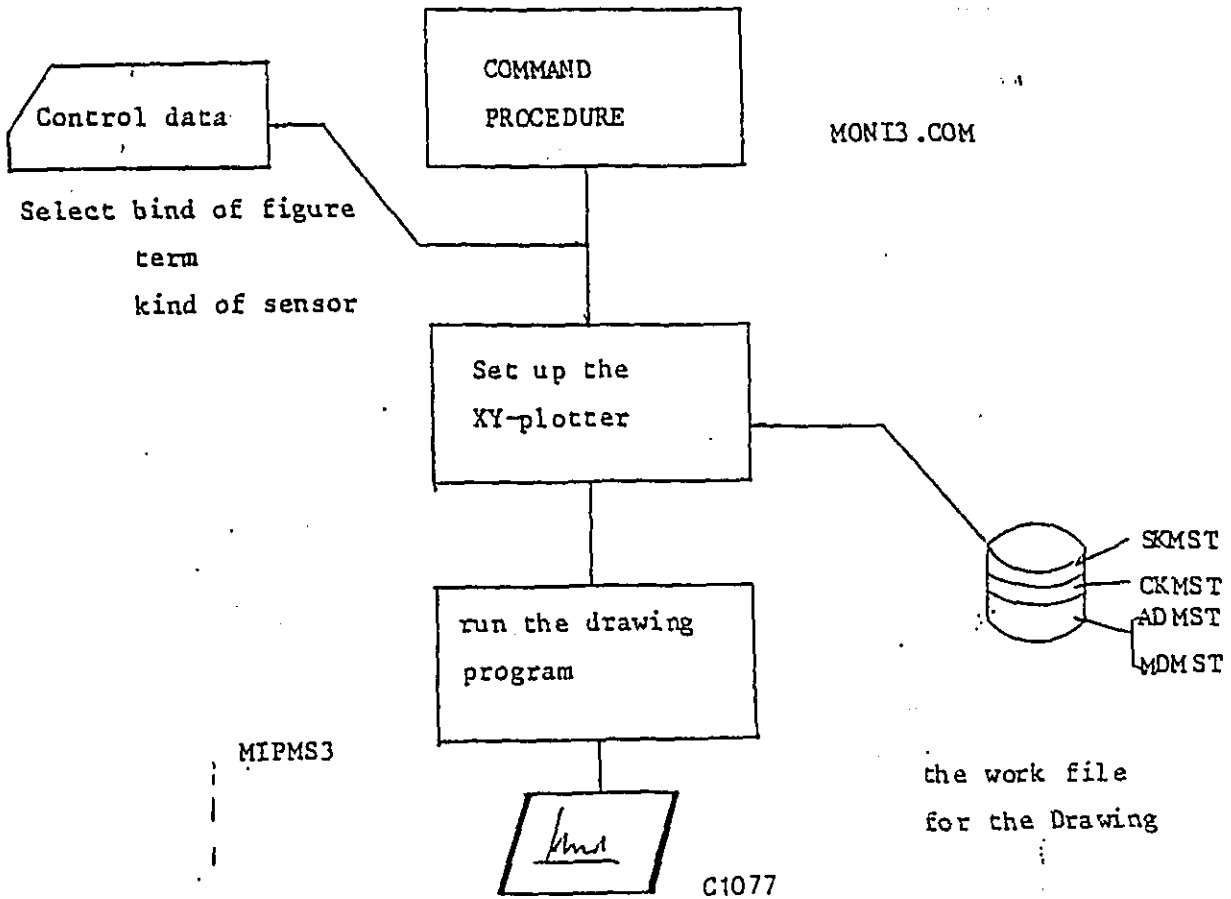


Fig.3-41 The Procedure of Drawing by MIPMS3

Control data records are composed of the following 5 types of data records, and they determine the type of graphs, the period over which data measurement is taken and the name of the sensors.

Control data records

- i) Parameter records for plotting designation
- ii) Title record (1)
- iii) Title record (2)
- iv) Sensors' name records
- v) Sensors designation records for plotting

i) Parameter record for plotting designation (Free format)

Table 3-8

Record name	Variables
Parameters for plotting designation	1. NFYY, 2. NFMM, 3. NFDD, 4. NTTY, 5. NTMM, 6. NTDD, 7. NELF, 8. NELT, 9. NYEAR, 10. NMONTH, 11. NEP, 12. WTH, 13. NTYPE1, 14. NTYPE2, 15. NTYPE3, 16. DEL, 17. NPROH, 18. NTH, 19. NTYPE4, 20. NTYPE5, 21. NTYPE6, 22. NTYPE7, 23. NTYPE8

Table 3-9

Column	Variables	Type	Contents
	1. NFYY	I2	Year of commencement of plotting graphs
	2. NFMM	*	Month of commencement of plotting graphs
	3. NFDD	*	Day of commencement of plotting graphs
	4. NTTY	*	Year of termination of plotting graphs
	5. NTMM	*	Month of termination of plotting graphs
	6. NTDD	*	Day of termination of plotting graphs
	7. NELF	*	The upper limit of evaluation to be considered when plotting graphs (+ or - figures are both acceptable)
	8. NELT	*	The lower limit of evaluation to be considered when plotting graphs (+ or - figures are both acceptable)
	9. NYEAR	*	Parameter for creation of yearly historical graph
	10. NMONTH	*	Parameter for creation of monthly historical graph
	11. NEP	*	Maximum value of strain ratio axis (unit : 10 ⁻⁴ /min)
	12. WTH	F2.1	Width of strain ratio bar graph (unit : mm)
	13. NTYPE1	I2	Parameter for plotting historical graph of strain ratios (Kurihara's method)
	14. NTYPE2	*	Parameter for historical graph of steady creep-strain ratios (Saito's method (1))
	15. NTYPE3	*	Parameter for historical graph of tertiary creep-strain ratios (Saito's method (2))
	16. DEL	F5.2	Dummy parameter
	17. NPROH	I2	The upper limit of the historical axis
	18. NTH	*	The lower limit of the historical axis
	19. NTYPE4	*	Parameter for plotting vertical distribution graph of horizontal displacement
	20. NTYPE5	*	Parameter for plotting vertical distribution graph of vertical displacement
	21. NTYPE6	*	Parameter for plotting horizontal displacement graph for the location of each inclinometer
	22. NTYPE7	*	Parameter for plotting vertical displacement graph for the location each settlement gauge
	23. NTYPE8	*	Parameter for plotting relative displacement graph

User should designate the value of parameters of 9. NYEAR, 10. NMONTH, 13. NTYPE1, 14. NTYPE2, 15. NTYPE3, 19. NTYPE4, 20. NTYPE5, 21. NTYPE6, 22. NTYPE7, 23. NTYPE8 as follows

In the case of not plotting graph : 0
 In the case of plotting graph : 1

ii) Title record (1) (Character type A20)
 Title written above the graph (the upper line)

iii) Title record (2) (Character type A20)
 Title written above the graph (the lower line)

iv) Sensors' name records (Character type 16 byte)
 Sensors' name should be input in order of sensors' code.
 User can arbitrarily change the code numbers, but should fix them during monitoring period.

Table 3-10

Record name	Variables
Sensors' name records	KEIDI (II), II = 1, 12

Table 3-11

Variable	Type	Contents
KEIKI (1)	A16	INCLINOMETER
" (2)	"	EXTENSOMETER
" (3)	"	PIEZOMETER
" (4)	"	SETTLEMENT GAUGE
" (5)	"	SURVEY FILE
" (6)	"	DUMMY
" (7)	"	DUMMY
" (8)	"	DUMMY
" (9)	"	DUMMY
" (10)	"	DUMMY
" (11)	"	WATER LEVEL
" (12)	"	GROUNDWATER LEVEL
ENCODE	A20	ENCODE '999 - 999'

Note: KEIKI (II), II = 1, 12 should have the name in accordance with the measuring instruments codes (KCD (I)) which have been determined at step 2.

Remark: At the end of these data, user has to add '999 - 999' as an endcode.

- v) Sensors designation records for plotting (character type 16 byte)
 User designate the installation number of the sensor. In the case of plotting several sensors' data simultaneously, the installation numbers of the necessary sensors should be input (the maximum number of input is 100)

Table 3-12

Record name	Items
Sensors designation records	AP (I), I = 1, N (N < 100)

Table 3-13

Variable	Type	Contents
AP (1)	A16	Installation number of sensor designated ex. NO 256+41
AP (2)	"	Installation number of sensor designated ex. NO 257+43
AP (N)	"	Installation number of sensor designated ex. NO 259+18
ENCODE	"	Endcode '999 - 999'

Remark: If some of the measuring instruments have not been installed, the user has to check whether the measuring instrument is the one whose data has been input or not and then the user can prepare the input data.

③ Preparation of command procedure

The control data records and the Work File for plotting graphs have already been prepared through the processes of 1 and 2 mentioned above. Then, the user has to prepare and modify the command procedure using edit function in order to run the plotting program S32MS3. FOR.

Command procedure " MON13. COM "

④ Setting X Y plotter

Initialize the X Y plotter (C 1077).

⑤ Execution of plotting graphs

After preparation from 1 to 4, user can run the plotting program S82MS3.
FOR using the command procedure " MON13.COM" Input command is as follows.
MON_13. COM (R)

The designated graph shall be output in X Y plotter through these processes.

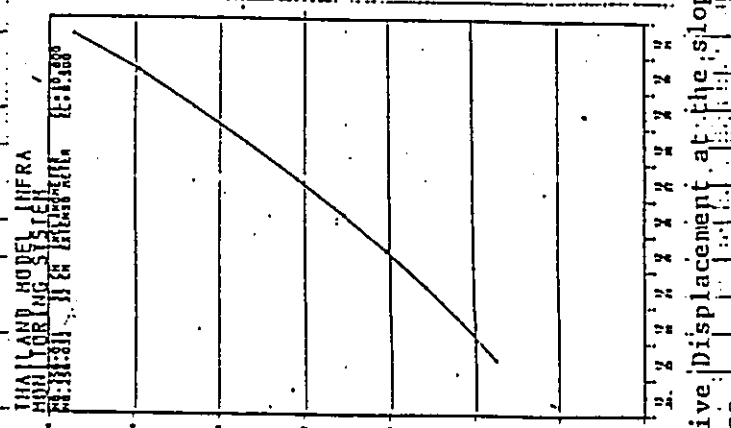
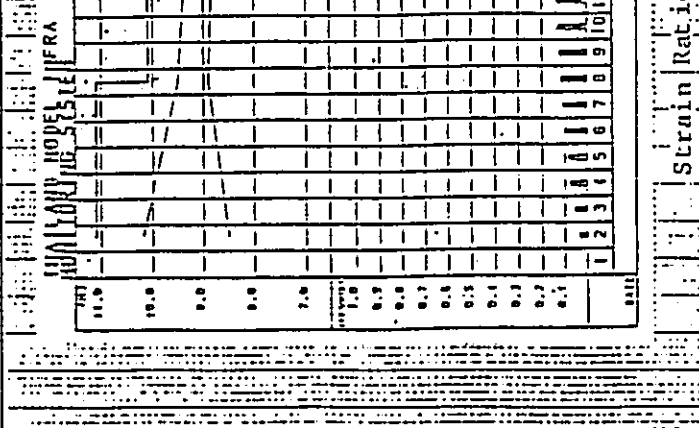
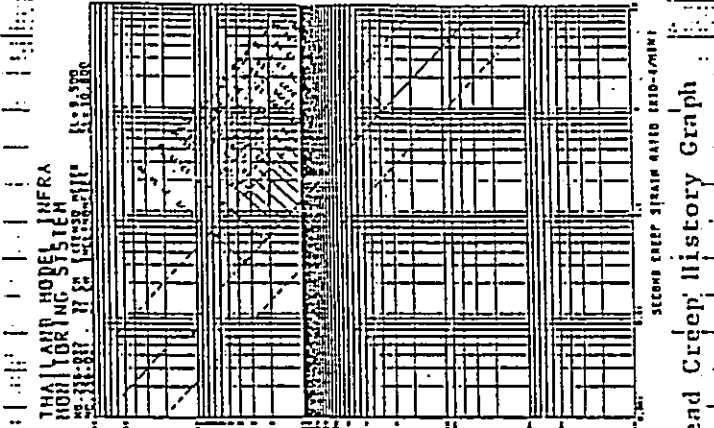
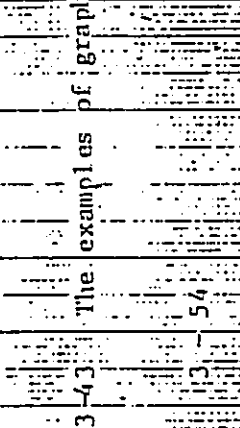
These are the procedure for plotting figures in the Monitoring System.
On the next page, examples of input control data record and data image of
Work Files for the plotting graphs Measured Data Master the Files, the
Measuring Instruments Master File and the Construction Data Master File
are shown for your reference. And, Fig 3-42~ 3-43 are examples of
plotting nine (9) kinds of graph output.

Figure Type	Arrangement Plotting Data Item	Plotting Format
1. Inclinator	Lateral flow	
2. Extensometer	Relative displacement	
3. Pore Pressure Gauge	Pore pressure	
4. Differential Settlement Gauge	Vertical Displacement	
5. Displacement Pile	Horizontal and Vertical Displacement	

Figure Type	Arrangement Plotting Data Item	Plotting Format
1. Lateral Flow at a cross section	Lateral Flow obtained from Inclinator	
2. Vertical Displacement at a cross section	Vertical Displacement obtained from Differential Settlement Gauge	

Figure Type	Arrangement Plotting Data Item	Plotting Format
3. Lateral Flow at each measuring point	Lateral flow obtained from Inclinator or Extensometer	
4. Vertical Displacement at each measuring point	Vertical Displacement obtained from Inclinator or Extensometer	

Fig 3-42 Five examples of graph output.

Figure Type	Arrangement Data Item	Plotting Format
5. Relative Displacement at the slope surface	Relative Displacement at the slope surface placement obtained from Extensometer	
1. Strain Ratio History Graph (Kurihara's Method)	Strain Ratio calculated data obtained from Extensometer.	
2. Steady Creep History Graph (Saito's Method)	Steady Creep History Graph	
3. The Third Creep History Graph (Saito's Method)	The Third Creep History Graph	

Prediction of Slope Failure

FIG. 3-43 The examples of graph output

4 F.E.M Analysis Method

4-1 Objectives and Analysis Method

(1) Objectives

The purposes of setting up the F.E.M Analysis System are as follows:

- 1) To predict stress, deformation and pore water pressure behaviour of Bangkok Clay in which the passage of time is taken into consideration, and to reflect the results of analysis in construction and design methods.
- 2) To apply the results of analysis to the other 2 systems
 - ① Regarding the installation plan of the measuring instruments, especially determination of the places where the measuring instruments will be installed, the results of analysis can give useful suggestions.
 - ② Slope failure control graphs and the distribution of zones which have had their strength decreased because of excavation work will be verified using the results of analysis.
- 3) To estimate the properties of Bangkok Clay from the data obtained from the Monitoring System, and to examine its deformation and failure mechanisms.

(2) Analysis method

In the case of a soft soil foundation like Bangkok Clay, in order to examine the excavated slope stability, it is necessary to consider several phenomena and factors as follows.

When the soft soil is excavated, the phenomena of rebounding and swelling occur due to removal of load. As a result, the strength of the foundation decreases around the excavated soil surface and pore water pressure increases with the passage of time and sometimes slope failure occurs in the end. These phenomena are well known.

For an understanding of these phenomena, elasto-viscoplastic properties of soil and time dependence such as creep are very important

factors. And it is necessary to apply Darcy's law of pore water flow.

In order to express the phenomena mentioned above, this F.E.M. Analysis System applies the Sekiguchi-Ohta elasto-viscoplastic model as a constitutive law of the relationship between stress and strain. And concerning pore water flow, this system adopts the concept of the Akai-Tamura multi-dimensional consolidation model.

Using the F.E.M. Analysis Program 'DACSAR' which takes these concepts into consideration, the excavated slope stability of Bangkok Clay can be examined.

For details of these models, please refer to Appendices 4-1 and 4-2.

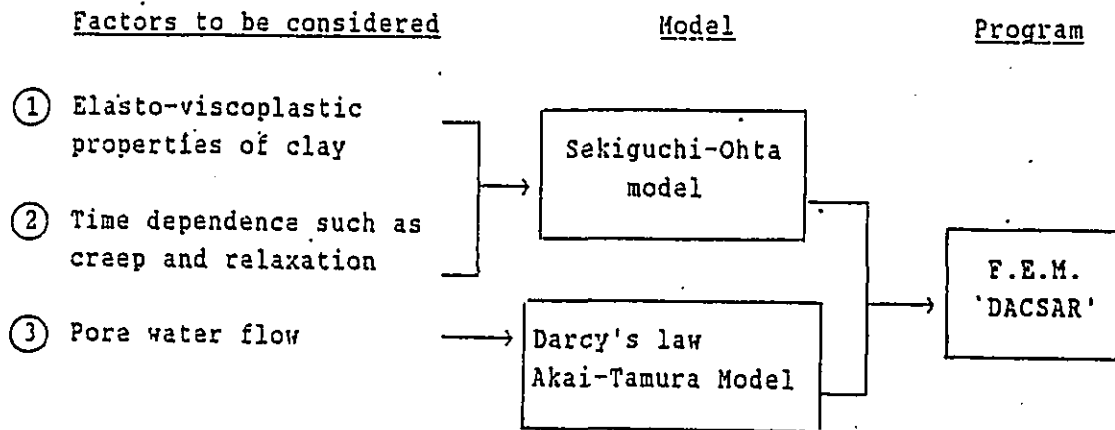


Fig. 4-1 Factors and Models necessary to analyze the behaviour of Bangkok Clay

4-2. Procedure of Analysis

Analysis procedure of the excavated slope behaviour on the soft soil foundation by the F.E.M. analysis program 'DACSAR' is as follows (refer to flowchart Fig. 4-2).

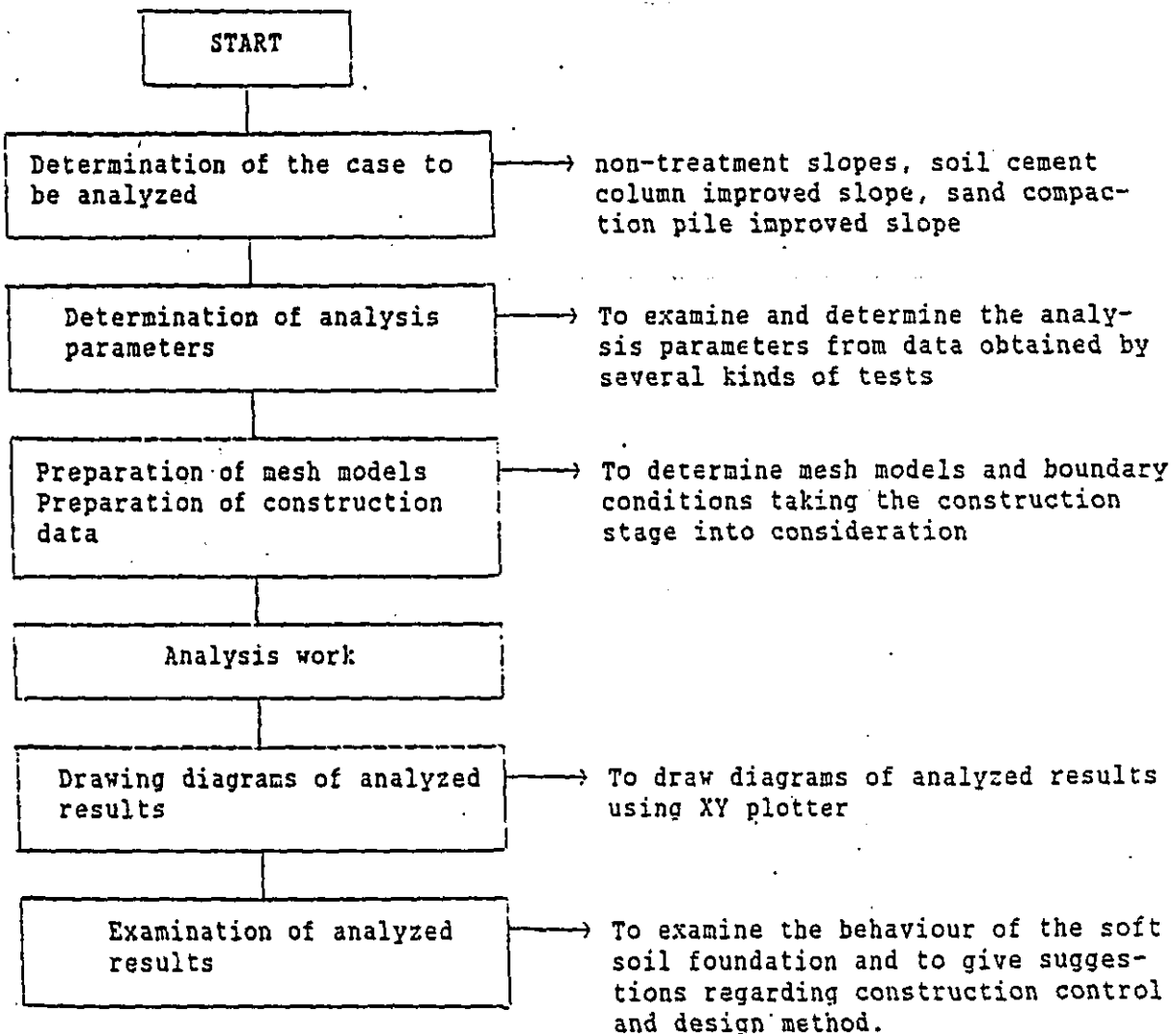


Fig. 4-2 F.E.M. analysis flow chart

Firstly, the cases to be analyzed should be determined as the non-treatment slopes, the soil cement column improved slope, and the sand compaction pile improved slope etc.

Secondly, mesh models of the excavated foundations and construction data at each construction stage should be prepared. Then, analysis work will be conducted after checking these analysis-parameters, mesh models and the construction stage data.

Finally, the results of the analysis should be drawn in several diagrams and examination of these results should be done.

Further details after the determination of the analysis parameters' stage are explained in the following sections 4-3.

4-3. Determination of Parameters for Analysis

The adequacy of the results obtained from F.E.M. analysis depends directly on the parameters which express material properties.

Consequently, it is necessary for analyzers to know the determination method of parameters for F.E.M. analysis.

In the case of soft clay, eleven (11) parameters are needed for analysis since elasto-viscoplastic properties should be considered, but in the case of sand compaction piles and soil cement columns, since the improved foundation can be considered to be elastic or elasto-plastic, we can apply ordinary analysis parameters. The following is how to determine the analysis parameters for soft clay.

In order to carry out F.E.M. analysis using the program 'DACSAR', we have to determine 11 parameters as shown in Table 4-1. There are two ways to determine the parameters. One way is determining them directly from the results of laboratory tests and the other way is estimating them indirectly using parameters obtained from the easy tests such as tests for physical properties and consolidation tests (hereinafter for the former referred to as "The Direct Method" and for the latter referred to as "The Indirect Method").

Before determination of analysis parameters, it is necessary to grasp the soft soil conditions in both plane section and vertically by in situ tests such as Standard Penetration Test, Dutch Cone Test or Boring. Zoning for analysis model should be conducted based on the investigated results and analysis parameters should be determined in every zone on every layer.

Fig. 4-3 is a flowchart which shows how to determine the analysis parameters. The followings are the explanation of determination of analysis parameters in accordance with this flowchart.

Table 4 - 1 Parameters for Analysis and its Test Method

	Parameters for Analysis	Laboratory Test	Remarks
Mechanical Properties:	D : Coefficient of dilatancy	Drained triaxial compression test #1 (CD)	$D = \frac{\lambda - K}{M(1 + e_0)}$ 1)
	Λ : Irreversibility ratio	Standard consolidation test	$\Lambda = 1 - K/\lambda$ or $M/1.75$
	M : Critical state parameter	Ko- triaxial compression test	$M = \frac{6 \sin \phi'}{3 - \sin \phi'}$
	v' : Effective Poisson ratio	- ditto -	
	α : Coefficient of secondary consolidation	Standard consolidation test	$\alpha = dv/d(\ln t)$
	v_0 = Initial volumetric strain rate	- ditto -	$v_0 = \alpha/t_c$ 2)
Pre-load	σ_{v0} : Pre-consolidation vertical pressure	Standard consolidation test	
	κ_0 : Coefficient of earth pressure at rest	Ko- triaxial compression test #2	
Initial Stress	σ'_{vi} : Effective overburden pressure	Consolidation test	$\sigma'_{vi} = \sigma$ sub Z
	κ_i : Coefficient of in-situ earth pressure at rest	Triaxial Ko-swelling test	
	K : Coefficient of permeability	Standard consolidation test	$K = \gamma W_m v C_v$

Parameter of stress	$n^* = \sqrt{\frac{3}{2} \cdot (n_{ij} - n_{ijo})(n_{ij} - n_{ijo})}$ $n_{ij} = \frac{S_{ij}}{P}, S_{ij} = \sigma'_{ij} - p \sigma'_{ij}$ $p^i = \frac{1}{3} \sigma'_{ij}$
---------------------	--

- Where 1) $\lambda = 0.434 C_c$, $K = 0.434 C_s$ (in the case of natural logarithm)
 2) t_c : When primary consolidation completed
 3) σ' : Weight of soil in water
 4) σ'_{ij} : Effective stress tensor

*1 In this project undrained triaxial compression test is not performed, therefore, D is obtained from calculation.

*2 The value of κ_0 is obtained by Alpan's method (1967).

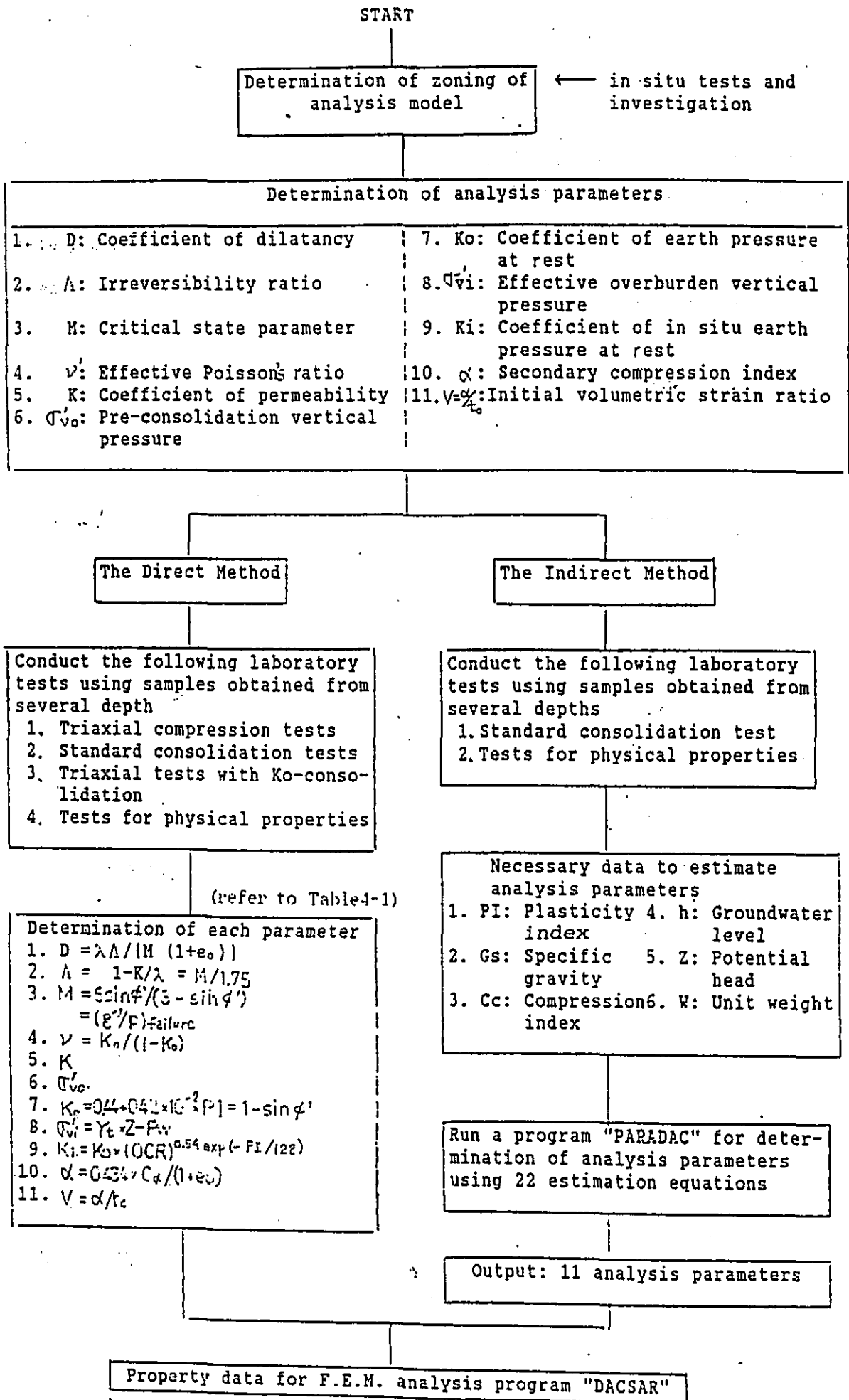


Fig. 4-3 Flowchart for determination of analysis parameters

(1) The Direct Method

As shown in Table 4-1, eleven (11) parameters for the F.E.M. analysis can be obtained from the several kinds of tests.

The following are the methods to obtain those parameters directly using the results of the tests in order of data input in the "DACSAR" program.

1) D: Coefficient of dilatancy

Coefficient of dilatancy is expressed by the following equation (4.1). Before calculation of the coefficient of dilatancy (D), it is necessary to obtain the compression index (Cc), void ratio at preconsolidation pressure (e_c) and irreversible ratio (Λ) from standard consolidation tests. It is also necessary to calculate critical state parameter (M). This parameter M can be calculated from the effective angle of friction (θ') obtained from Ko-note triaxial compression tests or triaxial compression tests, or the value of (q / P') at the time of failure can directly be used in deviatric stress-effective principal stress relations (q-P' plane).

$$D = \lambda \cdot \Lambda / [M (1 + e_0)] \dots\dots\dots (4.1)$$

$$\text{where, } \lambda = 0.343 Cc \dots\dots\dots (4.2)$$

e₀ = void ratio at σ_{v0}

$$M = 6 \sin \theta' / (3 - \sin \theta') \dots\dots\dots (4.3)$$

$$= (q' / P') \text{ at failure} \dots\dots\dots (4.3')$$

$$\Lambda = 1 - K / \lambda \dots\dots\dots (4.4)$$

$$K = 0.434 Cc$$

$$\lambda = 0.434 Cc$$

$$= M / 1.75 \dots\dots\dots (4.5)$$

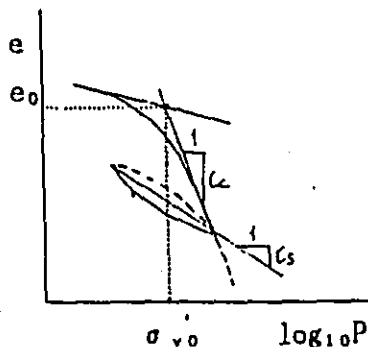


Fig. 4-4 a) e-log P relations from standard consolidation test

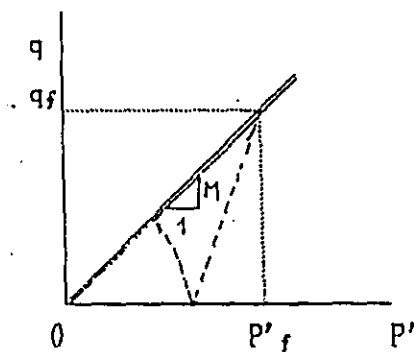


Fig. 4-4 b) Deviatric stress-effective principal stress relations

2) Λ : Irreversible ratio

Irreversible ratio (Λ) can be calculated by equation (4.4) or (4.5) mentioned above in 1).

3) M: Critical state parameter

Critical state parameter (M) can be calculated by equation (4.3) or (4.3') mentioned in 1).

4) ν' : Effective Poisson ratio

Effective Poisson ratio can be obtained from the following equation using coefficient of earth pressure at rest (K_0) .

$$\nu' = \frac{K_0}{1+K_0} \dots\dots\dots (4.6)$$

Coefficient of earth pressure at rest can be obtained from K_0 -note triaxial compression tests or the following estimation equations.
(refer to Appendix 4-3)

$$K_0 = 0.19 + 0.233 \log I_n \dots\dots\dots (4.7)$$

(by Alpan (1967))

$$K_0 = 1 - \sin \phi' \dots\dots\dots (4.8)$$

(by Jaky (1944))

where, PI : Plastic index

ϕ' : effective angle of friction

5) K: Coefficient of permeability

Coefficient of permeability (k) can be obtained from standard consolidation tests using the following equation.

$$k = m_v C_v \gamma_w \dots\dots\dots (4.9)$$

where, m_v : Coefficient of volume compressibility

C_v : Coefficient of consolidation

γ_w : Unit weight of water

Coefficient of permeability can also be obtained directly from permeability test. If there is anisotropy in permeability between horizontal and vertical directions each coefficient (K_x, K_y) can be input.

6) σ'_{vo} : Preconsolidation pressure

Preconsolidation pressure can be obtained from standard consolidation test as shown in Fig. 4-4 (a).

7) K_o : Coefficient of earth pressure at rest

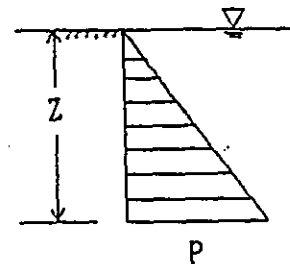
Coefficient of earth pressure at rest (K_o) can be obtained as mentioned in 4).

8) σ'_{vi} : Effective overburden pressure

Effective overburden pressure (σ'_{vi}) can be calculated by the following equation.

$$\sigma'_{vi} = \gamma t \cdot Z - P \dots\dots\dots (4.10)$$

where, t : unit weight of soil
 Z : depth
 P : pore water pressure



$$\sigma'_{vi} = \gamma \cdot Z - P$$

Fig.4- 5

9) K_i : In situ coefficient earth pressure at rest

Several estimation equations are suggested for in situ coefficient earth pressure at rest (K_i). As a result of examination of their applicability, Alpan's equation mentioned below is considered to be the most appropriate, so that this equation is adopted.

$$K_i = K_o (OCR)^{0.54} \exp (-PI/122) \dots\dots\dots (4.11)$$

where, K_o : Coefficient of earth pressure at rest
 OCR : Overconsolidation ratio = $\sigma'_{vi} / \sigma'_{vo}$
 PI : Plasticity index

10) α : Secondary consolidation index

Secondary consolidation index (α) can be calculated by the following equation from consolidation theory.

$$\alpha = \frac{0.434}{H e_c} \cdot C_\alpha = \frac{0.434}{1 + e_c} \frac{-de}{d(\log t)} \dots\dots\dots (4.12)$$

where, C_{α} : Secondary compression rate
 $\frac{-de}{d(\log t)}$, Slope of straight line in secondary consolidation
in relationship curve between time and void ratio

There are two (2) methods to determine secondary consolidation ratios. One is the means of obtaining the slope of a straight line in secondary consolidation tests. The other is the means, in the case that the secondary consolidation stage is not tested, to determine C_{α} by reading it on a relationship diagram between secondary consolidation ratio and natural moisture content (w_n) as shown in Fig. 4-6.

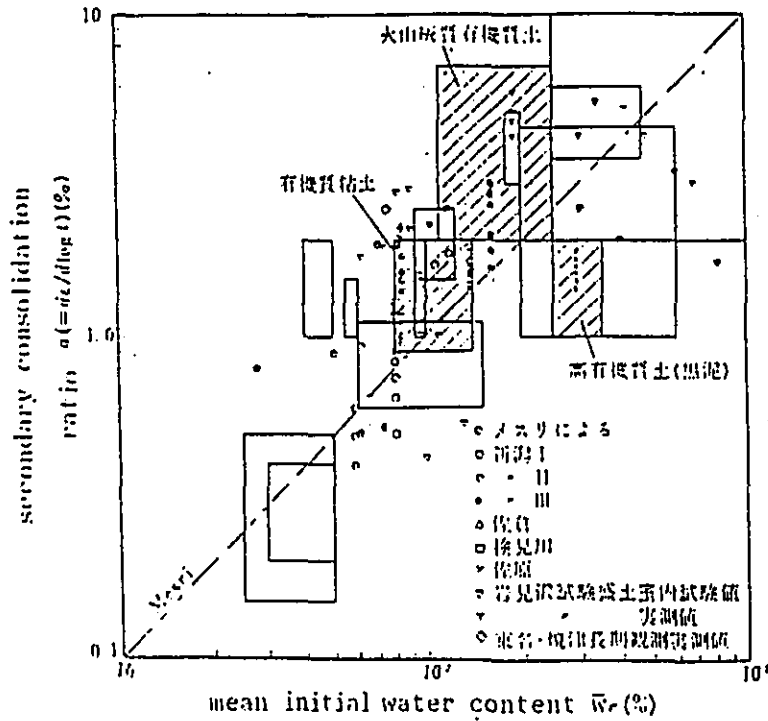


Fig. 4-6 Relationship between secondary consolidation ratio and natural moisture content (by Dr. Mesri)

11) v : Initial volumetric strain ratio

Initial volumetric strain ratio (v) can be obtained by the following equation.

$$v = \delta / t_c \approx \delta / t_{90} \dots\dots\dots (4.13)$$

(by Sekiguchi, 1977)

where, t_c : Time of completion of primary consolidation

It is possible to substitute this t_c for t_{90} which is the time of 90% degree of consolidation, consequently t_{90} is adopted as follows

$$t_c \approx t_{90} = H^2 T_v \text{ (at } U = 90\%) / C_v \dots\dots\dots (4.14)$$

The eleven (11) analysis parameters can be obtained for the F.E.M. analysis program 'DACSAR' by the foregoing methods based on several tests. Table 4-2 shows the list of parameters for F.E.M. analysis at the detailed design stage.

(2) Indirect Method

In the Direct Method mentioned above, it is necessary to carry out triaxial compression tests, Ko-note triaxial consolidation tests, standard consolidation tests and tests for physical properties in order to obtain the eleven (11) parameters for analysis. In the case of analysis for important structures, it is desirable to obtain the parameters by the Direct Method. But, in the case that the tests are insufficient or that you only need the tendency of soil foundation behaviour, it is possible to determine the parameters by the Indirect Method more easily than by the Direct Method.

The Indirect Method is the method to calculate the eleven (11) parameters for analysis using several estimation equations. This method was proposed by Dr. Iizuka and Dr. Ohta in 1986.

Using this concept, a parameter determination program named 'PAPADAC' has been developed and introduced coupled with the F.E.M. analysis program 'DACSAR' in the VAX System.

In several estimation equations in the program 'PAPADAC', each coefficient was obtained from the clay properties in various parts by means of statistical treatment. Consequently, it is necessary to consider whether these coefficients are appropriate to Bangkok Clay or not. It will be necessary to modify these coefficient to adjust to Bangkok Clay's properties. For this reason it is desirable to collect existing data from various tests about Bangkok Clay and to analyze these data statistically in way similar to that of Dr. Iizuka et al.

The following are the parameter determination methods for analysis by Dr. Iizuka et al.

1) Parameter determination method for analysis

Dr. Iizuka et al. considered the plasticity index (PI) to be a very important factor which influences clay properties and proposed a flowchart for parameter determination for analysis as shown in Fig. 4-7.

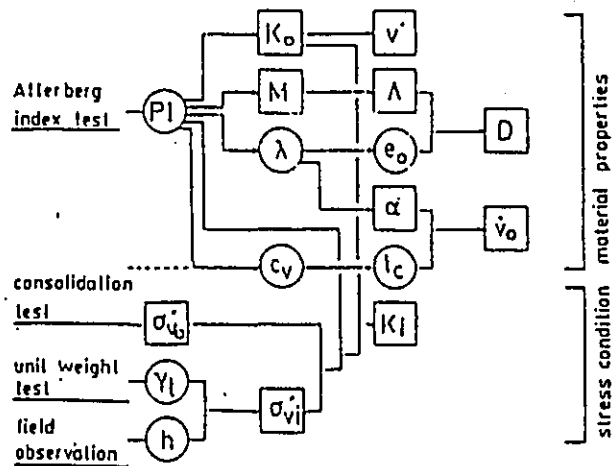


Fig.4-7. Determination procedure of input parameters from plasticity index

As in Fig. 4-7, in order to determine parameters for analysis, several tests and observations are necessary, that is, Atterberg limit tests and unit weight tests as tests for physical properties, consolidation tests as tests for mechanical properties and observation of groundwater by open piezometers as field observation. All of these tests and observation are easy to carry out.

The bases of Fig. 4-7 are correlations between the plasticity index (PI) and each parameter of properties and correlations between several parameters except the plasticity index (PI) of various clays. Fig.5. 4-8 ~ 4-2 are the diagrams when the correlations were analyzed statistically.

Based on these Figs. twenty two (22) correlation functions were proposed as in Fig. 4-2 . Fig. 4-2 shows the flowchart of determination procedure for parameters in Fig. 4-7 and various correlation functions at the same time, and the program 'PAPADAC' was developed using these correlations.

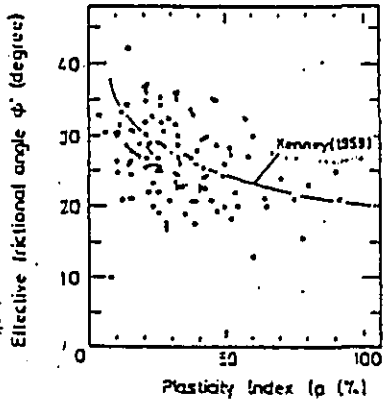


Fig.4-8 Relationship between PI and ϕ'

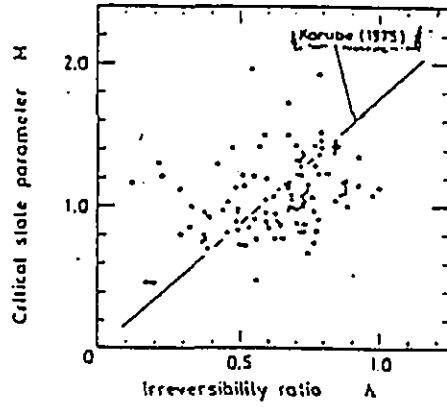


Fig.4-9 Relationship between λ and M

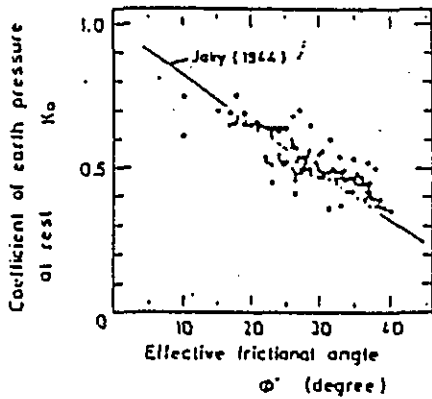


Fig.4-10 Relationship between ϕ' and K_0

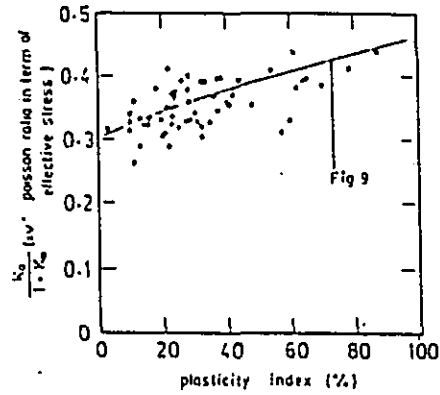


Fig.4-11 Relationship between effective Poisson's ratio and plasticity index

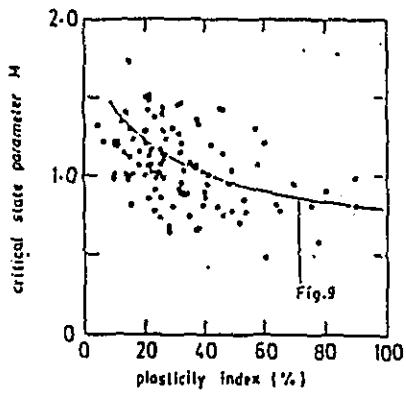


Fig. 4-12 Relationship between critical state parameter and plasticity index

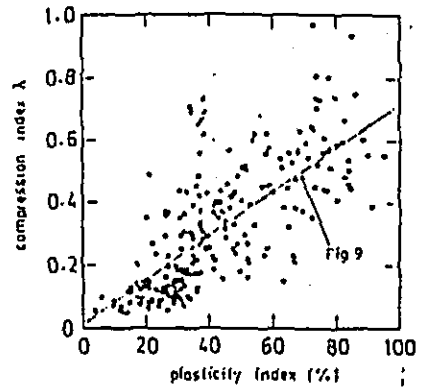


Fig. 4-13 Relationship between compression index and plasticity index

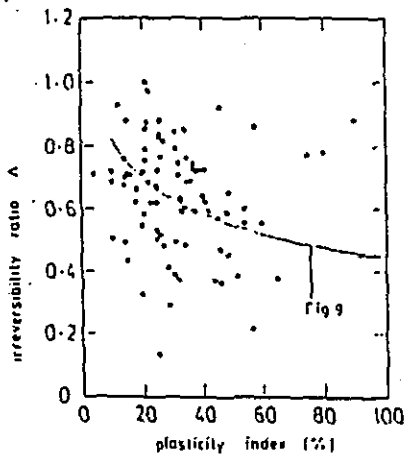


Fig. 4-14 Relationship between irreversibility ratio and plasticity index

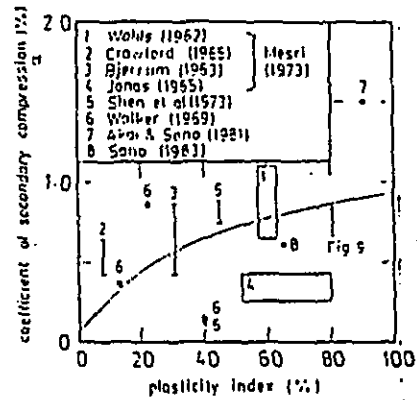


Fig. 4-15 Relationship between coefficient of secondary compression and plasticity index

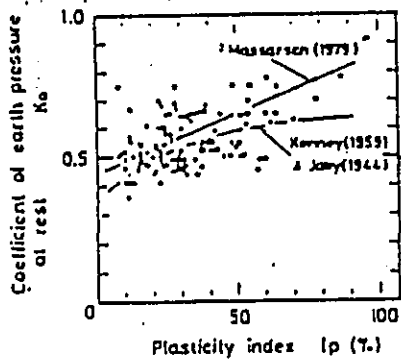


Fig.4-16 Relationship between coefficient of earth pressure and plasticity index

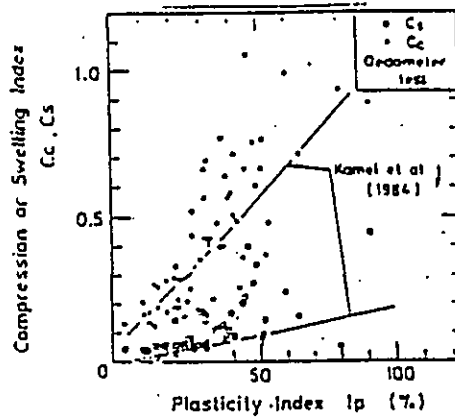


Fig.4-17 Relationship between compression or swelling index and plasticity index

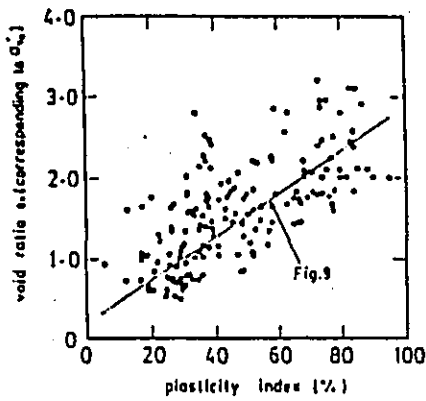


Fig.4-18 Relationship between void ratio at preconsolidation state and plasticity index

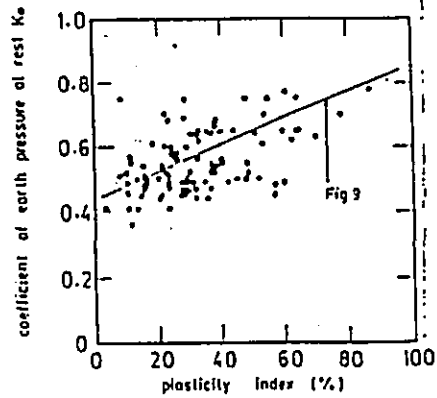


Fig. 4-19 Relationship between coefficient of earth pressure at rest (K_0) and plasticity index

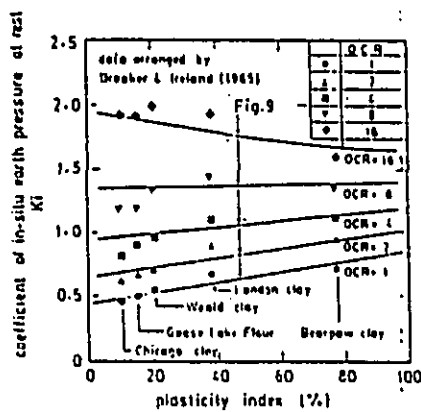


Fig.4-20 Relationship between coefficient of in situ earth pressure at rest (K_1) and plasticity index (data by Brooker and Ireland, 1965)

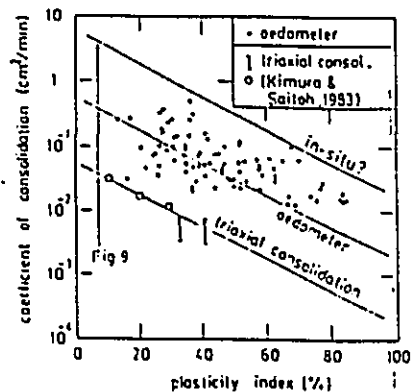
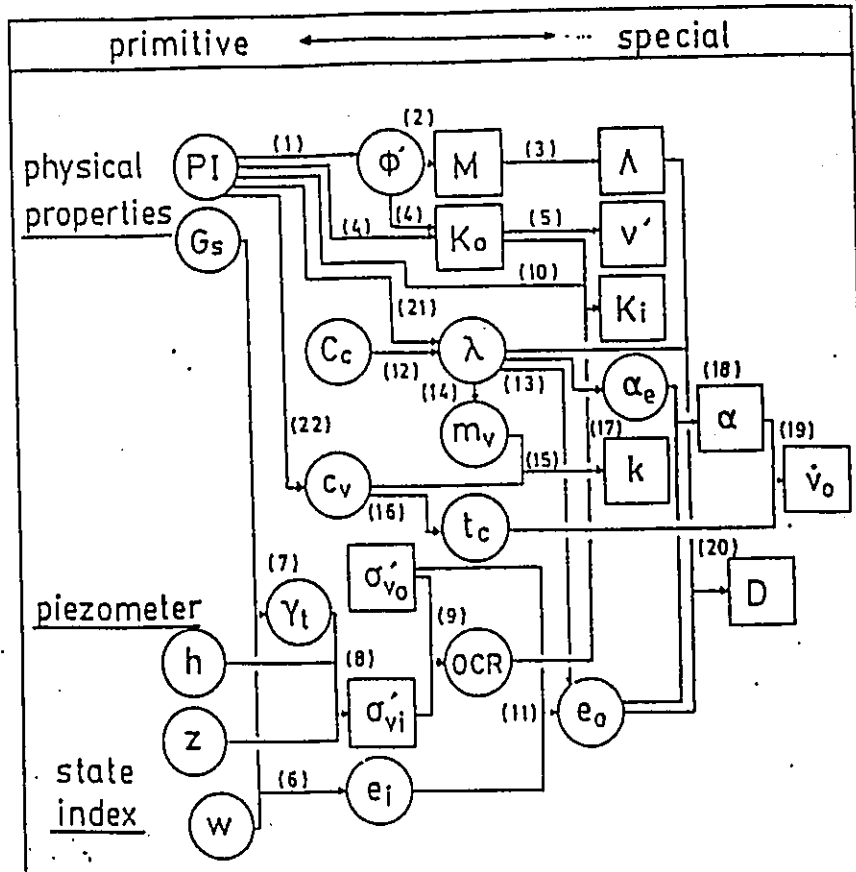


Fig.4-21 Relationship between coefficient of consolidation and plasticity index



- | | | | |
|---|--|--|--------------------------|
| (1) $\sin\phi = 0.81 - 0.233 \log PI$ | Kenney (1959) | (12) $\lambda = 0.434 C_c$ | |
| (2) $M = 6s(\ln\phi' / (3 - \sin\phi'))$ | | (13) $e_o = 3.78\lambda \cdot 0.156$ | |
| (3) $\Lambda = M / 1.75$ | Karube (1975) | (14) $m_v = 3\lambda / [(1 - e_o)(1 - 2K_o)\sigma'_{v_o}]$ | |
| (4) $K_o = 0.44 \cdot 0.42 \cdot 10^2 PI$ | Massarsch (1979) | (15) $k = m_v c_v \gamma_w$ | |
| $K_o = 1 - \sin\phi'$ | Jáky (1944) | (16) $t_c \doteq t_{90} = H^2 T_v (U = 90\%) / c_v$ | |
| (5) $v' = K_o / (1 - K_o)$ | | (17) $\alpha_e / \lambda = 0.05 \pm 0.02$ (clay) | Mesri & Godlewski (1977) |
| (6) $e_i = w G_s$ | | $= 0.07 \pm 0.02$ (peat) | |
| (7) $\gamma_t = G_s \gamma_w (1 + w) / (1 + G_s w)$ | | (18) $\alpha = \alpha_e / (1 - e_o)$ | Sekiguchi (1977) |
| (8) $\sigma'_{vi} = \gamma_t z - p_w$ | | (19) $\dot{v}_o = \alpha / t_c$ | Sekiguchi (1977) |
| (9) $OCR = \sigma'_{v_o} / \sigma'_{vi}$ | | (20) $D = \lambda \Lambda / [M(1 - e_o)]$ | Ohla (1971) |
| (10) $K_i = K_o (OCR)^{0.54 \exp(-PI/122)}$ | Alpan (1967) | (21) $\lambda = 0.015 \cdot 0.007 PI$ | |
| (11) $e_o = e_i - \lambda(1 - \Lambda) \ln(OCR)$ | $\overline{OCR} = \frac{1 - 2K_o}{1.2K_i} OCR$ | (22) $\log c_v (cm^2/min) = -0.025 PI - 0.25 \pm 1$ | |

Fig.4-22 Proposed determination procedure for input parameters

2) Execution of the parameter determination program 'PARADAC' for analysis

The following are examples of input and output data regarding the execution of the parameter determination program 'PARADAC' for analysis.

① Example of input data

a) control data records (Free format)

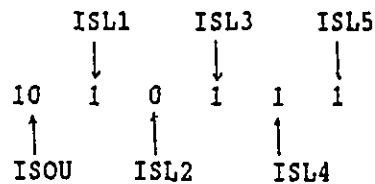


Table 4-3

Variables	Type	Contents
ISOU	Integer	The number of layers
ISL1	-ditto-	Selection flag $\left\{ \begin{array}{l} 0: K_a = 0.44 + (0.42/100 * PI) \\ 1: K_a = 1 - \sin \phi \end{array} \right.$
ISL2	-ditto-	-ditto- $\left\{ \begin{array}{l} 0: e_a = 3.78 + 0.156 \\ 1: e_a = e^{-\lambda(1-\lambda) \ln(\overline{OCR})} \end{array} \right.$
ISL3	-ditto-	-ditto- $\left\{ \begin{array}{l} 0: \phi_a = 0.05 + 0.02 \\ 1: \phi_a = 0.05 - 0.02 \end{array} \right.$ } (clay)
ISL4	-ditto-	-ditto- $\left\{ \begin{array}{l} 0: \phi_a = 0.05 + 0.02 \\ 1: \phi_a = 0.05 - 0.02 \end{array} \right.$
ISL5	-ditto-	-ditto- $\left\{ \begin{array}{l} 0: \phi_a = 0.07 + 0.02 \\ 1: \phi_a = 0.07 - 0.02 \end{array} \right.$ } (peat)

Notes: User should select the flags ISL1~ISL5 by judging which is appropriate for the clay being analyzed.

b) Material parameter records (free format)

User should input material parameter records the same number of times as the number of ISOU (the number of layers)

① 57.0, 0.0128736, 1.0, 2.5, 0.5, 0.5, 0.010, 1.47, 0.35

PI
CV
EI
SVO
Z
PW
T90
GT
AKIX

- ② 57.0, 0.0101088, 1.0, 2.8, 2.0, 2.0, 0.012, 1.47, 0.35
- ③ 57.0, 0.007344, 1.0, 4.0, 4.0, 4.0, 0.017, 1.47, 0.35
- ④ 60.0, 0.0048384, 1.0, 4.5, 6.0, 6.0, 0.025, 1.44, 0.35
- ⑤ 60.0, 0.009936, 1.0, 7.0, 8.0, 8.0, 0.013, 1.4, 0.34
- ⑥ 71.4, 0.0120096, 1.0, 7.2, 10.0, 10.0, 0.010, 1.41, 0.34
- ⑦ 71.4, 0.00864, 1.0, 9.0, 12.0, 12.0, 0.010, 1.43, 0.34
- ⑧ 71.4, 0.0201312, 1.0, 14.0, 14.0, 14.0, 0.003, 1.54, 0.34
- ⑨ 22.0, 0.02376, 1.0, 16.16, 16.0, 16.0, 0.001, 1.54, 0.34
- ⑩ 20.0, 0.0250214, 1.0, 45.3, 23.5, 23.5, 0.001, 1.54, 0.34

Table.4-4

variable	type	contents
PI	Real	Plasticity index
CV	Real	compression index
EI	Real	initial void ratio e_i
SVO	Real	preconsolidation overburden stress σ_{vo}
Z	Real	depth
PW	Real	pore water pressure
T90	Real	consolidation time
GT	Real	unit weight γ_c
AKIX	Real	$0.54 \exp(-PI/122)^{11}$

Note : 1) AKIX is the value of the exponent in Alpan's equation
 $K_i = K_o (OCR)^{0.34} \exp(-PI/122)$

2. Example of output

Executing the program 'PARADAC' by inputting the above data ①, the following output can be obtained.

Table 4-5 Example of output

===== MATERIAL PARAMETER =====											
	DIR	RAM	HMM	MIV	PK (M/DAY)	SVD (TF/MEEZ)	KD	SVI (TF/MEEZ)	KI	ALF	V0
SCUN: 1	0.147	0.529	0.925	0.375	0.1000-02	2.500	0.599	0.275	1.113	0.013	0.1270-01
SCUN: 2	0.125	0.529	0.925	0.375	0.1110-02	2.200	0.599	0.940	0.957	0.011	0.9360-01
SCUN: 3	0.124	0.529	0.925	0.375	0.5450-03	4.000	0.599	1.290	0.919	0.011	0.8400-01
SCUN: 4	0.129	0.521	0.912	0.377	0.3210-03	4.500	0.604	2.240	0.901	0.011	0.6400-01
SCUN: 5	0.132	0.521	0.912	0.377	0.4440-03	7.000	0.604	3.200	0.925	0.012	0.9250-01
SCUN: 6	0.154	0.494	0.965	0.393	0.6000-03	7.200	0.622	4.100	0.915	0.013	0.1340-01
SCUN: 7	0.154	0.494	0.965	0.393	0.3450-03	7.000	0.622	5.160	0.915	0.013	0.1340-01
SCUN: 8	0.155	0.494	0.965	0.393	0.5200-03	14.000	0.622	7.550	0.924	0.014	0.4510-01
SCUN: 9	0.349	0.621	1.192	0.335	0.1820-02	15.100	0.503	2.640	0.907	0.004	0.4270-01
SCUN: 10	0.045	0.677	1.220	0.330	0.5610-04	45.300	0.493	12.690	0.882	0.004	0.3050-01

These are all to explain parameter determination for analysis by the Direct Method and the Indirect Method. Whichever method is used for the determination of parameters, it is necessary to examine these values carefully.

Regarding the input formats of analysis parameters in the F.E.M. analysis program 'DACSAR', please refer to '4-6, Operation Manual of F.E.M. Analysis System'.

4-4 Procedure for Analysis Model Preparation

This section explains how to prepare an analysis model and how to prepare boundary condition data and construction state data in accordance with the flowchart illustrated below.

(1) Mesh models for analysis

Firstly, the general composition of the soft soil should be grasped by in-situ tests etc. and should be classified into several layers. At the testing site, according to Dutch cone penetration tests, soft clay are heaped to a depth of 17 meters and there is a stiff clay layer below this. Consequently, the layers can be divided into two.

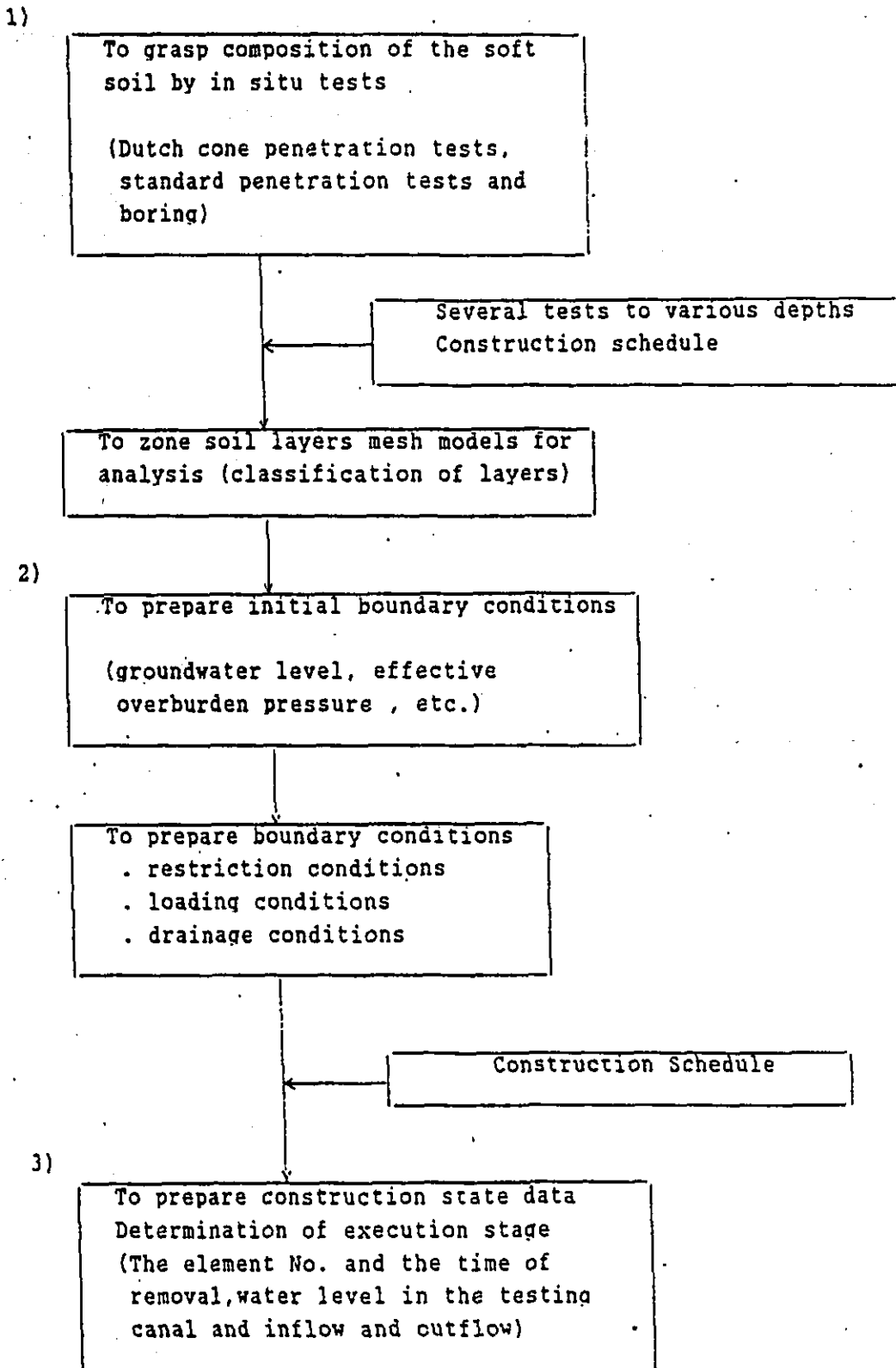


Fig.4-24, Analysis model and construction state data

Then the soft clay layer should be divided into small parts based on data obtained from several tests at various depths.

At the detailed design stage, in order to analyze in detail, the thickness of every layer was considered to be 2.0 meters and the change in its property parameter with depth was considered. Moreover, the mesh configuration to be removed was determined taking the excavation stage into consideration based on the construction stage as shown in Fig.4-25.

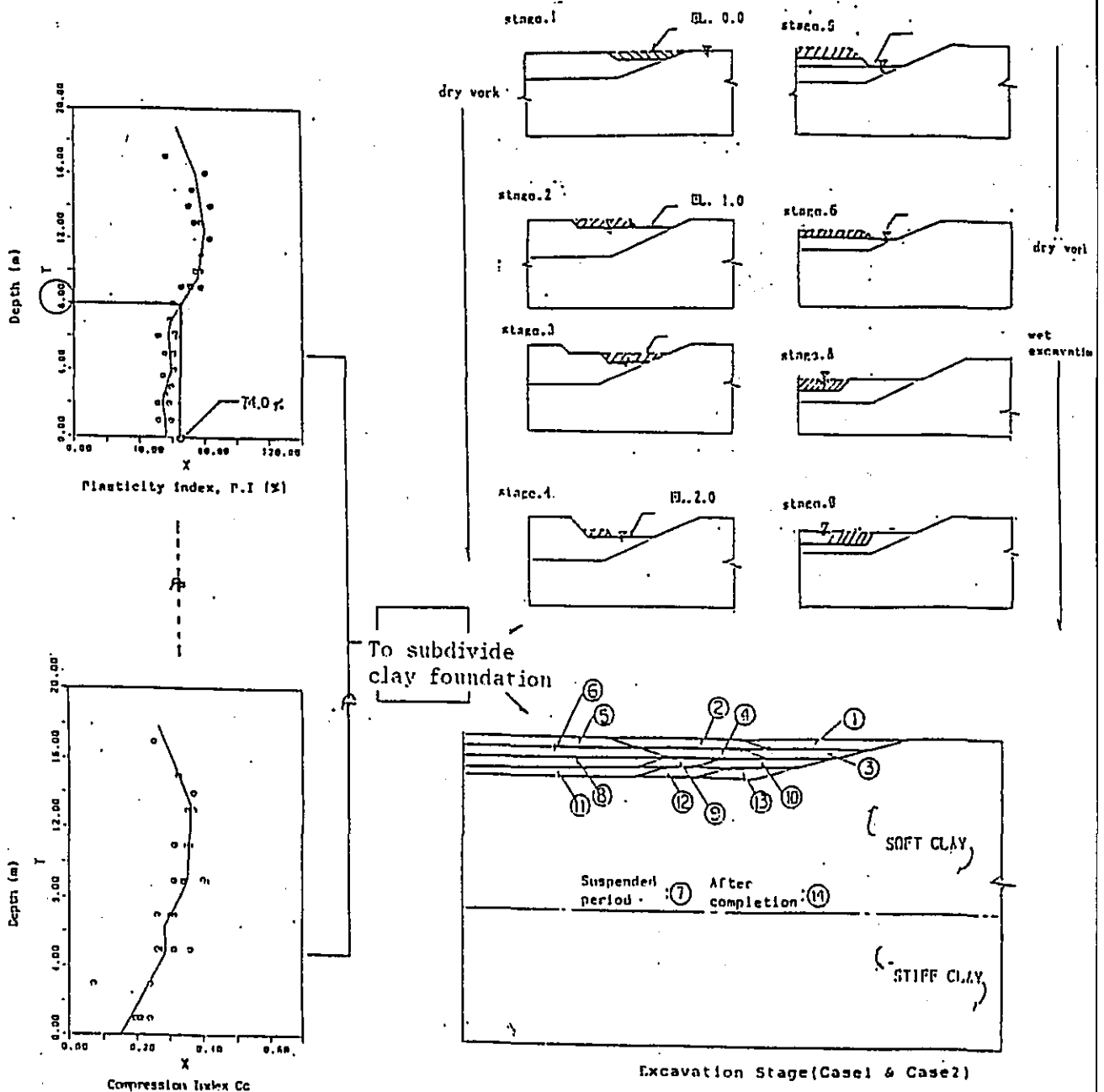


Fig.4-25 Mesh generation of the analyzed model

(2) Initial condition setting

It is necessary to consider the following items as the initial conditions for analysis model.

Table 4-6 Initial conditions for the analysis model

Items	Operation manual
1. Groundwater level and water level in the canal	---> See data record (5) " Setting up Initial Values " in 4-6-1 Operation Manual
2. Effective overburden pressure of each element (σ'_{vi}) This value is necessary for calculation of OCR and for initial compression stress of the joint element	---> See data record (6) ①②⑤ " Material Properties' Data "

The groundwater level can be expressed by WPZ as in Fig. 4-25, and it is the height from a base line, which is decided freely, to the groundwater level. Initial effective overburden pressure (σ'_{vi}) at point A in the ground can be expressed by the following equation (See Fig. 4-26).

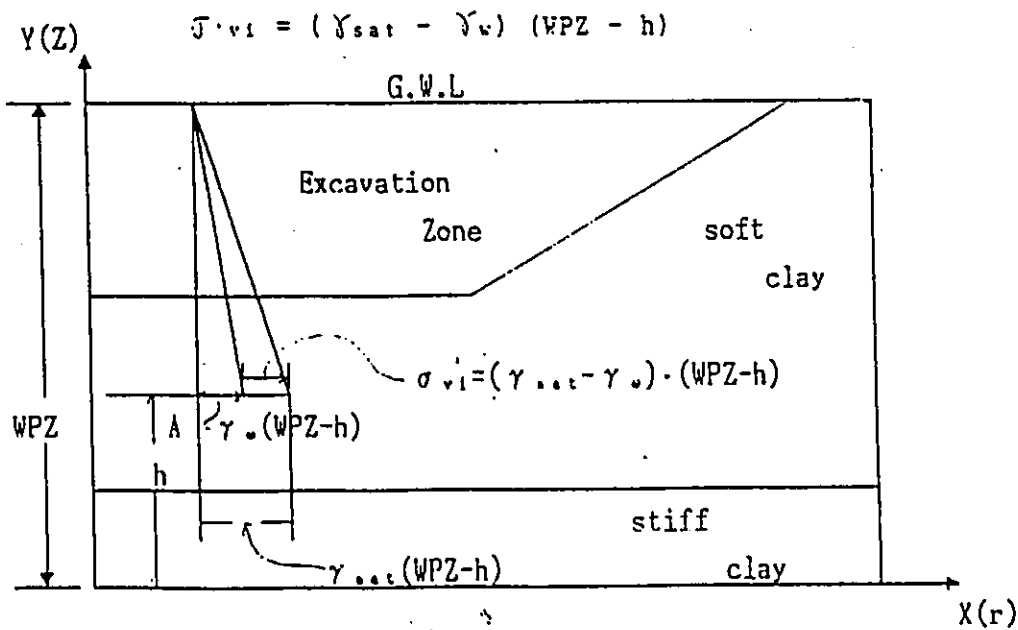


Fig.4-26 Analysis conditions of a model

(3) Boundary condition setting

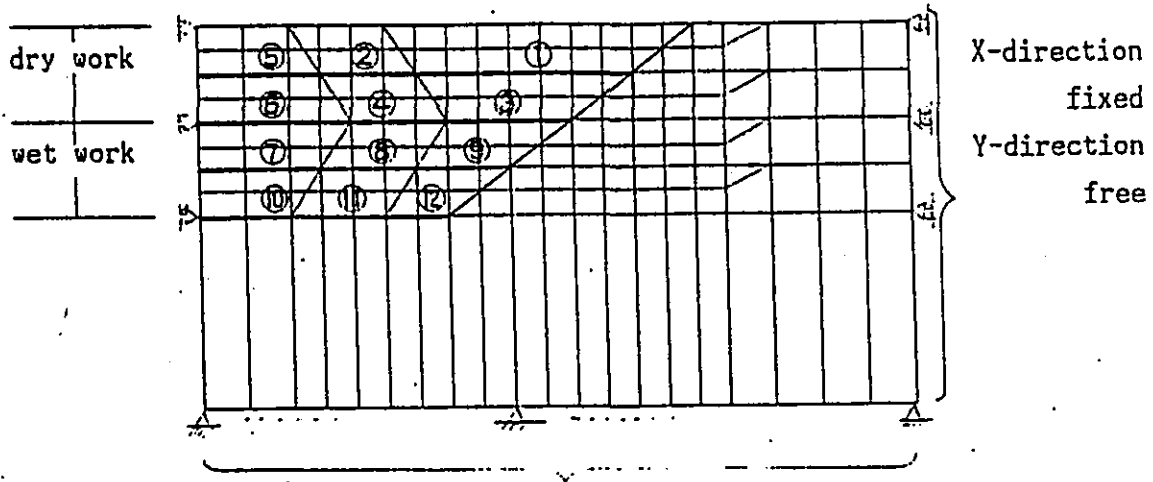
It is necessary to consider the items shown in Table 4-7 as boundary conditions for analysis: Special care should be taken with drainage conditions and overburden conditions because they have a close relationship with the construction state and change with the passage of time.

Table 4-7 Boundary conditions

Items	Operation manual
<p>1. Geometric boundary conditions ---</p> <p>Boundary conditions of nodal points</p>	<p>---> Data record (7) - c</p> <p>Geometric boundary condition data</p>
<p>2. Drainage condition ---</p> <p>Designation of drainage boundary</p> <p>drainage boundary will change in accordance with fluctuations in water level in the canal and construction state</p>	<p>---> Data record (7) - d</p> <p>Drainage condition data</p>
<p>3. Loading conditions --</p> <p>Designation of places to be loaded and unloaded and types of load.</p> <p>There are three (3) types of loads, namely concentrated loads, distributed loads and elementary forces.</p> <p>In the case of excavation or embankment work, elementary forces should be used.</p>	<p>---> Data record (7) - e</p> <p>Loading condition data</p>

① Geometric boundary conditions

Geometric boundary conditions are illustrated in Fig. 4-27 at the nodal points of both sides, the abscissas are fixed and the ordinates are free. At the nodal points on the bottom line, both the abscissas and the ordinates are fixed.



X,Y-direction fixed

Fig.4-27. Geometric condition of the mesh model.

②. Drainage conditions

Fig.4-28 shows a drainage condition. At the wet work stage, care should be taken that there is water in the testing canal and there is pore water pressure as much as the water level on the drainage boundary.

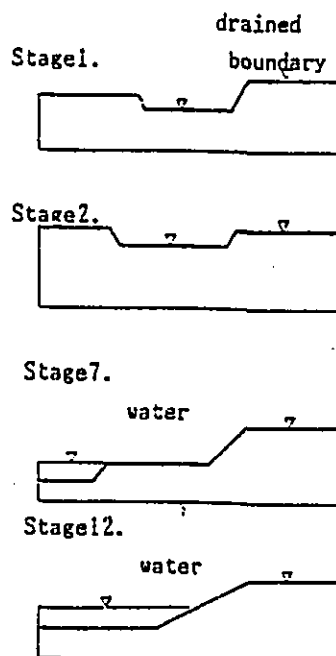


Fig.4-28. Drainage Condition

Considering an element M as shown in Fig.4-29, the drainage boundary is side ③ and the boundary has water-head h_B .

Supposing that the element adjacent to the element M is L, and let us consider these two elements, drainage boundary condition data should be prepared as follows:

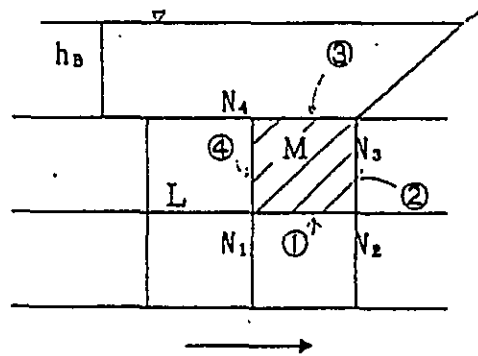


Fig.4-29. Explanation of drainage boundary conditions.

Example of data records of drainage boundary condition

Δ	L	M	ξ	h_B
	⋮	⋮	⋮	⋮
	①	②	③	④

- ①. Number of the first element among the elements in the same drainage condition.
- ②. Number of the last element among the elements in the same drainage condition.
- ③. Drainage boundary side of the element and boundary condition.
- ④. Height from the boundary to the water level

(3) Loading conditions

We can take account of concentrated loads and distributed loads on nodal-points and sides respectively and body forces which act on centroids in elements as loading conditions.

In the case of embankment work or excavation work, the work should be considered as a loading or unloading of the body forces (i.e. the weight of the elements). The unit weight of elements γ is consequently needed. If the elements are in the water or below the groundwater level, the submerged unit weight is necessary. Regarding preparation of input data for analysis, refer to Section 4-6 'Operation Manual'.

(4) Preparation of construction state data

Construction states should be divided into several stages taking account of excavation area and depth and passage of time, and construction state data should be prepared based on the proposed or actual construction schedule as shown in Fig. 4-27 and Table 4-8. At the same time, the drainage conditions and loading conditions mentioned above should be prepared.

In case of excavation work, negative signs should be assigned to the element numbers which correspond to the excavation area, and in the case of embankment work, the sign will be positive. Negative and positive signs mean unloading and loading respectively.

For more details about input data preparation for analysis, refer to Section 4-6 ' Operation Manual '

Table.4-8 Excavation Stage

Construction method	Stage number	term	removed element No.
	1		
dry	2		
work	3		
	4		
	5		
	6		
	7		
wet	8		
work	9		
	10		
	11		
	12		
	13		

4-5 Output of the results of analysis

In order to make the results of F.M.E analysis easy to understand visually, programs for drawing diagrams as in Table 4-9 will be set up.

Table 4-9

Program name	Diagram	Details
MIPPL01	Displacement diagram	To grasp displacement and deformation on the slope surfaces and in the ground.
MIPPL02	Displacement vector diagram	To grasp the size and directions of displacement at nodal points.
MIPPL03	Stress diagram	To grasp distribution of principal stress
MIPPL04	Distribution diagram of analyzed results (e.g.pore water pressure, stresses displacement)	To grasp distribution of displacement stresses, pore water pressure or strain etc.
MIPPL05	Contour diagram	- ditto -
MIPPL06	Effective stress Path diagram	To predict the place where a slope failure will occur.

Examples of each diagram are shown below.

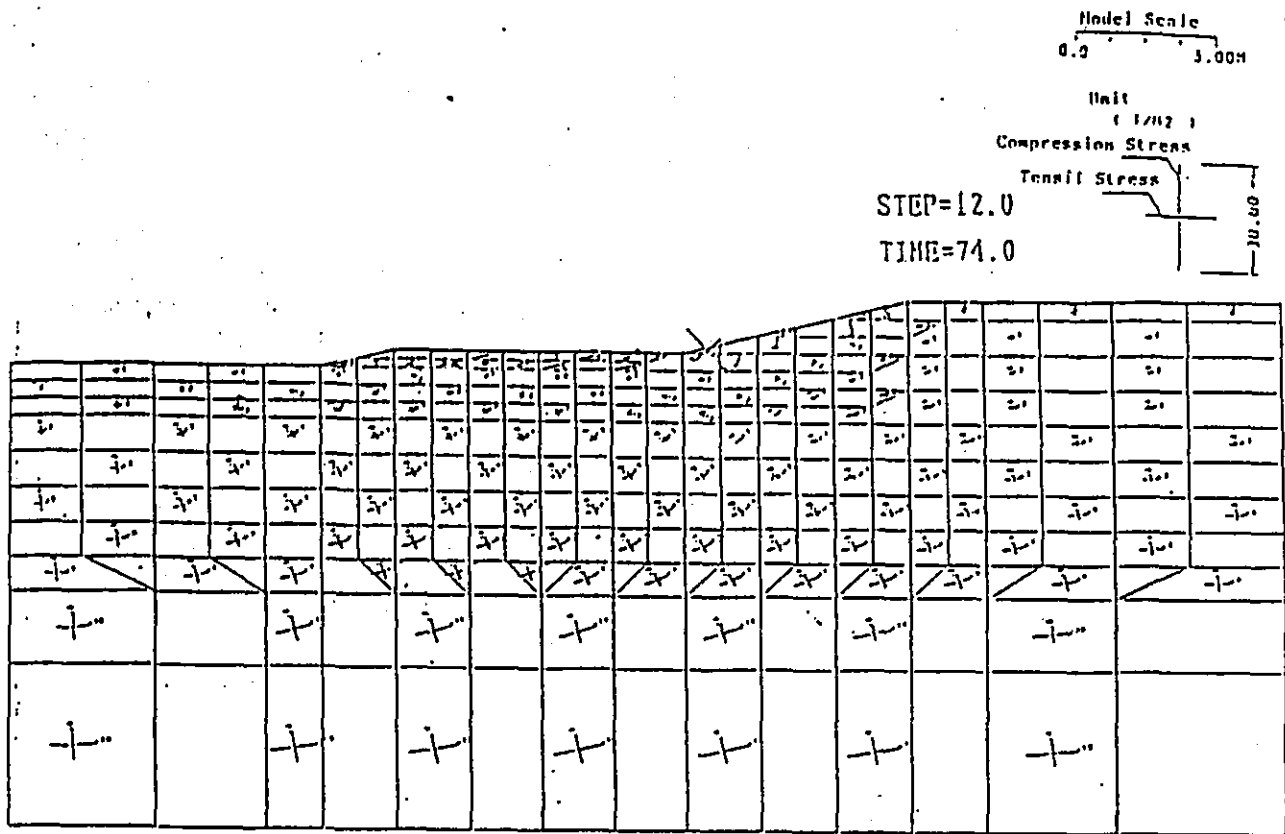


Fig.4-30, Stresses occurring in the non-treated slope for short-term slope stability

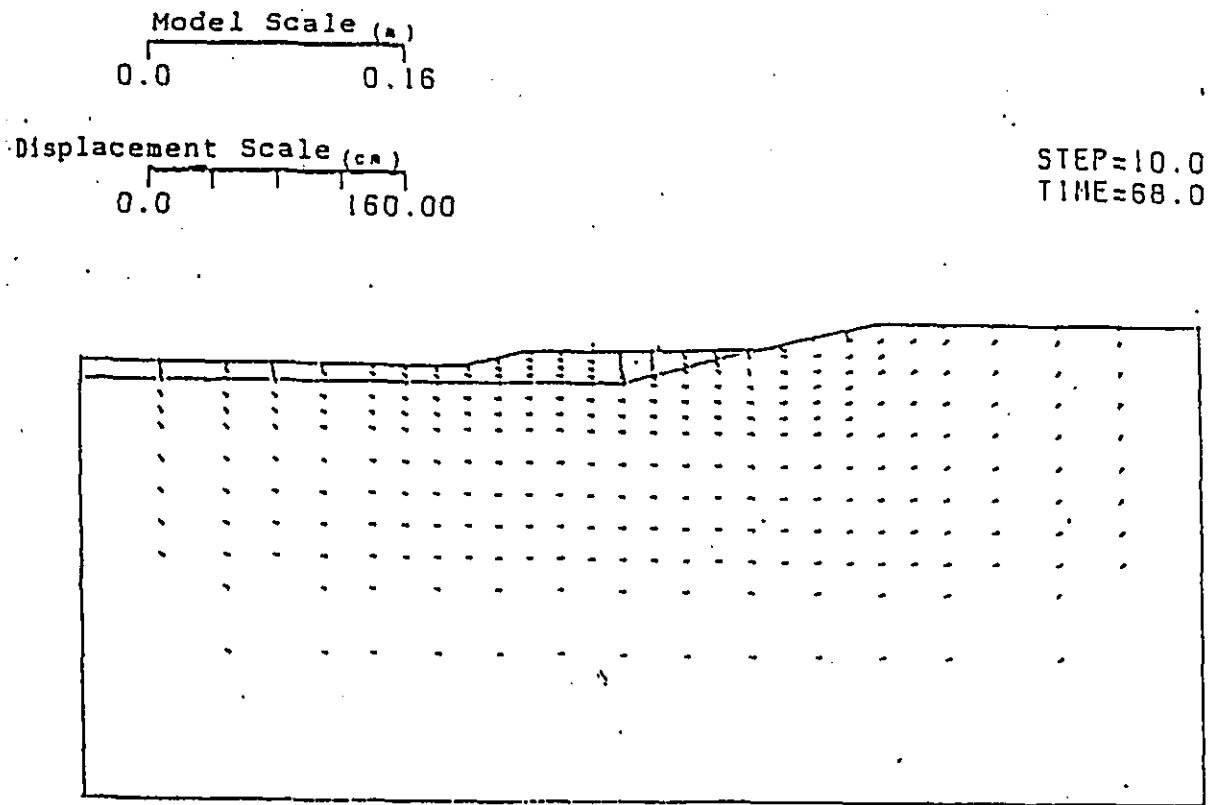


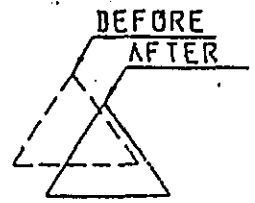
Fig.4-31 Deformation Vector in Non-treatment Slope for Short Term Slope Stability

DISPLACEMENT

MODEL SCALE (")
0.0 16.00

DISPLACEMENT SCALE (")
0.0 64.00

LEGEND



STEP=12.0
TIME=74.0

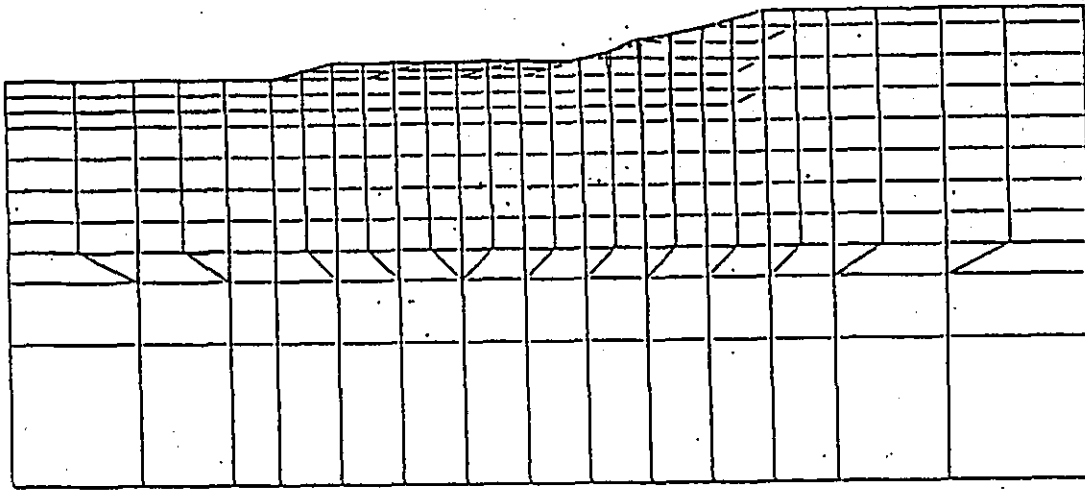


Fig.4-32(1) Overall displacement in the non-treated slope for short-term slope stability

STEP=13.0
TIME=77.0

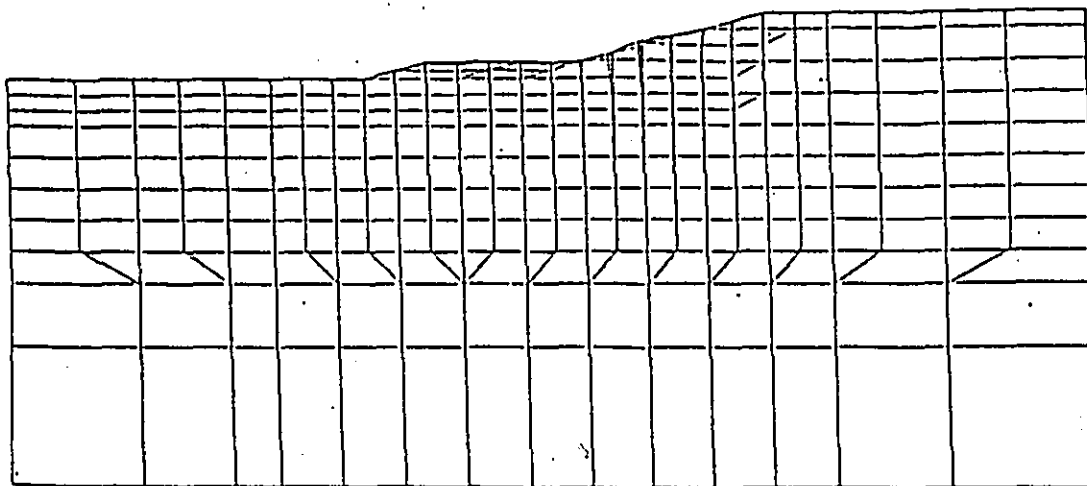
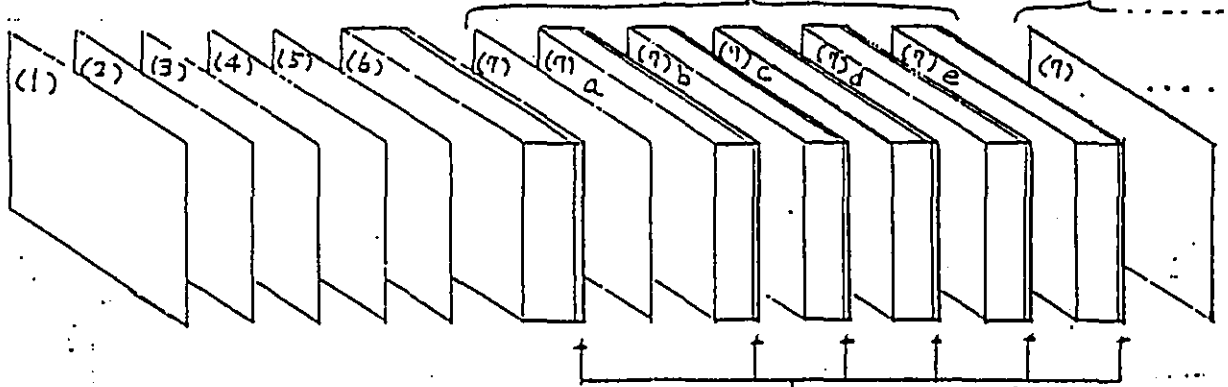


Fig.4-32(2) Overall displacement in the non-treated slope for short-term slope stability

4-6. Operation Manual for the F.E.M Analysis
(for Soft Soil Foundation Analysis)

INPUT USAGE

1. Procedure for inputting data with a Card Image preparing progressive steps.



Keyin E on the Keyboard on the first column indicates the end of each data records

where

- (1) Title Card
- (2) Analysis Control Card
- (3) Output Control Card
- (4) Output Control Card for checking purposes
- * (5) Setting up Initial Values
- * (6) Material Properties' Data
- (7) Step Control Card
- (7)-a Nodal Points' Data
- (7)-b Elements' Data
- (7)-c Geometric Boundary Condition Data
- (7)-d Drinage Boundary Condition Data
- (7)-e Loading Condition Data

In continuous calculation, (5) and (6) are not necessary

2. Input Data Procedure

(1) Title Card

READ (MAIN) (UNIT (i), i=1,3), (TITL(i), i=1,63)

col	variable (format)	contents
1-9	UNIT(i), i=1,3 (3A3)	indication of dimension used in analysis
10-72	TITL(i), i=1,63 (63A1)	title name of the analysis

Remarks:

UNIT(i) : indicates the dimension /L/T/M/ with every 3cd.

(2) Analysis Control Card

READ (MAIN) IPSN, ICON, IPLAS, IEXC, ICAL

col	variables (format)	contents
1-5	IPSN (i5)	whether plane-strain or axi-symmetric
6-10	ICON (i5)	whether coupled analysis or not
11-15	IPLAS (i5)	whether considering viscosity or not
16-20	IEXC (i5)	dealing with the equivalent nodal forces at excavation expressed as remove elements.
*21-25	ICAL (i5)	whether new calculation or continuous one

Notes

IPSN { 0 : plane strain condition
1 : axi-symmetric condition

ICON { 0 : considering pore water flow (coupled analysis)
1 : not considering pore water flow (ordinary F.E.M)

IPLAS { 0 : considering viscosity of material (elasto-viscoplastic)
1 : not considering viscosity (elasto-plastic)

IEXC { 0 : the equivalent nodal forces calculated from total stress (including water pressure) of the elements taken away as excavation
1 : the equivalent nodal forces calculated from effective stress of the elements

ICAL { 0 : new calculation (from beginning)
1 : continuous calculation (data and results of the previous calculation gotten from file on disk)

(3) Output Control Card

READ (MAIN) (IWRITE(i), i=1,4), NFT10, NFT20, ITRM

col	variables (format)	contents
1-5	IWRITE(1) (i5)	nodal displacement output
6-10	IWRITE(2) (i5)	stress component output
11-15	IWRITE(3) (i5)	strain component output
16-20	IWRITE(4) (i5)	strain rate component output
*21-25	NFT10 (i5)	use data file (No.10) to write or read the input data and calculation results for the later continuous calculation
26-30	NFT20 (i5)	use data file (No.20) to write the calculation results in order to draw figures
31-35		Maximum number of iterations in each step

Notes

IWRITE (1-3) $\left\{ \begin{array}{l} 0 \text{ output} \\ 1 \text{ not output} \end{array} \right.$

NFT10, NFT20 $\left\{ \begin{array}{l} 0 \text{ use data file (No.10 or No.20)} \\ 1 \text{ do not use} \end{array} \right.$

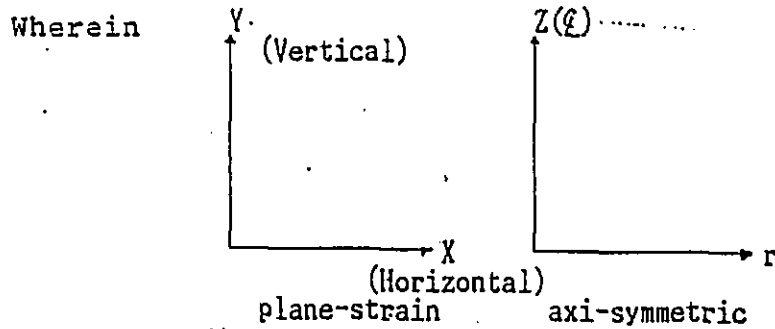
In the case of using data files to write or read, it is necessary to make up a data file to use beforehand. (need to ALLOCATE)

ITRM = 0 meaning ordinary step by step calculation
(superposition of incremental form)

Explanation of Contents of Outputs

① IWRITE(1)=0

- N : the number of the nodal point
- DU : incremental displacement in X (r)-direction
- DV : incremental displacement in Y (Z)-direction
- U : total displacement in X(r)-direction
- V : total displacement in Y(Z)-direction



② IWRITE(2)=0

(i) plane-elements (ground material)

M : the number of the element

STATE : the stress state of the element

STATE	1	2	3	4	5
MEANING	linear-elastic material	elastic region	elasto-(visco) plastic region	failure region	$P' < 0$

SX(N) (SR(N)) : σ'_x (σ'_r)
 SY(Q) (SZ(Q)) : σ'_y (σ'_z)
 SXY(M) (SRZ(M)) : τ_{xy} (τ_{rz})
 SZ (STH) : σ'_z (σ'_θ)
 SM : P' effective mean stress
 QQ : q generalized deviatoric shear stress

$$\text{where } q = \sqrt{\frac{3}{2} s_{11}s_{11}} \text{ , } s_{11} = \sigma'_{11} - P' \delta_{11}$$

HEAD : h total head
 where $h = P_w / \gamma_w + \Omega$, Ω head of position potential
 PW : P_v pore water pressure
 EHTA : η^* generalized stress ratio proposed by Sekiguchi and Ohta (1977)

$$\text{where } \eta^* = \sqrt{\frac{3}{2} (\eta_{11} - \eta_{110}) \lambda (\eta_{11} - \eta_{110})} \text{ , } \eta_{11} = S_{11} / P'$$

Q/SM : q/P' stress ratio
 S1 : σ'_1 effective maximum principal stress
 S3 : σ'_3 effective minimum principal stress
 TAUMAX : τ_{max} maximum shear stress
 THETA : θ rotation angle of principal stress
 where anti-clockwise is positive
 VOID : e void ratio

(ii) beam-elements

M : the number of the element
 STATE : the number of the material property
 SX(N) : N axial force ($N = \sigma_N A$)
 SY(Q) : Q shear force ($Q = \tau A$)
 SXY(M) : M moment

(iii) truss-elements

M : the number of the element
 STATE : the number of the material property

SX(N) : N axial stress ($N = \sigma_N A$)

(iv) Joint-elements

M : the number of the element
 STATE : the number of the material property
 SX(N) (SR(N)) : the state of the element

SX	1	2	3	4
meaning	/	no yield	shearing yield	exfoliation ($\sigma_N < 0$)

SY(Q) (SZ (Q)) : τ shear stress
 SKY(M) (SRZ(M)) : σ_N normal stress
 SZ : M moment



where 1) this M is introduced in order to consider fan-shaped exfoliation of 4-nodal joint elements, so that this is different from ordinarily defined moments
 2) moment M is calculated in the case of plane-strain condition

(v) Axi-symmetric shell elements

M : the number of the element
 STATE : the number of the material property
 SR(N) : N_s normal stress in longitudinal direction
 SZ(Q) : N normal stress in circumferential direction
 SRZ(M) : M_s moment
 STH : M_θ moment

MT	0		1	2	3	4	5
Array	elasto-viscoplastic	elasto-plastic	elastic	beam	truss	joint	shell
SIG(M, 1)	σ'_x		σ'_x	N	N	τ	N_z
SIG(M, 2)	σ'_y		σ'_y	Q		σ_w	N_θ
SIG(M, 3)	τ'_{xy}		τ'_{xy}	M		M^*	M_s
SIG(M, 4)	σ'_z		σ'_z				M_θ
SIG(M, 5)	P'		P'				
SIG(M, 6)	P'	P'_y					

- ③ IWRITE(3)=0 only in the case of plane elements
- M : the number of the element
- MM : the number of the material property
- STATE : the stress state of the element
- EPS-X (EPS-R) : $\epsilon_x(\epsilon_r)$ strain in X(r) direction
- EPS-Y (EPS-Z) : $\epsilon_y(\epsilon_z)$ strain in Y(z) direction
- EPS-XY (EPS-RZ) : $\gamma_{xy}(\gamma_{rz})$ shear strain
- (EPS-TH) : ϵ_θ strain in θ direction
- V : ϵ_v volumetric strain
- VP : ϵ_v^p viscoplastic part of volumetric strain
- FF : f scalar function

$$f = MD \ln \frac{P'}{P'_0} + D \eta^* \quad (\text{elasto-viscoplastic analysis})$$

$$f = MD \ln \frac{P'}{P'_y} + D \eta^* \quad (\text{elasto-plastic analysis})$$

CRITIC : scalar function of failure criterion

$$= M - \frac{\xi}{2\eta^*} \eta_{,1}(\eta_{k1} - \eta_{k10})$$

④ IWRITE(4)=0 only in the case of the plane elements

M	:	the number of the element
MM	:	the number of the material property
STATE	:	the stress state
DEPS-X(DEPS-R)	:	$\Delta \epsilon_x (\Delta \epsilon_r)$ incremental strain in x(r) direction
DEPS-Y(DEPS-Z)	:	$\Delta \epsilon_y (\Delta \epsilon_z)$ incremental strain in y(z) direction
DEPS-XY(DEPS-RZ)	:	$\Delta \gamma_{xy} (\Delta \gamma_{rz})$ incremental shear strain
(DEPS-TH)	:	$(\Delta \epsilon_\theta)$ incremental strain in θ direction
DV	:	$\Delta \epsilon_v$ incremental volumetric strain
DPS-X/DT(DPS-R/DT)	:	$\Delta \dot{\epsilon}_x (\Delta \dot{\epsilon}_r)$ strain rate in x(r) direction
DPS-Y/DT(DPS-Z/DT)	:	$\Delta \dot{\epsilon}_y (\Delta \dot{\epsilon}_z)$ strain rate in y(z) direction
DPS-XY/DT(DPS-RZ/DT)	:	$\Delta \dot{\gamma}_{xy} (\Delta \dot{\gamma}_{rz})$ shear strain rate
(DPS-TH/DT)	:	$(\Delta \dot{\epsilon}_\theta)$ the strain rate in θ direction
DV/DT	:	$\Delta \dot{\epsilon}_v$ volumetric strain rate

⑤ etc

The equivalent nodal forces
 (see (7)-c Geometry Boundary Condition Data about output
 command)

N	:	the number of the nodal point
DFX	:	increment of the equivalent nodal force in X-direction
DFY	:	increment of the equivalent nodal force in Y-direction
DMOMENT	:	increment of the equivalent nodal moment
FX	:	equivalent nodal force in X-direction
FY	:	equivalent nodal force in Y-direction
MOMENT	:	equivalent nodal moment

(4) Output Control Card for Checking Purpose

READ (MAIN) (ICHECK(i), i=1,10)

col.	variables (format)	contents of output
1-5	ICHECK(1) (i5)	XY(N,2), NKIND(N), FORCE(N,3) NCOND(N,3), JP(N), JPP(N,3) NEXCA(N)
6-10	ICHECK(2) (i5)	NOD(M,6), MDRN(M,4), MKIND(M) BODY(M), MEXCA(M), NAEL(M,4) JPE(M), JE(M), GXY(M,2)
11-15	ICHECK(3) (i5)	DEP(M,4,3)
16-20	ICHECK(4) (i5)	$\int \nu B(4,8) dv$
21-25	ICHECK(5) (i5)	DB(4,8)
26-30	ICHECK(6) (i5)	FEM(8,8)
31-35	ICHECK(7) (i5)	B(4,8)
36-40	ICHECK(8) (i5)	ALPH(M), DRAIG(M)
41-45	ICHECK(9) (i5)	F(LLNEL), GS(LLNEL), MJB)

ICHECK(i) { 0 not output
1 output

(5) Setting up Initial Values (not necessary in continuous calculation)

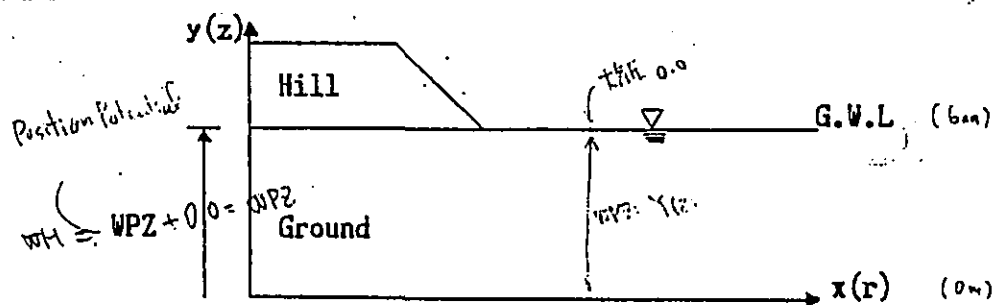
READ(MAIN) GMW, WPZ, EPSMIN

col.	variables (format)	contents
1-10	GMW (F10.0)	γ_w a unit weight of pore water
11-20	WPZ (F10.0)	Z height of head of position potential
21-30	EPSMIN (F10.0)	judging constant of iteration

remark

GMW : ex. 1.0(t/m³), 0.001(kg/cm³)

WPZ : though choice of height of position potential head up is a arbitrary, the head of excess pore water pressure is given instead of the total head in the case of setting wpz to the same height as the groundwater level.



EPSMIN : setting up EPSMIN = 1.0×10^{-3} automatically in the program in the case of input of 0.0 as judging constant.

(6) Material Properties' Data

READ (SUB, INMAT) L, MT, MM, (AA(j), j=1,6)

① Elasto-(visco) plastic Material (MT=0)

a unit consisting of 3 cards

col.	variables (format)	contents
[1st Card]		
1	L (A1)	key in 'E' on the last card
2-5	MT (i5)	0 because of the elasto-(visco) plastic material
6-10	MM (i5)	the number of the material property
11-20	AA(1) (F10.0)	D Coefficient of dilatancy proposed by Shibata (1963)
21-30	AA(2) (F10.0)	Λ Irreversibility Ratio expressed as $\Lambda = 1 - k/\lambda$
31-40	AA(3) (F10.0)	M Critical State Parameter
41-50	AA(4) (F10.0)	ν' Effective Poisson Ratio
51-60	AA(5) (F10.0)	$k_x(r)/\gamma_w$ Coefficient of permeability in x(r) direction at the reference stress state
61-70	AA(6) (F10.0)	$k_x(z)/\gamma_w$ Coefficient of permeability in y(z) direction at the reference stress state

col.	variables (format)	contents
[2nd Card]		
11~20	AA(7) (F10.0)	σ'_{v_0} Preconsolidation Pressure
21~30	AA(8) (F10.0)	K_0 Coefficient of Earth Pressure at rest
31~40	AA(9) (F10.0)	σ'_{v_1} Effective Overburden Pressure
41~50	AA(10) (F10.0)	K_t Coefficient of Earth Pressure at rest in-situ
51~60	AA(11) (F10.0)	α Coefficient of Secondary Compression expressed as $\alpha \equiv \frac{dv}{d(\ln t/t_0)}$
61~70	AA(12) (F10.0)	\dot{v}_0 Initial Volumetric Strain Rate at reference state
[3rd Card]		
11~20	AA(13) (F10.0)	λ Compression Index in the $e-\ln(p'/p'_0)$ relationship
21~30	AA(14) (F10.0)	e_0 Void Ratio corresponding with σ'_{v_0} (at preconsolidation)
31~40	AA(15) (F10.0)	λ_k Gradient of k (coefficient of permeability) and $\ln p'/p'_0$ relationship

remark

e_0 : this value is used to calculate the coefficient of permeability, and is automatically estimated from D, Λ, M, λ in the case of inputting 0.0

$$e_0 = \frac{\lambda \Lambda}{MD} - 1$$

λ_k : using λ (compression index) as λ_k in the case of inputting 0.0

$k_{x_0}/\gamma_w, k_{y_0}/\gamma_w$: on the basis of Taylor (1948) the coefficient of permeability is calculated as follows

$$k_i/\gamma_w = (k_{i_0}/\gamma_w) \exp\left(\frac{e - e_0}{\lambda_k}\right) \quad i = x(r), y(z) \quad (*)$$

λ : making the coefficient of permeability constant without using eq. (*) in the case of inputting 0.0

② Linear-elastic Material. (MT=1)....plane elements a unit consisting of 2 cards

col.	variables (format)	contents
[1st Card] 1	L (A1)	Keyin 'E' on the last card
2-5	MT (i5) i4	1 because of the linear-elastic material
6-10	MM (i5)	the number of the material property
11-12	AA(1) (F10.0)	$\bar{\lambda}$ } $\bar{\mu}$ } Lamé's constants
21-30	AA(2) (F10.0)	
31-40	AA(3) (F10.0)	σ'_{vi} Effective Overburden Pressure
41-50	AA(4) (F10.0)	k_i Coefficient of in-situ Earth Pressure at rest
51-60	AA(5) (F10.0)	k_{x_0}/γ_w Coefficient of permeability in x(r) direction at the reference stress state
61-70	AA(6) (F10.0)	k_{y_0}/γ_w Coefficient of permeability in y(z) direction at the reference stress state

col.	variables (format)	contents
[2nd Card] 11~20	AA(7) (F10.0)	e_1 Initial Void Ratio
21~30	AA(3) (F10.0)	λk Gradient of k (coefficient of permeability) and $\ln p'/p_0$ relationship

remarks

: making the coefficient of permeability constant in the case of inputting 0.0

$$\tilde{\lambda}, \tilde{\mu} : \tilde{\lambda} = \frac{\nu E}{(1+\nu)(1-2\nu)}, \tilde{\mu} = G = \frac{E}{2(1+\nu)}, \text{ where}$$

E is Youngs' modulus
 ν is Poisson ratio

③ Beam Material (MT=2) (only in plane strain condition)

col.	variables (format)	contents
1	L (A1)	Keyin 'E' on the last card
2~5	MT (i5)	2 because of the beam material
6~10	MM (i5)	the number of the material property
11~20	AA(1) (F10.0)	E Youngs' modulus of the beam
21~30	AA(2) (F10.0)	A sectional area per a unit of depth
31~40	AA(3) (F10.0)	I moment of inertia of area

④ Truss Material (MT=3) (only in plane-strain condition)

col.	variables (format)	contents
1	L (A1)	Keyin 'E' on the last card
2-5	MT (i5)	3 because of the truss material
6-10	MM (i5)	the number of the material property
11-20	AA(1) (F10.0)	E Youngs' modulus
21-30	AA(2) (F10.0)	A sectional area per a unit of depth

⑤ Joint Material (MT=4)

col.	variables (format)	contents
1	L (A1)	Keyin 'E' on the last card
2-5	MT (i5)	4 because of the joint material
6-10	MM (i5)	the number of the material property
11-20	AA(1) (F10.0)	K_s Shear Stiffness
21-30	AA(2) (F10.0)	k_n Normal Stiffness
31-40	AA(3) (F10.0)	σ_v Overburden Pressure
41-50	AA(4) (F10.0)	K_1 Coefficient of in-situ Earth Pressure at rest
51-60	AA(5) (F10.0)	C Cohesion Stress
61-70	AA(6) (F10.0)	$\tan\phi$ Gradient of Internal Frictional Angle

⑥ Axi-symmetric Shell Material (MT=5) (only in axi-symmetric condition)

col.	variables (format)	contents
1	L (A1)	Keyin 'E' on the last card
2~5	MT (i5)	5 because of the shell element
6~10	MH (i5)	the number of the material property
11~20	AA(10) (F10.0)	E Young's Modulus
21~30	AA(2) (F10.0)	t Thickness
31~40	AA(3) (F10.0)	Poisson Ratio

remark

t : in case of inputting 0.0, automatically setting up unit thickness

7 Step Control Card

READ (MAIN) LE, ISTEP, INOD, IELM, ICOND, IDRNM, ILOAD, IOUT,
DTIME, IISTEP

col.	variables (format)	contents
1	LE (A1)	Keyin 'E' on the last card
6-10	ISTEP (i5)	the number of the step
11-15	INOD (i5)	whether nodal point data exist or not
16-20	IELM (i5)	whether element data exist or not
21-25	ICOND (i5)	whether geometry boundary condition data exist or not
26-30	IDRM (i5)	whether the drainage boundary condition data exist or not
31-35	ILOAD (i5)	whether the loading condition data exist or not
36-40	IOUT (i5)	whether the calculation results at this step are printed out or not
41-50	DTIME (F10.0)	the incremental time of this step
51-55	IISTEP (i5)	(repeating step by step calculation IISTEP times per step)

in these flags : { 1 means Yes
0 means NO

In the continuous calculation the number of steps also starts from the continuous one

on INOD=1

(7) Nodal Point Data

READ (SUB, INNOD) L, N1, X1, Y1, N2, X2, Y2

col.	variables (format)	contents
1	L (A1)	Keyin 'E' on the last card
6~10	N1 (i5)	the number of the nodal point (the beginning)
11~20	X1 (F10.0)	x (or r) coordinate of the nodal point N1
21~30	Y1 (F10.0)	y (or z) coordinate of the nodal point N1
31~35	N2 (i5)	the number of the nodal point (the end)
36~45	X2 (F10.0)	x (or r) coordinates of the nodal point N2
46~55	Y2 (F10.0)	y (or z) coordinates of the nodal point N2

remarks

- (x,y) or (r,z) coordinates between N1 and N2 are automatically interpolated at regular intervals
- Nodal point data which are not yet used in the steps are allowed to input together in the step

on IELM=1

(7) -b Element Data

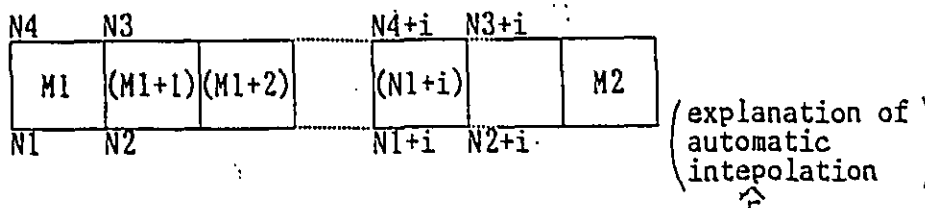
READ (SUB, INELM) L, M1, (ND(i), i= 1,4), MM, M2, WH

col.	variables (format)	contents
1	L (A1)	Keyin 'E' on the last card
6-10	M1 (i5)	the number of the element (the beginning) *1)
11-15	ND(1) (i5)	N1*2)
16-20	ND(2) (i5)	N2*2)
21-25	ND(3) (i5)	M3 (be blank in line elements)*2)
26-30	ND(4) (i5)	M4 (be blank in line & triangular elements)
31-35	MM (i5)	the number of the material property
36-40	M2 (i5)	the number of the element*1) (the end)
41-50	WH (F10.0)	h _i the initial total water head (h _i = $\rho_w i / \gamma_w + z$)

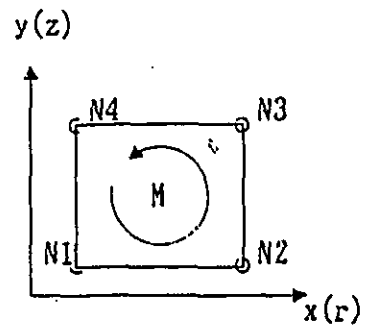
remarks

*1) In the case of taking away elements at excavation, mark the minus sign (-) at the head of the numbers of these elements

The nodal points between M1 and M2 are automatically interpolated but this option is not allowed to be used in line and triangular elements



*2) the order of N_1, \dots, N_4 is anti-clockwise



on ICOND = 1

(7) - c Geometric Boundary Condition Data

READ (SUB,INCCND) L, NB, NL, (NBB(i), i=1,3), (BB(i), i=1,3) NN

col.	variables (format)	contents
1	L (A1)	Keyin 'E' on the last card
6 - 10	NB (i5)	the number of the nodal point (the beginning)*1)
11 - 15	NL (i5)	the number of nodal point (the end)*1)
16 - 20	NBB(1) (i5)	whether restriction condition in x(r) direction exists or not*2)
21 - 25	NBB(2) (i5)	whether restriction condition in y(z) direction exists or not*2)
26 - 30	NBB(3) (i5)	whether restriction condition in rotation exists or not*2)
31 - 40	BB(1) (F10.0)	amount of compelled nodal displacement in x(r) direction*3)
41 - 50	BB(2) (F10.0)	amount of compelled nodal displacement in y(z) direction*3)
51 - 60	BB(3) (F10.0)	amount of compelled rotation (anti-clockwise is positive)*3)
61 - 65	NN (i5)	output indication of the equivalent nodal forces with compelled nodal displacement*4)

remarks

- * 1) The number of nodal points between NB and NL are set up to the same geometric boundary conditions corresponding to NBB (1-3) and BB(1-3)

Geometric boundary condition data which are not yet used in the steps are allowed to input together

The geometric boundary conditions are changed to the new one in inputting again

- *2) NBB(1-3) $\left\{ \begin{array}{l} 0 \text{ no restriction} \\ 1 \text{ restriction} \end{array} \right.$

In the case of indicating "restriction", it is necessary to input the amount of "restriction" to BB(1)-BB(3)

It means "fixed" condition to input 0.0 as the compelled displacement or rotation

- * 3) NN $\left\{ \begin{array}{l} 0 \text{ no requirement of output} \\ 1 \text{ requirement} \end{array} \right.$

on IDRN=1

(7) - d Drainage Boundary Condition Data

READ (SUB, INDRN) L, MB, IC, BW

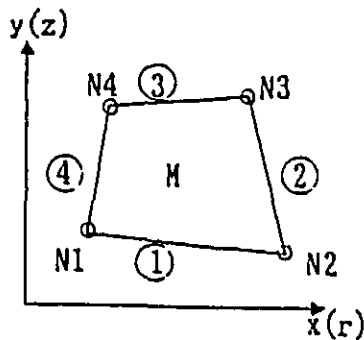
col.	variables (format)	contents
1	L (A1)	Keyin 'E' on the last card
6 - 10	MB (i5)	the number of the element <u>(the*1)</u> <u>begining)</u>
11 - 15	ML (i5)	the number of the element <u>(the end)*1)</u>
16 - 20	IC (i5)	indication of the kind of drainage condition and its position*2)
21-30	BW (F10.0)	hs total water head on the boundary

remarks

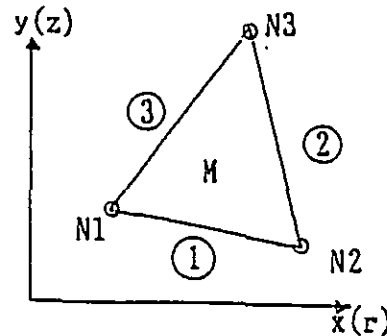
* 1) The boundary of elements between MB and ML is automatically set up to the same drainage boundary conditions corresponding to IC and BW

* 2) The boundary is opositted corresponding with the input

order (N1~N4 constituting the element M) as in the figures.



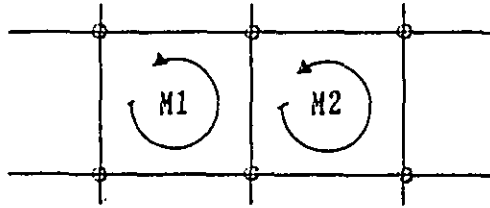
the quadrilateral element



the triangular element

- IC = 1⁻⁴ : drainage boundary condition
(Pore water is allowed to flow across the boundary)
- IC = -1⁻⁴ : undrained boundary condition
(Pore water is not allowed to flow across the boundary)
- IC = 11⁻¹⁴ : cancelling undrained or drained boundaries set up before

As shown in the figure, in making the boundary between M1 and M2 undrained (or drained), it is necessary to input both data of M1 and M2 (IC=-2 (or 2) for M1 and IC = -4 (or 4) for M2)



Without any indication (not input), the boundary between elements is automatically set up to drainage condition and the outside boundary of the element is automatically set up to undrained condition.

on ILOAD=1

(7) - e Loading Condition Data

READ (SUB, INLOAD) L, KIND, N1, N2, FX, FY, FM

col.	variables (format)	contents
1	L (A1)	keyin 'E' on the last card
6-10	KIND (i5)	kind of loading*1)
11-15	N1 (i5)	the number of the nodal point or the element loaded (the beginning)*2)
16-20	N2 (i5)	the number of the nodal point or the element loaded (the end)*2)
21-30	FX (F10.0)	amount of incremental load in x(r) direction *3)
31-40	FY (F10.0)	amount of incremental load in y(z) direction in ^{the} case of nodal force γ , a unit weight of element in the case of body force expressed as elemental force *3)
41-50	FM (F10.0)	amount of incremental moment (anti-clockwise is positive)*3)

remark

| *1) KIND { 0 elemental force
| | 1 nodal force

*2) The loading conditions between N1 and N2 are automatically set up to the same conditions

*3) In the case of nodal forces.

Input the amount of load acting on the nodal point to FX, FY, FM

In the case of acting elemental forces.

Input the amount of a unit weight γ of the element to FY

§ Explanation of Components of COMMON Block

COMMON/A/

NNOD Maximum number of Nodal Point in each step

NNEL Maximum number of Element in each step

LLNEL Maximum length of column or row of total stiffness matrix in each step

MJB Band width of reduced total stiffness matrix in each step

COMMON/B/

SIG(M,6) Array of stress components

Array	Plane Element			Line Element			
	Elasto-visco plastic	Elasto-plastic	Elastic	Beam	Truss	Joint	Shell
SIG(M,1)	$\sigma'_x(\sigma'_x)$	$\sigma'_y(\sigma'_y)$	$\sigma'_z(\sigma'_z)$	N	N	τ	N_s
SIG(M,2)	$\sigma'_y(\sigma'_z)$	$\sigma'_y(\sigma'_z)$	$\sigma'_y(\sigma'_z)$	Q	/	σ_N	N_s
SIG(M,3)	$\tau_{xy}(\tau_{xy})$	$\tau_{xy}(\tau_{xy})$	$\tau_{xy}(\tau_{xy})$	M		M	M_s
SIG(M,4)	$\sigma'_z(\sigma'_z)$	$\sigma'_z(\sigma'_z)$	$\sigma'_z(\sigma'_z)$	/		/	PS
SIG(M,5)	P'	P'	P'		/		/
SIG(M,6)	$\Delta P'$	P'_y	/	/		/	
	Axi-symmetric			Plane-strain			Axi-symmetric

remark : PS : shearing stiffness, PN : normal stiffness

SIGC(M,5) Array of stress histories of elasto-(visco) plastic elements

Array	Elasto-(visco) plastic	Elasto-plastic
SIGC(M,1)	$\sigma'_{x0}(\sigma'_{x0})$	$\sigma'_{x0}(\sigma'_{x0})$
SIGC(M,2)	$\sigma'_{y0}(\sigma'_{y0})$	$\sigma'_{y0}(\sigma'_{y0})$
SIGC(M,3)	$\tau'_{xy0}(\tau'_{xy0})$	$\tau'_{xy0}(\tau'_{xy0})$
SIGC(M,4)	$\sigma'_{z0}(\sigma'_{z0})$	$\sigma'_{z0}(\sigma'_{z0})$
SIGC(M,5)	P'_0	P'_0

RSIG(M,4) : Array of incremental relaxation stress $\Delta \sigma'$ of elasto-viscoplastic elements

A constitutive relationship of elasto-viscoplastic material is

$$\dot{\underline{\sigma}} = \underline{D}^{*vp} \dot{\underline{\epsilon}} - \dot{\underline{\sigma}}'$$

PW(M) : Array of total water head $h * \gamma_w$.

where $h = p_w / \gamma_w + \Omega$, p_w is pore water pressure, γ_w is unit weight of water, Ω is position potential height.

The value of $h * \gamma_w$ is put into its array

FF(M) : Array of scalar function f , which shows yield surface in an elasto-plastic material

$$f = MD \ln \frac{p'}{p'_0} + D \eta'$$

ISTATE(M) : Array of flags which show the stress state of element

ISTATE(M)	Elasto-visco plastic material	Elasto plastic material	Joint element
1			
2	elastic region	elastic region	not yield
3	elasto-visco plastic	elasto-plastic	shearing yield
4	failure	failure	exfoliation
5	$p' < 0$	$p' < 0$	

other elements are dealt with linear elastic material

ISTATE(M)=1

VP(M) : Array of visco-plastic part of volumetric strain of element

VOID(M) : Array of void ratio

TIME : Elapsed time

DTIME : Incremental time in each step

COMMON/C/

XY(N,2) : Array of (x,y) or (r,z) coordinates of nodal points

GXY(M,2) : Array of (x,y) or (r,z) coordinates of center of gravity of element

NOD(M,6) : Array of numbers of nodal points constituting an element and characteristics of the element

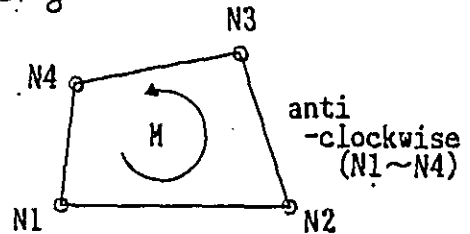
Array	NOD(M,1)	NOD(M,2)	NOD(M,3)	NOD(M,4)	NOD(M,5)	NOD(M,6)
contents	N1	N2	N3	N4	MM	MT

N1,N2,N3,N4 are ^{the} number of nodal points consisting the element

M is the number of the element

MM is the number of material

MT is the number of ^{the} sorts of _{the} element



MT	0	1	2	3
sorts of element	elasto-(visco) plastic plane element	linear elastic plane element	linear elastic beam element	linear elastic truss element
analysis condition	Axi-symmetric		Plane strain	

4	5
elastic-perfect plastic joint element	linear elastic shell element
Axi-symmetric	
Plane strain	

MT Array	0	1	2	3	4	5
EYM(MM.1)	D	$\tilde{\lambda}$	E	E	K_s	E
EYM(MM.2)	Λ	$\tilde{\mu}$	A	A	K_s	h
EYM(MM.3)	M	σ'_{v1}	I		σ'_{v1}	ν
EYM(MM.4)	ν'	k_x			k_x	
EYM(MM.5)	k_x/γ_s	k_x/γ_s			C	
EYM(MM.6)	k_y/γ_s	k_y/γ_s			$\tan \phi$	
EYM(MM.7)	σ'_{v0}					
EYM(MM.8)	k_0					
EYM(MM.9)	σ'_{v1}					
EYM(MM.10)	k_1					
EYM(MM.11)	α					
EYM(MM.12)	\dot{v}_0					
EYM(MM.13)	λ					
EYM(MM.14)	e_0	e_1				
EYM(MM.15)	λ_s	λ_s				

remark

D : coefficient of dilatancy proposed by Shibata (1963)

Λ : irreversibility ratio as $\Lambda = 1 - k/\lambda$

M : critical state parameter

ν' : effective Poisson ratio

k_x, k_y : coefficient of permeability

σ'_{v0} : preconsolidation vertical stress

k_0 : coefficient of earth pressure at rest in preconsolidation

σ'_{v1} : effective overburden pressure

k_1 : coefficient of earth pressure at rest in situ

α : coefficient of secondary compression

\dot{v}_0 : initial volumetric strain rate of secondary compression

λ : compression index

e_0 : void ratio at preconsolidation (void ratio in reference state)
 λ_k : gradient of $e \sim \log k/k_0$ relationship
 λ, μ : Lamé's constants (linear elasticity)
 E : Young's modulus
 A : sectional area
 I : moment of inertia of area
 k_s : shearing stiffness of joint
 k_n : normal stiffness of joint
 σ_{v1} : overburden pressure
 C : cohesion stress
 $\tan \phi$: gradient of internal friction angle ϕ
 h : thickness of shell element

GMW Weight of unit volume of water

WPZ Height of reference of position potential

COMMON/D/

F(LLNEL) Array of load vector including the equation of water continuity

BODY(M) Array of unit weight γ of the loading element

FORCE(M) Array of applied normal forces

WB(M) Array of height of total head of boundary, where housing as $h * \gamma$.

COMMON/E/

HATER(MM) : Array of material numbers

NEXCA(N) : Array of flag whether the nodal point N is made use of or not in each step

MEXCA(M) : Array of flag whether the element M is made use of or not at a step

NCOND(N,3) : Array of restriction conditions of the nodal point N

Array	NCOND(N,1)	NCOND(N,2)	NCOND(N,3)	NCOND	0	1
direction of restriction	x(r)	y(z)	rotation θ	Contents	free	Compelled displacement

remark : anti-clockwise is positive

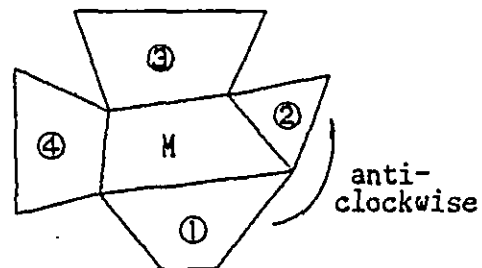
MDRN(M,4) : Array of drainage boundary conditions of 3 or 4 sides of the element M

MDRN(M,1) between M and ①

MDRN(M,2) between M and ②

MDRN(M,3) between M and ③

MDRN(M,4) between M and ④



where $ic = MDRN(M,i)$, $i = 1,4$

ic	1~4	-1~-4	11~14
contents	drained condition corresponding to permeability	undrained condition (not allowed pore water to flow)	changing undrained to drained condition

NKIND(N) : Array of flag whether nodal force is loaded with the nodal point N or not

NKIND(N)	0	1
nodal force	not applied	applied

MKIND(M) : Array of flag for judging whether the element M is applied as load of body force

MKIND(M)	0	1
element M	not applied	applied

COMMON/F/

JP(N) : Array of degree of freedom of the nodal point N

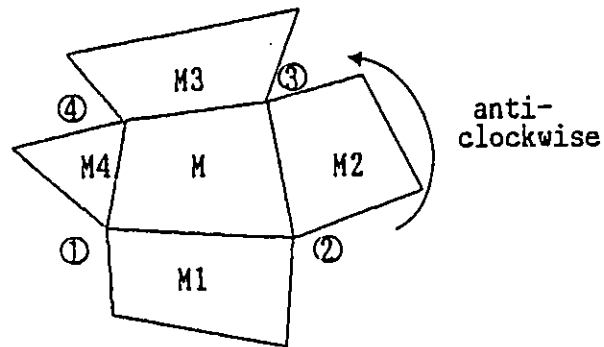
JE(M) : Array of flag, which indicates the number of nodal points corresponding with the element M [^]the

remark :

In the case of coupling analysis, the extended total stiffness matrix consists of soil structure parts and pore water flow parts. Displacements and forces of soil structure parts correspond with nodal points, on the other hand total head and flux of pore water flow correspond with elements.

So that it is necessary to combine the number of element and one of nodal point.

NAEL(M,4) : Array of number of elements which enclose the element M



where

NAEL(M,i) = 0 : undrained boundary

= -1 : drained boundary

JPE(M) : Array of order number of unknown total head ($h + \gamma \cdot$) among the unknown vector in the extended total stiffness equation

$$\begin{array}{c} \left(\begin{array}{c} \\ \\ \\ \end{array} \right) \\ \text{load vector} \end{array} = \begin{array}{c} \left(\begin{array}{c} \text{extended} \\ \text{total stiffness} \\ \text{matrix} \end{array} \right) \cdot \begin{array}{c} \left(\begin{array}{c} \vdots \\ h_M \\ \vdots \\ \gamma \cdot \end{array} \right) \\ \text{unknown vector} \end{array} \downarrow \text{JPE(M)}
 \end{array}$$

JPP(N,3) : Array of order numbers of unknown displacements
 $(\Delta u, \Delta v, \Delta \theta)$ among the unknown vectors in the extended
total stiffness equation.

$$\begin{array}{c} \left[\begin{array}{c} \\ \\ \end{array} \right] \\ \text{load vector} \end{array} = \begin{array}{c} \left[\begin{array}{c} \text{the extended} \\ \text{stiffness} \\ \text{equation} \end{array} \right] \cdot \begin{array}{c} \left[\begin{array}{c} \vdots \\ \Delta u_N \\ \Delta v_N \\ \Delta \theta_N \\ \vdots \end{array} \right] \\ \text{unknown} \\ \text{vector} \end{array}
 \end{array}$$

where Δu_N incremental displacement of the nodal point N
in x(r)-direction

Δv_N incremental displacement of the nodal point N
in y(z)-direction

$\Delta \theta_N$ incremental rotation of the nodal point N
(anti-clockwise is positive)

COMMON/G/

ALPH(M) : Array of components concerned with permeability of pore
water flow in the stiffness equation

DRAIG(M,4) : Array of variables meaning permeability of pore water flow
between boundaries surrounding the plane element M

CRITIC(M) : Array of values of scalar function employed as failure
criteria

$$f_{critic} = M - \frac{3}{2\eta} \eta_{k1} (\eta_{r1} - \eta_{k10})$$

COMMON/H/

- B(4,8) : Matrix of displacements and strain relationship of a \hat{n} element
- DB(4,8) : Matrix of displacements and effective stress relationship of a element
- FEM(8,8) : Elementary stiffness matrix
- DEP(M,4,4) : Matrix of incremental stress and strain relationship of the plane element M
- ARE(M) : Array of area of the plane element M

COMMON/I/

- DUVT(N,3) : Array of incremental displacements given by solving the extended total stiffness equation

DUVT(N,1)	DUVT(N,2)	DUVT(N,3)
ΔU_N	ΔV_N	$\Delta \theta_N$
in x(r)- direction	in y(z)- direction	anti-clockwise is positive

- UVT(N,3) : Array of displacements given by superposing incremental displacements \hat{im}

UVT(N,1)	UVT(N,2)	UVT(N,3)
U_N	V_N	θ_N
$U_N = \Sigma \Delta U_N$	$V_N = \Sigma \Delta V_N$	$\theta_N = \Sigma \Delta \theta_N$

COMMON/J/

GS(LLNEL,MAXBAN) : Extended total stiffness matrix deformed by Band method

COMMON/K/

IWRITE(4) : Output control flags

IPSN : Control flag^{for} judging whether plane-strain condition (IPSN=0) or axi-symmetric condition (IPSN=1)

ICON : Control flag^{for} judging whether coupling analysis (ICON=0) or not

IPLAS : Control flag meaning the kinds of analysis

IPLAS=0	IPLAS=1
considering	not considering
viscosity of	viscosity of
soil materials	soil materials
elasto-visco	elasto-plastic
plastic analysis	analysis

IEXC : Control flag^{for} considering whether pore water pressure or not at excavation expressed as removing the elements

IEXC=0	The equivalent nodal forces are calculated from total stress of the element removing at excavation
IEXC=1	The equivalent nodal forces are calculated from effective stress of the element removing at excavation

ISTEP : Step number in incremental F.E. scheme

COMMON/M/

ICHECK(10) : Array of control flags for checking output

COMMON/N/

EPS(M,5) : Array of strain components of the plane element M

DPS(M,5) : Array of incremental strain components of the plane element M

EPS(M,1)	EPS(M,2)	EPS(M,3)	EPS(M,4)	EPS(M,5)	
ϵ_x or ϵ_r	ϵ_y or ϵ_s	γ_{xy} or γ_{rs}	- ϵ_θ	ϵ_v	plane strain axi-symmetric

DPS(M,1)	DPS(M,2)	DPS(M,3)	DPS(M,4)	DPS(M,5)	
$\Delta \epsilon_x$ or $\Delta \epsilon_r$	$\Delta \epsilon_y$ or $\Delta \epsilon_s$	$\Delta \gamma_{xy}$ or $\Delta \gamma_{rs}$	- $\Delta \epsilon_\theta$	$\Delta \epsilon_v$	plane strain axi-symmetric

COMMON/O/

TF(N,3) : Array of the equivalent nodal forces of the nodal point N

DF(N,3) : Array of the incremental equivalent nodal forces of the nodal forces of the nodal point N

TF(N,1)	TF(N,2)	TF(N,3)	DF(N,1)	DF(N,2)	DF(N,3)
f_x or f_r	f_y or f_s	M	Δf_x or Δf_r	Δf_y or Δf_s	ΔM

NNGS(N) Array of flags indicating whether equivalent nodal forces of the nodal point N are calculated or not.

NNGS(N)	contents
0	calculated
1	not calculated

COMMON/P/

PWB(M) : Array of total water head (housing as $h * \gamma_w$) of previous step

SIGB(M) : Array of stress components of previous step

JIRM(M) : Array of flags for judging iteration

VPI(M) : Array of viscoplastic volumetric strain of previous step

DATA definition of the capacity of the program DACSAR

MAXNOD : Maximum number of nodal points (400)

MAXNEL : Maximum number of elements (300)

MAXMAT : Maximum number of kinds of material properties (50)

MAXBAN : Maximum band width

IFLNG : Maximum length of unknown vectors of the extended total stiffness equation

According to the program DACSAR now in use

MAXNOD = 400

MAXNEL = 300

MAXMAT = 50

MAXBAN = 150

IFLNG = 1200

It is possible to extend the capacity of the program

4-6-2

DACSAR CHECK

In this section the computation scheme of DACSAR F.E.M. is verified by comparison with theoretical values obtained in some boundary conditions.

The performed calculations are follows;

- (1) In order to verify the coupling scheme, simulating one-dimensional consolidation tests (oedometer tests) under both plane-strain and axi-symmetric conditions are employed and compared with one-dimensional theoretical solutions given by Terzaghi.
- (2) In order to verify the constitutive relationship, simulating K_0 -consolidated undrained triaxial compression and extension tests under both plane-strain and axi-symmetric conditions are employed.
- (3) In order to see viscid behavior and to verify its computation, simulating isotropic consolidated undrained creep tests under axi-symmetric condition are employed and compared with theoretical values obtained as numerical solutions of the Runge-Kutta-Gill method.

1. One-dimensional Consolidation

F.E. mesh and parameters used in calculation are summarized in Fig. 1-1. Only the upper boundary is made drained boundary and others are set up as undrained, so that the drainage length H becomes 3.5 cm. The load of $\sigma = 4.0 \text{ kg/cm}^2$ is made to act on the nodal point at the first calculation step in an instance and time is divided into increments to see dissipation of pore water pressure.

Fig. 1-2 and 1-3 show the dissipation of pore water pressure of each element under plane strain and axi-symmetric conditions respectively, where pore water pressure is estimated in the center of elements.

Figs. 1-4 and 1-5 show dissipation of consolidation similar to Figs. 1-2 and 1-3.

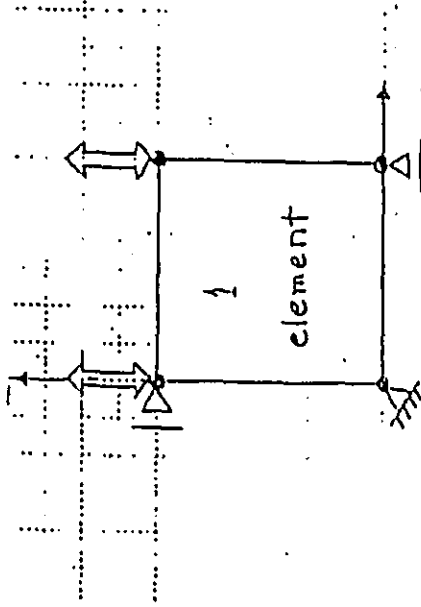
2. Constitutive Relationship

The simulations of K_0 -consolidated undrained triaxial compression and extension shearing tests are performed under plane strain and axi-symmetric conditions.

Sekiguchi-Ohta's constitutive model has two faces.

One is the constitutive equation based on plasticity theory, and the other is the constitutive equation based on flow surface theory which is able to express time dependent behavior. The boundary conditions and input parameters which are set up in order to verify calculation of DACSAR F.E.M. summarized in Fig. 1, where properties of specimen correspond with $PI = 50$ (%).

The results of calculation of the elasto-plastic constitutive model are shown in Fig. 2-2 (a) (b) and Fig. 2-3 (a) (b). Fig. 2-2 (a) (b) are effective stress paths normalized by preconsolidation stress σ'_{v0} , otherwise Fig. 2-3 (a) (b) are stress-strain relationships. In these figures, the results of F.E.M. are shown in figures (a), theoretical values in figures (b).



F. E. mesh

input paramater	its value
D	0.076
$\Delta \left(= 1 - \frac{\kappa}{\lambda} \right)$	0.549
M	0.961
ν'	0.394
σ'_{vo} (kg/cm ²)	1.0
K_o	0.65
σ'_{vz} (kg/cm ²)	1.0
Ki	0.65
α	0.00666
$\dot{\nu}_o$ (1/min.)	4.625×10^{-6}
e_o	0.84
λ	0.245

Fig.2-1 calculation condition

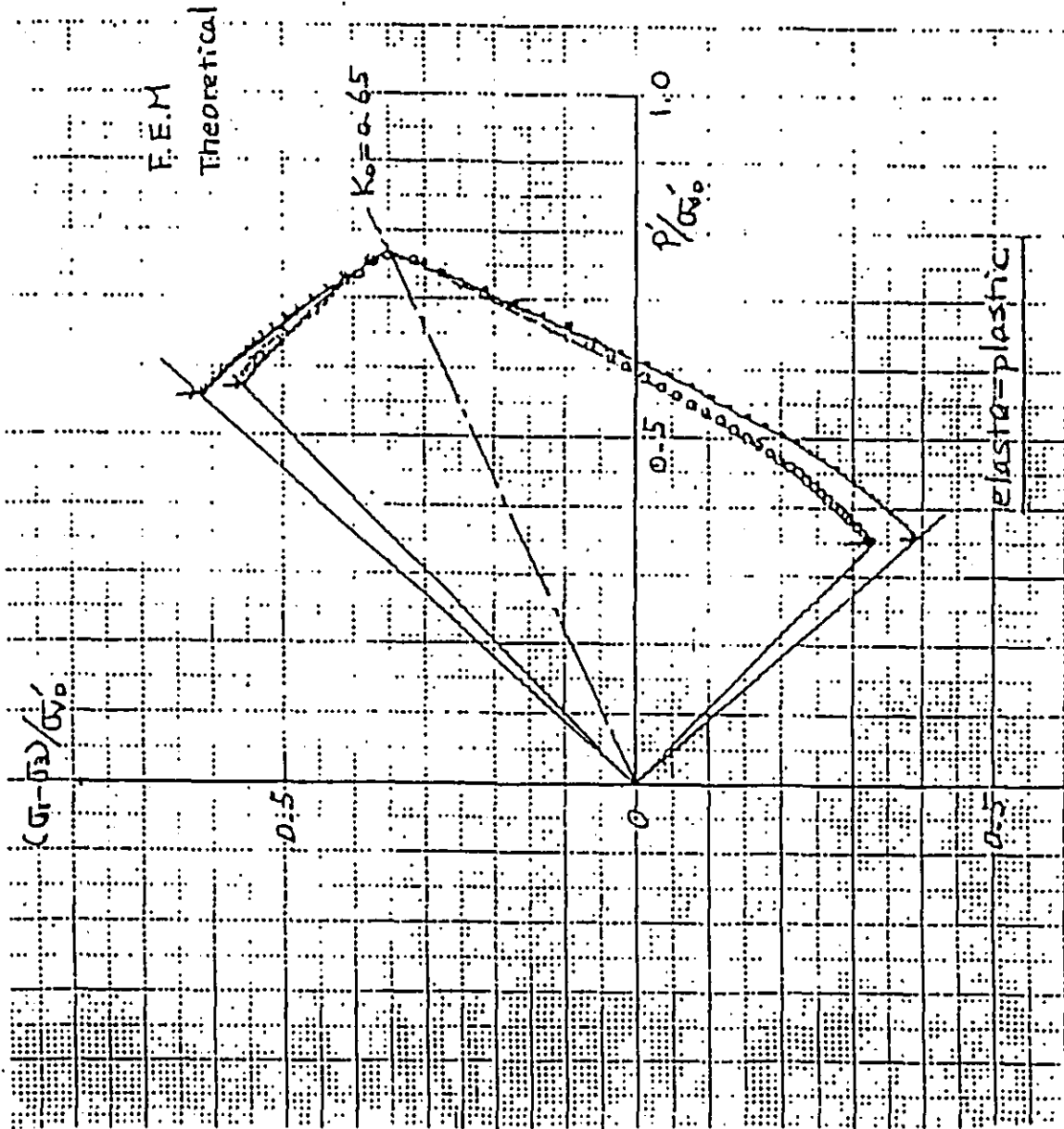


Fig.2-2 (a) (b) F Theoretical values

Fig.2-2 stress-path of elasto-plastic constitutive model

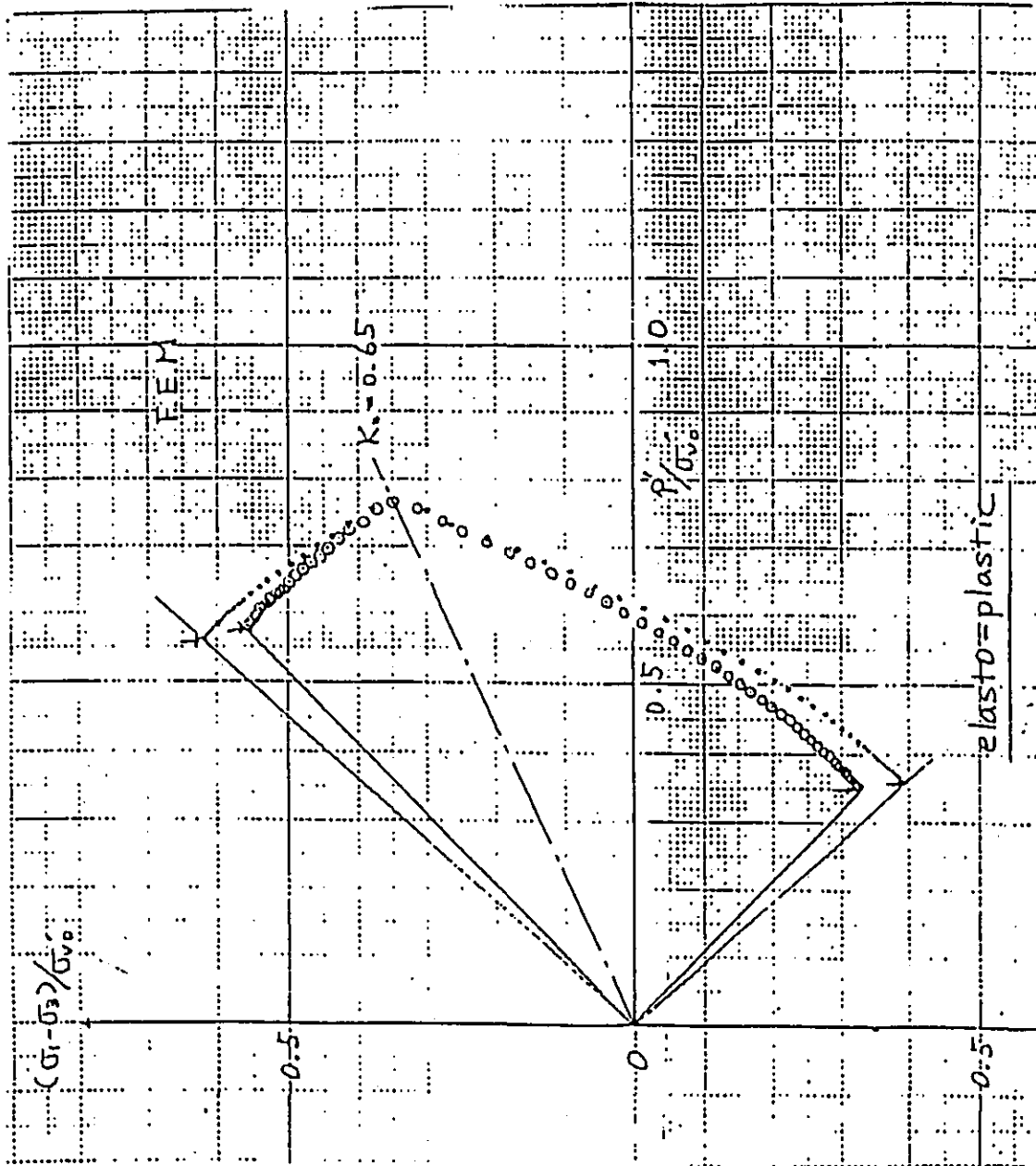


Fig.2-2 (a) F.E.M results

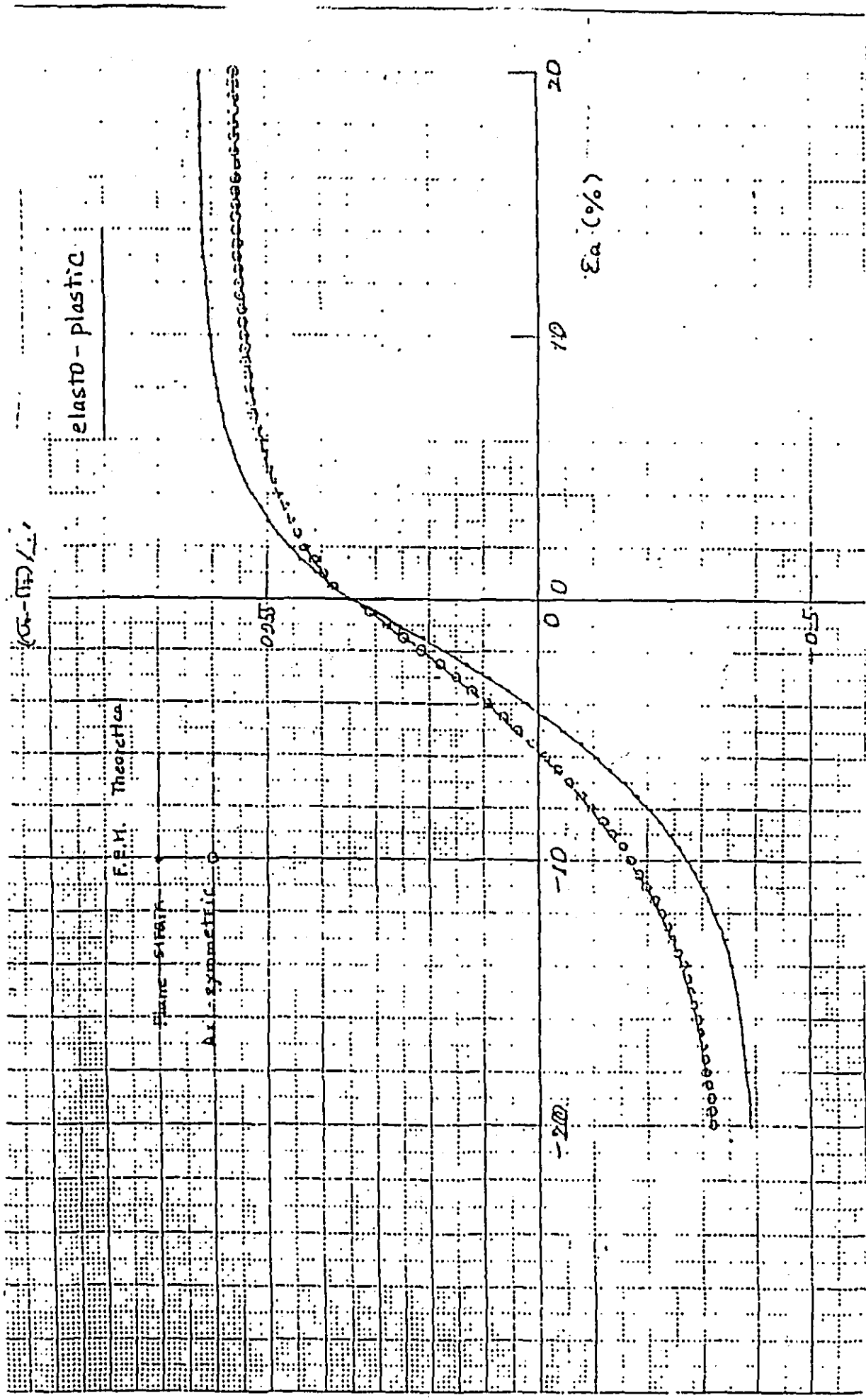


Fig. 2-3 (a) (b) Theoretical values

Fig. 2-2 representation of elasto-plastic constitutive model

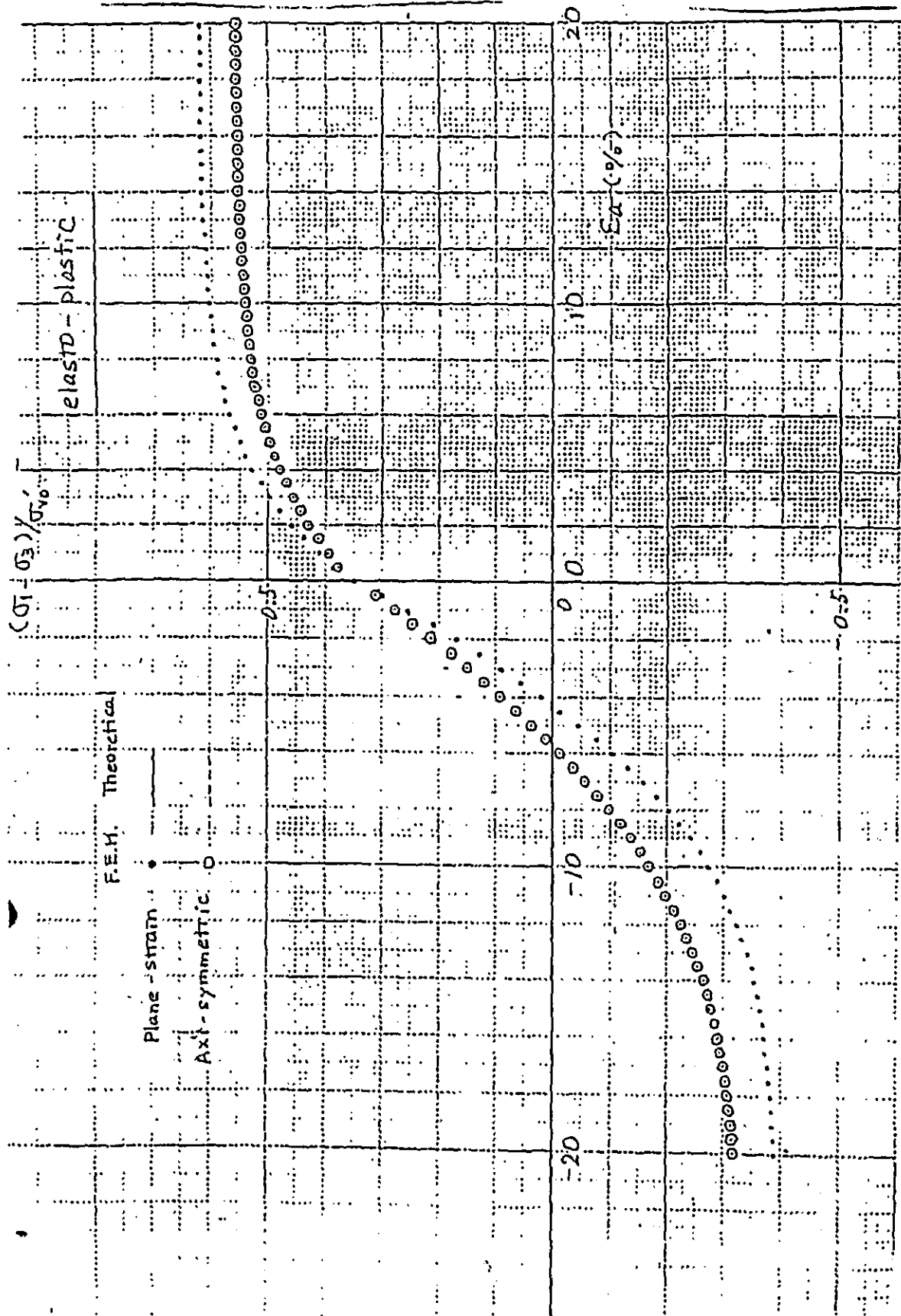


Fig. 2-3 (a) F.E.M results

Fig. 2-4 and Fig. 2-5 indicate the comparison of calculation results of the elasto-viscoplastic constitutive model. Two cases of different shearing rates $\dot{\epsilon}_a = 0.1\%/min.$ and $0.001\%/min$ against plane strain condition and axi-symmetric condition respectively are chosen to see the effect of time dependency.

Fig. 2-4 (a) (b) are effective stress paths normalized by preconsolidation stress σ'_{vo} , otherwise Fig. 2-5 (a) (b) are the stress-strain relationship. The theoretical curves (Fig. 2-4 (b) and Fig. 2-5 (b)) are obtained by numerical calculation of Euler's method but attention must be paid to make sure that the incremental range is made enough small not to accumulate errors.

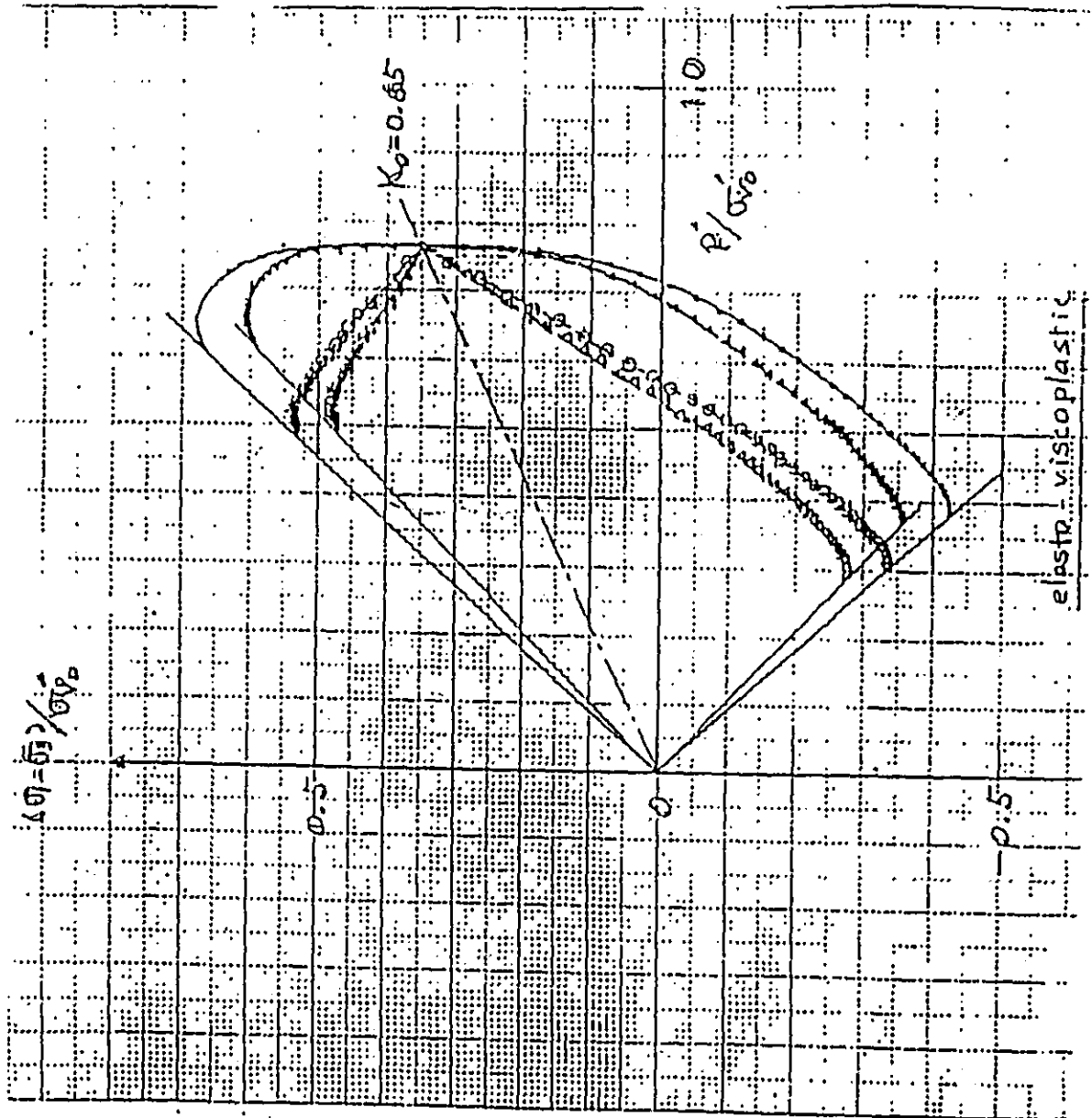


Fig. 2-4 (a) (b) Theoretical values
 Fig. 2-4 Theoretical values of elasto-viscoplastic material model.

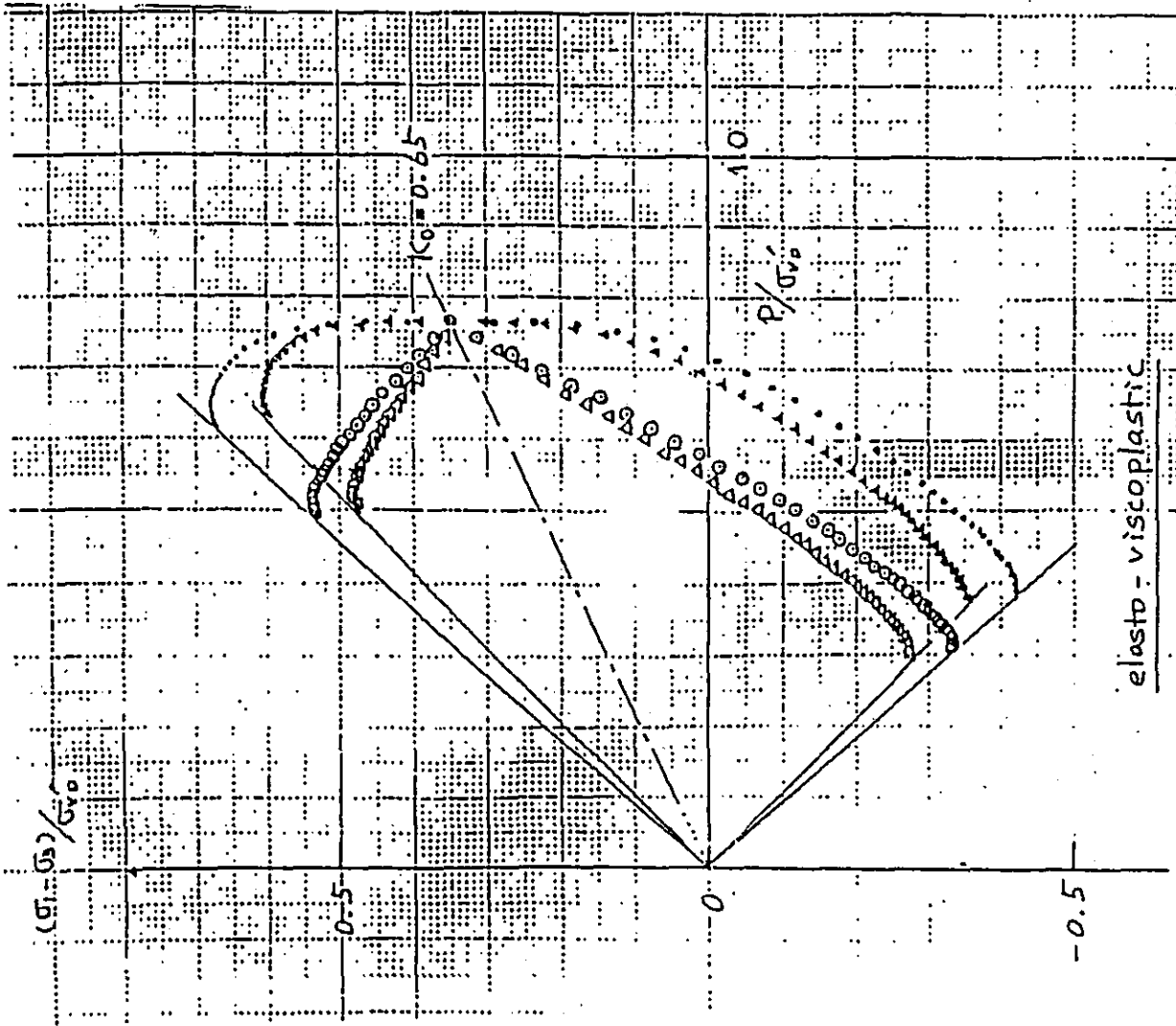


Fig.2-4 (a) F.E.M results

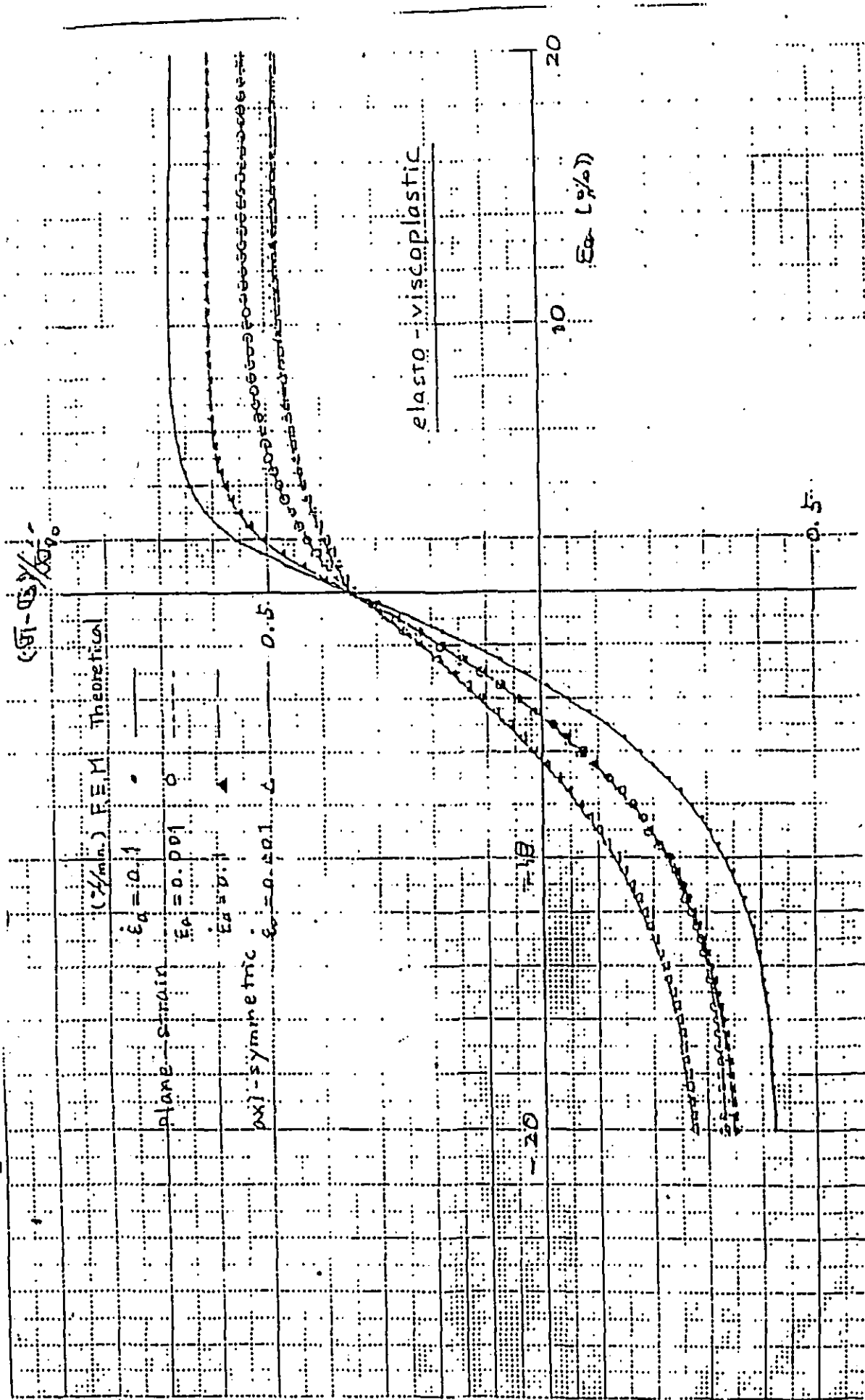


Fig.2-5 (a) (b) Theoretical values

Fig.2-5 stress-strain of elasto-viscoplastic constitutive model

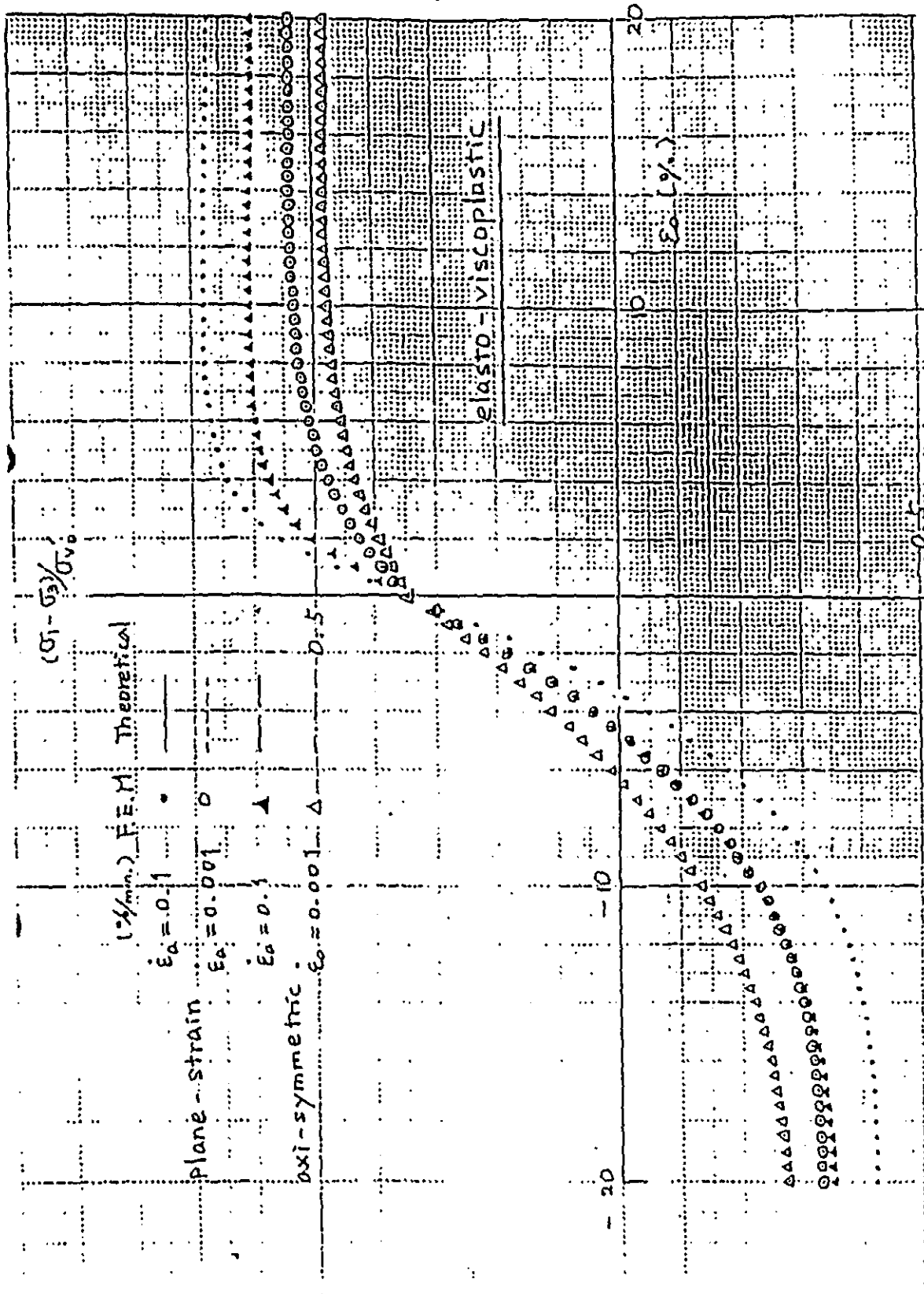


Fig.2-5 (a) F. E. M results

3. Creep Behavior

The simulations of undrained creep are performed by making various loads of q/p_0 act on the isotropically consolidated specimen under axi-symmetric conditions.

The input parameters and F.E. mesh are the same as those used in 2. The relationships of $\log (\dot{\epsilon}_a)$ (1/min.) and $\log (t)$ (min.) are shown in Fig. 2-6 (a) (b), where Fig. 2-6 (a) and (b) are F.E.M results and theoretical values respectively. The stress paths and equivalent elapsing time of creep are shown in Fig. 2-7 (a) (b) and Fig. 2-7 (a) and Fig. 2-7 (b) are F.E.M results and theoretical values respectively.

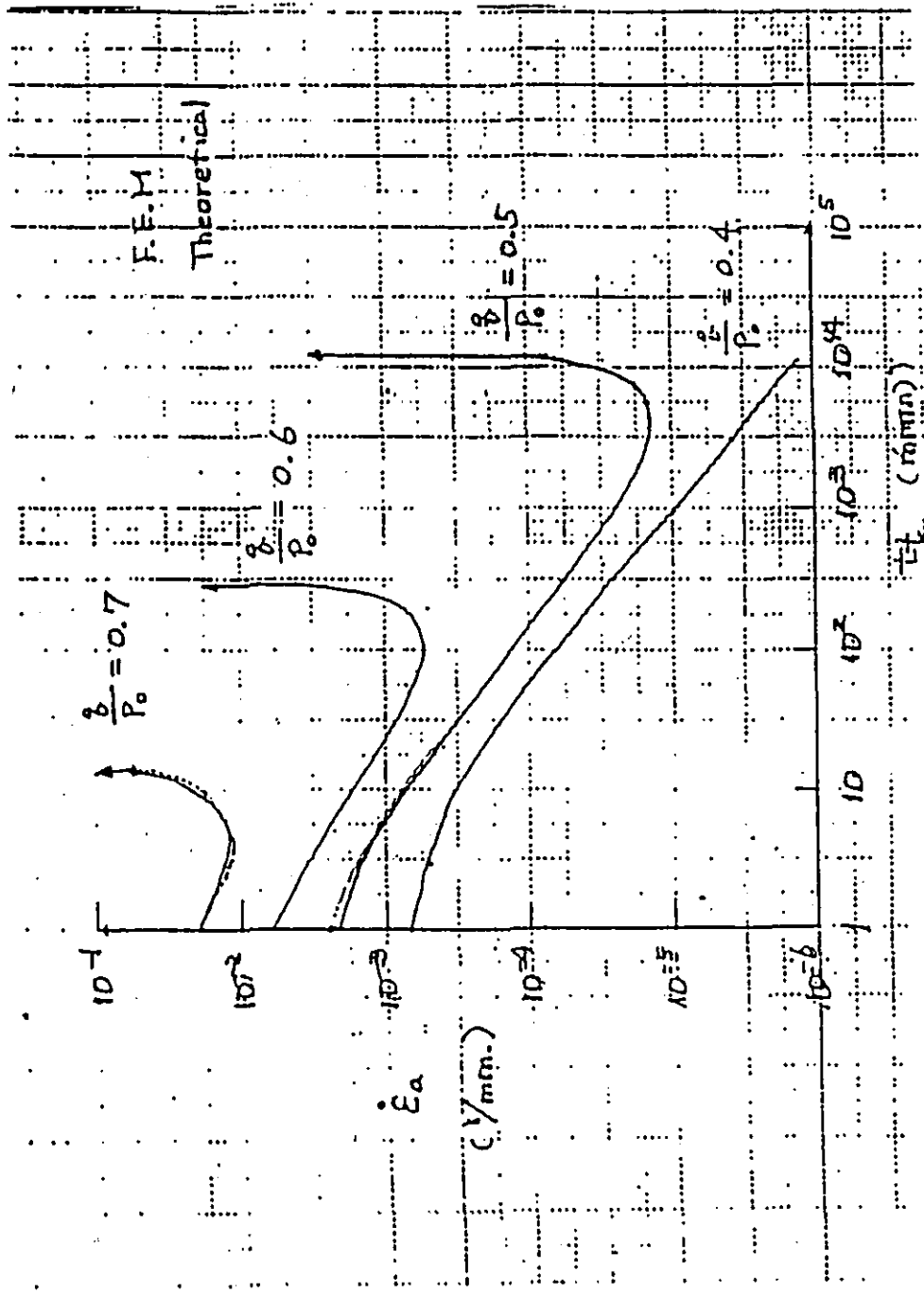


Fig.2-6 (a) (b) Theoretical values

Fig.2-6 log $\dot{\epsilon}_a \sim \log t$ relationship undrained creep

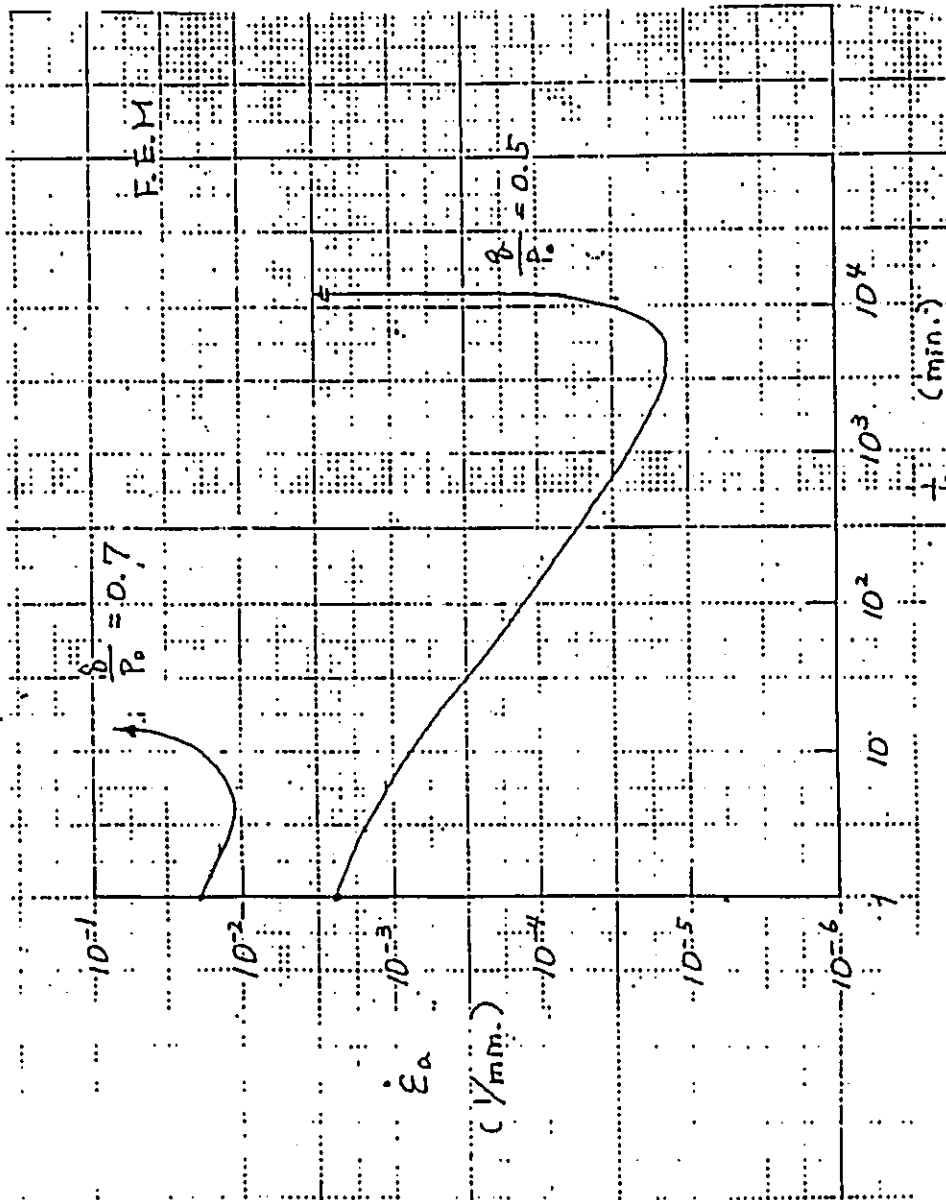


Fig. 2-6 (a) F.E.M results

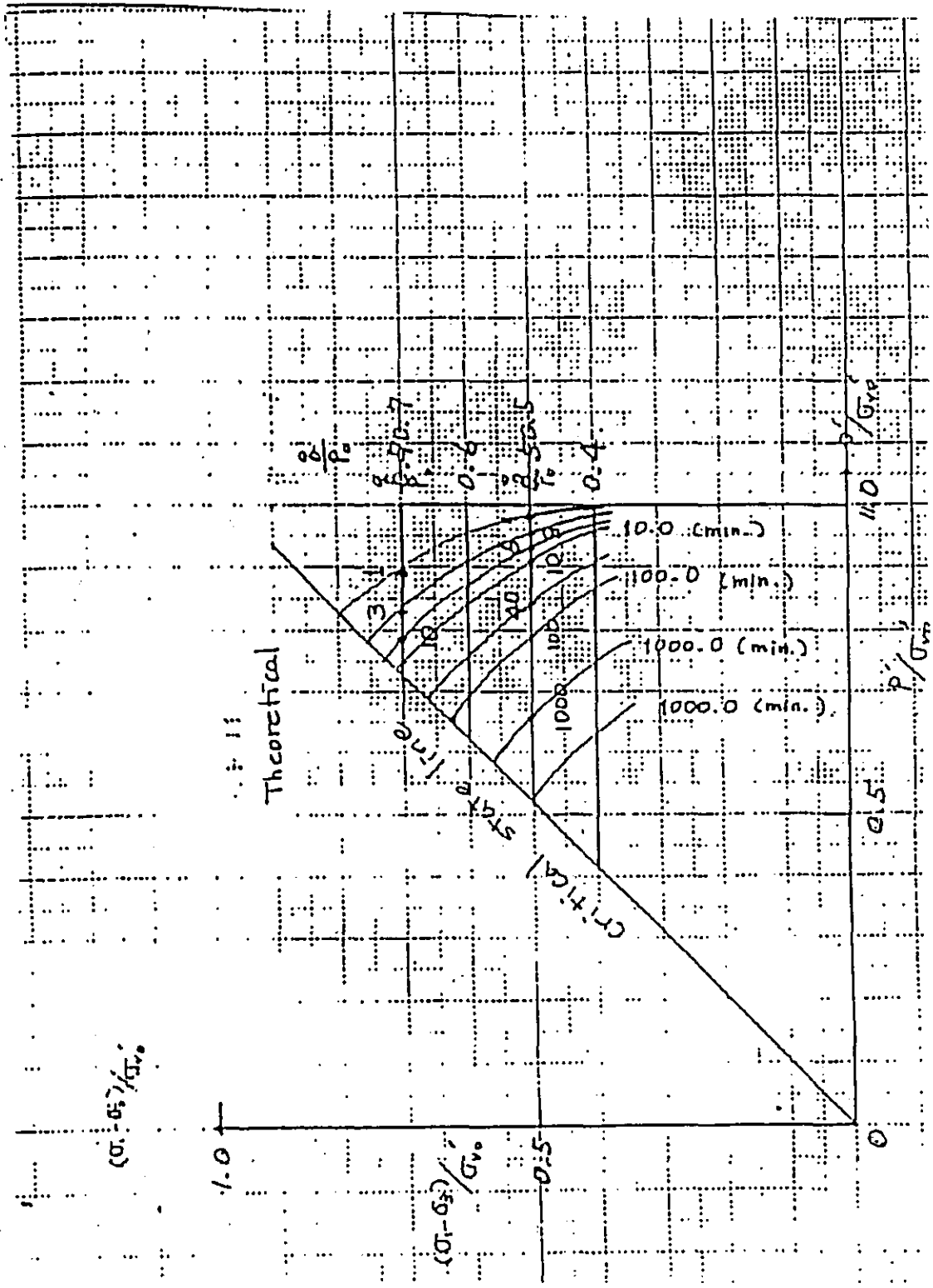


Fig.2-7 (a) (b) Theoretical values

Fig.2-7 stress-paths and equivalent time curves of undrained creep

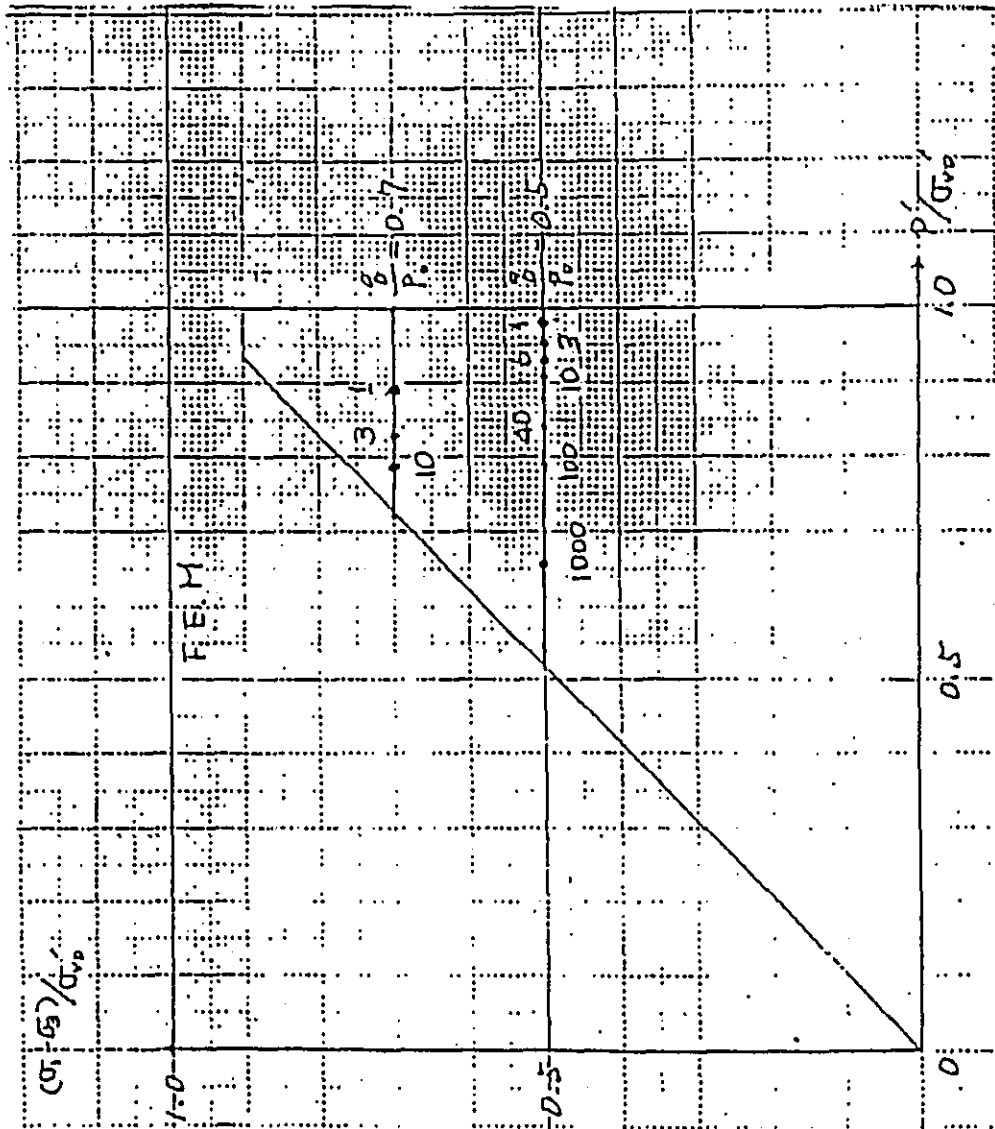


Fig. 2-7 (a) F.E.M results

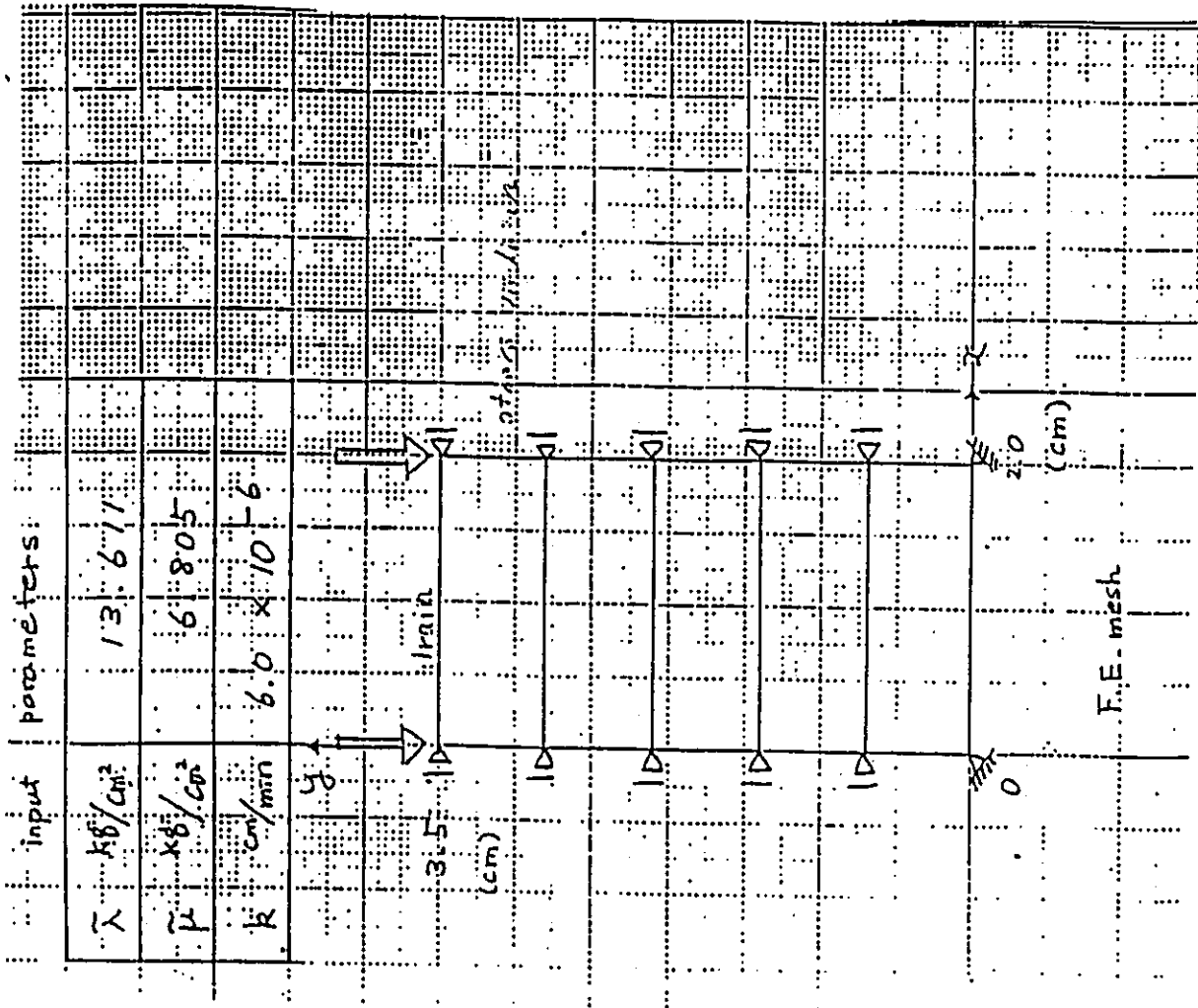


Fig.1-1 problem conditions

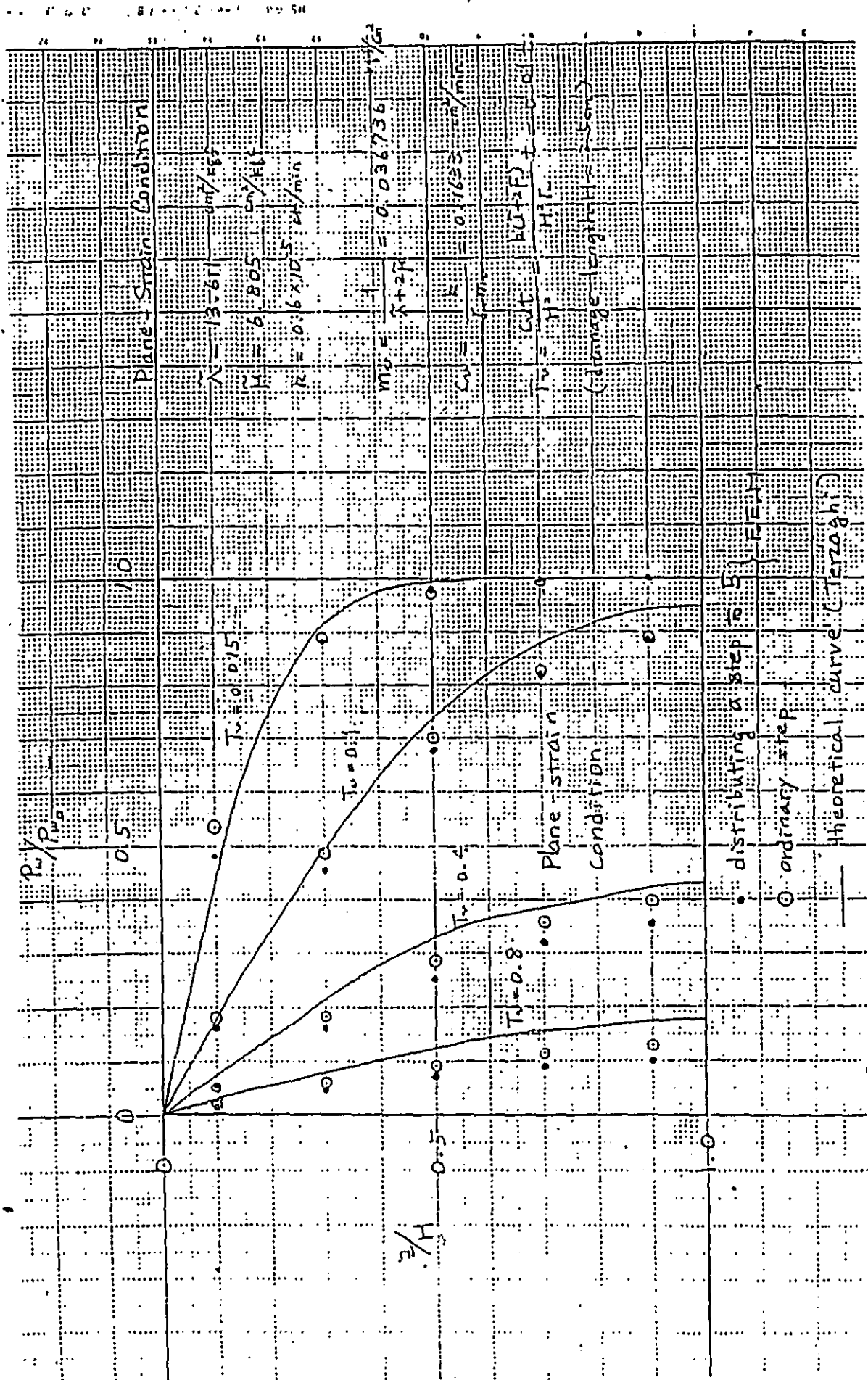


Fig.1-2 dissipation of pore water pressure

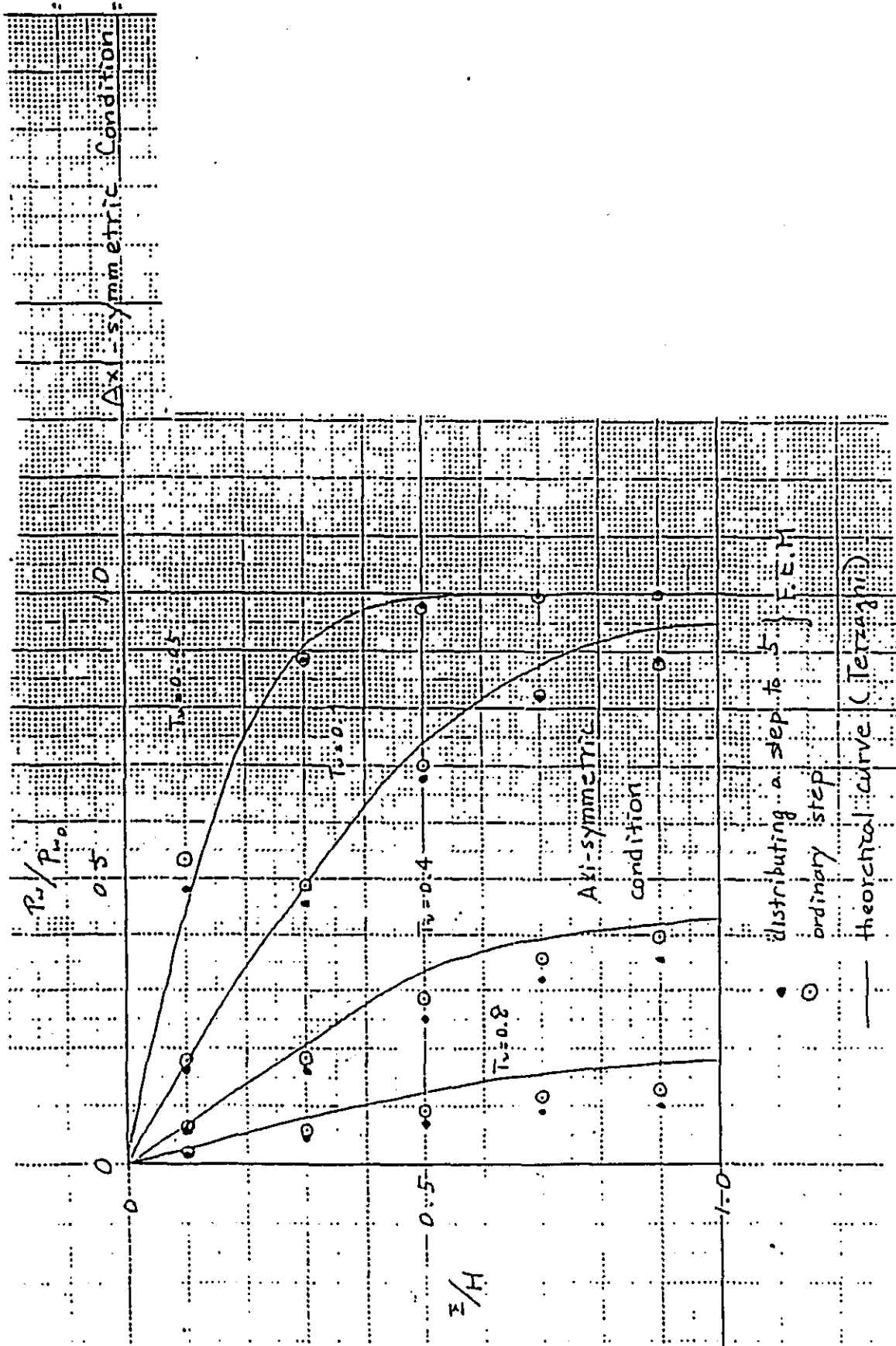


Fig.1-3 dissipation of pore water pressure

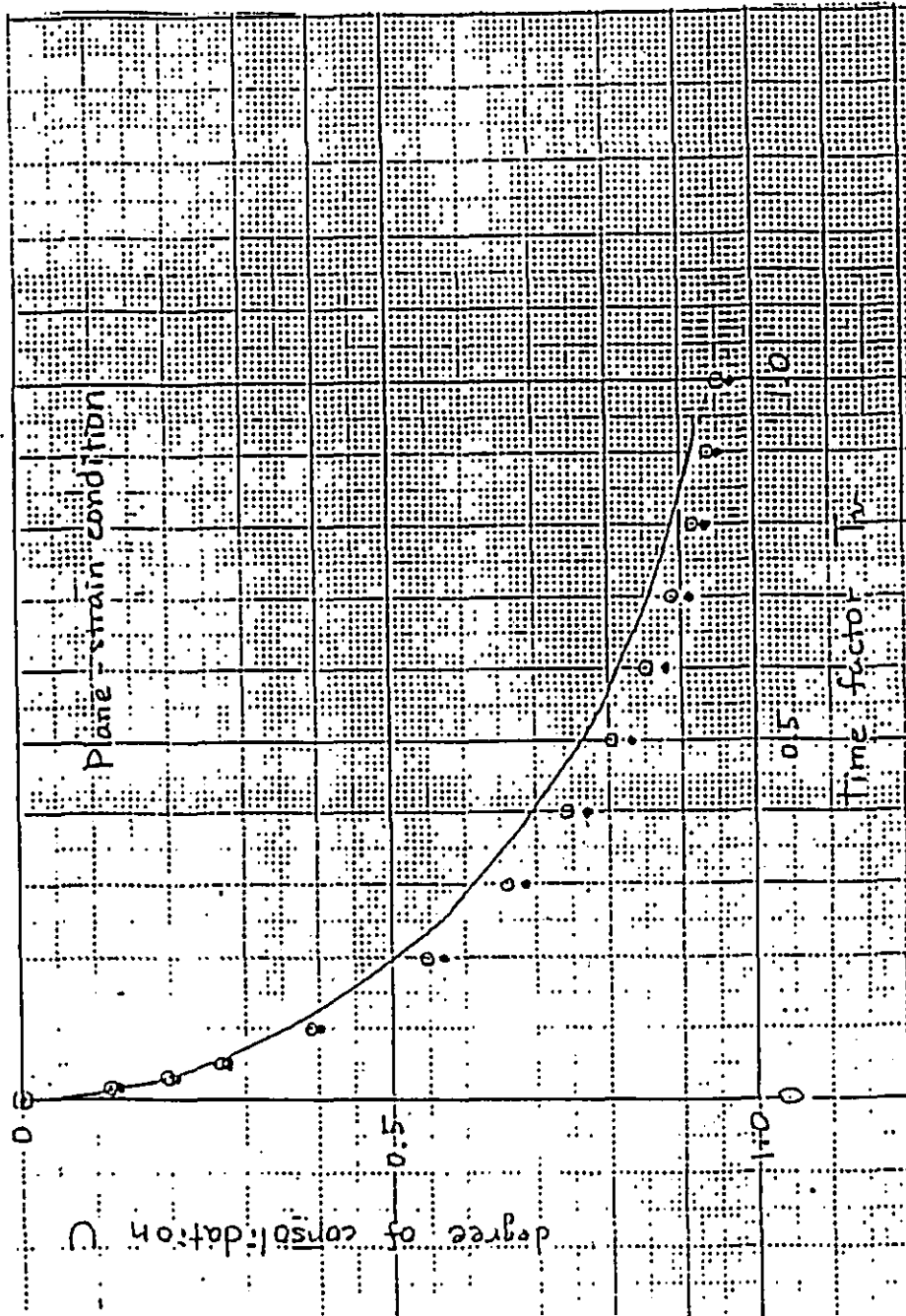


Fig. 1-4 dissipation of consolidation

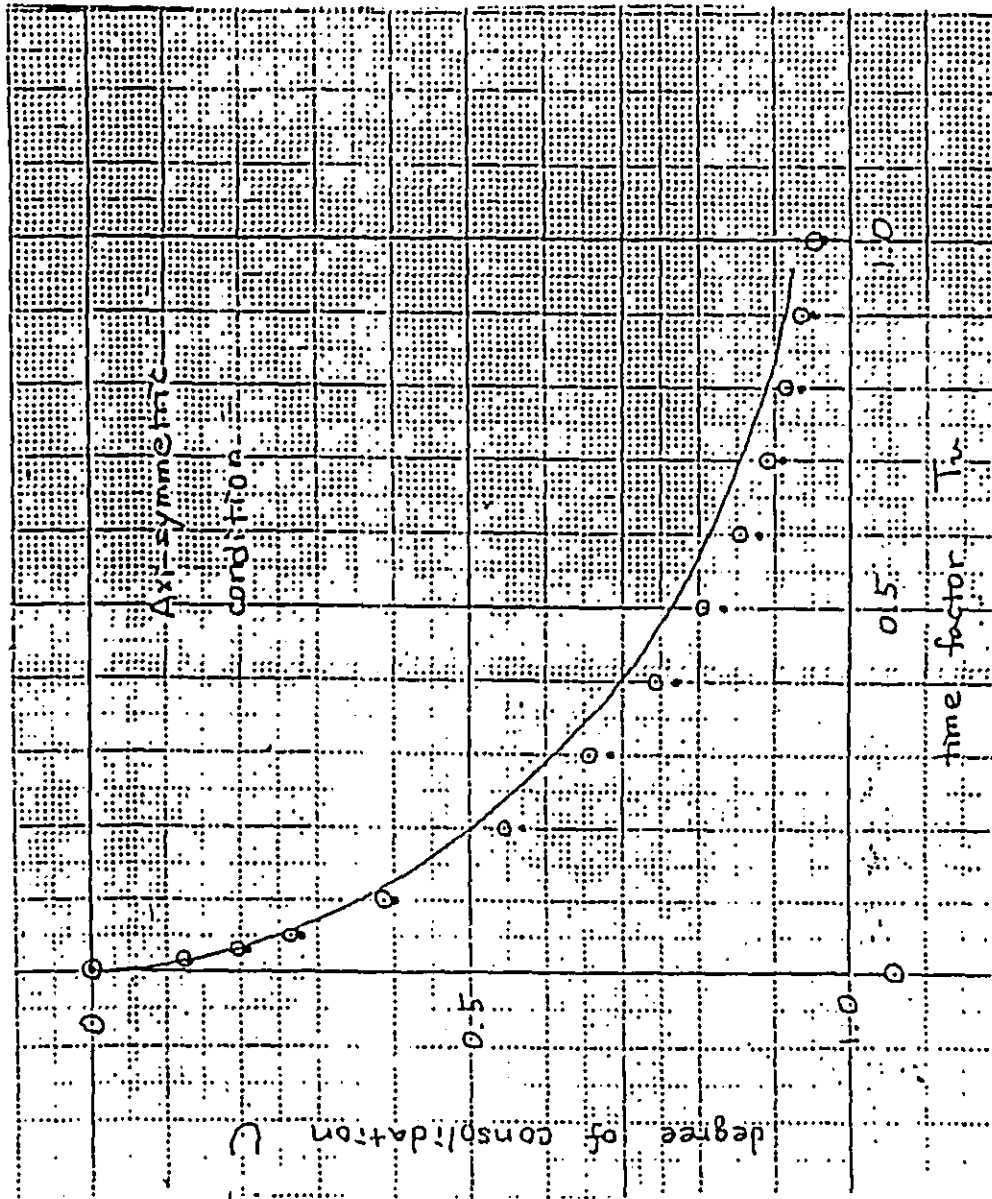


Fig. 1-5 dissipation of consolidation

Practical Example

1. Introduction

Here we now take up the construction site shown in Fig. 1 as a practical example. The hill is constructed first of all and then the trench is excavated near the foot of hill after setting up the sheet piles in the accumulating layers as shown in Fig. 1.

The construction procedure of this site and F.E. simulation of it are indicated in Table.1.

Soil properties of the ground are summarized in Fig.2, provided that clay layers and sand layers are considered as respectively elasto-vicoplastic material and linear elastic material.

Input parameters needed in computation are listed in Table 2, herein input parameters concerning with clay layers are estimated from the value of plasticity index.

In Fig. 3 and Fig. 4 data of F.E. mesh are shown.

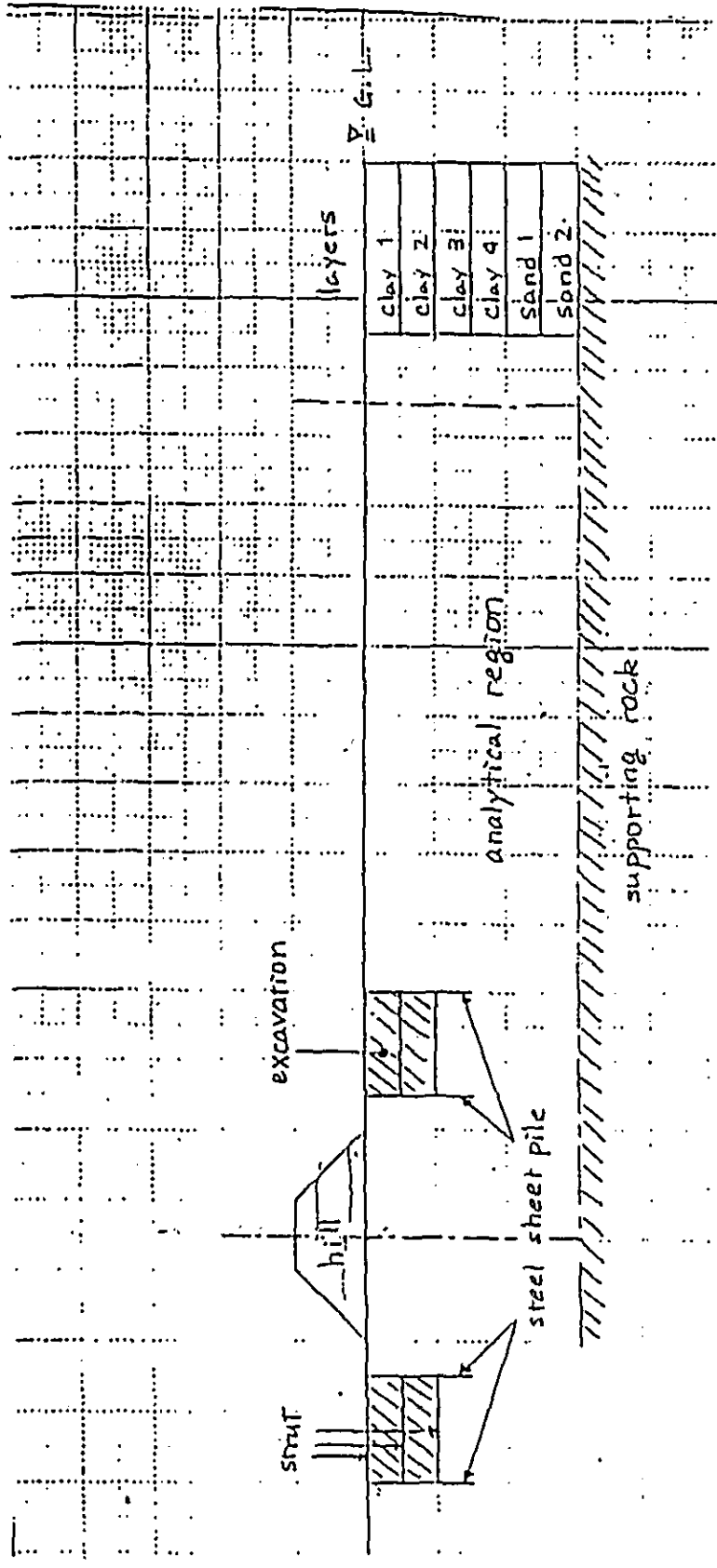


Fig.1 profile of imaginary construction site.

Table 1. construction procedure and F.E.M simulation of it.

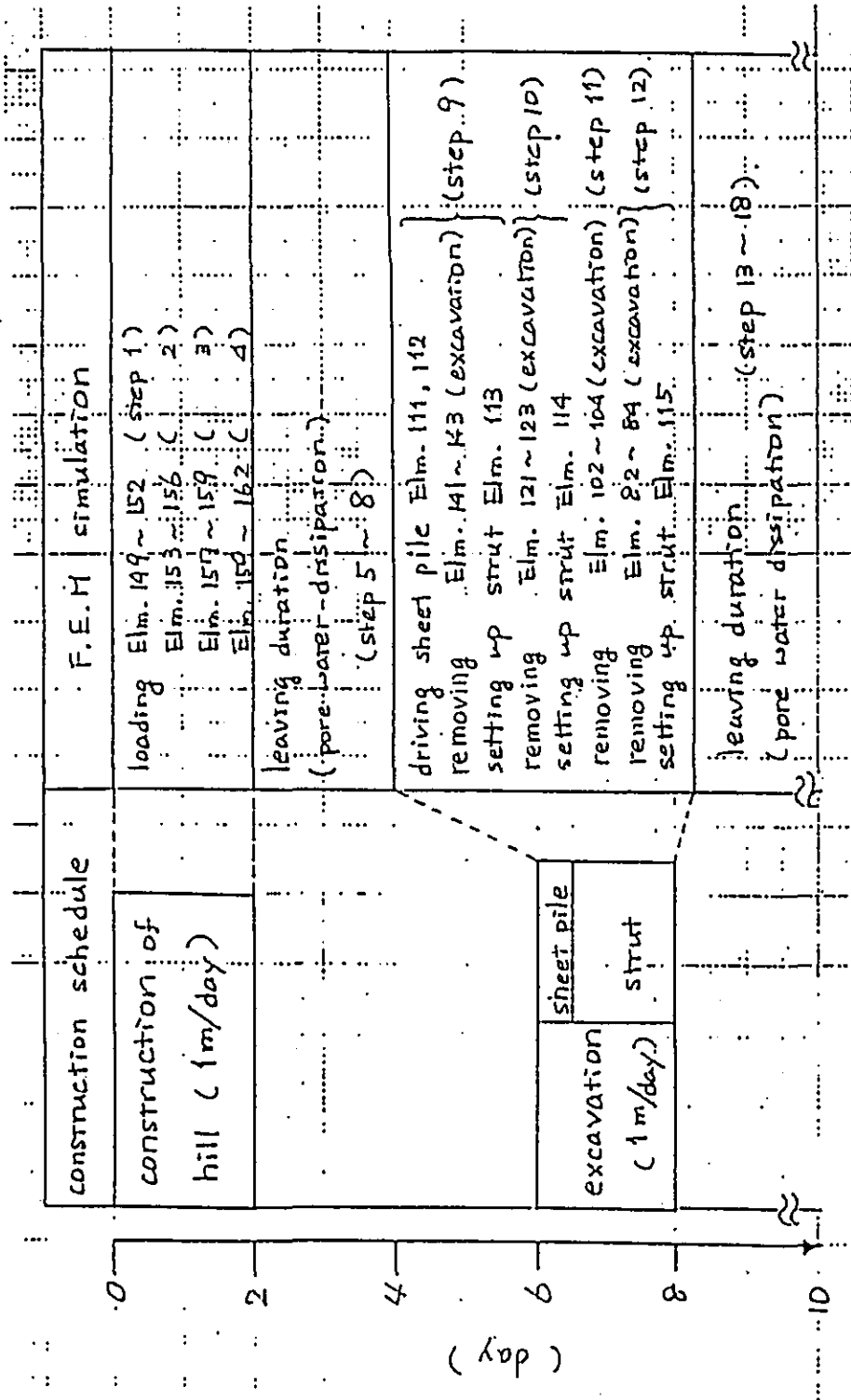


Table 2. List of input parameters.

Layer	M	α	λ	ν	ν'	ν_0	σ_{v_0}	σ_{v_0}'	K_0	K	ν_0	Order	
Clay 1	0.961					1.43×10^{-3}	2.0	0.3	1.28	0.0202		6	
Clay 2	PI = 50	$\lambda = 0.549$	$\nu = 0.076$	$\nu' = 0.394$	$\alpha = 0.00666$	1.57×10^{-4}	2.0	0.9	0.86	0.0055		5	
													$K_0 = 0.65$
Clay 3						1.57×10^{-4}	2.0	1.5	0.72	0.0040		4	
Clay 4						1.43×10^{-4}	2.0	1.0	0.65	0.0030		3	
Sand 1								2.7	0.65	0.05	865.1	5.76-9	2
Sand 2								3.3	0.65	0.05	1442.3	961.5	1
<p>Hill is $\sigma = 1.5 \text{ (t/m}^2\text{)}$ $E = 500$</p>												10	
<p>Beam: $A = 0.0062$ $E = 2.1 \times 10^7$ $I = 0.0055$ $\nu = 0.3$</p>												8	
<p>Truss: $A = 0.00795$ $E = 2.1 \times 10^7$</p>												9	

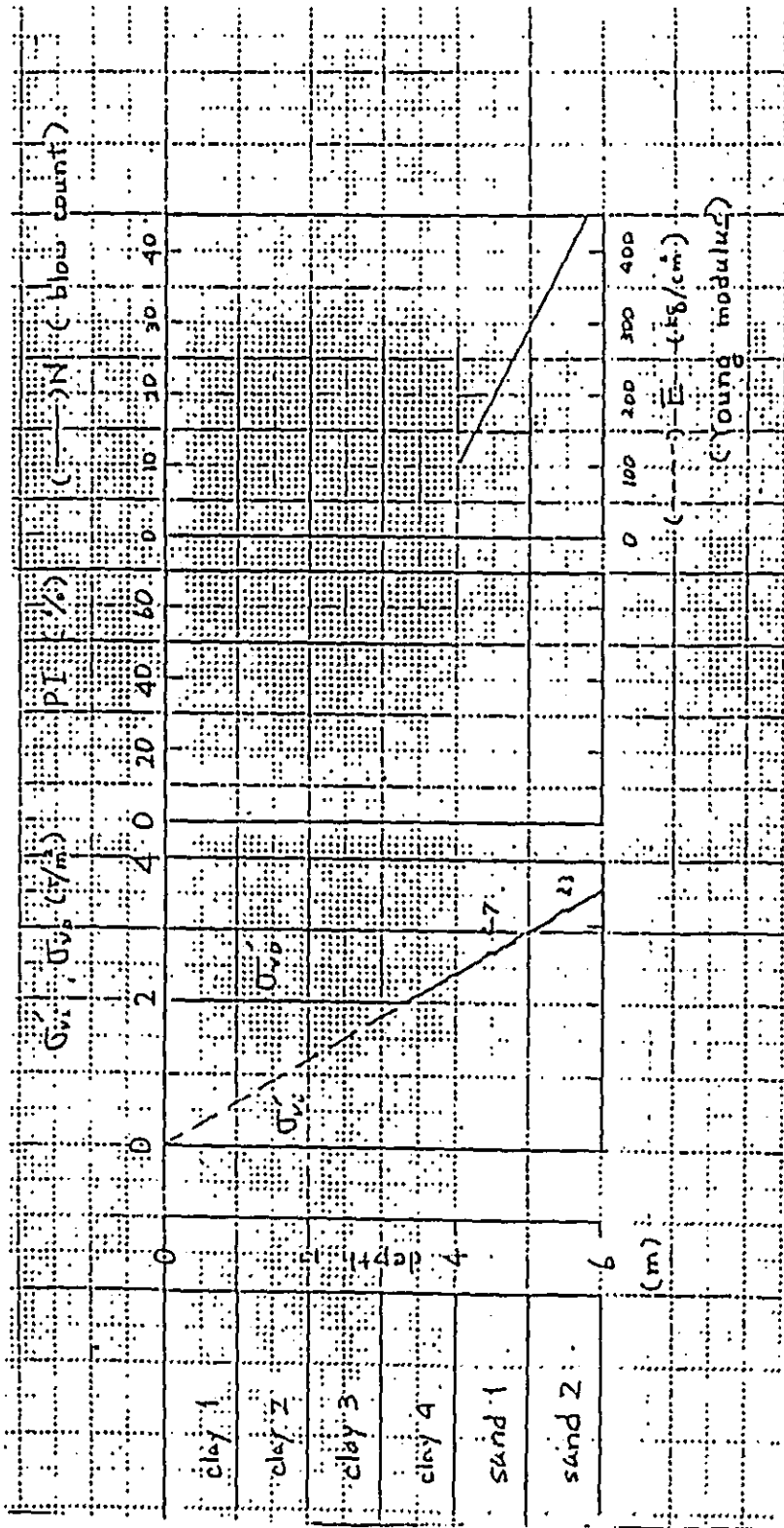


Fig. 2 soil properties

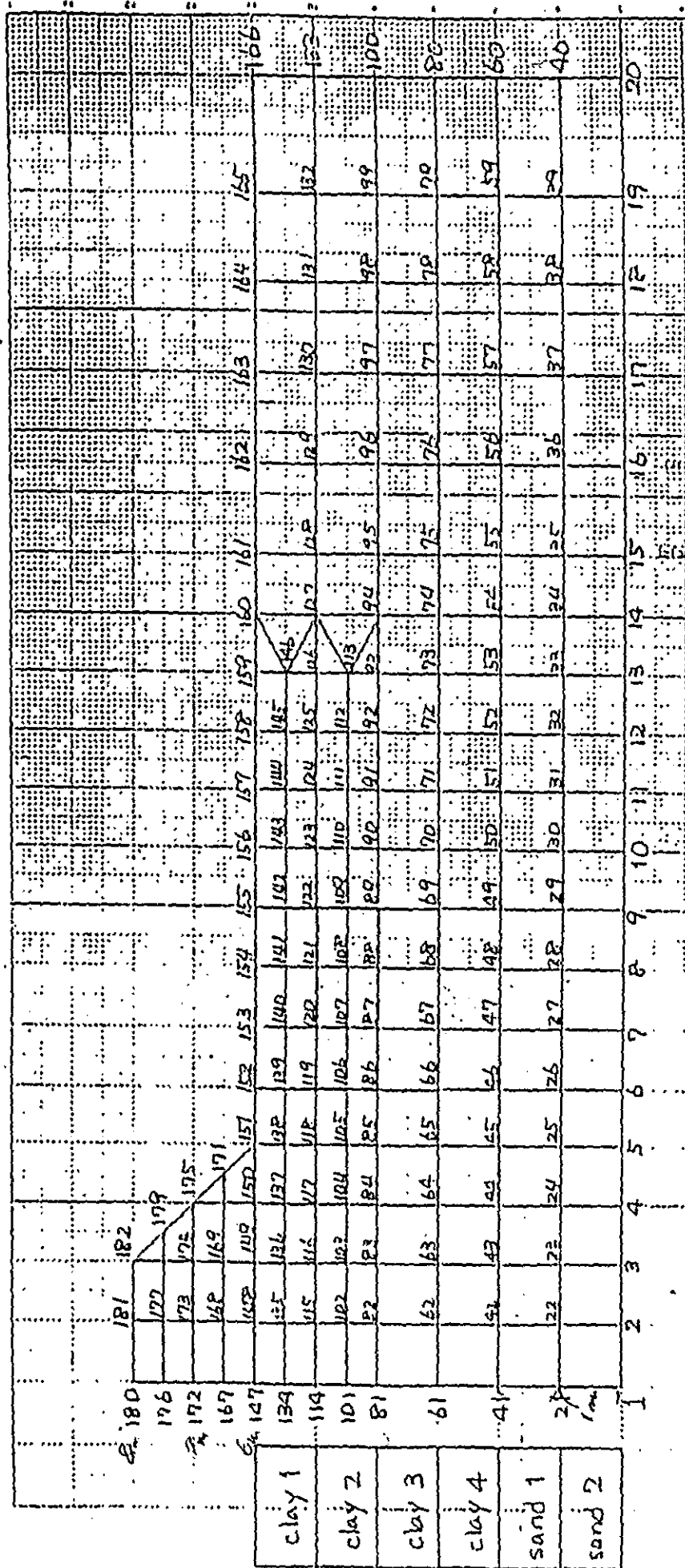


Fig. 3 the number of nodal points

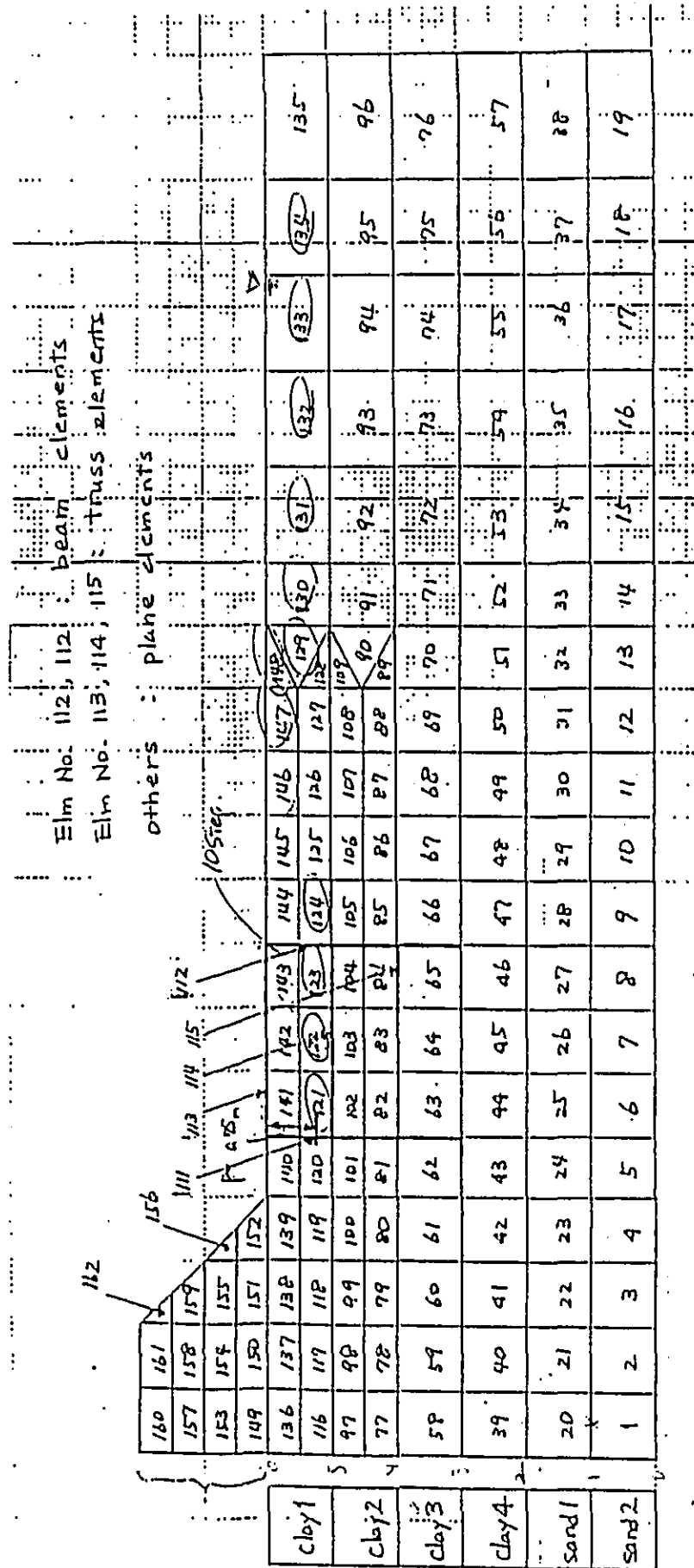


Fig. 4 the number of elements

2. List of DACSAR input data

Input data of this analytical case are shown as follows, and comments written on the right mean the kind of data which has already been explained.

Line	T	M	DAY	PRACTICAL EXAMPLE 1 1986. APRIL					
1									
2	0	0	0	0	0	0			
3	0	0	1	1	1	0	0		
4	0	0	0	0	0	0	0	0	
5	1.0			6.0					
6	1	1	1	1442.3	941.5	3.3	0.65	0.05	0.05
7				1.2					
8	1	2	2	845.4	576.9	2.7	0.65	0.05	0.05
9				1.2					
10		3	3	0.076	0.549	0.961	0.384	0.003	0.003
11				2.0	0.65	2.0	0.64999	0.00666	0.000143
12				0.245	0.84				
13		4	4	0.076	0.549	0.961	0.394	0.004	0.004
14				2.0	0.65	1.5	0.72	0.00666	0.000159
15				0.245	0.84				
16		5	5	0.076	0.549	0.961	0.394	0.0055	0.0055
17				2.0	0.65	0.9	0.86	0.00666	0.000159
18				0.245	0.84				
19		6	6	0.076	0.549	0.961	0.394	-0.0202	0.0202
20				2.0	0.65	0.3	1.28	0.00666	0.000143
21				0.245	0.84				
22	2	8	8	2.1E07	0.0462	0.0056			
23	3	9	9	2.1E07	0.00795				
24	E	1	10	288.5	192.3	1.0	1.0	0.05	0.05
25				1.5					
26		1	1	1	1	1	0.5	2	
27		1	1	0.0	0.0	15	14.0	0.0	
28		14	14	15.5	0.0	19	20.0	0.0	
29		20	20	22.0	0.0				
30		21	21	0.0	1.0	35	14.0	1.0	
31		36	36	15.5	1.0	39	20.0	1.0	
32		40	40	22.0	1.0				
33		41	41		2.0	55	14.0	2.0	
34		56	56	15.5	2.0	59	20.0	2.0	
35		60	60	22.0	2.0				
36		61	61		3.0	75	14.0	3.0	
37		76	76	15.5	3.0	79	20.0	3.0	
38		80	80	22.0	3.0				
39		81	81		4.0	95	14.0	4.0	
40		96	96	15.5	4.0	99	20.0	4.0	
41		100	100	22.0	4.0				
42		101	101		4.5	113	12.0	4.5	
43		114	114		5.0	128	14.0	5.0	
44		129	129	15.5	5.0	132	20.0	5.0	
45		133	133	22.0	5.0				
46		134	134		5.5	146	12.0	5.5	
47		147	147		6.0	161	14.0	6.0	
48		162	162	15.5	6.0	165	20.0	6.0	
49		166	166	22.0	6.0				
50		167	167		6.5	170	3.0	6.5	
51		171	171	3.5	6.5				
52		172	172		7.0	174	2.0	7.0	
53		175	175	3.0	7.0				
54		176	176		7.5	178	2.0	7.5	
55		179	179	2.5	7.5				
56	E	180	180		8.0	182	2.0	8.0	
57		1	1	2	22	21	19		
58		20	20	21	22	42	41	2	18

- (1) title card
- (2) control card
- (3) control card
- (4) control card
- (5) initial setting

(6) material properties data

(7) step control card

(7) a nodal point data (on INOD=1)

59	39	41	42	62	61	3	57		
60	50	61	62	82	81	4	76		
61	77	81	82	102	101	5	88		
62	89	93	94	113		5			
63	90	113	94	127		5			
64	91	94	95	128	127	5	96		
65	97	101	102	115	114	5	100		(7)-b element data
66	109	113	127	126		5			
67	116	114	115	135	134	6	127		
68	128	126	127	146		6			
69	129	146	127	160		6			
70	130	127	128	161	160	6	135		
71	136	134	135	148	147	6	147		
72	148	146	160	159		6			
73	E	149	147	148	168	167	10	152	
74		1	20	1	1				
75		21		1					
76		40	41	1					
77		60	61	1					(7)-c geometric bound
78		80	81	1					condition data
79		100	101	1					
80		114		1					
81		133	134	1					
82		147		1					
83	E	166	167	1					
84		140	147	3	0.0				*4)
85		148		2	0.0				
86		130	135	3	0.0				(7)-d drainage bound
87		149	152	3	0.0				condition data
88	E	152		2	0.0				
89	E	0	149	152					(7)-e
90		2	151	152	1	1	1	0.5	2 (7)
91		153	167	168	173	172	10	155	(7)-b
92	E	156	170	171	175		10		(7)-c
93	E	172		1					(7)-d
94		149	152	13					(7)-e
95		153	155	3					
96	E	156		2					
97	E	0	153	156					
98		3	0	1	1	1	1	0.5	2
99	E	157	172	173	177	176	10	159	(7)-b
100	E	176		1					(7)-c
101		153	155	13					(7)-d
102		157	159	3					(7)-e
103	E	159		2					
104	E	0	157	159					
105		4	0	1	1	1	1	0.5	2
106		160	176	177	181	180	10	161	(7)-b
107	E	162	170	179	182		10		(7)-c
108	E	180		1					(7)-d
109		157	159	13					
110		160	161	3					
111	E	162		2					
112	E	0	160	162					(7)-e
113		5	0	0	0	0	0	1	2
114		6	0	0	0	0	0	1	2
115		7	0	0	0	0	0	1	2
116		8	0	0	0	0	0	1	1

117		-2	0	1	0	1	0	1	0.5	2
118		111	152	66			8			
119		112	155	69			8			
120		-141						-143		
121	E	113	152	155			9			
122	E	121	123	3	-0.5					
123		10	0	1	0	1	0	1	0.5	2
124		-121						-123		
125	E	114	119	122			9			
126	E	102	104	3	-1.0					
127		11	0	1	0	1	0	1	0.5	2
128	E	-102						-104		
129	E	82	84	3	-1.5					
130		12	0	1	0	1	0	1	0.5	2
131		-82						-84		
132	E	115	86	89			9			
133	E	63	65	3	-2.0					
134		13	0	0	0	0	0	1	1.0	4
135		14	0	0	0	0	0	1	1.0	2
136		15	0	0	0	0	0	1	1.0	1
137		16	0	0	0	0	0	1	2.0	
138		17	0	0	0	0	0	1	5.0	2
139	E	18	0	0	0	0	0	1	10.0	2

Remarks

- * 1) All material data used in this analysis including the case of the continuous calculation have to be defined here. Material number (MM) 1,2 and 10 are linear elastic material, 3, 4, 5 and 6 are elasto-viscoplastic material, 8 is beam material and 9 is truss material, herein 7 is a missing number.
- * 2) At the first step this control data shows that data of (a) nodal points, (b) elements, (c) geometry boundary conditions, (d) drainage boundary conditions and (e) loading condition exist, incremental time is 0.5 (day) and the dividing step is two.
- * 3) All nodal points including the nodal points which have not yet been used at this step can be defined. In this example all nodal points have been defined at the first step.
- * 4) The ground surface is set to drainage condition. As the height of head of position potential have already been set to the level of ground surface, the head of ground surface boundary is set to 0.0.

3. Calculation results of the example

A part of the results are shown in Fig. 6-Fig. 9 In Fig. 5 F.E. mesh is shown, in others deformation of this F.E. mesh are shown.

These figures are drawn by using computer soft library () after writing the computational results on temporary files (FT20F001).

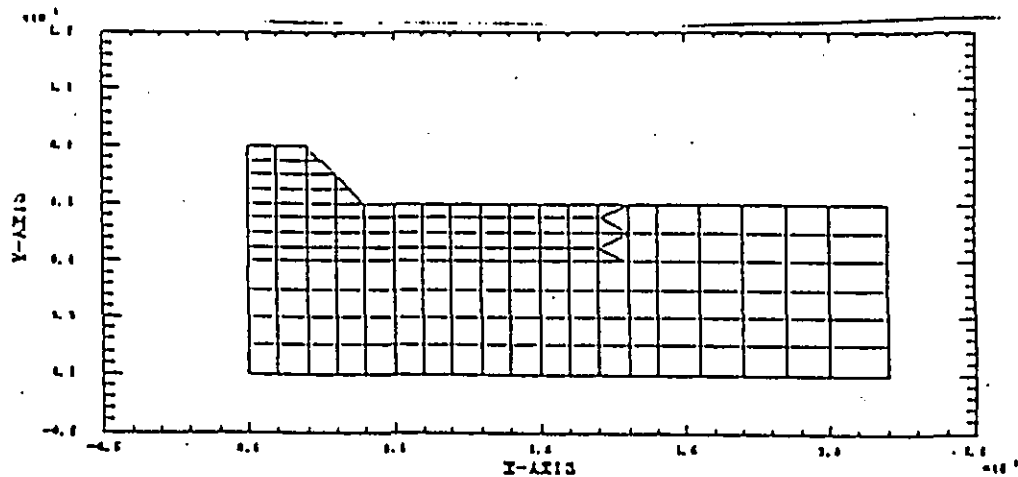


Fig.5 F.E. mesh in cluding all elements and nodal points.

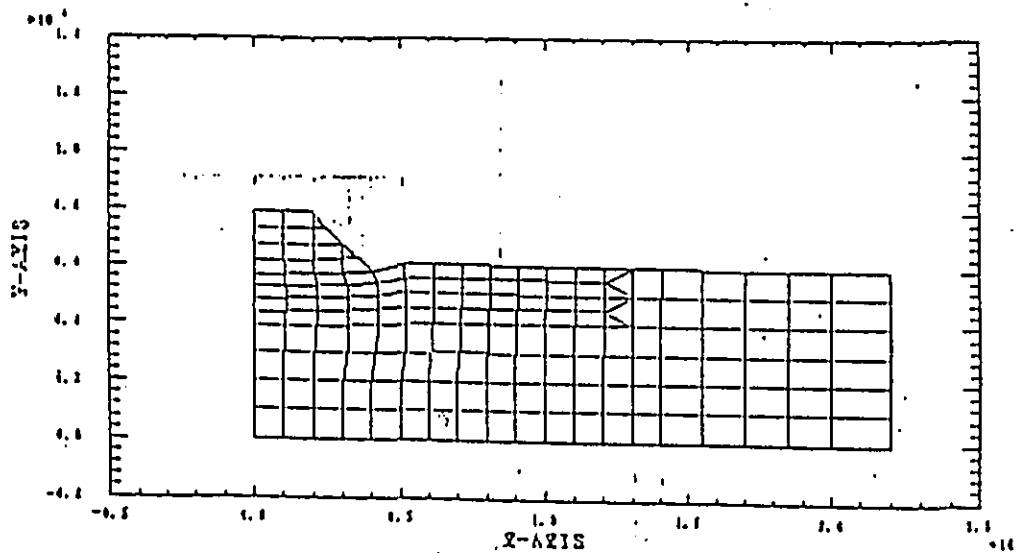


Fig.6 deformation of the mesh at step 4.
(just after building hill).

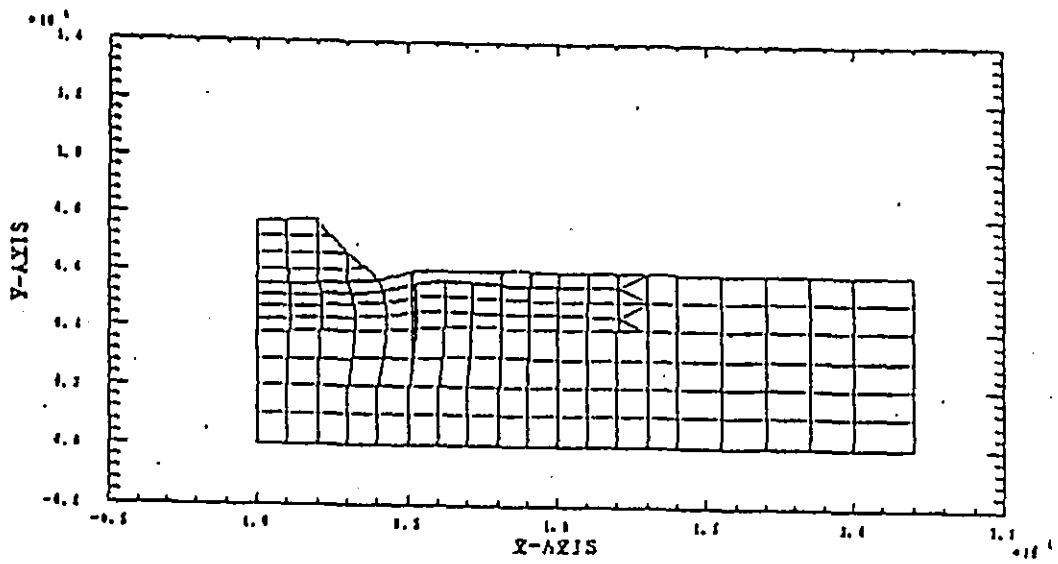


Fig.7 deformation of the mesh at step 9.

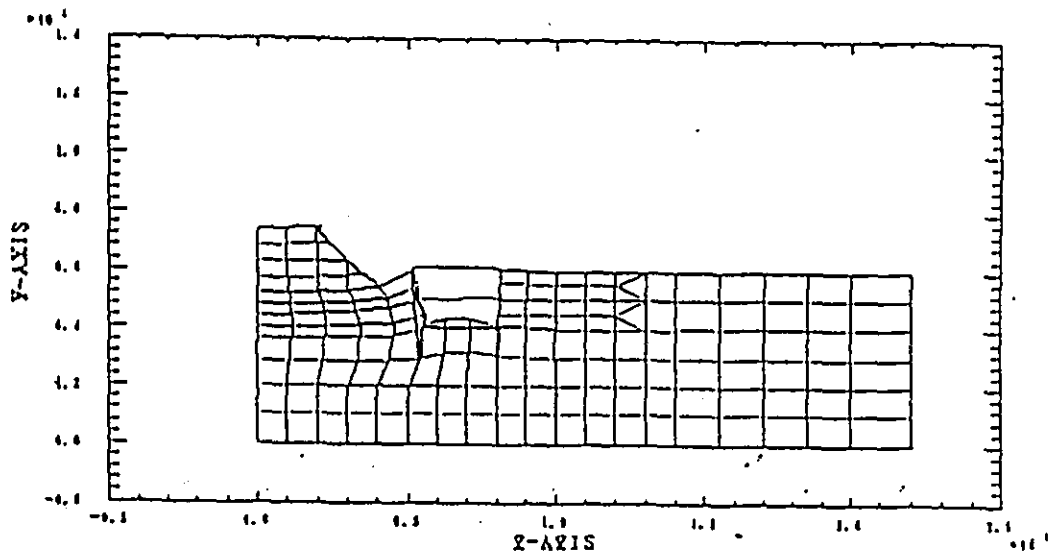


Fig.8 deformation of the mesh at step 12.

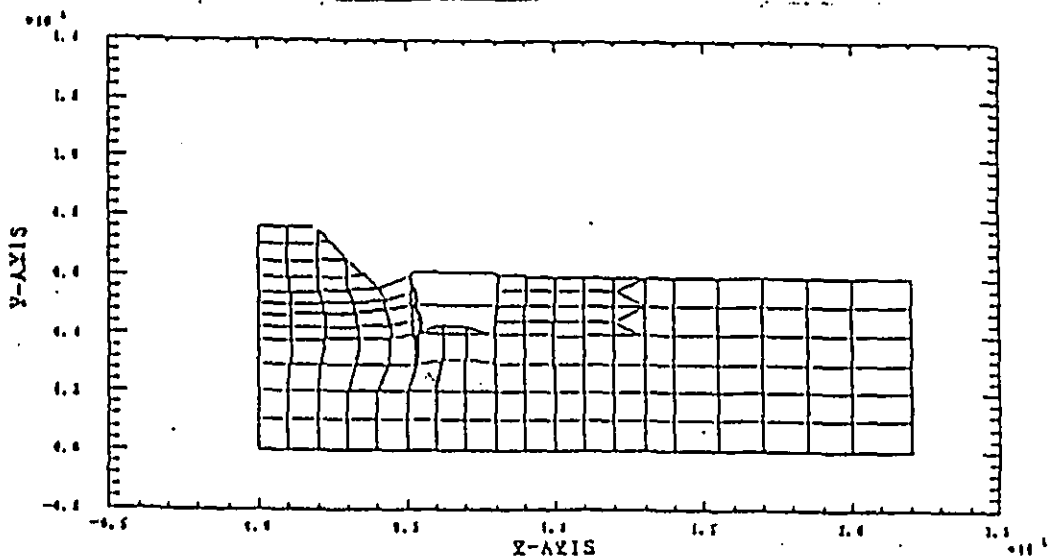


Fig.9 deformation of the mesh at step 16.

4. Output list of the example

A part of the output list is shown as follows in the case of appointing output of nodal displacement and stress and state in elements.

```

.....
THE RESULTS OF BACAR F.E.M.----- ON THE PLANE-STRAIN CONDITION

REGATION  1. IPEN 2-D PLANE-STRAIN CONDITION      [SIAM]-SYMMETRIC CONDITION
           2. ICON 8-DIGIT CONSOLIDATION          SIMISHOME CONSOLIDATION
           3. IPLAS 2-ELASTO/VISCOPLASTIC ANALYSIS  2-ELASTO/PLASTIC ANALYSIS
           4. IENC 2-TOTAL STRESS (EXCAVATION)     2-EFFECTIVE STRESS (EXCAVATION)
           5. ICAL 2-DIPAST ANALYSIS              2-CONTINUOUS ANALYSIS (READING FROM F10 FILES)

UNIT      6  TITLE
T / M / DAY/ PRACTICAL EXAMPLE 1 1966. APRIL

IPEN  ICON  IPLAS  IENC  ICAL
0      0      0      0      0

DISP  EIAS  EPS  OP/DT  F10  F120  ITHM
0      0      1      1      1      0      0

OUTPUT FLAG OF CHECK
0      0      0      0      0      0      0

WATER DENSITY = 0.1000-01      POTENTIAL LEVEL V= 0.000      - EPENIN= 0.1000-02

MATERIAL DATA
1  1  1642.300  741.200  1.300  0.650  0.1000-01  0.1000-01  20LIE-11
1  2  845.400  374.900  2.700  0.650  0.1000-01  0.1000-01  20LIE-21
0  3  0.074  0.349  0.161  0.304  0.2000-02  0.2000-02  20LIEVP-11
0  4  0.074  0.349  0.161  0.304  0.2000-02  0.2000-02  20LIEVP-21
0  5  0.074  0.349  0.161  0.304  0.2000-02  0.2000-02  20LIEVP-31
0  6  0.074  0.349  0.161  0.304  0.2000-02  0.2000-02  20LIEVP-41
0  7  0.074  0.349  0.161  0.304  0.2000-02  0.2000-02  20LIEVP-51
0  8  0.074  0.349  0.161  0.304  0.2000-02  0.2000-02  20LIEVP-61
0  9  0.074  0.349  0.161  0.304  0.2000-02  0.2000-02  20LIEVP-71
0 10  0.074  0.349  0.161  0.304  0.2000-02  0.2000-02  20LIEVP-81
2  0  0.2100+00  0.1420-01  0.1400-01  20LIEVP-11
2  1  0.2100+00  0.1420-01  0.1400-01  20LIEVP-21
1  10  200.100  172.100  1.000  1.000  0.1000-01  0.1000-01  20LIE-11
1  11  1.100  0.0  0.0  0.0  0.1000-01  0.1000-01  20LIE-21
.....
KEEP  HOB  ILM  COND  SAN  LOAD  SWF  DT  ISTEP
1  1  1  1  1  1  1  0.1000  1
.....
NODAL POINT DATA
1  0.0  0.0  15  14.000  0.0
14  15.100  0.0  19  10.000  0.0
20  22.000  0.0  0  0.0  0.0
31  0.0  1.000  25  14.000  1.000
.....
data control { 1:Yes
                0:No
    
```

20	15.100	2.000	19	20.000	1.000
40	15.100	2.000	0	0.0	0.0
41	0.0	2.000	12	14.000	7.000
56	15.100	2.000	19	20.000	1.000
80	15.100	2.000	0	0.0	0.0
65	0.0	2.000	75	14.000	3.000
76	15.100	2.000	79	20.000	3.000
80	15.100	2.000	0	0.0	0.0
85	0.0	2.000	75	14.000	4.000
94	15.100	4.000	19	20.000	1.000
100	12.000	4.000	0	0.0	0.0
101	0.0	4.000	113	12.000	4.100
114	0.0	2.000	120	14.000	3.000
129	15.100	1.000	122	20.000	1.000
133	18.000	1.000	0	0.0	0.0
134	0.0	2.000	145	12.000	1.100
142	0.0	5.000	141	14.000	2.000
142	15.100	6.000	145	20.000	4.000
144	12.000	1.000	0	0.0	0.0
147	0.0	4.000	120	3.000	4.100
171	3.100	6.500	0	0.0	0.0
172	0.0	7.000	174	2.000	7.000
175	3.000	7.000	0	0.0	0.0
176	0.0	7.000	170	2.100	7.100
179	7.100	7.100	0	0.0	0.0
180	0.0	0.000	107	2.000	0.000

x,y coordinates of the nodal point
the number of nodal point

ELEMENTAL DATA

1	1	1	22	21	1	17	0.
20	21	22	41	41	1	30	0.
30	41	42	42	41	1	17	0.
56	45	42	42	41	4	74	0.
77	41	42	102	101	1	40	0.
89	75	74	123	0	1	0	0.
90	153	94	127	0	1	0	0.
91	74	95	120	127	1	76	0.
97	100	102	110	114	1	100	0.
109	113	127	224	0	1	0	0.
114	114	115	135	134	1	127	0.
120	120	127	104	0	1	0	0.
129	146	127	160	0	1	0	0.
130	127	120	103	140	1	122	0.
134	134	135	140	147	1	147	0.
140	146	140	139	0	1	0	0.
143	147	140	140	147	10	152	0.

material number (MM)
the number of nodal point
constituting the element
the number of element

BOUNDARY CONDITION

1	20	1	1	0	0.0	0.0	0.0	0
40	41	1	0	0	0.0	0.0	0.0	0
40	41	1	0	0	0.0	0.0	0.0	0
80	81	1	0	0	0.0	0.0	0.0	0
100	101	1	0	0	0.0	0.0	0.0	0
114	114	1	0	0	0.0	0.0	0.0	0
122	124	1	0	0	0.0	0.0	0.0	0
141	0	1	0	0	0.0	0.0	0.0	0
144	147	1	0	0	0.0	0.0	0.0	0

DRAINING COEFFICIENT

140	147	3	0.0
140	0	7	0.0
120	125	3	0.0
145	133	3	0.0
152	0	3	0.0

LOADING DATA

0	140	152	0.0	-1.100	0.0
---	-----	-----	-----	--------	-----

***** INITIAL CONDITION *****

N	MM	ME	SET	EX	EY	ENZ	EZ	EM	EN	HEAD	WRES1	WRES2	WRES3	WRES4	INTA	VOID
1	1	1	1	2.145	2.100	0.0	2.141	2.130	0.0	0.0	0.0	0.0	0.0	0.0	0.0	1.200
2	1	1	1	2.145	2.100	0.0	2.141	2.130	0.0	0.0	0.0	0.0	0.0	0.0	0.0	1.200
3	1	1	1	2.145	2.100	0.0	2.141	2.130	0.0	0.0	0.0	0.0	0.0	0.0	0.0	1.200
4	1	1	1	2.145	2.100	0.0	2.141	2.130	0.0	0.0	0.0	0.0	0.0	0.0	0.0	1.200
5	1	1	1	2.145	2.100	0.0	2.141	2.130	0.0	0.0	0.0	0.0	0.0	0.0	0.0	1.200
6	1	1	1	2.145	2.100	0.0	2.141	2.130	0.0	0.0	0.0	0.0	0.0	0.0	0.0	1.200
7	1	1	1	2.145	2.100	0.0	2.141	2.130	0.0	0.0	0.0	0.0	0.0	0.0	0.0	1.200
8	1	1	1	2.145	2.100	0.0	2.141	2.130	0.0	0.0	0.0	0.0	0.0	0.0	0.0	1.200
9	1	1	1	2.145	2.100	0.0	2.141	2.130	0.0	0.0	0.0	0.0	0.0	0.0	0.0	1.200
10	1	1	1	2.145	2.100	0.0	2.141	2.130	0.0	0.0	0.0	0.0	0.0	0.0	0.0	1.200
11	1	1	1	2.145	2.100	0.0	2.141	2.130	0.0	0.0	0.0	0.0	0.0	0.0	0.0	1.200
12	1	1	1	2.145	2.100	0.0	2.141	2.130	0.0	0.0	0.0	0.0	0.0	0.0	0.0	1.200
13	1	1	1	2.145	2.100	0.0	2.141	2.130	0.0	0.0	0.0	0.0	0.0	0.0	0.0	1.200
14	1	1	1	2.145	2.100	0.0	2.141	2.130	0.0	0.0	0.0	0.0	0.0	0.0	0.0	1.200
15	1	1	1	2.145	2.100	0.0	2.141	2.130	0.0	0.0	0.0	0.0	0.0	0.0	0.0	1.200
16	1	1	1	2.145	2.100	0.0	2.141	2.130	0.0	0.0	0.0	0.0	0.0	0.0	0.0	1.200
17	1	1	1	2.145	2.100	0.0	2.141	2.130	0.0	0.0	0.0	0.0	0.0	0.0	0.0	1.200
18	1	1	1	2.145	2.100	0.0	2.141	2.130	0.0	0.0	0.0	0.0	0.0	0.0	0.0	1.200
19	1	1	1	2.145	2.100	0.0	2.141	2.130	0.0	0.0	0.0	0.0	0.0	0.0	0.0	1.200
20	1	1	1	2.145	2.100	0.0	2.141	2.130	0.0	0.0	0.0	0.0	0.0	0.0	0.0	1.200
21	1	1	1	2.145	2.100	0.0	2.141	2.130	0.0	0.0	0.0	0.0	0.0	0.0	0.0	1.200
22	1	1	1	2.145	2.100	0.0	2.141	2.130	0.0	0.0	0.0	0.0	0.0	0.0	0.0	1.200
23	1	1	1	2.145	2.100	0.0	2.141	2.130	0.0	0.0	0.0	0.0	0.0	0.0	0.0	1.200
24	1	1	1	2.145	2.100	0.0	2.141	2.130	0.0	0.0	0.0	0.0	0.0	0.0	0.0	1.200
25	1	1	1	2.145	2.100	0.0	2.141	2.130	0.0	0.0	0.0	0.0	0.0	0.0	0.0	1.200
26	1	1	1	2.145	2.100	0.0	2.141	2.130	0.0	0.0	0.0	0.0	0.0	0.0	0.0	1.200
27	1	1	1	2.145	2.100	0.0	2.141	2.130	0.0	0.0	0.0	0.0	0.0	0.0	0.0	1.200
28	1	1	1	2.145	2.100	0.0	2.141	2.130	0.0	0.0	0.0	0.0	0.0	0.0	0.0	1.200
29	1	1	1	2.145	2.100	0.0	2.141	2.130	0.0	0.0	0.0	0.0	0.0	0.0	0.0	1.200
30	1	1	1	2.145	2.100	0.0	2.141	2.130	0.0	0.0	0.0	0.0	0.0	0.0	0.0	1.200
31	1	1	1	2.145	2.100	0.0	2.141	2.130	0.0	0.0	0.0	0.0	0.0	0.0	0.0	1.200
32	1	1	1	2.145	2.100	0.0	2.141	2.130	0.0	0.0	0.0	0.0	0.0	0.0	0.0	1.200
33	1	1	1	2.145	2.100	0.0	2.141	2.130	0.0	0.0	0.0	0.0	0.0	0.0	0.0	1.200
34	1	1	1	2.145	2.100	0.0	2.141	2.130	0.0	0.0	0.0	0.0	0.0	0.0	0.0	1.200
35	1	1	1	2.145	2.100	0.0	2.141	2.130	0.0	0.0	0.0	0.0	0.0	0.0	0.0	1.200
36	1	1	1	2.145	2.100	0.0	2.141	2.130	0.0	0.0	0.0	0.0	0.0	0.0	0.0	1.200
37	1	1	1	2.145	2.100	0.0	2.141	2.130	0.0	0.0	0.0	0.0	0.0	0.0	0.0	1.200

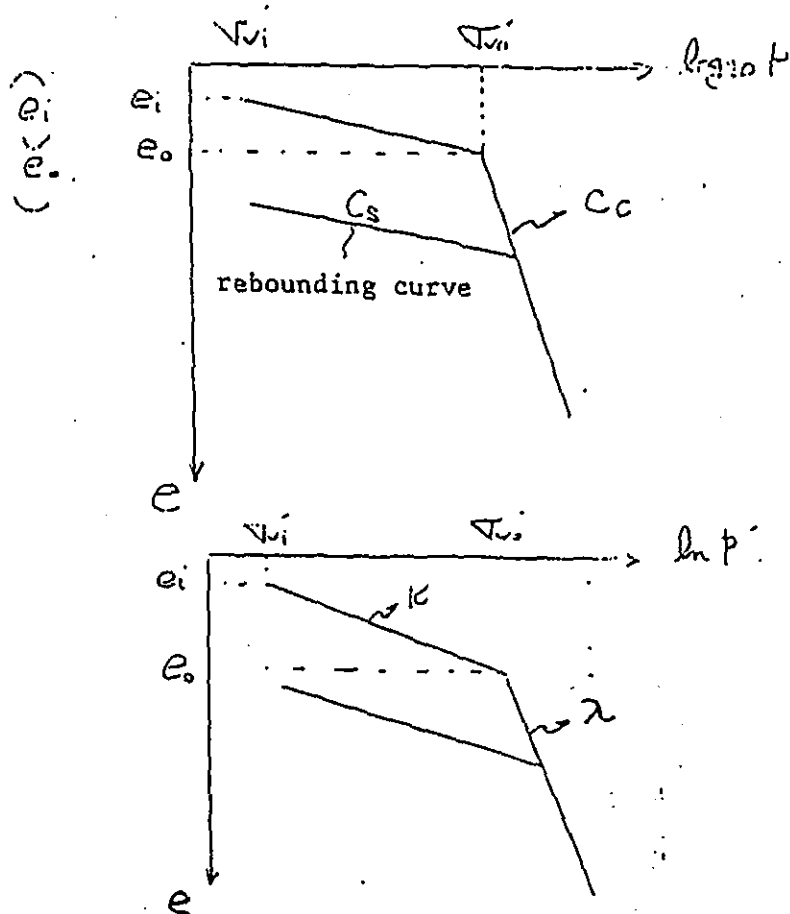
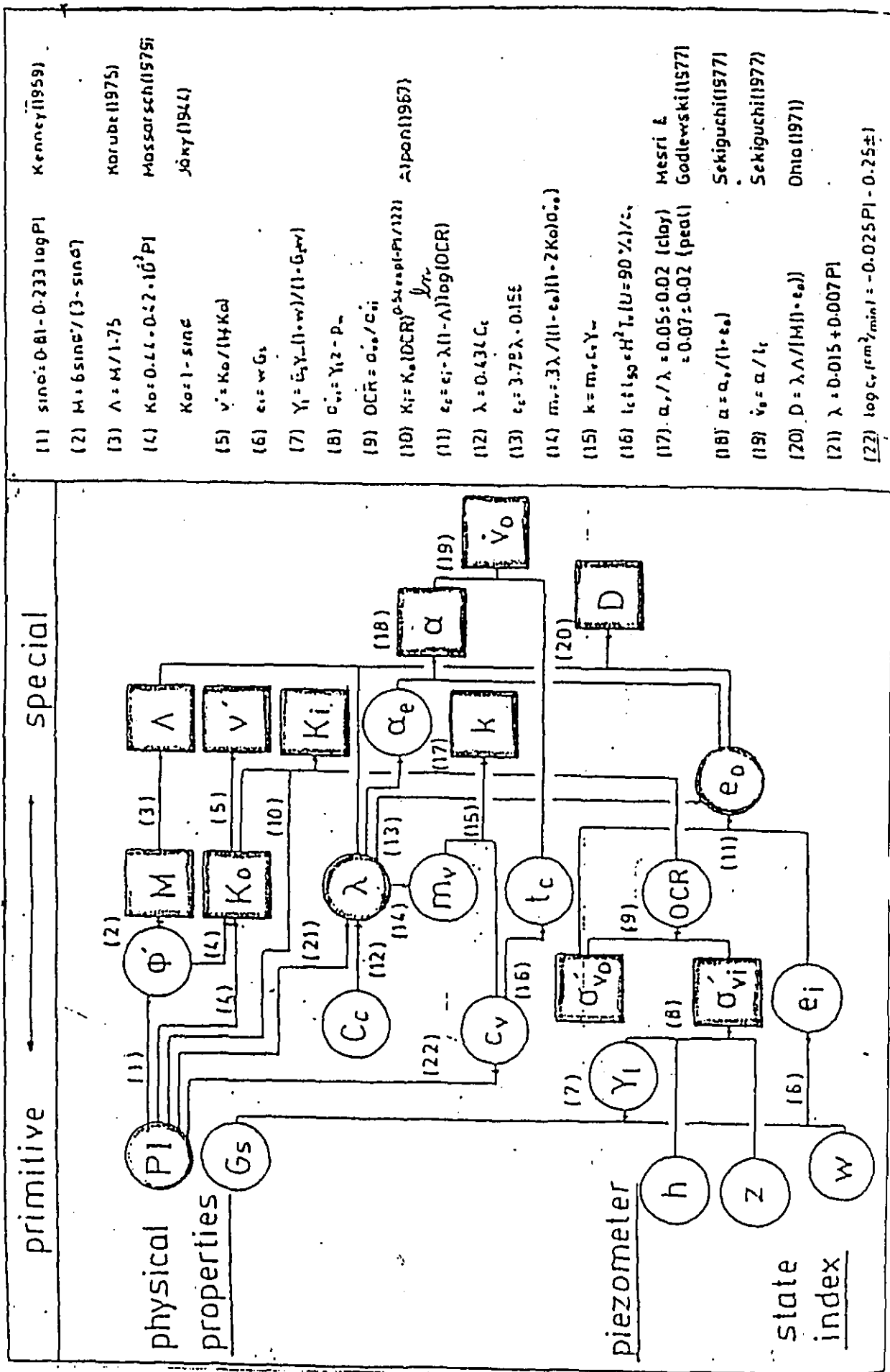


TABLE I Stress and Material Parameters

MATERIAL PARAMETERS	λ	$= 0.434 C_c$ (C_c ; compression index)
	κ	$= 0.434 C_s$ (C_s ; swelling index)
	D	Dilatancy coefficient proposed by Skibaca (1963)
	Λ	$= 1 - \kappa/\lambda$; irreversibility ratio
	H	$= \frac{\lambda - \kappa}{D(1+e_o)} = \frac{b \sin \phi'}{1 - \sin \phi'}$; critical state parameter
	K_0	Coefficient of earth pressure at rest
	B	$= \frac{\sqrt{3} \eta_0 \Lambda}{2H}$
STRESS PARAMETERS	η^*	$= \sqrt{\frac{1}{2} \left(\frac{s_{11}}{p'} - \frac{s_{11}^0}{p_0'} \right) \left(\frac{s_{11}}{p'} - \frac{s_{11}^0}{p_0'} \right)}$; Normalized shear stress
	p'	effective mean principal stress
	s_{11}	$= \sigma_{11} - p' \delta_{11}$ (δ_{11} ; Kronecker's delta) ; deviatoric stress tensor
	σ_0'	effective overburden pressure
	τ	undrained shear resistance along slip line
	η_0	$= \frac{3(1-K_0)}{1+2K_0}$
Note: Subscript 0 specifies the value at the time of completion of K_0 -consolidation. Subscript 1 specifies the value at the initial state prior to undrained loading.		



primitive ← → special

- (1) $\sin \delta = 0.81 - 0.233 \log PI$ Kenney (1959)
- (2) $M = 6 \sin \delta / (3 - \sin \delta)$
- (3) $\Lambda = M / 1.75$ Karube (1975)
- (4) $K_0 = 0.44 - 0.2 \cdot 10^{-2} PI$ Massarsch (1975)
- $K_0 = 1 - \sin \delta$ Jaky (1944)
- (5) $v' = K_0 / (1 + K_0)$
- (6) $e_s = v' G_s$
- (7) $\gamma_1 = \gamma_2 \cdot (1 + v) / (1 - G_s v)$
- (8) $\sigma_{vi} = \gamma_1 z - p_u$
- (9) $OCR = \sigma_{vi} / c_{vi}$
- (10) $K_i = K_0 (OCR)^{0.54 + 0.01 \cdot PI / 122}$ Japan (1967)
- (11) $e_s = e_i - \lambda (1 - \Lambda) \log (OCR)$
- (12) $\lambda = 0.43 C_c$
- (13) $e_s = 3.75 \lambda \cdot 0.15 e$
- (14) $m_v = 3 \lambda / (1 - e_s) (1 - 2 K_0 \sigma_{vi})$
- (15) $k = m_v c_v \gamma_w$
- (16) $t_c = 1.99 \cdot H^2 \cdot (U = 90\%) / c_v$
- (17) $\alpha_r / \lambda = 0.05 \pm 0.02$ (clay) Mesri &
 $= 0.07 \pm 0.02$ (peat) Godlewski (1977)
- (18) $\alpha = \alpha_r / (1 - e_s)$ Sekiguchi (1977)
- (19) $v_0 = \alpha / t_c$ Sekiguchi (1977)
- (20) $D = \lambda \Lambda / (M) (1 - e_s)$ Onio (1971)
- (21) $\lambda = 0.015 + 0.007 PI$
- (22) $\log c_v / (m_v^2 \cdot \min I) = -0.025 PI - 0.25 \pm 1$

physical properties

piezometer

state index

4-6-3. Plotter Program of Results of F.E.M. Analysis

- (1) MIPDPL1 (Displacement Diagram)
- (2) MIPVPL2 (Displacement Vector Diagram)
- (3) MIPSPL3 (Stress Diagram)
- (4) MIPZPL4 (Zone Partition Diagram)

The programs mentioned later are programs that plot the results of F.E.M. analysis on XY plotter.

(1) MIPDPL1

① Program Contents

This is a program which plots displacement diagrams such as model and displacement diagrams on XY plotter, using file output of analyzing conditions and results by F.E.M. program.

② Usage

To use command procedure

③ Input

1) Control record

The control record specifies the number of diagrams and the time of overplot.

Record	Variables
Control record	MAI, KAI

Variables	Type	Contents
MAI	Real Real	Total number of diagrams (≤ 20)
KAI	Integer	Time of overplot

2) Plotting condition record

The plotting condition record specifies the condition of diagram to be plotted on Mth paper.

Record	Variables
Plotting condition record	LY(M), (SCAL (i, M), i=1, 2)

Variables	Type	Contents
LY(M)	Real	Plotting layer number on Mth paper.
SCAL (1,M)	Real	Total scale. In the case of 1/100, 100.0 is input.
SCAL (2,M)	Real	Displacement scale. In the case that displacement of 1cm is shown in 0.5 cm, namely in the scale of 1/2, 2.0 is input.

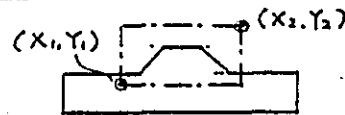
3) Plotting range record

If a part of a diagram to be plotted on Mth paper is enlarged, input the range in units of meters which means the actual size of a model.

Record	Variables
Plotting range record	XYL (i, M), i= 1, 4

Variables	Type	Contents
XYL (1, M)	Real	x abscissa (m) at bottom left [x_1 , Total range-1000000
XYL (2, M)	Real	y ordinate (m) at bottom left [y_1 , Total range-1000000
XYL (3, M)	Real	x abscissa (m) at top right [x_2 , Total range 10000000
XYL (4, M)	Real	y ordinate (m) at top right [y_2 , Total range 10000000

Remarks



- A total scale should be specified within the possible range because the possible range is limited by a XY plotter ordinate of 22 cm. It should be considered for all of the diagram programs mentioned later.
- A diagram is easily visible if the maximum displacement is about 1.0 cm.
- A plotting range is input in unit of meters because the coordinates of the output file are shown in cm.

Input data (x, y) ----> Output file (x*SCALX, y*SCALY).

Here, SCALX and SCALY are conversion scales of x and y axes specified in the stress analysis program.

In the case that the total range is specified,

XYL (1, M) = -1000000000

XYL (2, M) = -1000000000

XYL (3, M) = 1000000000

XYL (4, M) = 1000000000

(2) MIPVPL2

① Program Content

The MIPVPL2 makes a diagram of displacement of nodal points as a displacement vector while the MIPDPL1 makes a displacement diagram.

② Usage

To use command procedure.

③ Input

The inputting method is the same as MIPDPL1.

(3) MIPSPL3

① Program Contents

The MIPSPL3 is a program to make a principal stress diagram in an analyzed model diagram, using principal stresses of each element as a result of F.E.M. analysis such as DACSAR program.

② Usage

To use command procedure.

③ Input

1) Record number

Record	Variable
Record number	MAi

Variable	Type	Contents
MAi	Integer	The number of diagrams is specified. (MAi \leq 20)

2) Plotting condition record

Record	Variables
Plotting condition record	LY(M), (SCAL(i,M)), IND(i,M), KAI (i,M); i=1,2

Variables	Type	Contents
LY (M)	Integer	Layer number to be plotted on Mth paper. Descending order.
SCAL (1, M)	Real	Total scale In the case of 1/100, 100.0 is input.
IND (1, M)	Integer	Specification of external frame, Number of external frame data. IND \leq 50, When IND = -1, a mesh diagram is drawn.
KAI (1, M)	Integer	Times of overplotting an external frame (>0)
SCAL (2, M)	Real	Stress scale In the case that 10 kg/cm ² is shown in 1cm, 10.0 is input.
IND (1, M)	Integer	Specification of principal stress Refer to Table 7.1
KAI (2, M)	Integer	Times of overplotting principal stress (>0)

Table 7.1 Value of iND (2, M)

To specify element for principal stress diagram	Not to plot principal stress	To plot principal stress
All elements	1	2
Odd numbered elements	11	12
Even numbered elements	21	22

Legend record 1

Record	Variables
Legend record	NCOD (i,M), i=1, iE (iE=iCOD(M))

Variables	Type	Contents
NCOD(i, M)	Integer	Plotting pattern of i th data on Mth paper is specified by legend numbers.

Legend record 2

Record	Variables
Legend record	(ZONE(i, J, M), i=1,2), J=1, iE

Variables	Type	Contents
ZONE(1, J, M)	Real	Lowest limit value responding to Jth plotting pattern
ZONE(2, J, M)	Real	Uppermost limit value responding to Jth plotting pattern

Plotting range record

Record	Variables
Plotting range record	XYL(i,M), i=1,4

Variables	Type	Contents
XYL(1,M)	Real	X1 coordinates at bottom left range (m)
XYL(2,M)	Real	y1 coordinates at bottom left range (m)
XYL(3,M)	Real	X2 coordinates at top right range (m)
XYL(4,M)	Real	y1 coordinates at top right range (m)

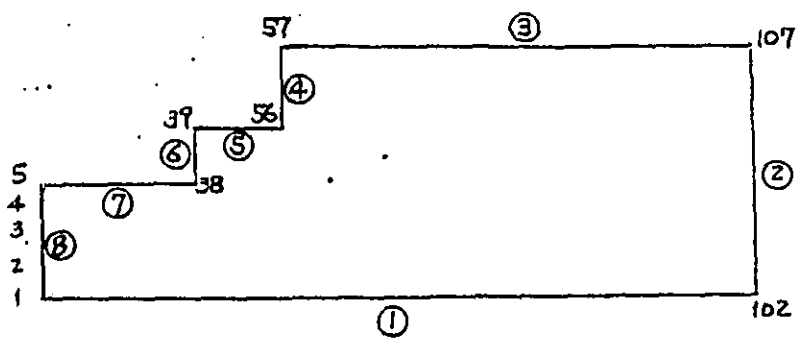
4) External frame data

In the case of $iND(1, M) > 0$, data is input.

In the case that the numbers of straight lines are specified by $iND(1, M)$, the nodal point number of beginning and ending points is given (Refer to Example)

Record	Variables
Model Data 2	KENDS (1, i), KENDS (2, i) i = 1, NKEND

Variables	Type	Contents
KENDS (1, i)	Integer	Number of beginning nodal point
KENDS (2, i)	Integer	Number of ending nodal point



In case of example of DACSAR program,

NKEND = 8

$\text{NENDS} = \overline{\text{①}}_{1,102} , \overline{\text{②}}_{102,107} , \overline{\text{③}}_{107,57} , \overline{\text{④}}_{57,56} , \overline{\text{⑤}}_{56,39}$
 $\overline{\text{⑥}}_{39,38} , \overline{\text{⑦}}_{38,5} , \overline{\text{⑧}}_{5,1}$

(4) MIPZPL4

① Program Content

The MIPZPL4 is a program to make a shaded distribution diagram of stresses and strains using the results of F.E.M. analysis.

② Usage

To use command procedure.

③ Input

1) Number record

Record	Variable
Number record	MAi

Variable	Type	Content
MAi	Integer	Number of diagrams (MAi \leq 20)

2) Control record

Record	Variable
Control record	LY(M), IND(M), TITLE (M), iCOD(M), SCAL(M)

Variable	Type	Contents
LY(M)	Integer	Layer number to be plotted on Mth paper
IND(M)	Integer	Selected data number to be plotted on Mth paper Refer to Table 7.2
TITLE(M)	Character 'R8'	Diagram title to be plotted on Mth paper Less than 8 letters, To be surrounded by ' '
iCOD(M)	Integer	Number of legend (≤ 20), Refer to FEMCHK3
SCAL(M)	Real	Total scale In the case of 1/100, input 100.0

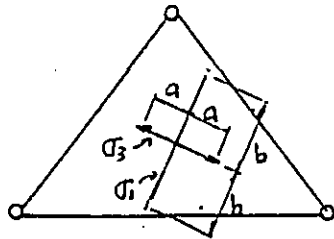
Table 7.2 Selected Data Number

IND	Contents	IND	Contents
1	x axial stress (Kg/cm^2)	12	x axial strain
2	y axial stress (Kg/cm^2)	13	y axial strain
3	z axial stress (Kg/cm^2)	14	Shear strain
4	Shear stress (Kg/cm^2)	15	Minimum principal strain
5	Minimum principal stress (Kg/cm^2)	16	Maximum principal strain
6	Maximum principal stress (Kg/cm^2)	17	Maximum shear strain
7	z axial principal stress (Kg/cm^2)	18	X axial stress by load
8	Angle between minimum stress and axis	19	Y axial stress by load
9	Maximum shear stress (Kg/cm^2)	20	Z axial stress by load
10	Young's modulus	21	Reciprocal of safety factor
11	Poisson's ratio		

Remark

A principal stress is given to maintain the center of a principal stress at the center of gravity of an element.

Example



If stresses in an element are as follows:

$$\sigma_3 = -5 \text{ Kg/cm}^2$$

$$\sigma_1 = -1.5 \text{ Kg/cm}^2$$

And the scale is specified to be 10:0,

$$2a = |\sigma_3| / 10.0 = 0.5 \text{ cm}$$

$$2b = |\sigma_1| / 10.0 = 1.5 \text{ cm}$$

Consequently,

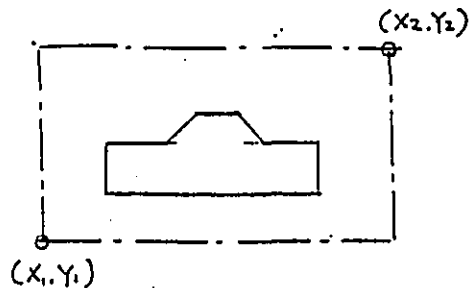
A diagram is drawn by $\sigma_3 = 0.5 \text{ cm}$

and $\sigma_1 = 1.5 \text{ cm}$.

3) Plotting range record

Record	Variables
Plotting range record	XYL (i,M), i = 1, 4

Variables	Type	Contents
XYL (1,M)	Real	x abscissa (m) at bottom left <x1>
XYL (2,M)	Real	y ordinate (m) at bottom left <y1>
XYL (3,M)	Real	x abscissa (m) at top right <x2>
XYL (4,M)	Real	y ordinate (m) at top right <y2>
		Refer MIPDPL1



If the total range is specified,

$$x1 = -1000000000$$

$$y1 = -1000000000$$




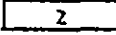

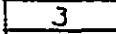

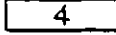









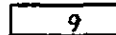

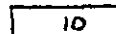
$$x2 = 1000000000$$

$$y2 = 1000000000$$

In this program, data selected from output file is judged by the following formula. And then a diagram is drawn by patterns specified by NCOD (i,M) responding to J Value. The relation between NCOD (i,M) and diagram patterns are shown in Table 7.3.

$$\text{ZONE (1,J,M)} \leq X_i \leq \text{ZONE (2,J,M)}$$

Table 7.3 Diagram Pattern Code

Legend	Diagram Pattern	Legend	Diagram Pattern
1		11	
2		12	
3		13	
4		14	
5		15	
6		16	
7		17	
8		18	
9		19	
10		20	

(5) MIPCHK 2

(F.E.M for element divide)

(5) MIPFCHK 2

① Program content

Data for this program are positive figures of area checked by MIPCHK1. Using these data, MIPCHK2 is a program which makes an element dividing diagram on XY plotter and checks whether the diagram is the same as the original one or not.

The program has the functions of enlarging a diagram of less than 20 parts at the same time and to specify a letter scale of a nodal point number and element number.

② Usage

Processing is only by batch processing and submitted jobs from a terminal in the CPU room.

③ Input

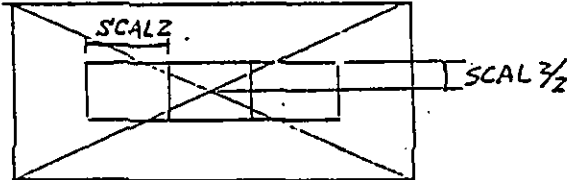
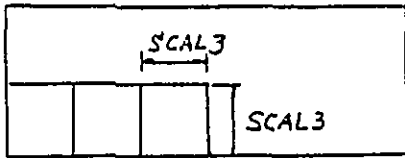
1) Control record

Record	Variables	
Control record	ISW, NELEM, NPOIN, MAI	

Variables	Type	Contents
ISW	Integer	To specify a triangular element or a square element. 1. For triangular elements 2. For square elements
NELEM	Integer	Total number of elements
NPOIN	Integer	Total number of nodal points
MAI	Integer	Number of diagrams to be plotted at a time

2) Scale record

Record	Variables
Scale record	SCAL1, SCAL2, SCAL3, IND1, IND2, IND3

Variables	Type	Contents
SCAL1	Real	Total scale In the case of scale=1/100, SCAL1=100.0
SCAL2	Real	Letter size of element number. Element number should be plotted to keep the center of element number at the center of element gravity.  Fig 1
SCAL3	Real	Letter size of nodal point number. A nodal point number is plotted, keeping nodal point coordinates at left down of number. 
IND1	Integer	Times of overplotting a mesh diagram
IND2	Integer	Times of overplotting element numbers
IND3	Integer	Times of overplotting nodal point numbers

Remarks

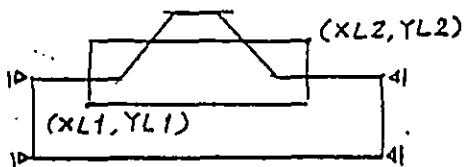
In the case of SCAL2 and SCAL3, 0.15 is usually specified.

In the case of enlargement, a scale is decided, referring to Fig.1.

3) Plotting range record

Record	Variables
Plotting range record	XL1, YL1, XL2, YL2

Variables	Type	Contents
XL1	Real	X coordinates of bottom left range. Responding to coordinate data to be put in
YL1	Real	Y coordinates of bottom left range. Responding to coordinate data to be put in
XL2	Real	X coordinates of top right range. Responding to coordinate data to be put in
YL2	Real	Y coordinates of top right range. Responding to coordinate data to be put in



(XL1, YL1) and (XL2, YL2) are not necessarily coincident with nodal point coordinates which are input later.

Input method of element and nodal point records are the same as MIPCHK1.

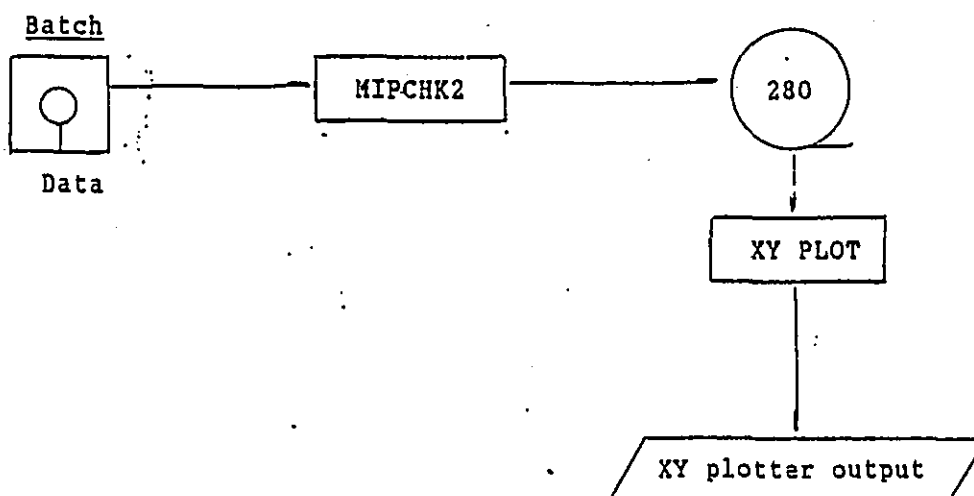
In the case of ISW = 1

- 4) Element record
- 5) Nodal point record

In the case of ISW = 2

- 4) Nodal point record
- 5) Element record

4 Hardware system



5. Slope Stability Analysis System

5-1 Objectives and Analysis Method

(1) Objectives

The purposes of the Slope Stability Analysis System are as follows

1) Analysis of excavated slope stability on the soft soil foundation

① It is almost impossible for excavated foundation slope stability analysis on the soft soil foundation to be carried out by normal slope stability analysis methods. But using this improved Slope Stability Analysis System, the excavated slope stability analysis on the soft soil foundation can be carried out.

② The slope stability analysis of improved slopes by the soil cement column method, etc. can be carried out by this improved slope stability analysis method using the concept of composite ground.*¹ Using this method of analysis, the method of design for excavated slopes and the construction method for improvement of slope stability can be examined.

*¹ By composite ground, we mean the areas that consist of original clay and the improvement method.

2) Application of the results of analysis to the other 2 systems as necessary information

① By offering information about the place where slope failure is expected to occur (obtained from the slope stability analysis), an effective installation plan of sensors can be made (e.g. extensometers, settlement gauges).

② And also by using information about the place where slope failure is expected to occur obtained from this analysis, examination of the results obtained from F.E.M. analysis (e.g. deformation and distribution of shear stress in the ground) can be done and the adequacy of

the parameters used in F.E.M. analysis can be examined.

(2) Analysis method

The features of this analysis method are as follows.

- 1) This method applies the following design shear strength Su^* based on shear strength obtained from Field Vane Tests Su , in which Su^* 2 kinds of correction coefficient are taken into consideration.

$$Su^* = \mu_A \times \mu_B \times Su$$

where, μ_A : Bjerrum's correction factor regarding shear strength obtained from Field Vane Tests

μ_B : Coefficient of strength decrease caused by excavation work

Su : Shear strength obtained from Field Vane Tests

- 2) In the analysis for improved slope stability, the original soft clay part and the parts improved by piles or columns (in the Sand Compaction Pile Method and Soil Cement Column Method respectively) are not distinguished from each other but are analyzed as a composite foundation. Shear strength of the composite foundation by Sand Compaction Piles and Soil Cement Columns are determined by each equation.

For details of the analysis method, please refer to the following section.

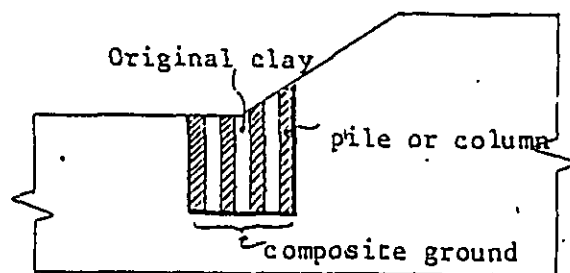


Fig 5-1 Composite ground

5-2. Determination of Design Parameters

In this chapter, we discuss the design parameters for excavated slopes and improved slopes by the sand compaction piles and soil cement columns on soft soil foundations. And we consider the modeling of soft clay foundation profiles.

(1) Excavated Slope Stability Analysis on soft soil foundations (in the case of a non-treatment slope).

1) Determination of the design parameters.

It has been reported in some investigation papers that normal slope stability methods tend to overestimate the actual safety factor values SF of excavated slopes on soft soil foundations.

And in the case of Bangkok Clay Foundation, we should take strength anisotropy of the clay into account in slope stability analysis. Therefore, it has been reported in another technical paper that shear strength is reduced due to swelling on unloading process.

And then, we have proposed the excavated slope stability analysis method should take Bjerrum's coefficient (including factors of strain rate and strength anisotropy) and the rate of strength decreased by excavation from the standpoint of the Advanced Total Stress Method into account.

① The rate of strength decrease of Bangkok Clay by unloading

In the case where a clay foundation is unloaded by excavation work or removal of preload, clay under a groundwater surface swells according to unloading and its strength is decreased.

The strength decrease rate has already been derived by Nakase et al.¹⁾ based on Hvorslev's failure criteria as expressed in equation (1). And Takayama et al.²⁾ proved the usefulness of this strength decrease rate equation experimentally.

The strength decrease rate is expressed as follows;

$$\frac{S_{un}}{S_u} = OCR^{-\lambda} \frac{K + (\sigma'_{fn}/P_e) \cdot \tan \phi_e}{K + (\sigma'_{f}/P_c) \cdot \tan \phi_e} = \mu B \text{ ----- (1)}$$

Where, S_{un} : Undrained strength of overconsolidated clay
 S_u : Undrained strength of normally consolidated clay
 OCR : Overconsolidation ratio
 K, ϕ_e : Hvorslev's parameters
 P_c : Preconsolidation pressure
 P_s : $(=P_c \cdot OCR^{-\lambda} : \lambda = C_s/C_c)$

In equation (1), the denominator values of equation (1) are constant values for the same soil. Otherwise, the numerator of equation (1) is approximately considered to be a function of OCR (over consolidation ratio)

TAKAYAMA et al.²⁾ had obtained results of direct shear tests for Ariake clay under constant volume as shown in Fig. 5-2 and Fig. 5-3.

Fig.5-3 shows the results of direct shear tests for remolded clay.

If clay is consolidated under normal stress P_c and later consolidation pressure is decreased to P_d , the strength of clay has a tendency to decrease linearly at a gentle gradient according to the unloading. But in the case where the over consolidation ratio value is more than 4.0, the strength of clay decreases forming a curve.

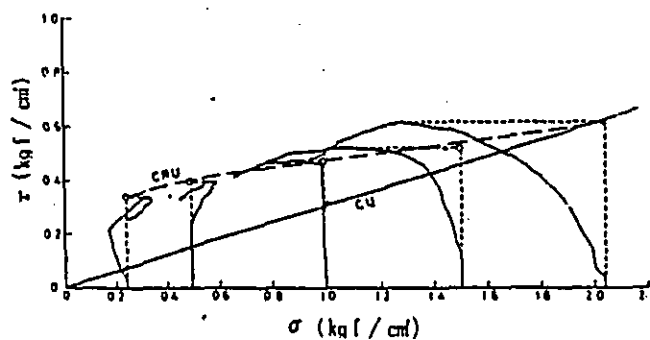


Fig. 5-2 The results of direct shear tests at constant volume under consolidation and swelling.

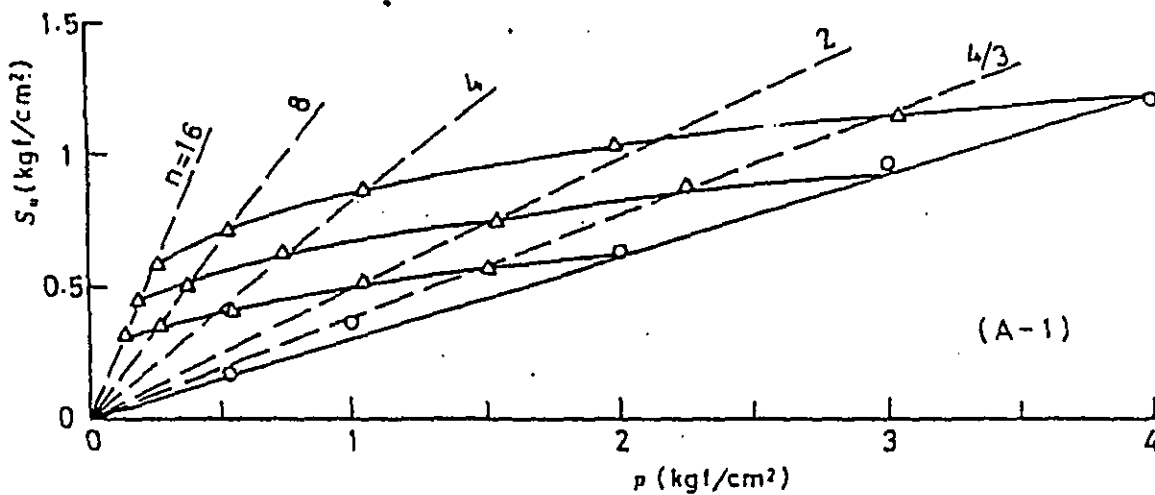


Fig. 5-3 Strength decrease according to unloading

And if the loading pressures P_c at the start of swelling are different, in the case where overconsolidation ratios, OCRs are equal; the ratios of undrained shear strength to loading pressures, S_u/P_c are considered to be an almost constant value.

Ratios of undrained shear strengths to loading pressures, S_u/P_c are expressed as the equation (2)

$$\frac{S_{un}}{P_c} = OCR^{1-\lambda} \cdot K + (\sigma'_{fn}/P_c) \cdot \tan \phi_e \quad \text{----- (2)}$$

In equation (2), K , ϕ_e and the ratios of effective normal stress to preconsolidation pressures are the characteristic values of soil, and the ratios of strength to overburden pressure are a function of only overconsolidation ratios, OCRs. But ratios of a swelling index to compression index, are not only a function of overconsolidation ratio OCR. But also preconsolidation pressures P_c .

However, in the case of usual excavation work, values of overconsolidation ratios, OCRs are less than 10 except for levels near the excavated surface which have values of more than 10. If overconsolidation ratio values are less than 10, the ratios of strength to overburden pressure, S_u/P_d are hardly influenced by the ratios of the swelling index to the compression index.

As above mentioned, in the case where an overconsolidation ratio, OCR is constant, the ratios of strength to overburden pressures, S_u/P_d can be considered constant.

Fig. 5-4 shows the relationship between S_u/P_d and OCR.

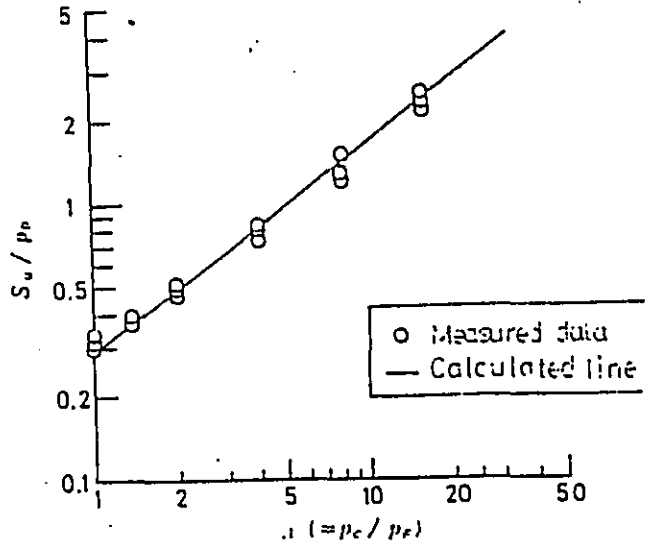


Fig. 5-4 The relationship between S_u/P_d and OCR under swelling

This proves that the denominator value of equation (1) is considered to be a constant value. And numerators of equation (1) can be considered to be a function of only overconsolidation ratios as mentioned above.

And so, the rates of strength decrease are considered to be a function of the overconsolidation ratios to first approximation, and TAKAYAMA et al.²⁾ have proved the above mentioned by a series of experiments as shown in Figs. 5-5 and 5-6.

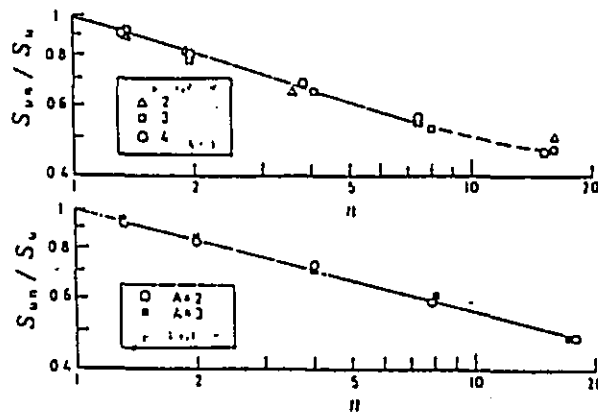


Fig. 5-5 The relationship between overconsolidation ratios and rates of strength reduce

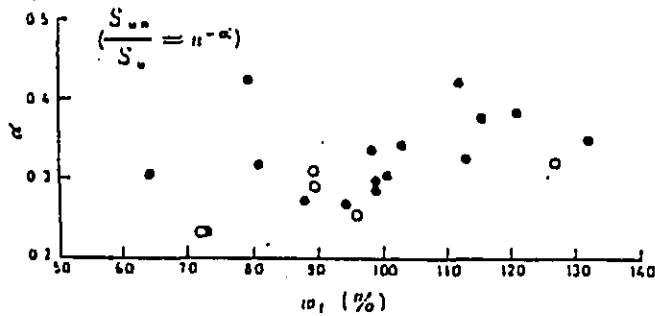


Fig. 5-6 The relationship between coefficient α and moisture content for
 ● : undisturbed Ariake clay
 ○ : remolded Ariake clay

Fig.5-7 shows the relationship between strength ratios, S_{un}/S_u . In the case where overconsolidation ratio values are less than 10, the relationship between overconsolidation ratios, (OCR) and rates of strength decrease due to unloading, (S_{un}/S_u) are linear on both axes of a logarithmic graph as in Fig.5-7 and are expressed as equation (3) approximately.

$$S_{un}/S_u = OCR^{-\alpha} = \mu B \quad \text{----- (3)}$$

The coefficient α in equation (3) is determined by the curve fitting method, using the values of S_u , S_{un} and OCR that are the results of Field Vane Tests or Direct Shear Tests or Dutch Cone Tests and Consolidation Tests.

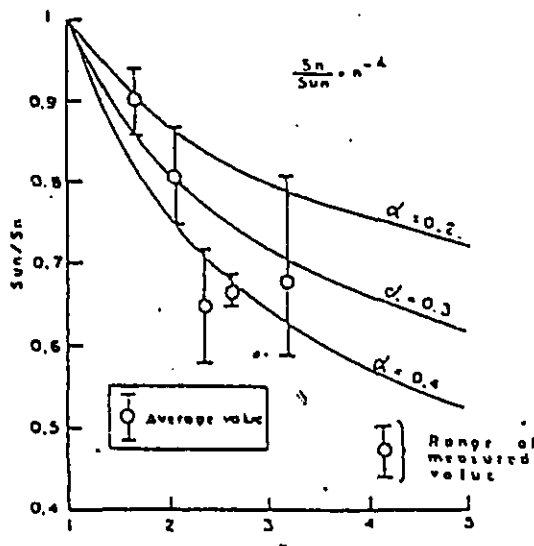


Fig. 5-7 The Relationship between OCR and strength decrease rate

② Bjerrum's coefficient

The shear strength of design is calculated by the results obtained from the Field Vane Tests. But, as mentioned above, the results of Field Vane Tests depend on the strain rate during vane shear process of soil.

Moreover, it was reported that Bangkok Clay foundation has shear strength anisotropy.

Therefore, it is necessary to correct shear strength obtained from Field Vane Tests by Bjerrum's coefficient and this is determined by the properties tests as in Fig. 5-8.

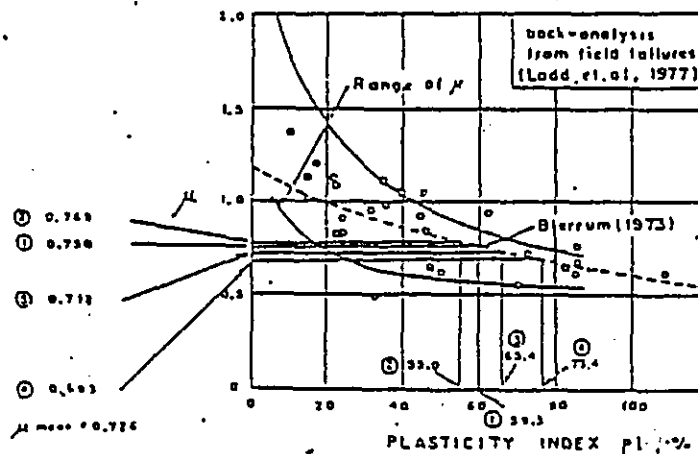


Fig. 5-8 Relationship between Bjerrum's Coefficient and Plasticity

In 1973, Bjerrum proposed the following equation to obtain the design shear strength of soil from the results of the Field Vane Tests¹⁾.

$$Su' = Su * \mu_a * \mu_r \quad \text{----- (4)}$$

where; Su' : Design shear strength

Su : Shear strength obtained from Field Vane Tests

μ_a : Corrected coefficient regarding anisotropy of strength

μ_r : Corrected coefficient regarding strain rate of shear process

μ_A : Bjerrum's coefficient ($\mu_A = \mu_a * \mu_r$)

Finally, in the case of excavated slope stability analysis, as mentioned above, we should determine the design shear strength taking into account two kinds of corrected coefficients μ_A and μ_B as follows,

$$Su^* = \mu A * \mu B * Su \quad \text{----- (5)}$$

Where, μA : Bjerrum's coefficient regarding shear strength obtained from Field Vane Tests

μB : Coefficient of strength decrease caused by excavation work

Su : Shear strength obtained from Field Vane Tests

Su^* : Design shear strength

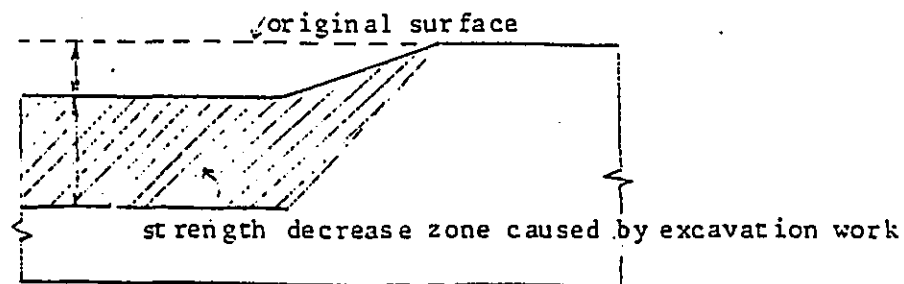


Fig.9 Strength Decrease Zone

Fig. 5-10 Shows the procedure for determination of design shear strength of excavated soft soil slopes.

Determination of shear strength decrease rate by excavation work

Apply Advanced Total Stress Method

Apply Nakase's Method
Formulization of undrained shear strength decrease rate after swelling by Hvorslev's criteria

- ① Direct shear test
- ② In situ tests
(Dutch Cone)
(Field Vane)

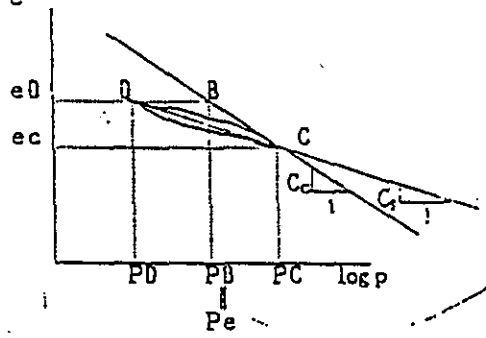
It is substantiated that the shear strength decrease rate is independent of consolidation pressure.

Hvorslev's failure criteria
 $\tau_f = C_e + \sigma'_f \cdot \tan \phi_e$ (1)
 C_e : Hvorslev's failure cohesion
 "Ce" is given by water content or void ratio.
 ϕ_e : Hvorslev's friction angle

$C_e = \kappa \cdot P_e$ (2)
 κ : Coefficient of cohesion
 P_e : Hvorslev's equivalent consolidation pressure

A

e - log P curve under isotropic and normal consolidation condition



Hvorslev's equivalent consolidation pressure

Fig. 5-10 (1) Excavated Slope Stability Problem for marine clay foundations

A

① Overconsolidation Ratio

$$OCR = P_c / P_D \quad \dots\dots(3)$$

② Equivalent Consolidation Stress(at P_D)

$$P_e (= P_B) = P_c \cdot OCR^{-1} \quad \dots\dots(4)$$

$$\lambda = \frac{C_s}{C_c} \quad \dots\dots(5)$$

swelling index compression index

Equations (2) to (5)
are substituted for equation (1)

Normally Consolidated Clay

$$\tau_f = S_u$$

$$= \kappa \cdot P_e + \sigma' f \cdot \tan \phi_e \quad \dots\dots(6)$$

$$\therefore \frac{S_u}{P_c} = \kappa + \left(\frac{\sigma' f}{P_c} \right) \cdot \tan \phi_e \quad \dots\dots(7)$$

Overconsolidated Clay

$$\tau_f = S_{un}$$

$$= \kappa \cdot P_D + \sigma' f_n \cdot \tan \phi_e$$

$$= \kappa \cdot P_c \cdot OCR^{-1} + \sigma' f_n \cdot \tan \phi_e \quad \dots\dots(8)$$

$$\frac{S_{un}}{P_D} = \kappa \cdot OCR^{1-1} + \frac{\sigma' f_n}{P_D} \cdot \tan \phi_e$$

$$= OCR^{1-1} \cdot \left(\kappa + \frac{1}{OCR^{1-1}} \cdot \frac{\sigma' f_n}{P_D} \cdot \tan \phi_e \right)$$

$$= OCR^{1-1} \cdot \left(\kappa + \frac{\sigma' f_n}{P_e} \cdot \tan \phi_e \right) \quad \dots\dots(9)$$

B

Fig. 5-10 (2) Excavated Slope Stability Problem for marine clay foundations

B

The shear strength decrease rate is derived by equations (7) and (9).

$$\frac{S_{un}}{S_u} = \frac{P_c \cdot OCR^{-1} \cdot OCR^{1-\alpha} \cdot \left[\kappa + \frac{\sigma'_{fn}}{P_e} \cdot \tan \phi_e \right]}{P_c \cdot \left[\kappa + \frac{\sigma'_{fn}}{P_e} \cdot \tan \phi_e \right]}$$

$$= OCR^{-1} \cdot \frac{\kappa + \frac{\sigma'_{fn}}{P_e} \cdot \tan \phi_e}{\kappa + \frac{\sigma'_{f}}{P_c} \cdot \tan \phi_e} \quad \text{---- (10)}$$

$OCR \sim \lambda, OCR \sim \sigma'_{f} / P_c$
 If λ and (σ'_{f}/P_c) of the soil are the characteristic value, the strength decrease rate can be considered to be a function of OCR.

$$\frac{S_{un}}{S_u} = OCR^{-\alpha} = \mu B \quad \text{---- (11)}$$

In the case of Ariake clay -
 $\alpha = 0.2 \sim 0.4$

Determine the strength rate under plain strain condition

Introduce the anisotropy of strength

Laboratory Test
 (K_0 -Triaxial Comp.)
 Nishihara & Ohta (1985)

In situ Test
 (Field Vane)
 Bjerrum's method

Compare the theory with the experimental values

M, Λ, K_0 STS
 K_0 - condition

↕ triaxial tests' values

M, Λ, K_0

Bjerrum's coefficient μA

- ① Take into account strain rate and strength anisotropy
- ② Determine Plasticity

C

D

Fig. 5-10 (3) Excavated Slope Stability Problem for marine clay foundations

C

D

(Normally consolidated clay)

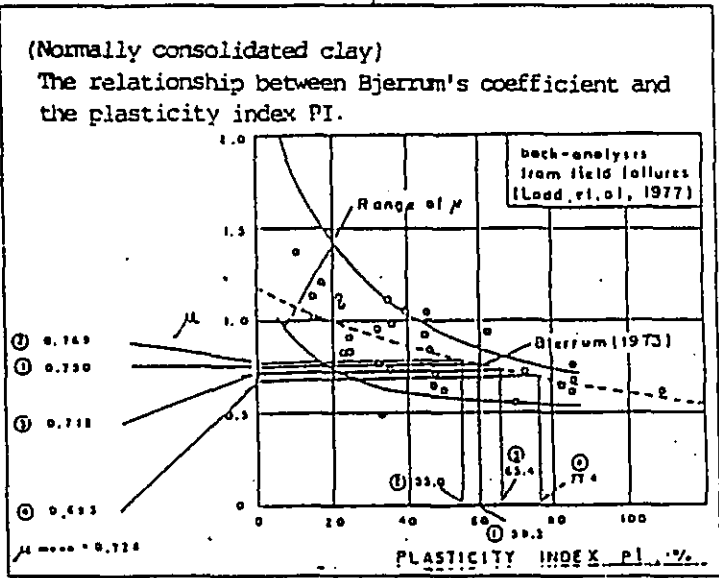
$$\frac{S}{\sigma'_{fo}} = \frac{1+2K_o}{6} M \cdot \exp \frac{\Lambda \mu_o}{M} - \Lambda$$

$$M = 6 \sin \phi' / (3 - \sin \phi')$$

$$\Lambda = 1 - C_s / C_c \text{ or } \Lambda = \mu / 1.75$$

$$\eta = 3(1 - K_o) / (1 + 2K_o)$$

$$\beta = \sqrt{3} \mu_o \Lambda / 2M$$



$M, \Lambda, \mu_o, K_o, OCR, \omega$

TYPE2
Bjerrum's coefficient is determined by the plastic index.

TYPE1

$$\frac{\tau}{\sigma'_{vi}} = \frac{OCR^\Lambda (1+2K_o) \cdot M \exp(-\Lambda)}{3\sqrt{3}(\sqrt{\cos^2 R^2 \beta \cdot \sinh^2 \beta \cdot \cos^2 2\omega - \sinh \beta \cdot \sin 2\omega})}$$

The anisotropic properties introduced by stress.

Apply type 2 method for the determination of a design strength for clay

Determine the design shear strength undrained (S_u^*)

$$S_u^* = S_u \cdot \mu_A \cdot \mu_B \quad \text{----- (12)}$$

S_u : Shear strength obtained from Field Vane Tests
 μ_A : Bjerrum's coefficient
 μ_B : Shear strength decrease rate caused by unloading

Fig. 5-10 (4) Excavated Slope Stability Problem for marine clay foundations

2) Preparation of slope stability analysis model

In the case of alluvium where marine clay has been sedimented horizontally, each layer has almost the same properties and tends to change in proportion to the depth.

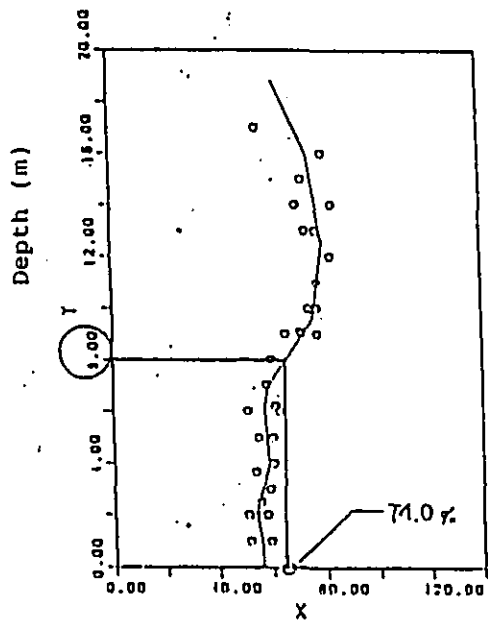
Consequently, the analysis model should be prepared by taking vertical distribution of parameters into account.

The number of physical property values or analysis parameters to be considered is twelve as follows;

- | | | | | |
|-----|---|----|---|---------------------------------------|
| A | } | 1 | Placticity index PI | |
| | | 2 | Bjerrum's coefficient | (μ_A) |
| B | } | 3 | Unit weight | γ_t |
| | | 4 | Groundwater level | h |
| | | 5 | Effective vertical stress before excavation | σ'_{vo} |
| | | 6 | Effective vertical stress during excavation | σ'_{vd} |
| | | 7 | Effective preconsolidation pressure | σ'_{vc} |
| | | 8 | Overconsolidation ratio | $OCR (= \sigma'_{vc} / \sigma'_{vd})$ |
| | | 9 | Strength decrease index | α |
| | | 10 | Strength decrease ratio | $(\mu_B) = OCR^{-\alpha}$ |
| Su* | } | 11 | Undrained shear strength | |
| | | | by Field Vane Test | $(S_u)_{FV}$ |
| | | 12 | Design strength of excavated slope | (S_u) |

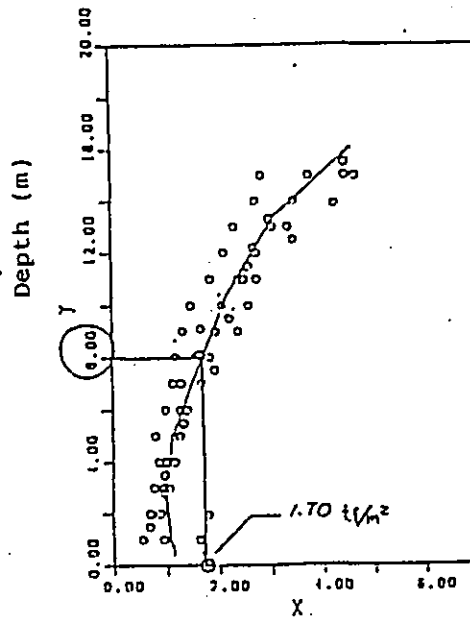
The twelve parameters mentioned above shall be determined through the procedure shown in Fig.5-10, and Figs.5-12 to 5-15 show examples of parameter distributions in soft soil foundations.

It is necessary to consider the strength-decreased zone beneath the excavated surface due to swelling by reduction of load. As shown in Figs.5-12 to 5-15, the strength-decreased zone is considered to be twice or three times as deep as the excavation depth.



Plasticity index, P.I. (%)

PI = 74.0



Undrained shear strength by F.V., S_u (tf/m^2)

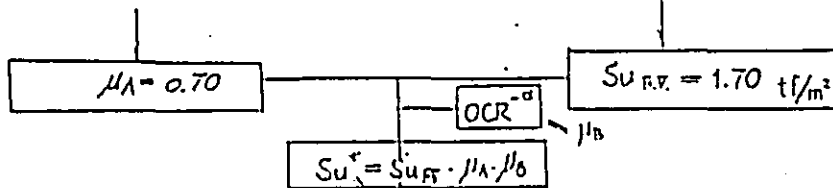
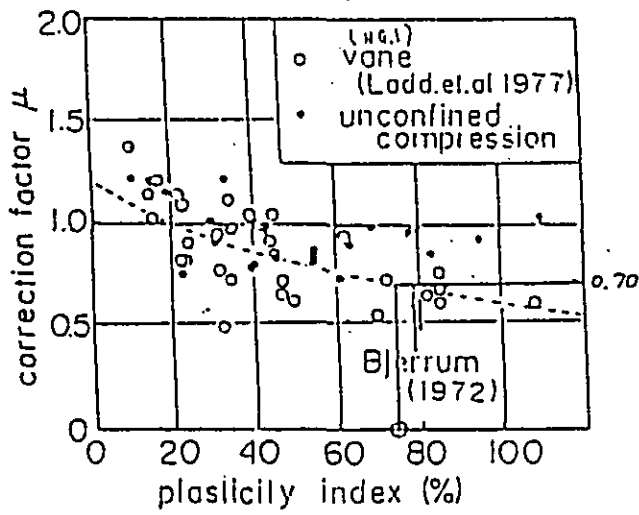


Fig. 5-11 Flowchart of Determination of Undrained Shear Strength

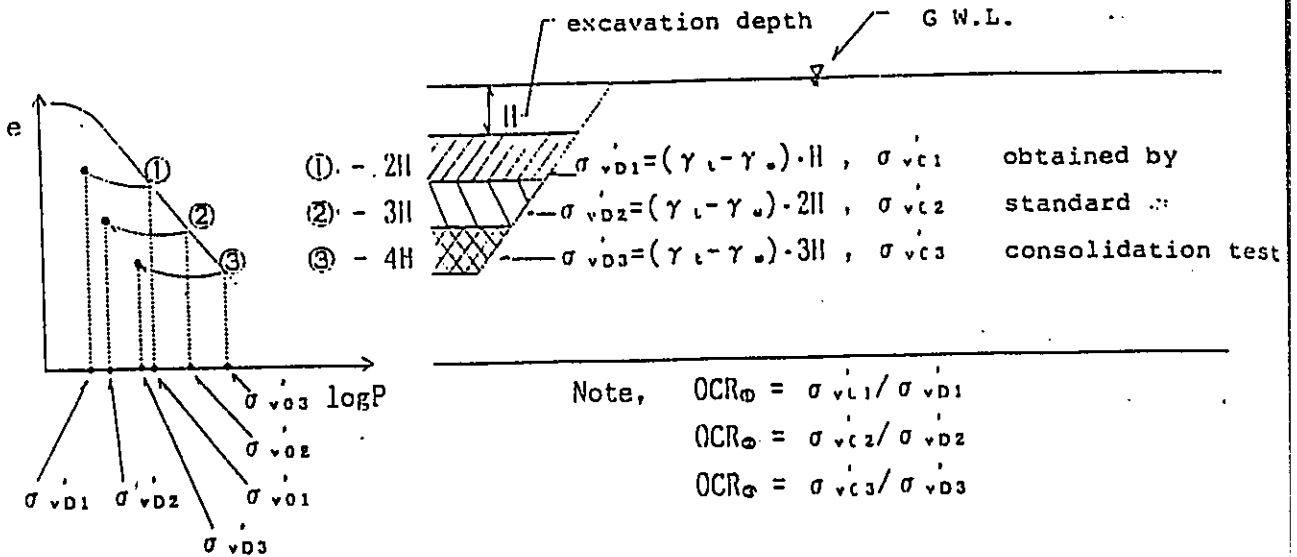


Fig. 5-12 Unloading process in every zone in soft soil foundation

Fig. 5-13 Distribution of effective overloading pressure before and after excavation in soft clay foundation

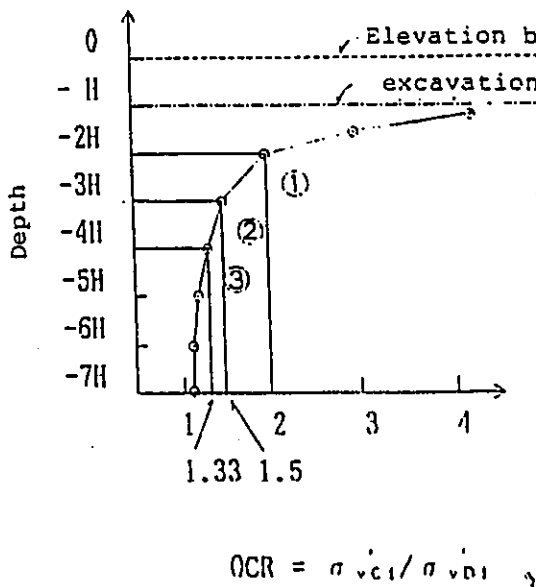


Fig. 5-14 O.C.R. at each depth in soft clay foundation

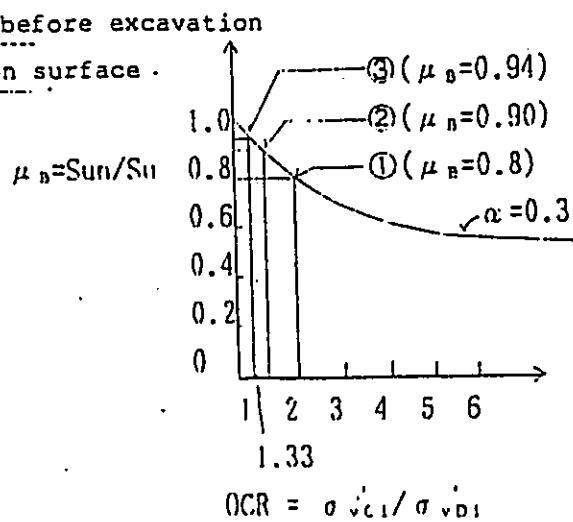


Fig. 5-15 Relationship between strength decrease rate and O.C.R.

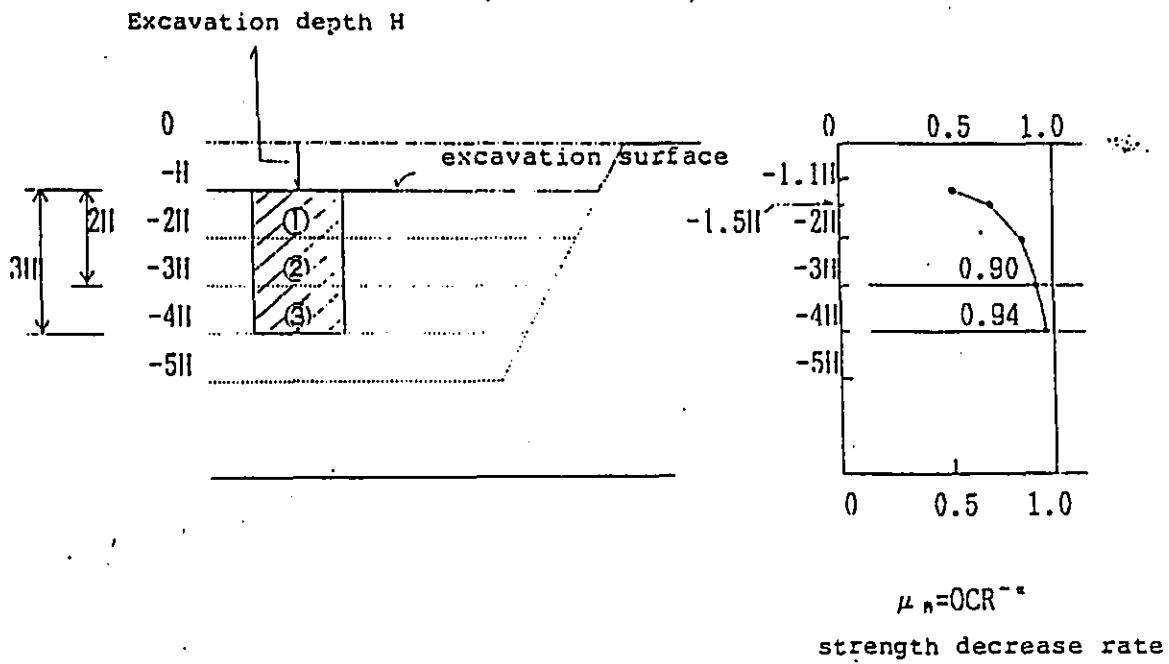


Fig. 5-16 Distribution of strength decrease rate

(μ_n) in vertical direction

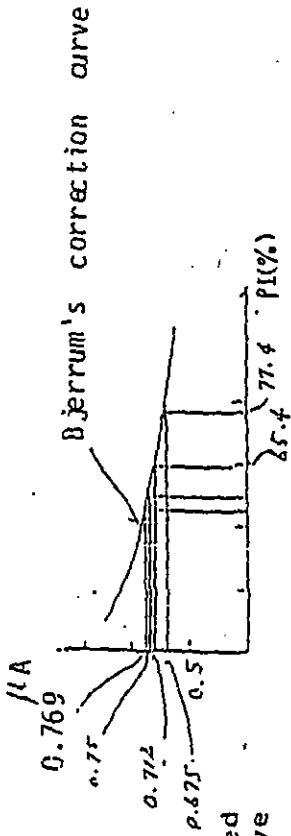


Table 5-1
Strength Decrease Ratio Obtained
from Bjerrum's Correction Curve

El. (m)	PI	μ_A	Remark
0.0	55	0.83	
-1.0	55	0.83	
-3.0	58.8	0.738	
-5.0	59.8	0.728	
-7.0	64.4	0.71	
-9.0	73.5	0.7	
-11.0	79.3	0.681	
-13.0	77.7	0.692	
-15.0	73.4	0.701	
-17.0			

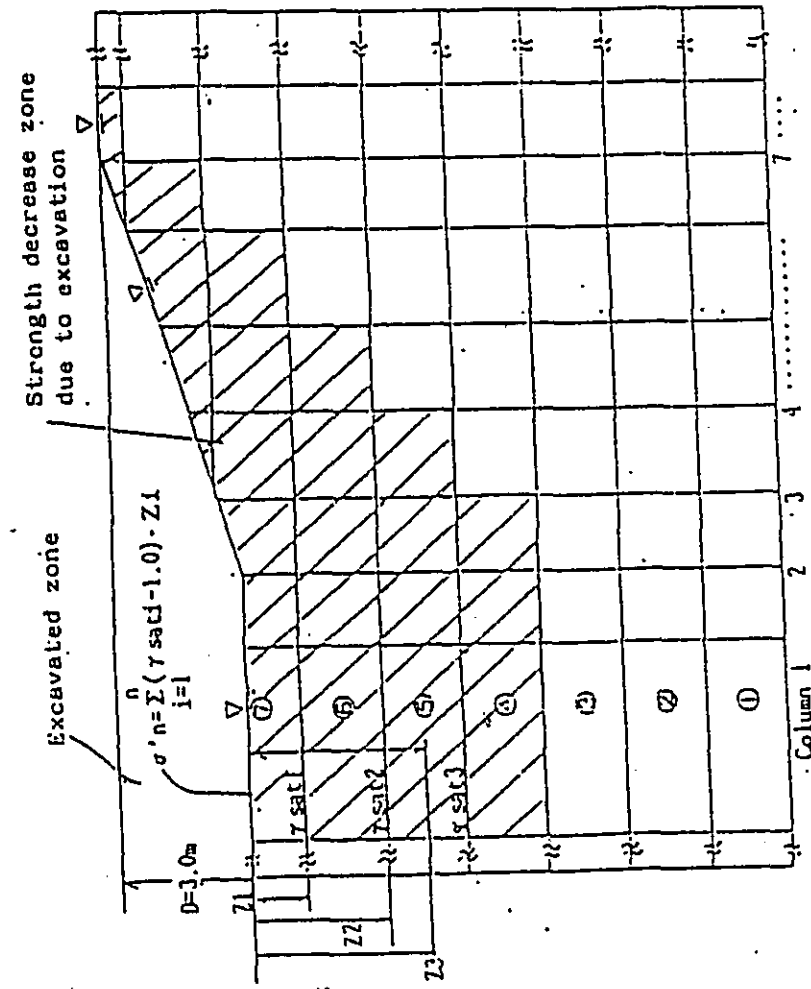
El.	Layer	μ -PI Relation curve	$\sigma'_{\Delta u}$	r_t	S_u
0.0	Layer (A)	∇	2.5	1.47	1.2
-1.0	Layer (B)	Δ	2.5	1.47	1.14
-3.0	Layer (C)	∇	2.88	1.47	1.04
-5.0	Layer (D)	Δ	4	1.47	1.27
-7.0	Layer (E)	∇	4.5	1.44	1.68
-9.0	Layer (F)	Δ	7	1.4	2.08
-11.0	Layer (G)	∇	7.2	1.41	2.62
-13.0	Layer (H)	Δ	9	1.43	3.38
-15.0	Layer (I)	∇	14	1.54	4.5
-17.0					

$\sigma'_{\Delta u}$: Preconsolidation pressure (t_f/m^2)
 S_u : Undrained shear strength (t_f/m^2)
 r_t : Wet density (t/m^3)

PI : Plasticity index
 μ_A : Bjerrum's correction factor

Fig.5-17. Deposit Layer Components

ELM	σ'_{vm}	σ'_n	OCR	α	μ_A	μ_B	SU	SU
7	2.8	0.225	11.915	0.3	0.83	0.476	1.04	0.411
6	4	0.94	4.253	0.3	0.738	0.642	1.27	0.607
5	4.5	1.82	2.395	0.3	0.71	0.765	1.66	0.912
4	7	2.82	2.482	0.3	0.7	0.767	2.02	1.108
3	7.2	—	—	—	0.681	—	2.62	1.72
2	9	—	—	—	0.693	—	3.35	2.322
1	14	—	—	—	0.701	—	4.5	3.152



Remarks : σ'_{vm} : Preconsolidation pressure (tf/m^2)
 σ'_n : Effective normal stress after excavation work (tf/m^2)
OCR : Overconsolidation ratio after excavation
 α : Constant parameter of strength decrease, $Su/Sn=OCR^{-\alpha}$
 μ_A : Bjerrum's correction factor
 μ_B : Correction factor ($=OCR^{-\beta}$)
Su : Shear strength from F.V. test data (tf/m^2)
 Su^* : Shear strength for design (tf/m^2), $Su^* = \mu_A \cdot \mu_B \cdot Su$

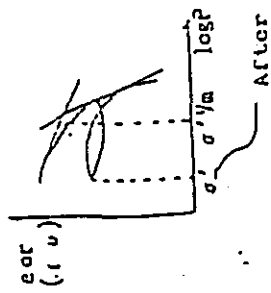


Fig. 5-13 Ratio of Strength Decrease and Design Parameters for Non-treatment Slope

(2) Slope stability analysis for the treated slopes

1) Determination method of design parameters for the treated slopes.

In the case of the excavated slopes treated by the cement column method or the sand compaction method, the design strength for slope stability analysis should be considered as follows;

① Strength of soft soil foundation

As mentioned in section (1), design strength (Su^*) should be determined as the product of the strength by Field Vane Tests (Su) and coefficient of correction ($\mu A, \mu B$)

② The strength of the improved areas composed of soft soil and sand piles or soft soil and cement columns

Improved areas are composite areas composed of soft soil and sand piles or soft soil and cement columns as in Fig.5-19.

Consequently, supposing that the improved zones are composite ground, the strength of the composite ground can be estimated by using the volumetric ratio of soft soil by sand piles or cement columns (A_s) and each strength of the soft soil itself and sand piles or cement columns.

Composite ground.....every layer (A) - (E) of composite ground (Improved zone) has its composite strength

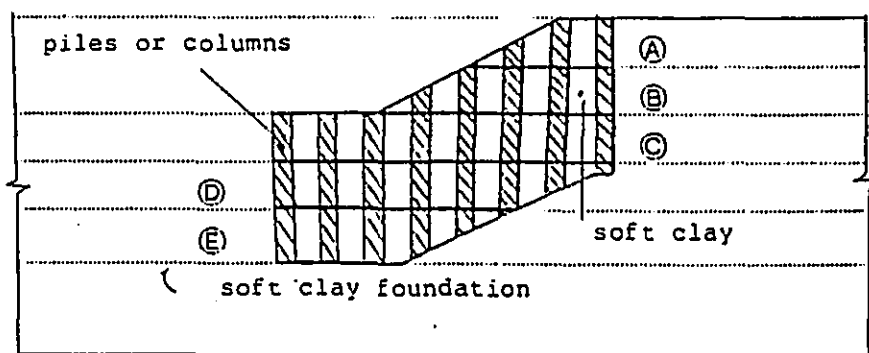


Fig.5-19 Excavated slope improved by sand compaction piles or cement columns

In the case of marine clay as shown in Fig. 5-19, the following matters should be taken into account.

- ① The composite strength of each layer of the improved zones is not the same but each layer has its own composite strength owing to different strengths of the clay layers.
- ② Concerning excavated clay parts in the improved zones, the strength decrease rate (μB) should be considered the same as for the soft soil foundation mentioned in ①

a) Soil cement column method (deep soil improvement)

The composite strength (τ_{csi}) of each layer improved by the soil cement column method is determined by the following equation.

$$\tau_{csi} = \frac{1}{n} [C_p \cdot A_{ss} + (1-A_{ss}) \cdot S_{u^*}] \dots (6)$$

where;

- n : Safety factor taking into account the scattering of soft cement column strength, usually $n = 1.2$
- C_p : Soil cement column strength, usually estimated from unconfined compression tests ($C_p = q_u/2$)
- A_{ss} : Volumetric replacement ratio by soil cement columns
- S_{u^*} : Undrained shear strength of clay part in improved zones ($S_{u^*} = \mu A + \mu B S_u$)

Fig. 5-20 gives an example of how to determine the design strength of the improved zone by soil cement columns and Table 5-2 expresses the value of parameter of each layer in the left column, that is, column 1 in Fig.5-20.

b) Sand compaction pile method

The composite strength (τ_{csi}) of each layer improved by the soil cement column method is determined by the following equation.

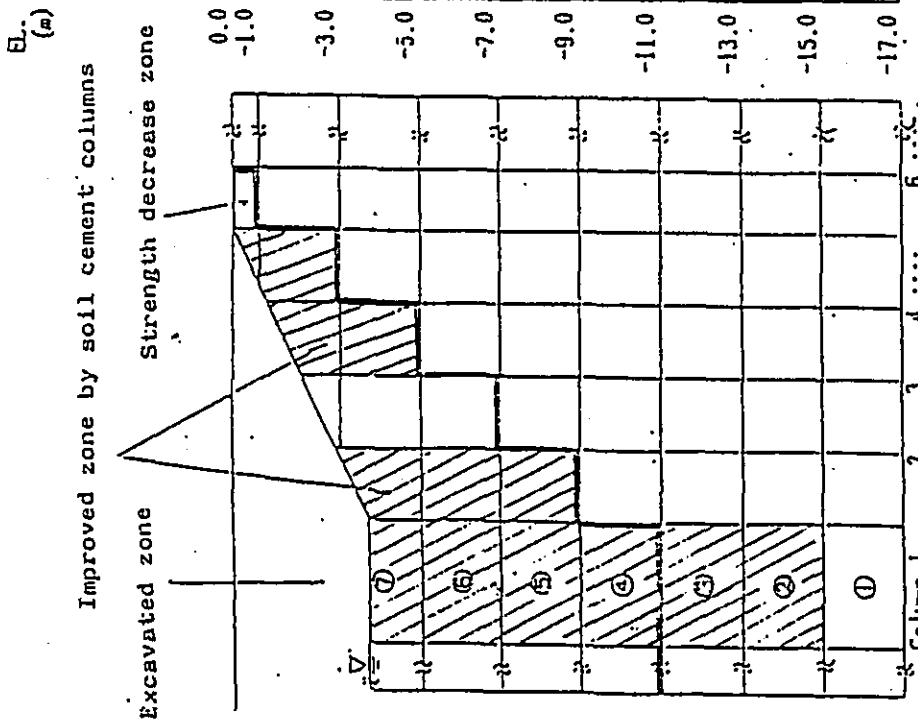
$$\tau_{csi} = (1-A_{ss}) \cdot \beta \cdot S_{u^*} + A_{ss} \cdot C_u \cdot \tan \theta \dots (7)$$

where;

- β : Coefficient of strength change taking into account the drain effect by sand compaction piles and disturbance during

Table 5-2 Design Parameters of Improved Zone by Soil Cement Columns

EL#	Mobilized shear strength in improved zone by soil cement columns									
	μA	μB	SU	SU	Ass	n	Cp	τ		
7	0.83	0.476	1.04	0.411	0.3	1.2	29	7.95	Strength decrease zone	
6	0.732	0.612	1.27	0.607	0.3	1.2	29	7.6	Improved zone	
5	0.71	0.765	1.62	0.917	0.3	1.2	29	7.78		
4	0.7	0.751	2.02	1.102	0.3	1.2	29	7.9		
3	0.681	1	2.62	1.784	0.3	1.2	29	8.25		
2	0.693	1	3.35	2.323	0.3	1.2	29	8.6		
1	0.701	1	4.3	3.155	0.3	1.2	29	9.09		



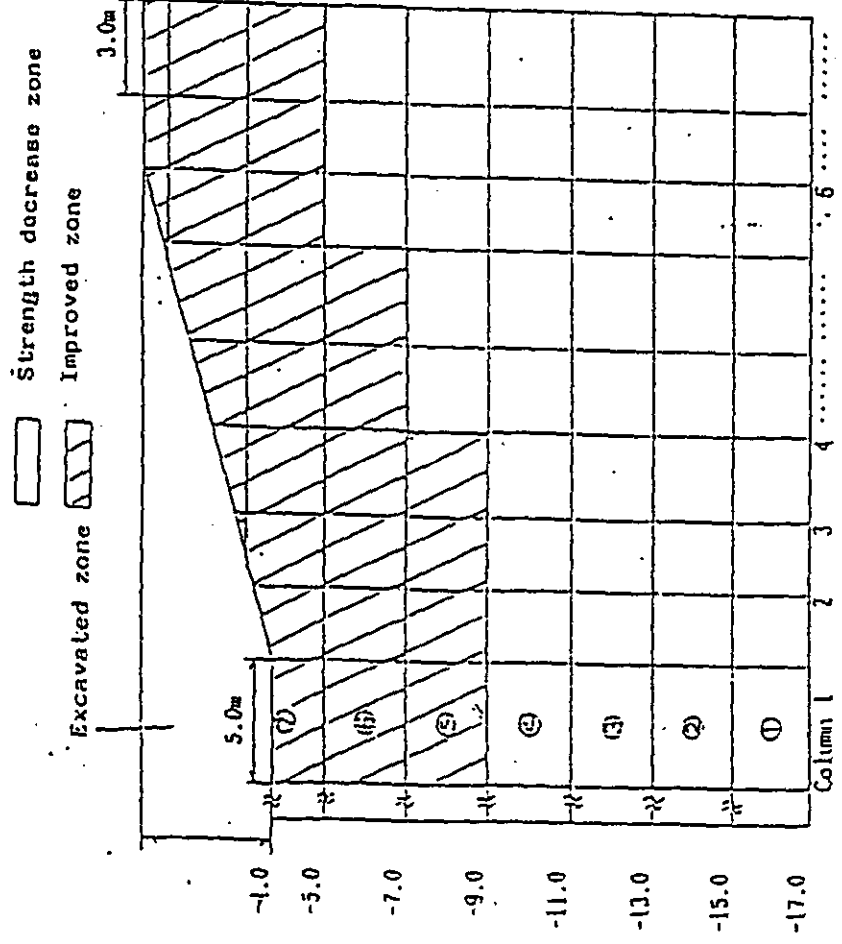
A : Bjerrum's correction factor
 B : Correction factor ($=0.0R^{-\alpha}$, $\alpha=0.3$) (tf/m^2)
 Su : Shear strength F.V test data (tf/m^2)
 Su* : Design shear strength (tf/m^2)
 Ass : Volume ratio
 n : Safety factor
 Cp : Shear strength of soil cement columns

Fig. 5-20 Strength Decrease Zone and Improved Zone by Soil Cement Columns

Strength decrease zone
 Improved zone

Table 5-3 Design Parameters of Improved Zone by Sand Compaction Piles

EL. (m)	μ_A	μ_B	SU	SU'	Ass	ϕ	$\frac{\Delta c}{\Delta P}$
0.0	—	—	—	—	—	—	—
-1.0	—	—	—	—	—	—	—
-3.0	—	—	—	—	—	—	—
-5.0	0.32	0.476	1.04	0.411	0.1	30	0.2
-7.0	0.738	0.648	1.27	0.507	0.1	30	0.2
-9.0	0.71	0.769	1.52	0.917	0.1	30	0.2
-11.0	0.7	0.761	2.02	1.102	0.1	30	0.2
-13.0	0.581	1	2.52	1.724	0.1	30	0.2
-15.0	0.592	1	3.35	2.322	0.1	30	0.2
-17.0	0.708	1	4.3	3.177	0.1	30	0.2

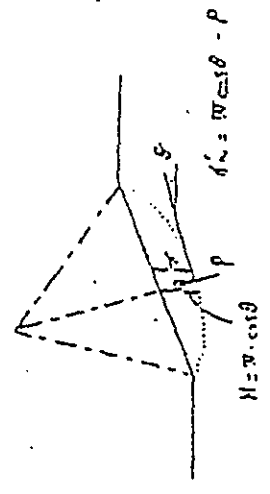


Original clay Sand compaction piles

Remarks:

- μ_A : Bjerrum's correction factor
- μ_B : $(\alpha - 0.3) \alpha$ Coefficient of strength decrease
- SU : Shear strength from F.V. test data
- SU' : $(\gamma_{sat}/\gamma_{sat})$ Shear strength for design
- Ass : Improved volume ratio
- ϕ : Internal friction angle of sand
- $\frac{\Delta c}{\Delta P}$: Coefficient of strength decrease in clay by drainage

Fig. 5-21 Strength Decrease Zone and Improved Zone by Sand Compaction Piles



driving piles.

Su^* : Undrained shear strength of clay part in improved zone

$$(Su^* = \frac{1}{2} A \cdot \frac{1}{B} \cdot Su)$$

Ass : Volumetric replacement ratio by sand compaction piles

$\sigma'_{n'}$: Effective surcharge load

ϕ : Internal friction angle of sand compaction piles (total stress analysis)

Fig.5-21 gives an example of how to determine the design strength of the improved zone by sand compaction piles and Table 5-3 expresses the values of the parameters of each layer in the left column, that is, column 1 in Fig.5-21.

2) Preparation of slope stability analysis model

When we prepare the excavated slope stability analysis model for zones improved by the cement column method or the sand compaction pile method, the following matters should be considered:

- ① Marine clay consists of horizontal sediment layers. Therefore, the analysis model should be prepared by being divided into horizontal layers taking into account the property values in each layer as mentioned in (2),1)
- ② The strength decrease zone due to excavation will be two or three times as deep as the depth of the excavated zone. It is desirable to check the depth of the strength decrease zone in soft soil foundation by in situ tests such as Dutch Cone Tests, Field Vane Tests or F.E.M analysis.

Analyzed models are shown in Figs.5-22 and 23.

References;

- 1) Akio NAKASE, Masaki KOBAYASHI, Hisashi KASUNO: Shear Strength Change in Saturated Soil due to Consolidation and Swelling, Technical Report of Research Institute of Harbor Engineering, 8-4 (1969) (in Japanese)
- 2) Masateru TKAYAMA : Channel Slope Stability in Ariake Clay Foundations (Research theme No 57460198) (in Japanese)

Slope Gradient 1:4

F.S.=1.408

R=40.0

(X, Y)=(45.0, 30.0)

F.S.=1.292

R=31.25

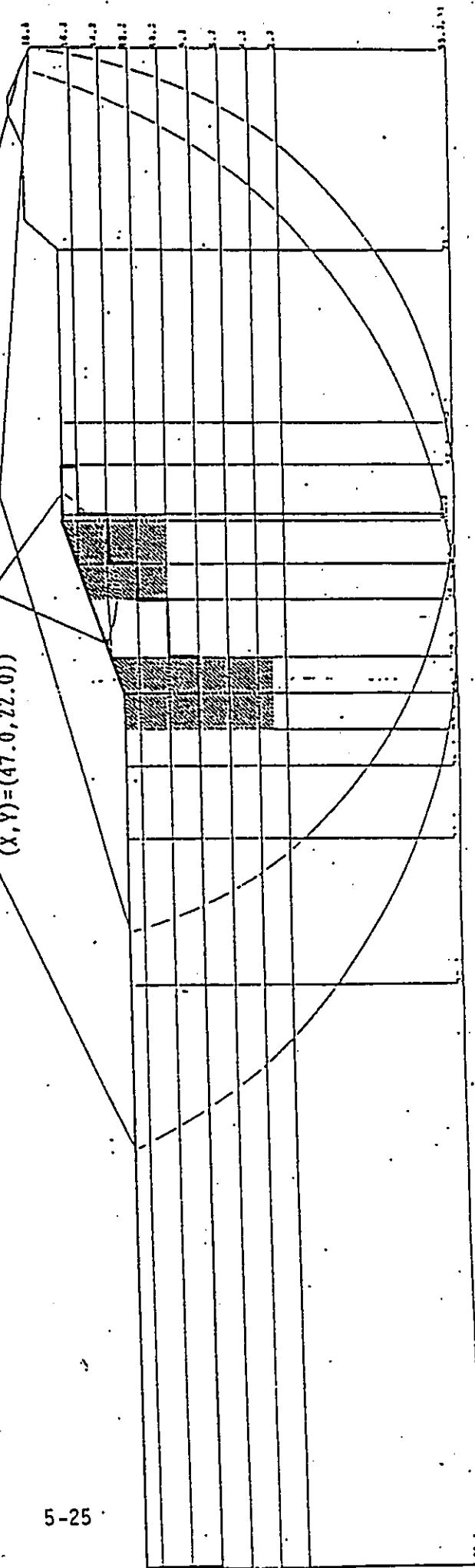
(X, Y)=(53.75, 21.25)

F.S.=9.402

R=8.54

(X, Y)=(47.0, 22.0)

Fig. 5-22 Critical Slip Circle in Improved Slope by Soil Cement Columns



Slope Gradient 1:3

F.S.=1.309

R=19.66

(X,Y)=(53.13,16.25)

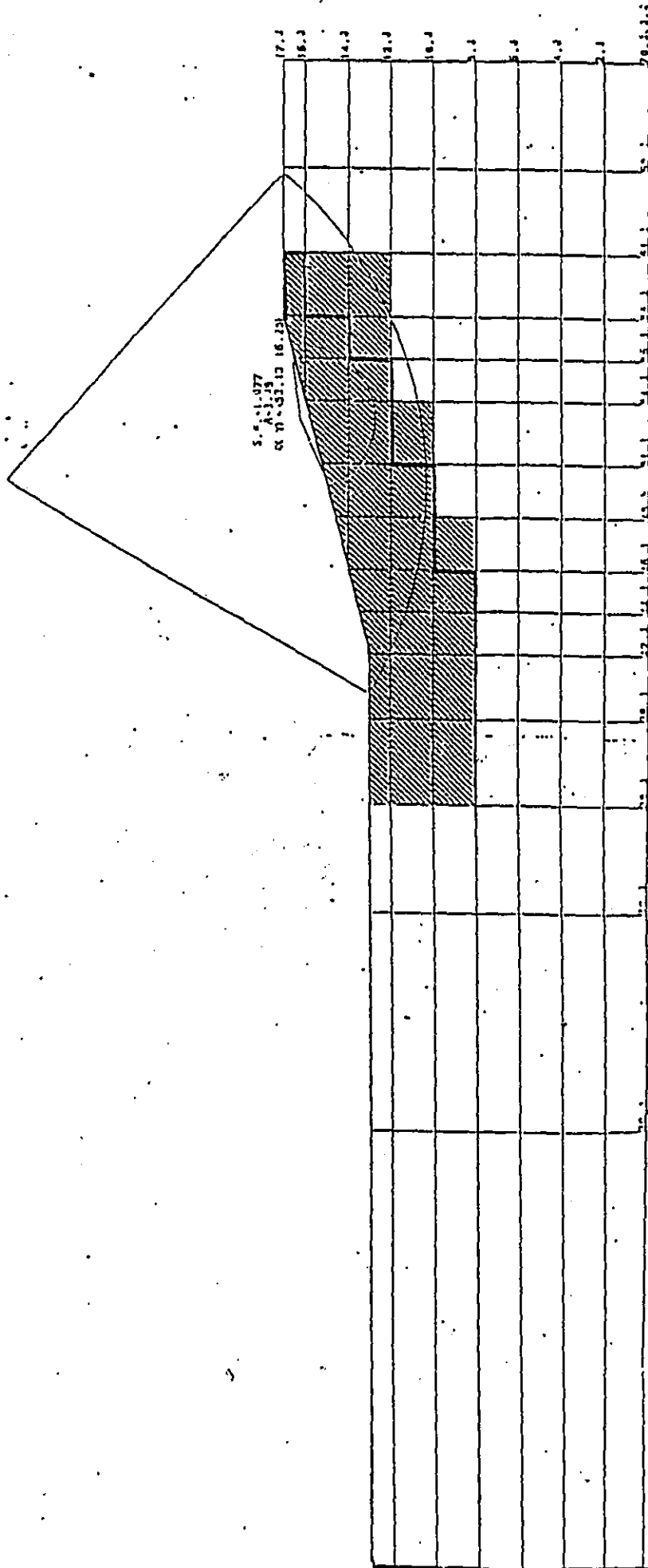


Fig.5-23 Critical Slip Circle in Improved Slope by Sand Compaction Piles

5-3

· OPERATION MANUAL

5-3 Operation Manual for Slope Stability Analysis System

1. Outline

These programs for slope stability analysis (hereinafter referred to as "the program") can be applied to the analysis in the case of excavated slopes on soft soil and composite ground by improvement construction method. The program is prepared by the improvement of the existing program which is for embankment slope stability based on Bishop's method. Though these results, excavated slope stability analysis, which has not been carried out before, will be possible in I.E.C. The computation can be executed by the program on embankment slopes and excavated slopes on soft soil, in accordance with the following case mentioned in Table-5.

Table-5 Cases for examination of slope stability at fill dam

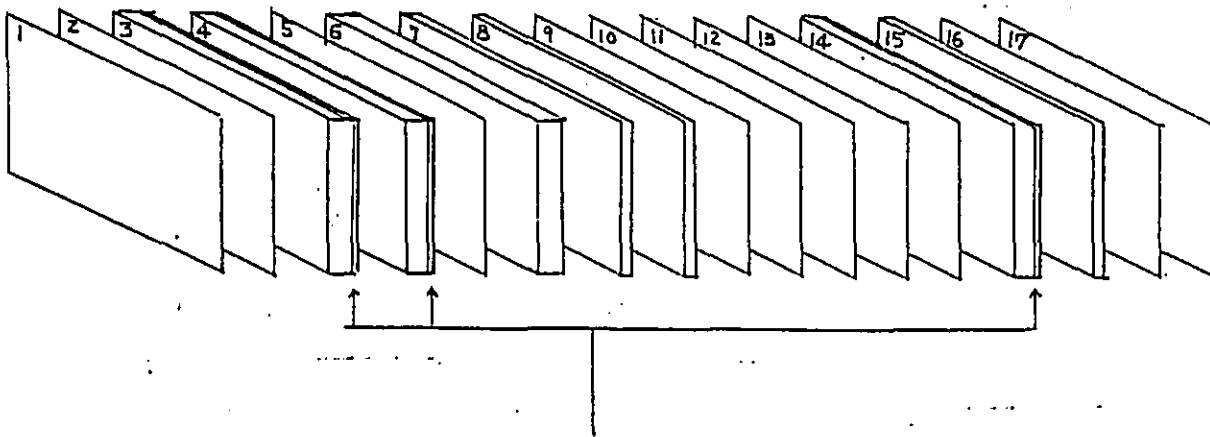
case	Dambody condition or reservoir water level	Hydro-static water level	Design seismic factor for seismic inertia force (%)	Application of circular arc
1	Normal full water level	Normal full water level	100	Effective stress
2	Immediately after completion (Empty)	-	50	Total stress or effective stress
3	Intermediate water level	Intermediate water level	100	Effective stress
4	Rapid drawdown	Lowest water level after draw down	100	Effective stress
5	Surcharge water level	Surcharge water level	50	Effective stress
6	Design flood level	Design flood level	-	Effective stress

* Remarks :

- 1 Analysis of the excavated slopes and composite ground slope can be carried out in case 1.
- 2 Water level can be changed randomly.

2. INPUT USAGE

[1] Constitution of Input data



key in '999' or '99' to indicate the end of data

where

- (1) Title Card
- (2) Calculation Case Control Card
- (3) Nodal Point Data
- (4) Element (or Zone) Data
- (5) Number of Elements Data
- (6) Material Properties Data
- (7) Corrected Coefficients for Excavated Slope of Clay Foundation Data
- (8) Foundation Improvement Condition Data
- (9) Loading Condition Data ①
- (13) Loading Condition Data ⑤
- (14) Calculation Point Data ①
- (15) Calculation Point Data ②
- (16) Control Card of Secondary Calculations
- (17) Calculation Radius Data

[2] Data Input Procedure

(1) Title Card

READ (SUB EXREAD) (HEAD) (I), I=1,10)

col.	variable (format)	contents
1-40	HEAD(i) i=1,10 (10A4)	Title name of the analysis

(2) Calculation Case Control Card

READ (SUB EXREAD) (IDAM)

col.	variable (format)	contents
11-15	IDAM (I5)	Calculation Case Index

Note :

According to the kind of structure computed by these programs,
" IDAM " can be designated as follows.

IDAM { = -1 --- fill dam
= 0 --- excavated slope of clay foundation

(3) Nodal Point Data

READ (SUB EXREAD) L, NPP(NPI), PX(NPI), PY(NPI), MPI=1, NPI-1

col.	Variable (format)	contents
1-10	L (i10)	Key in '999' after last data entry
11-15	NPP(NPI) (i5)	Number of Nodal points
21-30	PX(NPI) (F10.2)	X coordinate of the nodal point NPP(NPI)
31-40	PY(NPI) (F10.2)	Y coordinate of the nodal point NPP(NPI)

Remarks :

Maximum total number of Nodal points is 150, and the value of PX(NPI), PY(NPI) is more than zero.

$$NPP(NPI) \leq 150$$

$$PX(NPI) \geq 0$$

$$PY(NPI) \geq 0$$

(4) Element (or Zone) Data

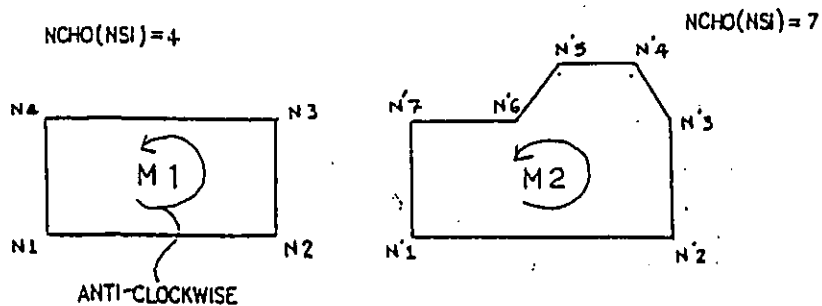
READ (SUB EXREAD),^{L,} KZ(NSI), NCHO(NSI), (LINK(NSI,J), J=1,12)

col.	Variable (format)	contents
1-9	L	Key in '999' on the last card*1)
10-12	KZ(NSI) (I3)	The number of the element
14-15	NCHO(NSI) (I2)	Nodal point numbers constituting the elements
18-21	LINK(NSI,1) (I4)	N1
22-25	LINK(NSI,2) (I4)	N2
		} The number of nodal point constituting the element
62-65	LINK(NSI,12) (I4)	N12

Remarks :

- *1) When we key in "999" on the last card, the others are blank.
- *2) Numbers of nodal points constituting the element (or zone) are less than twelve (12).

When keying in only the following data, i.e. nodal point numbers constituting the element, other are blank.



(5) Number of Elements Data

READ (SUB EXREAD) KZZZZZ

col.	Variable (format)	contents
11-13	KZZZZZ (I3)	number of Elements

(6) Material Properties Data

READ (SUB EXREAD) KZZ(i), LWRC(i), LWD(i), DE(i), DB(i), KDE,
KFU, C(i) i=1, KZZZZZ

col.	Variable (format)	contents
13-12	KZZ(i) (I3)	Element number
15	LWRC(I) (A1)	index of element material *1)
18	LWD(I) (A1)	index of element position compared of seepage flow surface *2)
21-30	DS(I) (F10.3)	saturated unit weight (tf/m ³)
31-40	DB(I) (F10.3)	wat unit weight (tf/m ³)
41-45	KDE (I5)	the internal friction angle (degrees)
45-50	KFU (I5)	the internal friction angle (minutes)
51-55	C(I) (F5.2)	cohesion

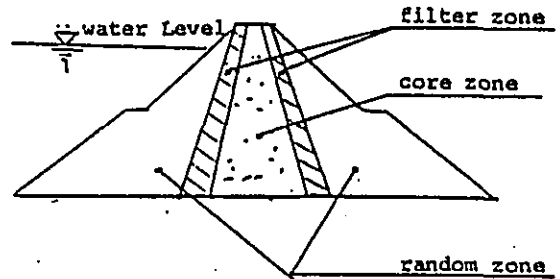
Note

*1) According to the kind of properties of the element, LWRC(I) can be designated as follows.

i) In the case of "fill dam"

$LWRC(I) = \left\{ \begin{array}{l} \text{filler} \\ R : \text{Random Rock} \\ C : \text{Core zone} \\ L : \text{water} \end{array} \right\} \text{ Zone}$

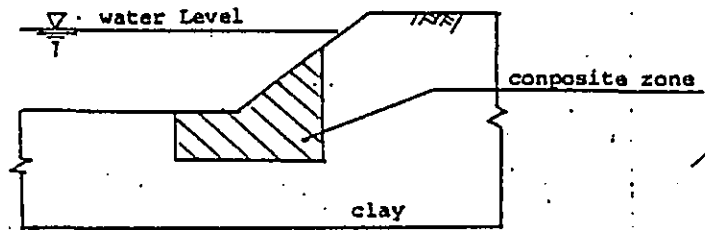
In the case of fill dam



ii) In the case of the excavated slope on clay foundation and of having the improvement zone in clay foundation.

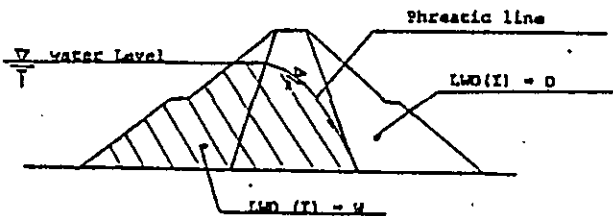
In the case of excavated slope on clay foundation

$LWRC(I) = C$



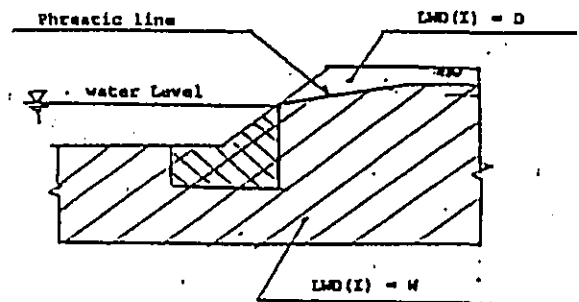
*2) $LWD(I)$ is the judgemental index as to whether the position of the element is above or below the phreatic line.

In the case of fill dam



above the Phreatic line

In the case of excavated slope on clay foundation



below the Phreatic line

(7) Corrected Coefficients for Excavated Slope of Clay Foundation Data.

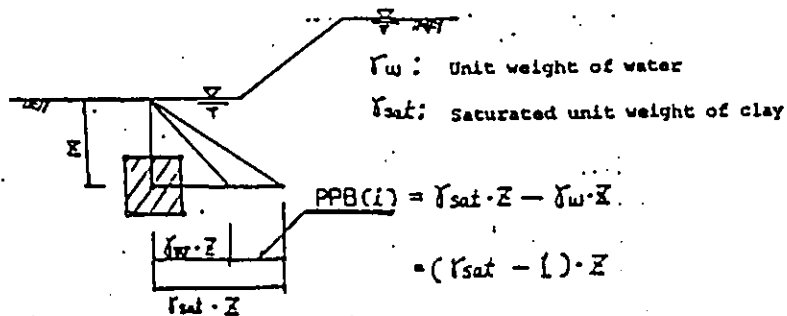
READ(SUB EXREAD) MEN, SU(I), PPB(I), PPC(I), ALF(1), IFLAG(I),
 AMIU(I), I=1, KZZZZZ

col.	variable (format)	contents
6-8	MEN (I3)	the number of element the
11-20	SU(I) (F10.3)	the original shear strength of clay from Field Vane Tests (tf/cm ²) *1)
23-32	PPB(I) (F10.3)	the effective overburden vertical pressure (tf/m ²) *2)
35-44	PPC(I) (F10.3)	the preconsolidation vertical*3) pressure
47-56	ALF(I) (F10.3)	the exponential coefficient*4) (OCR)
59-60	IFLAG(I) (I2)	the index of corrected shear strength of clay*5)
63-72	AMIU(I) (F10.3)	Bjerrum's corrected coefficient

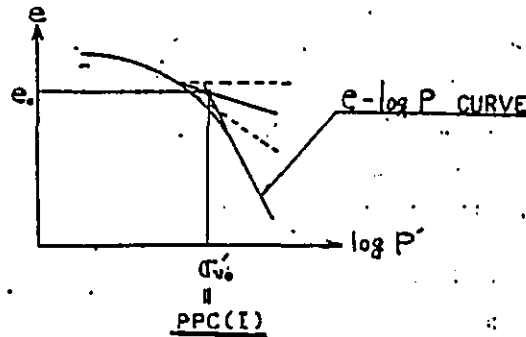
Remarks : In the case of fill dam, namely "IDAM-1", this data record is omitted.

Notes

- *1) SU(I) is the foundations' shear strength (tf/m²) obtained from the Field Vane Tests. In the case that shear strength which is obtained from tests except the Field Vane tests can be used, "AMIU(I)" has to be 1.0 (AMIU(I) = 1.0)
- *2) PPB(I) is effective vertical load on the centroid position of an element and can be obtained as follows:



- *3) PPC(I) is σ'_{vc} effective preconsolidation pressure and can be obtained from "e-logP' curve" gotten by standard consolidation tests.



- *4) ALF(I) is α , the index which shows the degree of the clay's shear strength decrease depending on over consolidation ratio, (OCR) due to the release of in-situ stress by the excavation.

$$\begin{aligned}
 Su^* &= Su * (OCR)^{-\alpha} \\
 &= Su * \mu_B \\
 &= Su(I) * \left\{ \frac{PPB(I)}{PPC(I)} \right\}^{*(-1,0*ALF(I))}
 \end{aligned}
 \tag{1}$$

where

- Su* : Design shear strength
- Su : Shear strength obtained from F.V tests
- μ_B : Coefficient of strength decrease
- OCR : Over consolidation ratio

Formula (1) was introduced based on the concepts of M.TAKAYAMA et al.¹⁾ and H.YAMAGUCHI²⁾

Regarding the details, refer to Chapter 5-1.

- *5) IFLAG (I) is the judgemental index for determination of whether it is necessary to correct clay's shear strength (su*) used for the design or not. These judgement are based on the following two ideas. One is to correct by using the coefficient of shear strength decrease due to the release of in-situ stress which is one of the important factors concerning the foundation's shear strength. The other is to correct by using Bjerrum's correction coefficient which

is to correct the shear strength obtained from F.V. tests, taking into account the anisotropy of clay and the shearing speed of clay.

$$IFLAG(I) = \begin{cases} -1 & Su^* = SU_{FV}; \text{non-correction} \\ 0 & Su^* = \mu_A * SU_{FV}; \text{Correction by } \mu_A \\ 1 & Su^* = \mu_A * \mu_B * SU_{FV}; \text{Correction by } \mu_A \text{ and } \mu_B \end{cases}$$

*6) AMIU(I) is Bjerrum's corrected coefficient for a correcting shearing strength (SU_{FV}) obtained from F.V. tests. It was confirmed by not only Bjerrum but also S.SAMBANDARAKSA et al that this coefficient could be used for Bangkok clay through the F.V tests on Bangkok clay foundation.

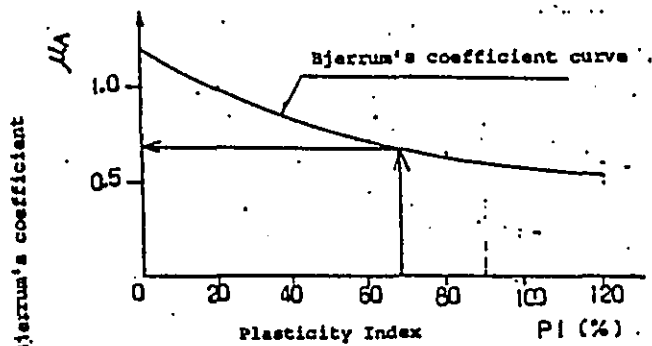


Fig.5 Relation between Bjerrum's coefficient and Plasticity Index

Fig.-5 Bjerrum's coefficient

reference

- 1)
- 2)
- 3)
- 4)

(8) Foundation Improvement Condition Data

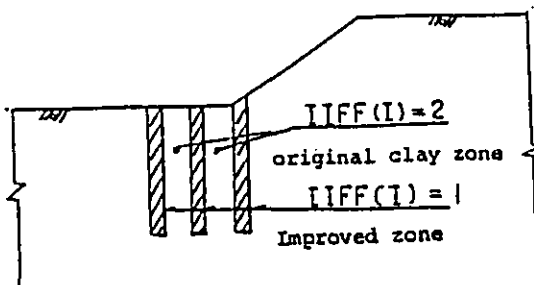
READ (SUB EXREAD) NNEN, IIFF(I), CPP(I), ASS(I)

col.	variable (format)	contents
11-15	NNEN (I5)	the number of element the
15-20	IIFF(I) (I5)	the index indicating the kind of improvement method*1)
20-30	CPP(I) (F10.3)	the cohesion of the improved zone*2)
31-40	ASS(I) (F10.3)	the volume ratio the of improved zone to total complex foundation volume*3)

Note :

- *1) IIFF(I) is an index to designate the kind of zone by selection of whether a zone is an improved zone or an original clay zone.

IIFF(I) {
 1 : In the case of an improved zone (for example, soil cement columns, etc.)
 2 : In the case of original clay foundation



- *2) CPP(I) is cohesion (C(tf/m²)) of the improved zone's property, for example soil cement columns, sand compaction piles, etc. In the case of soil cement columns, shear strength (cohesion) can be determined as follows :

$$C = \frac{1}{2} q_u$$

where

C : cohesion (tf/m²)

q_u : unconfined compression strength (tf/m²)

On the other hand, in the case of sand compaction piles or gravel compaction piles, the shear strength of the sand compaction pile or gravel compaction pile is determined by the internal friction angle (ϕ). CPP(I), therefore, can be blank, namely zero (0), but it is necessary to key in the friction angle (ϕ) of the improved zone's properties to KDE or KFU of (6) on Material Property Data.

- *3) ASS(I) is improved volume ratio, which is volume ratio of improved material to the original clay material in the improved zone under the consideration that the composite foundation consists of original clay and improved materials. ASS(I) can be described as follows:

$$ASS(I) = V_{imp} / (V_{clay} + V_{imp}) \text{ ----- (1)}$$

where

V_{imp} : Volume of the improved zone

V_{clay} : Volume of the original clay foundation

V_{imp} + V_{clay} : Total volume of the composite foundation

Using this ratio, ASS(I), the computation method of the design unit weight and the design shear strength on the composite foundation are presented by the following equation :

- i) Composite foundation improved by sand compaction piles. Unit weight

$$\begin{aligned} \gamma_t &= \gamma_{t,sand} * \frac{V_{sand}}{V_{sand} + V_{clay}} + \gamma_{t,clay} * \frac{V_{clay}}{V_{sand} + V_{clay}} \\ &= \gamma_{t,sand} * ASS(I) + \gamma_{t,clay} * (1 - ASS(I)) \text{ ----- (2)} \end{aligned}$$

Shear strength

$$\tau = c + \sigma_n \cdot \tan \phi$$

$$= s_u^* \cdot \frac{V_{clay}}{V_{sand} + V_{clay}} + \frac{V_{sand}}{V_{sand} + V_{clay}} \cdot \sigma_n \cdot \tan \phi$$

$$= s_u^* \cdot (1 - ASS(I)) + ASS(I) \cdot \sigma_n \cdot \tan \phi \quad \text{----- (3)}$$

where

γ_{sand} : Design unit weight of sand (tf/m³)

γ_{clay} : Design unit weight of clay (tf/m³)

V_{sand} : Volume of sand in the composite foundation (m³)

V_{clay} : Volume of clay in the composite foundation (m³)

σ_n : Effective overburden pressure

ϕ : Design internal friction angle

On the assumption that the consolidation effect caused by confining pressure due to the sand compaction piles drainage effect will occur on the original clay foundation, the equation (3) can be presented as follows :

$$\tau = (1 - ASS(I)) (s_u^* + \sigma_c \cdot \frac{\Delta C}{\Delta P} \cdot U \cdot s_u^* + ASS(I) \cdot \sigma_n' \cdot \tan \phi)$$

$$= (1 - ASS(I)) (1 + A) s_u^* + ASS(I) \cdot \sigma_n' \cdot \tan \phi \quad \text{----- (4)}$$

where

$A = \sigma_c \cdot \frac{\Delta C}{\Delta P} \cdot U$: Confined factor.

Changing ratio of shear strength in clay by the consolidation effect caused by confining pressure

$s_u^* = \mu_A \cdot \mu_B \cdot s_u$: Design shear strength of clay, taking into account the ratio of strength decrease by release of in-situ stress and Bjerrum's correction coefficient.

σ_n' : Effective overburden stress.

ii) Composite foundation improved by soil cement columns

Unit weight (γ_t)

$$\gamma_t = \gamma_{\text{soil cement}} \cdot \text{ASS(I)} + \gamma_{\text{clay}} \cdot (1 - \text{ASS(I)})$$

Shear strength (c)

$$C = \frac{1}{n} \{ C_p \cdot \text{ASS(I)} + (1 - \text{ASS(I)}) \cdot SU^* \} \text{----- (6)}$$

where

n : Safety factor commonly n = 1.2

C_p : Shear strength of soil cement

$$C_p = \frac{1}{2} q_u$$

q_u : unconfined compression strength

Design shear strength and design unit weight on the composite foundation are determined by the method mentioned above. Computation of excavated slope stability on the composite foundation can be carried out using this program. Likewise, from the viewpoint that these computation methods take into account the shear strength decrease by excavation and Bjerrum's coefficient on the composite foundation, it is considered that these programs are noteworthy.

Furthermore, the distribution in depth direction of the shear strength on composite foundation can be generally shown in the following figure :

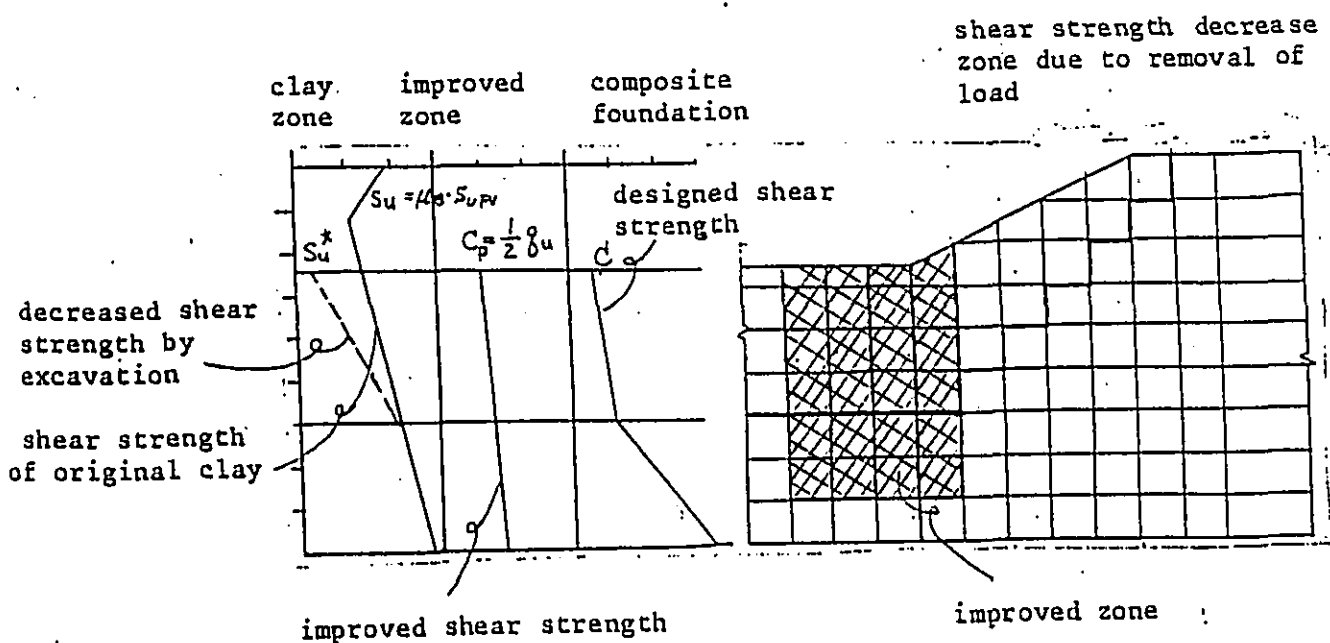


Fig.5- Shear strength of the excavated composite ground

(9) Loading Condition Data ①

READ (SUB EXREAD) IL

col.	variable (format)	contents
		kind of acting force
11~15	IL (I5)	{ 0 : no force 1 : nodal force 2 : elemental force 3 : nodal force + elemental force

(10) Loading Condition Data ②----- nodal force

READ (SUB EXREAD) NCL

col.	variable (format)	contents
11~15	NCL (I5)	the number of nodal force

Remarks NCL ≤ 10

(11) Loading Condition Data ③----- nodal force

READ (SUB EXREAD) XLP(I), YLP(I), XEC(I), YEC(I)

col.	variable (format)	contents
11~20	XLP(I) (F10.0)	X-coordinate of nodal force acting point
21~30	YLP(I) (F10.0)	Y-coordinate of nodal force acting point
31~40	XEC(I) (F10.0)	nodal force in component in X direction
41~50	YEC(I) (F10.0)	nodal force in component in Y direction

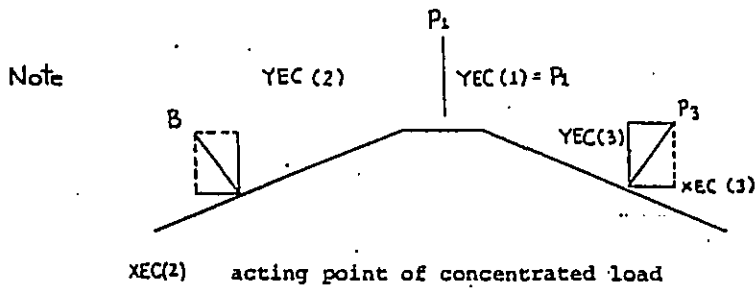


Fig.-5 The action of concentrated load

(12) Loading Condition Data (4) ----- elemental force

READ (SUB EXREAD) NDL

col.	variable (format)	contents
11-15	NDL (I5)	the number of elemental force

(13) Data of Loading Condition ----- (5)

READ (SUB EXREAD) XLD(I), YLD(I), XRD(I), YRD(I), FLD(I), FRD(I).

col.	variable (format)	contents
11-20	XLD(I)	X coordinate of "elemental force" acting point (left side)
21-30	YLD(I)	Y coordinate of "elemental force" acting point (left side)
31-40	XRD(I)	X coordinate of "elemental force" acting point (right side)
41-50	YRD(I)	Y coordinate of "elemental force" acting point (right side)
51-60	FLD(I)	the left component of "elemental force"
61-70	FRD(I)	the right component of "elemental force"

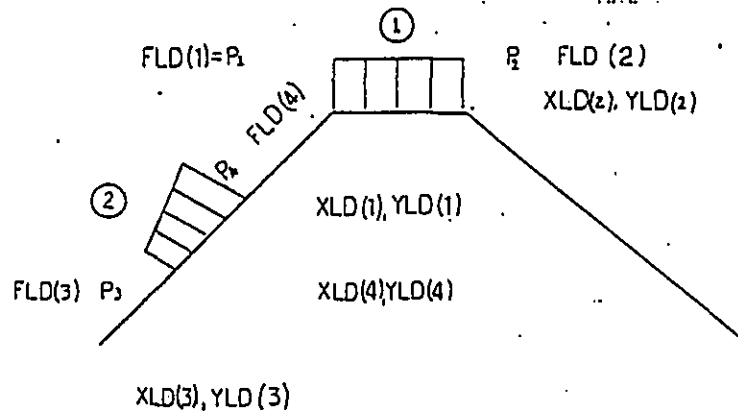


Fig. 5- Distributed load distribution

(14) Calculation Point Data ①

READ (SUB EXREAD) U, NKL, XKL, YKL, NKU, XKU, YKU

col.	variable (format)	contents
1-10	(I10)	Key in '999' on the last Card
11-15	NKL (I5)	Calculation vortex point number at the upper stream
16-25	XKL (F10.3)	X-coordinate of calculation point at the upper stream
26-35	YKL (F10.3)	Y coordinate of calculation point at the upper stream
41-45	NKU (I5)	calculation vortex point number at the downstream
46-55	XKU (F10.3)	X coordinate of calculation point at the downstream
56-65	YKU (F10.3)	Y coordinate of calculation point at the downstream

Remarks :

In the case that either calculation of upstream side or calculation of downstream side is carried out on a fill dam, the data of the calculated side is only keyed in, the others are blank.

On the other hand, in the case of excavated clay foundation, both calculation points of upstream side and downstream side are shown in Fig.5

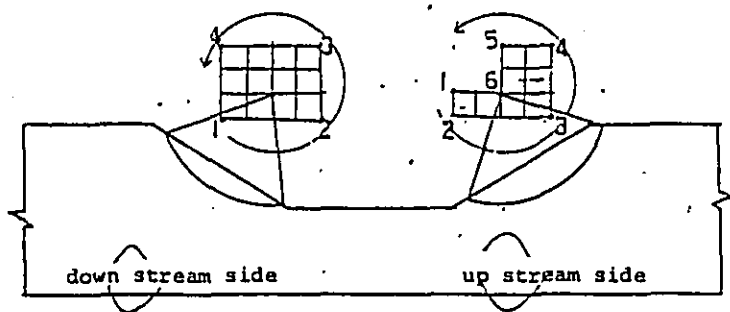


Fig.-5 Calculation point on excavated slope

(15) Calculation Point Data ②

```
READ (SUB EXREAD) MP, FX, EY, (KU(i), i=1,15)
```

col.	variable (format)	contents
11-13	MP	Number of calculation points-1)
16-20	DX	Mesh interval in x direction
21-25	ERY	Mesh interval in Y direccition
26-28	KU(1)	Calculation point number*2)
29-31	KU(2)	Calculation point number*2)
3	3	3
68-70	KU(15)	Calculation point number*2)

Remarks :

*1) number of calculation points is less than 15

$$MP \leq 15$$

*2) KU(i) is the only number of MP keyed in the other is blank.

(16) Control Card of Secondary Calculations

READ (SUB,EXREAD) NCBIT, KASE, NLIST, NRAD, FKH, ALPHA

col.	variable (format)	contents
11-15	NCBIT (I5)	index of secondary calculations { 0 : stop the calculation { 1 : execute Secondary calculation
16-20	KASE (I5)	index of calculation cases $1 \leq KASE \leq 6$
21-25	NLIST (I5)	index of output format is ordinarily NLIST = 2
26-30	NRAD (I5)	index of radius decrease ratio { 0 : Automatically { 1 : radius decrease ratio is determined by input data
31-40	FKH (F10.3)	horizontal earthquake force
41-50	ALPHA (F10.3)	corrected coefficient of pore pressure ordinarily ALPHA = 1.0

Remarks :

*1) refer to Table 5-

(17) Calculation Radius Data

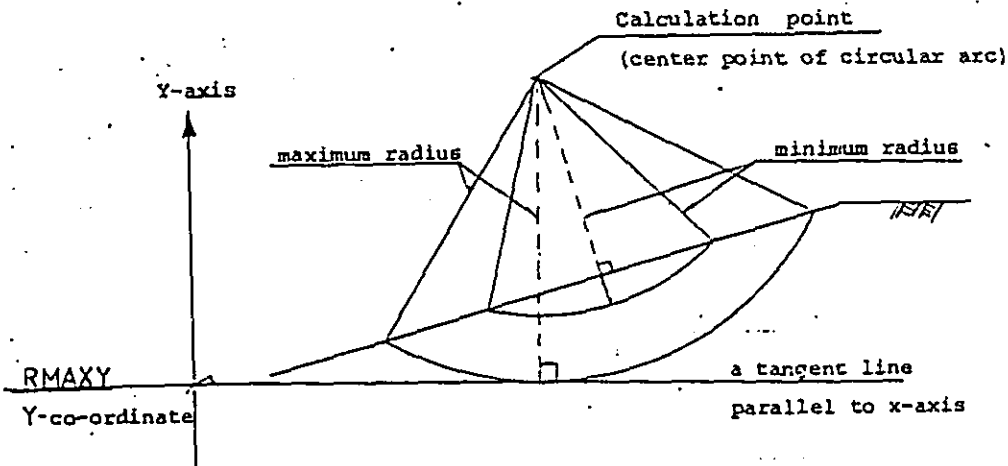
READ (SUB, EXREAD) DR, RMAX, RMINY

col.	variable (format)	contents
.11~20	DR (F10.3)	Decrease space of radius ΔR
21~30	RMAXY (F10.3)	Y-co-ordinate ^{*1)} of a tangent which touches the circle at maximum radius point
31~40	RMINY (F10.3)	Y-distance ^{*2)} of a tangent which touches the circle at minimum radius point

Remarks :

*1) RMAXY = RMINY in general.

*2) Maximum radius and minimum radius are shown in the following figure.



Appendices

- Appendix 3-1 Determination of the Installation Plan of the Measuring Instruments
 - 3-2 Evidential Study on Forecasting Occurrence of Slope Failure

- Appendix 4-1 Sekiguchi-Ohta Model (Elasto-viscoplastic model)
 - 4-2 Modeling of Soil Mass
 - 4-3 Estimation of Ko-value

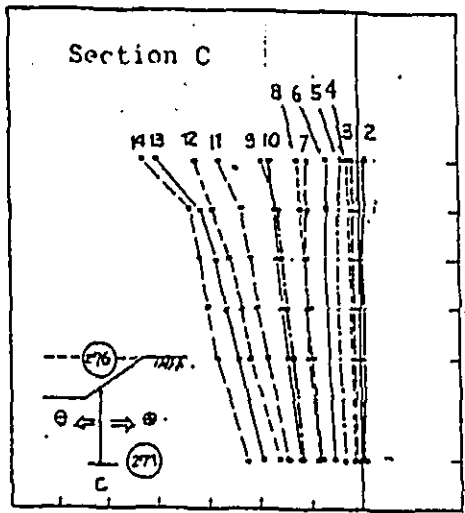
We determined this installation plan considering items as follows.

1. Displacement behavior

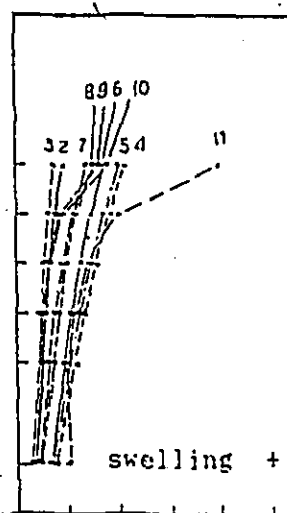
- 1) the position of slip surface line at the excavated slope surface
- 2) the position of the tension crack at top of the slope
- 3) the displacement of inner ground foundation

2. Pore Pressure behavior

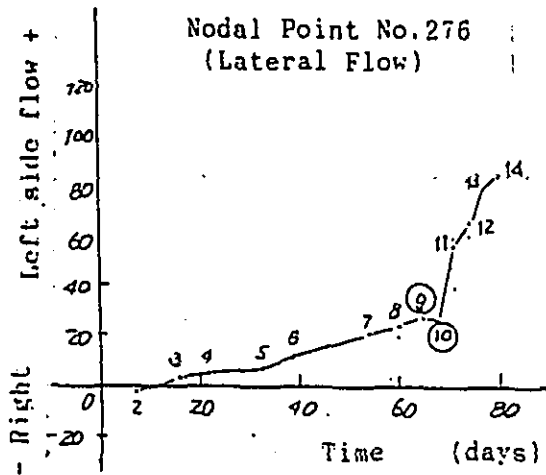
- 1) the temporary pore pressure reduction caused by excavation work.
- 2) the pore pressure increase caused by soil failure.



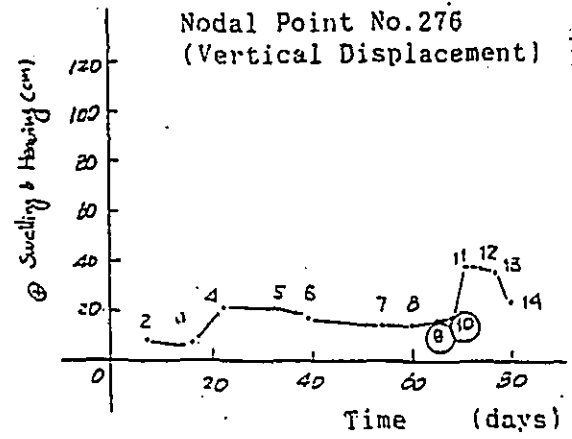
Lateral Flow (cm)



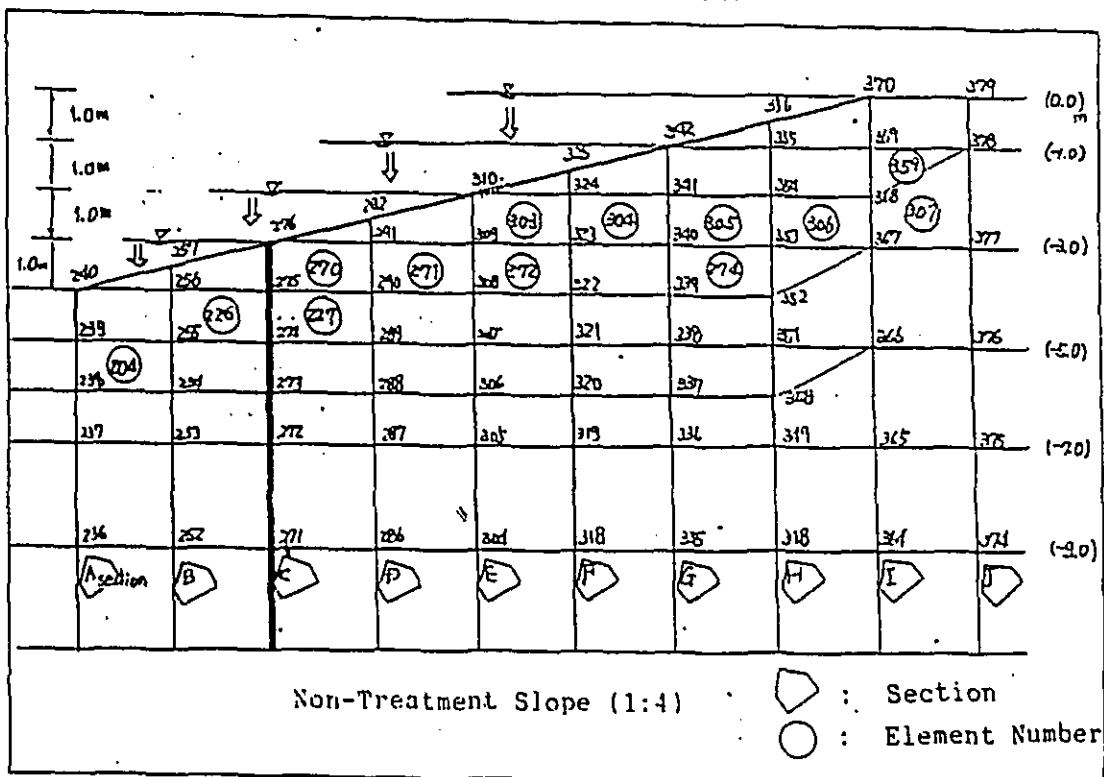
Vertical Displacement (cm)



Nodal Point No. 276 (Lateral Flow)



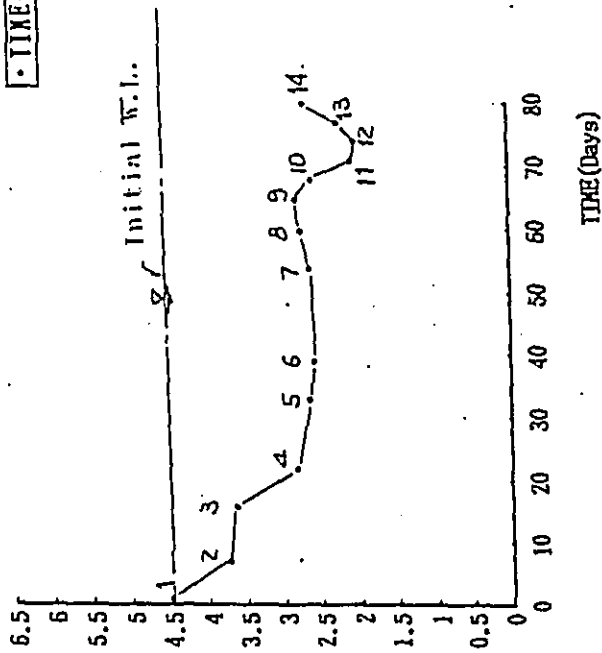
Nodal Point No. 276 (Vertical Displacement)



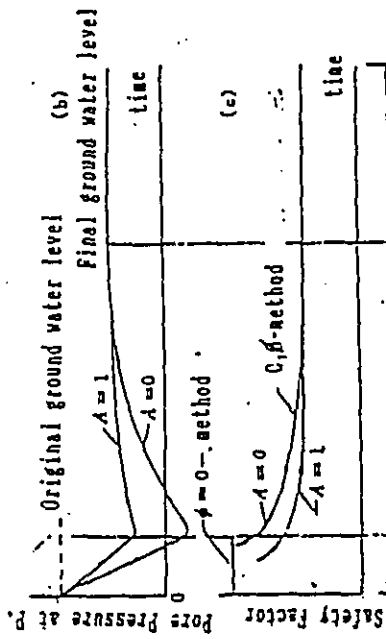
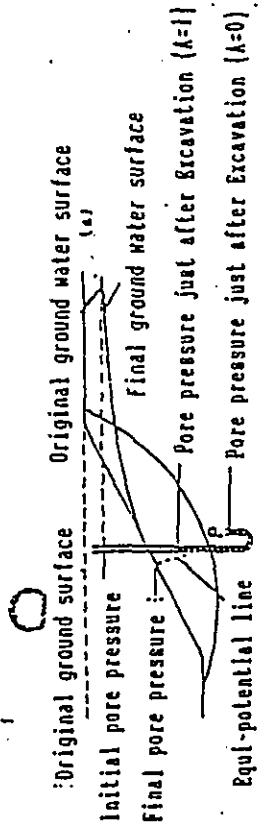
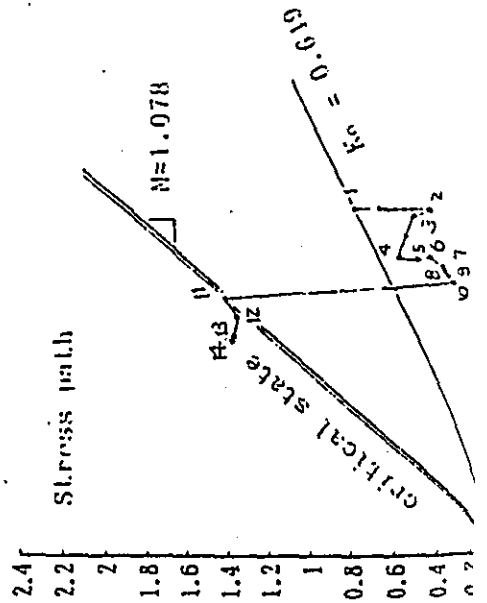
Non-Treatment Slope (1:4)

Section
Element Number

Pore.P. (tf/m²)



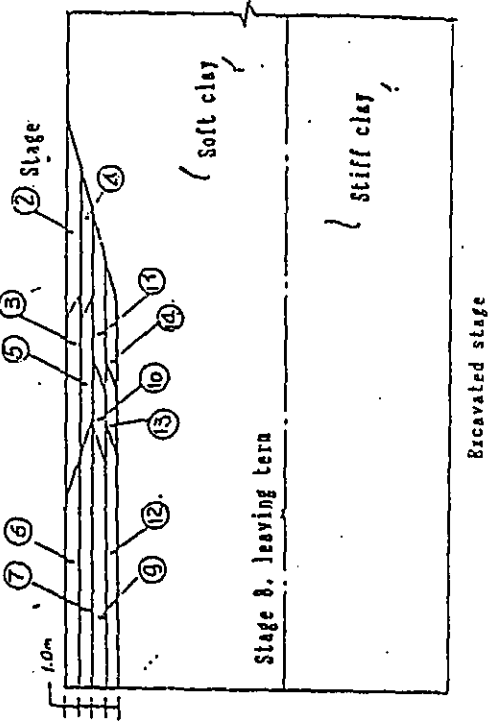
Q (tf/m²)



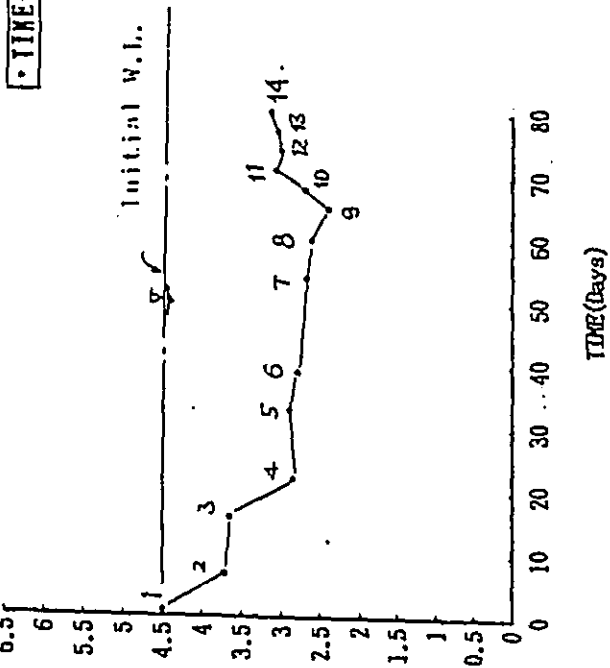
Rapid excavation work

Redistribution of pore pressure

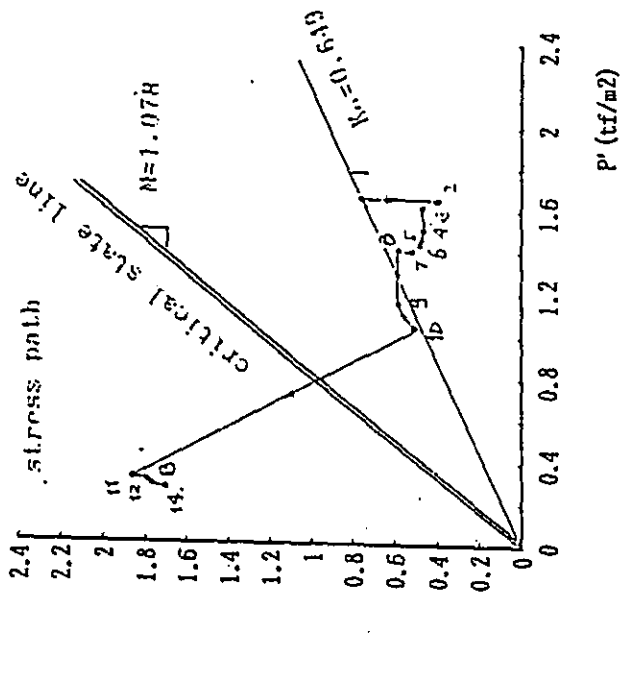
Slip Failure of Excavated Slope (Bishop-Bjerrum)



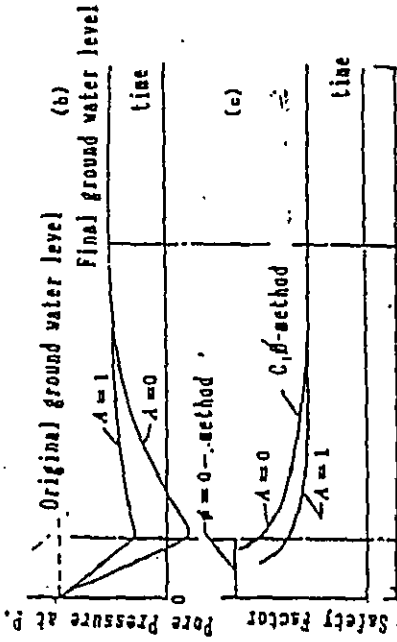
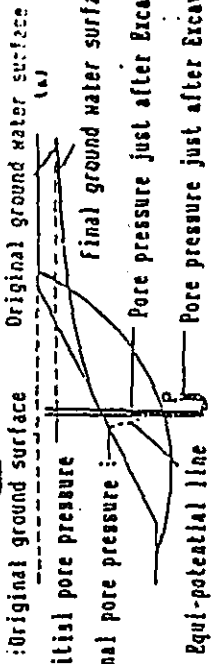
$\sigma' = 0$



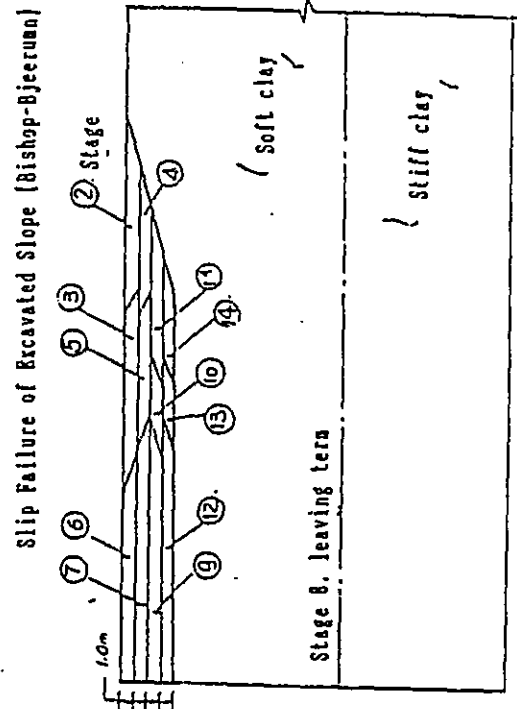
ELEMENT No. 277



TIME-Pore.P.



Redistribution of pore pressure

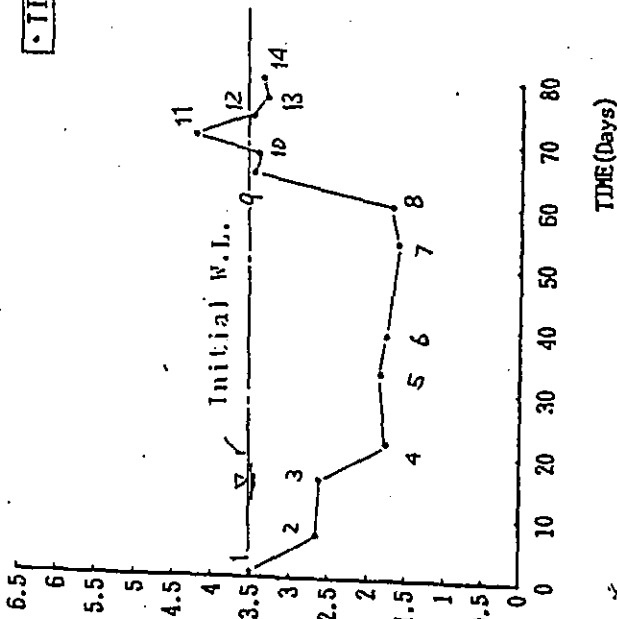


Excavated stage

P'-0

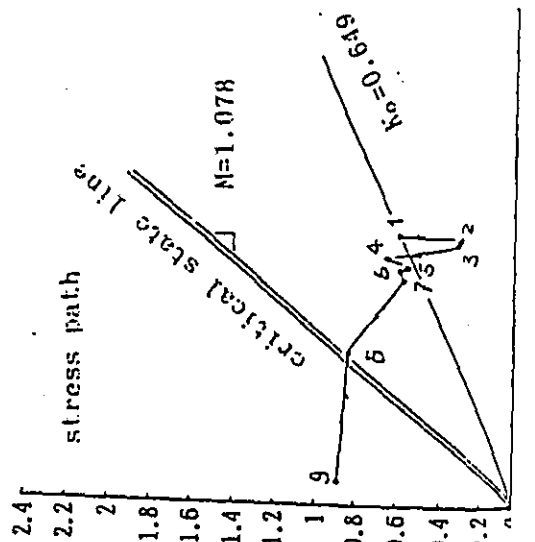
ELEMENT No. 270

Pore.P. (tf/m²)

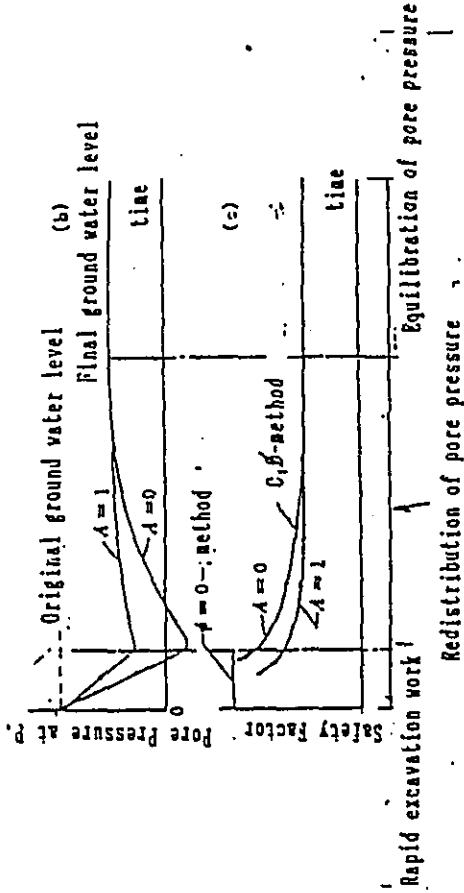
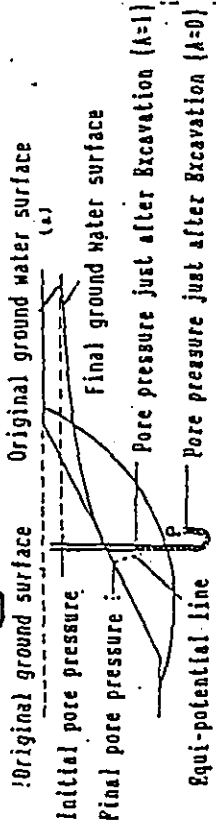


ELEMENT No. 270

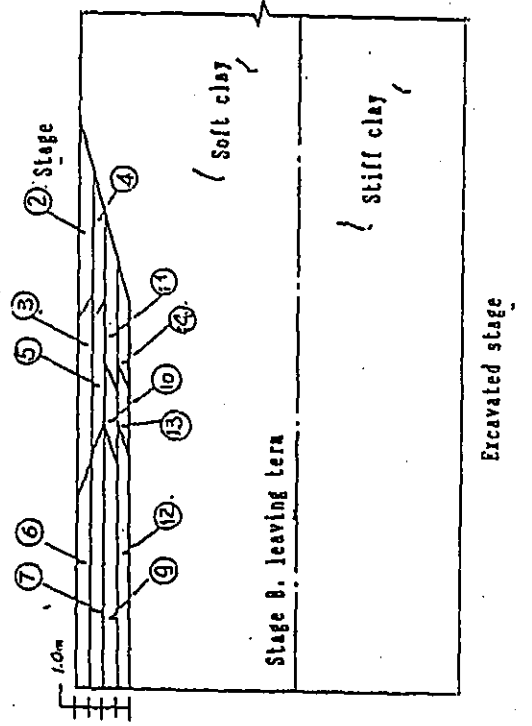
Q(tf/m²)



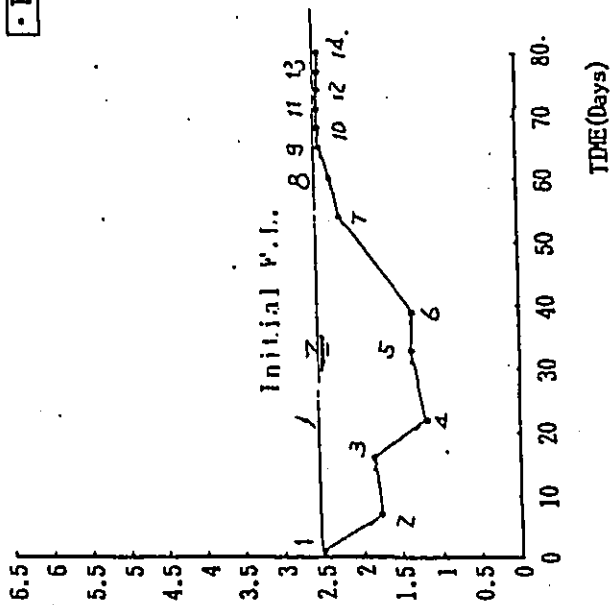
TIME-Pore.P.



Slip Failure of Excavated Slope (Bishop-Bjerrum)

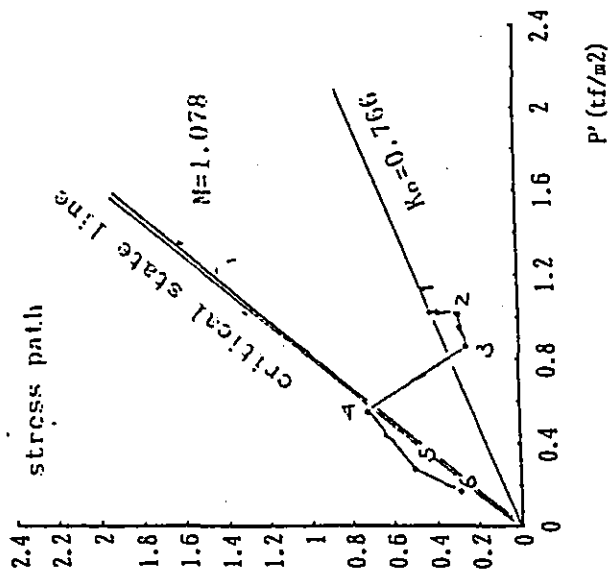


Pore.P. (tf/m²)

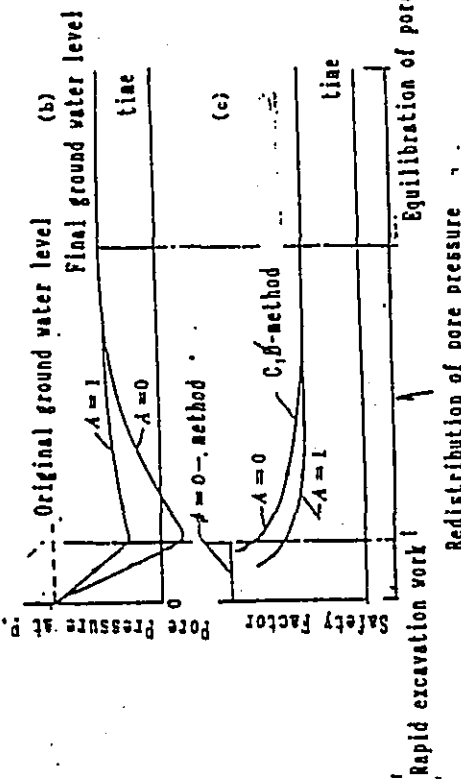
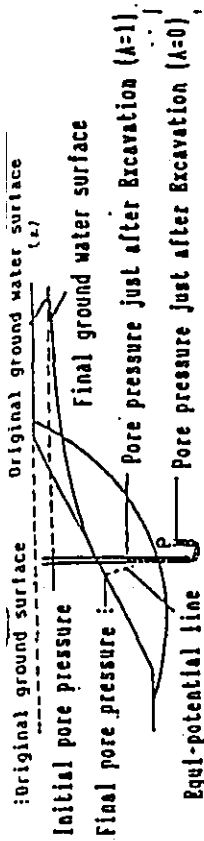


ELEMENT No.303

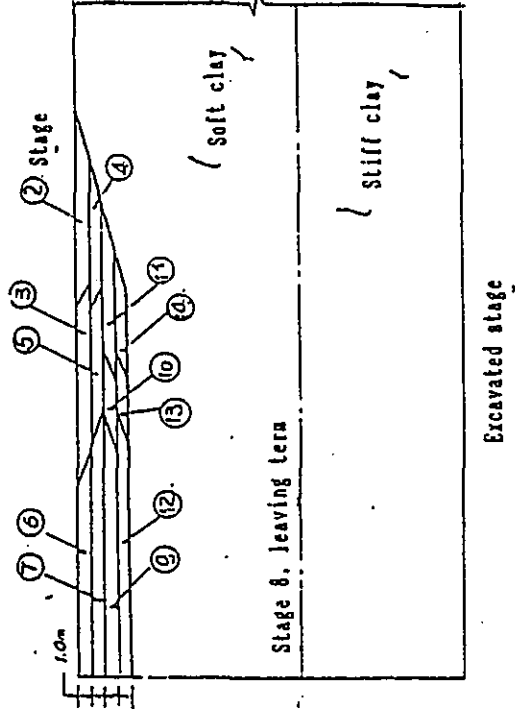
Q (tf/m²)



- TIME-Pore.P.

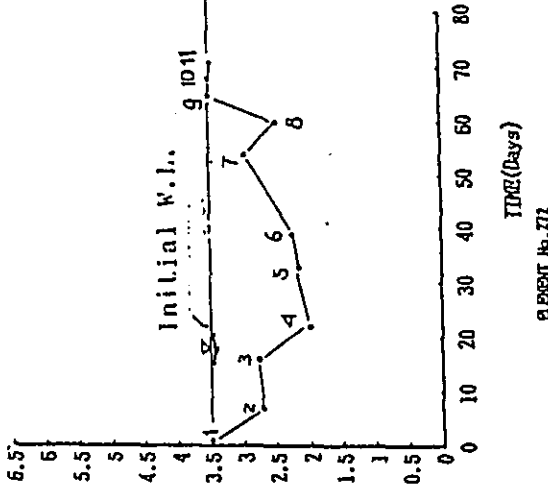


Slip Failure of Excavated Slope (Bishop-Bjerrum)

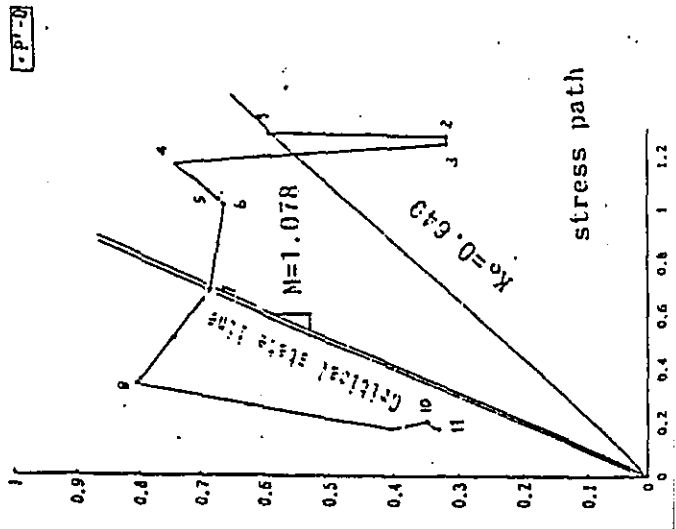


• P' = 0

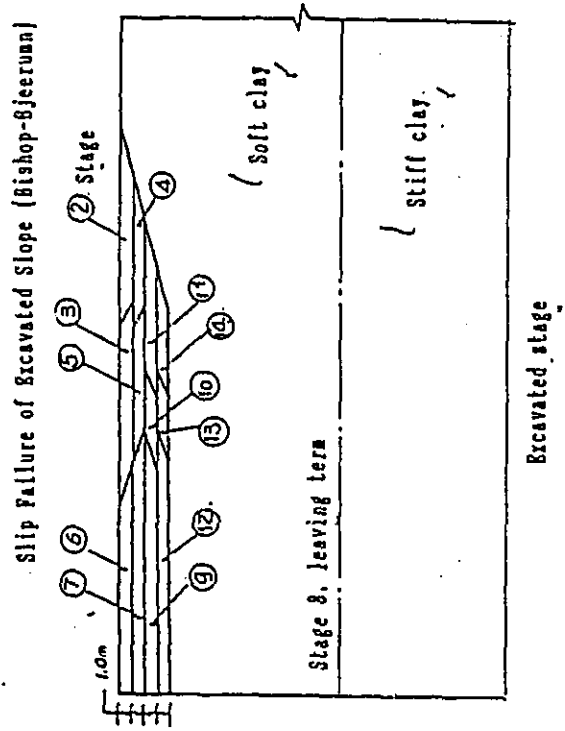
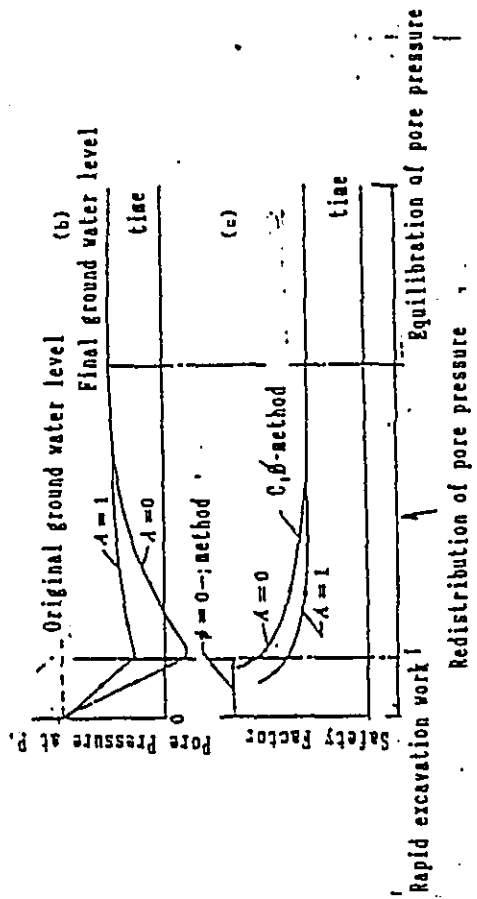
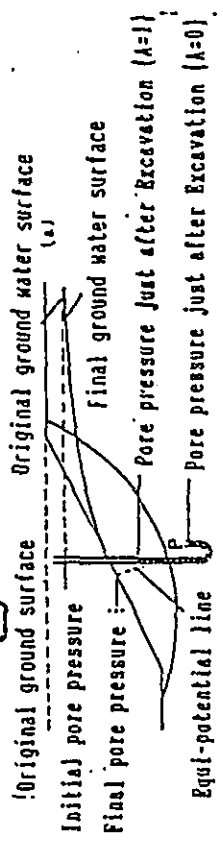
Pore P. ($t/\alpha z$)

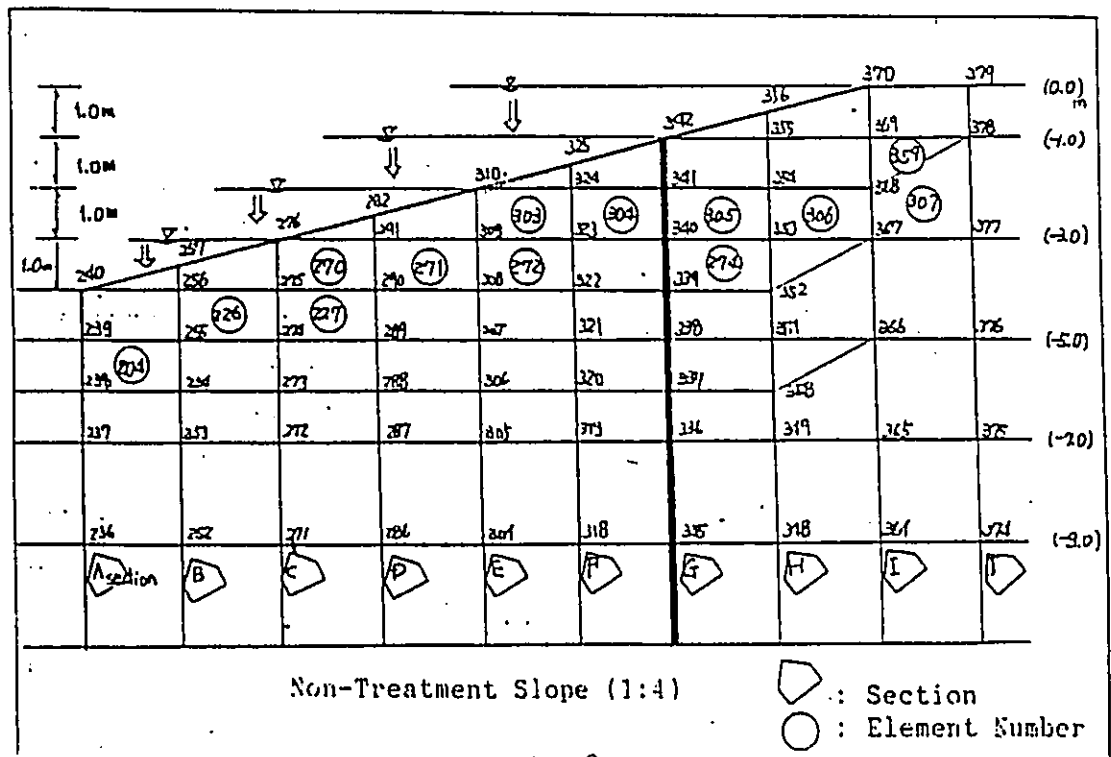
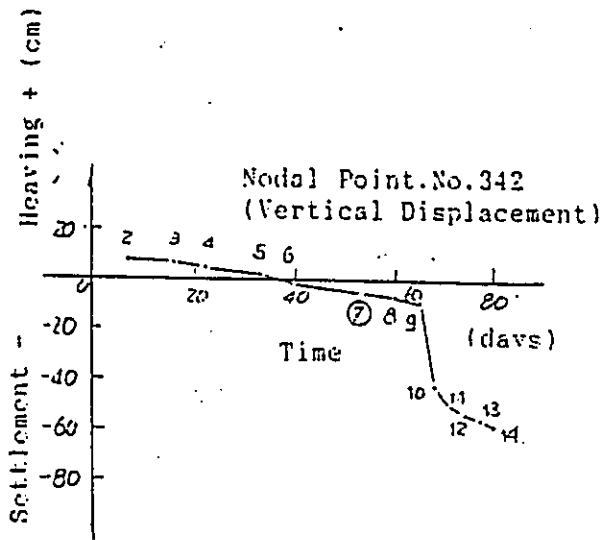
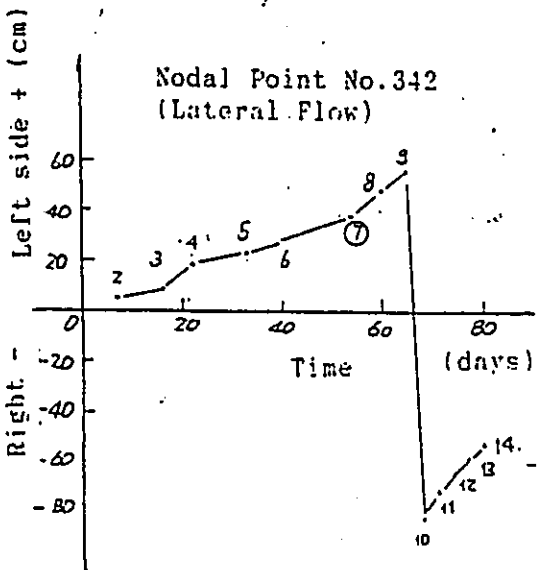
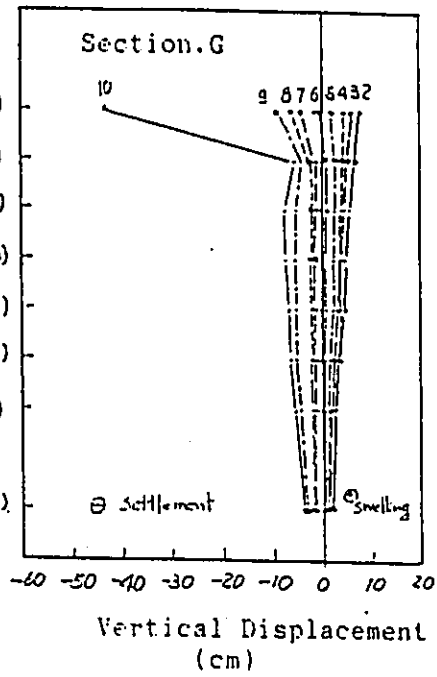
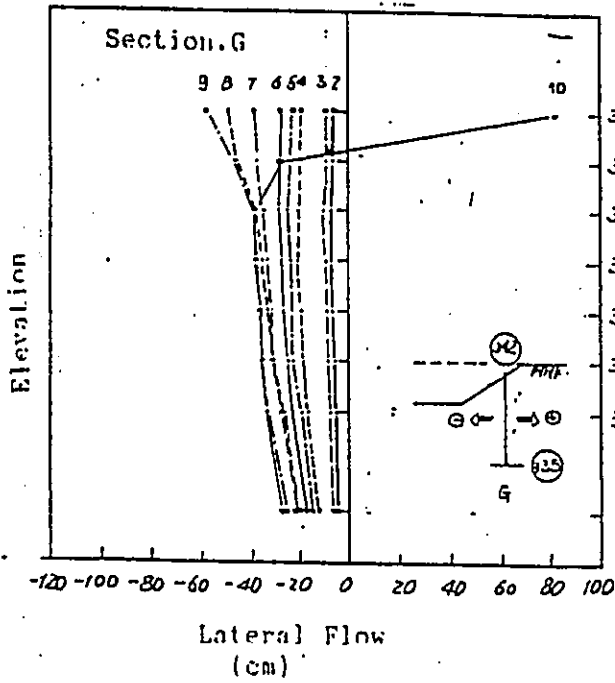


$q(\alpha t/\alpha z)$

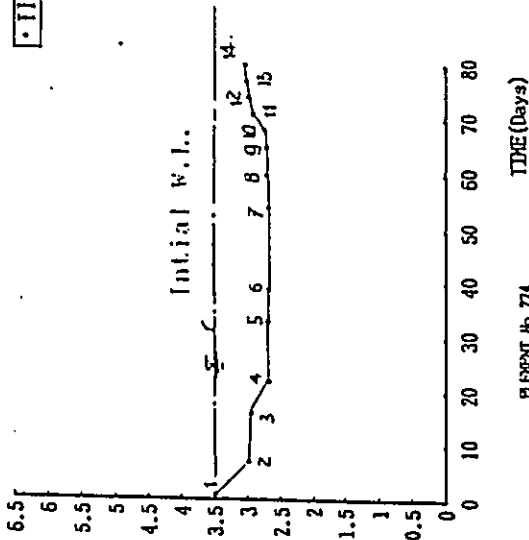


TIME-Pore.P.



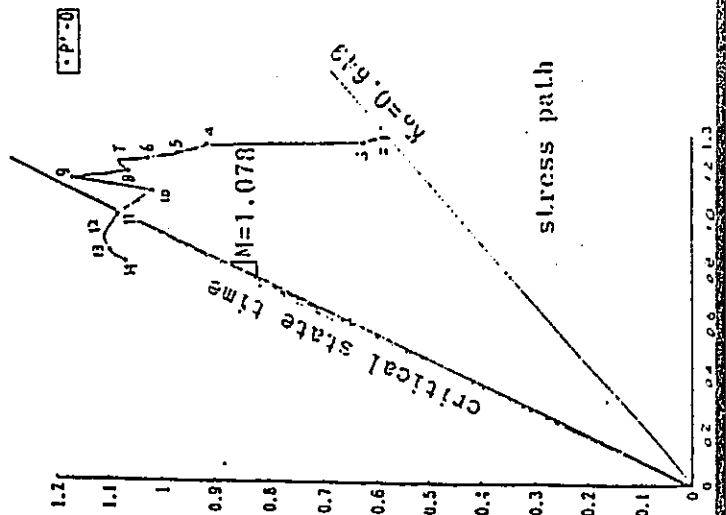


Pore.P. (tf/m²)

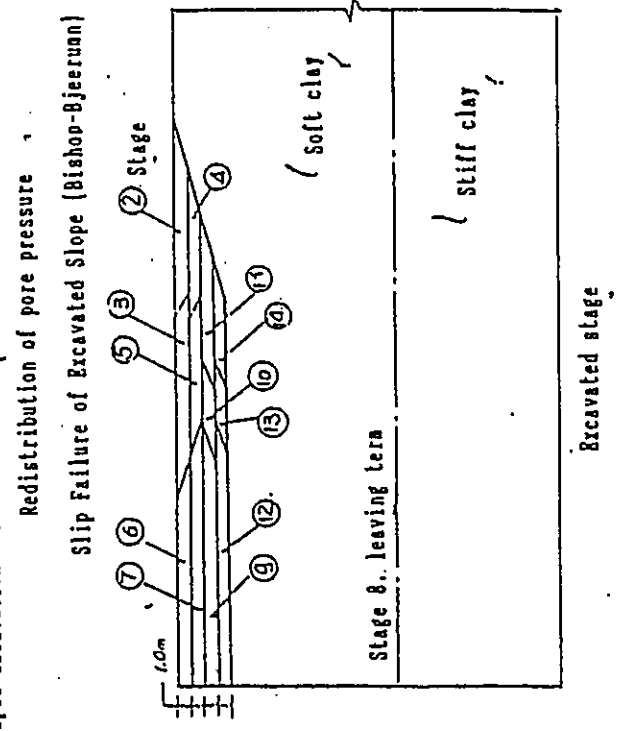
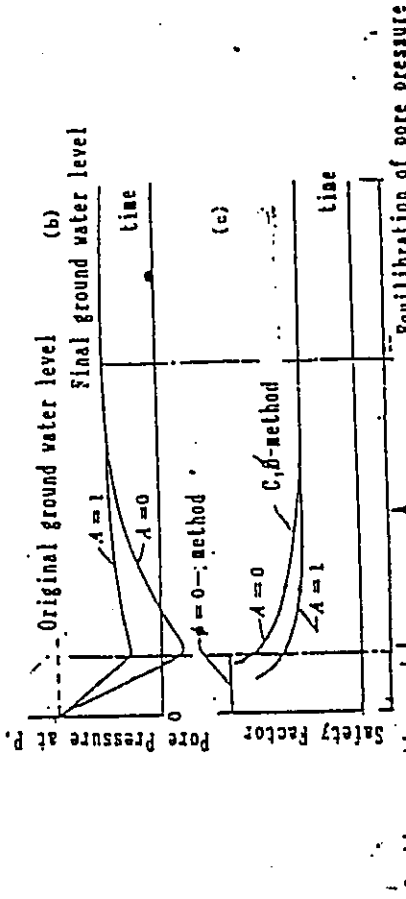
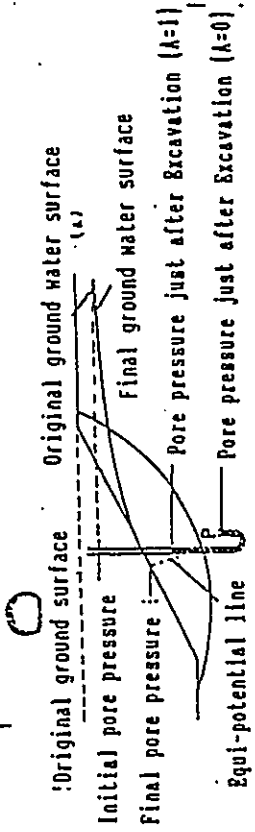


ELEMENT No. 274

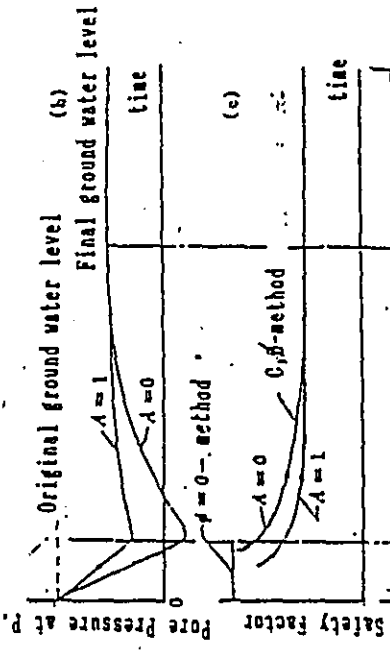
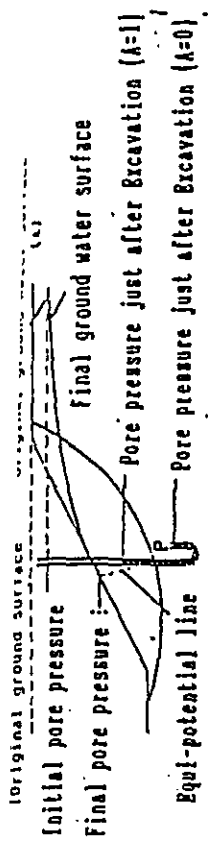
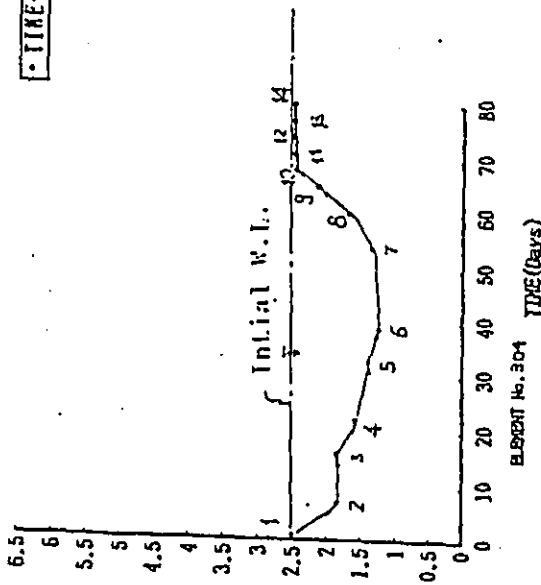
$\sigma(\text{tf/m}^2)$



TIME-Pore.P.

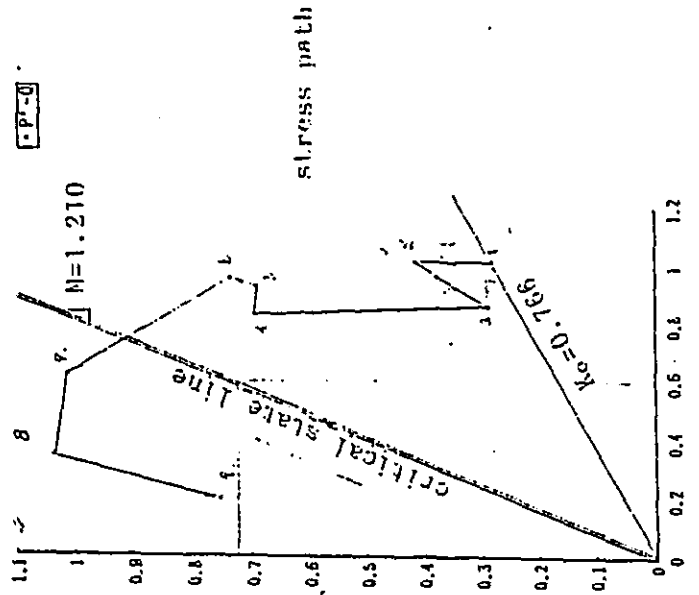


• TIME-Pore.P.

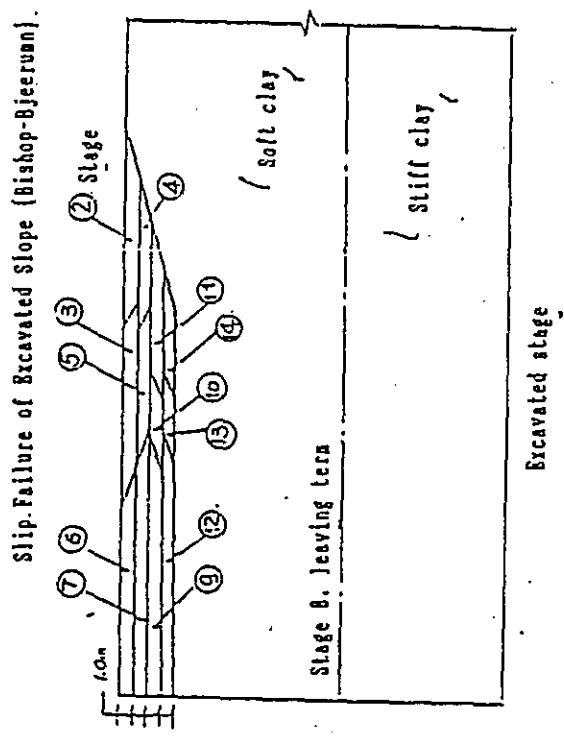


Rapid excavation work / Equilibration of pore pressure

0(11/42)

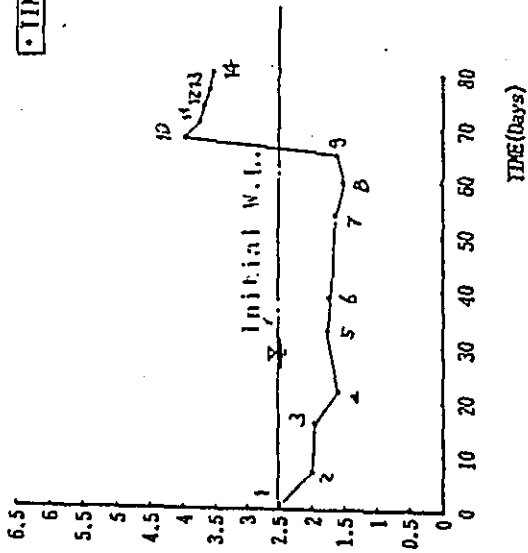


P' (11/42)

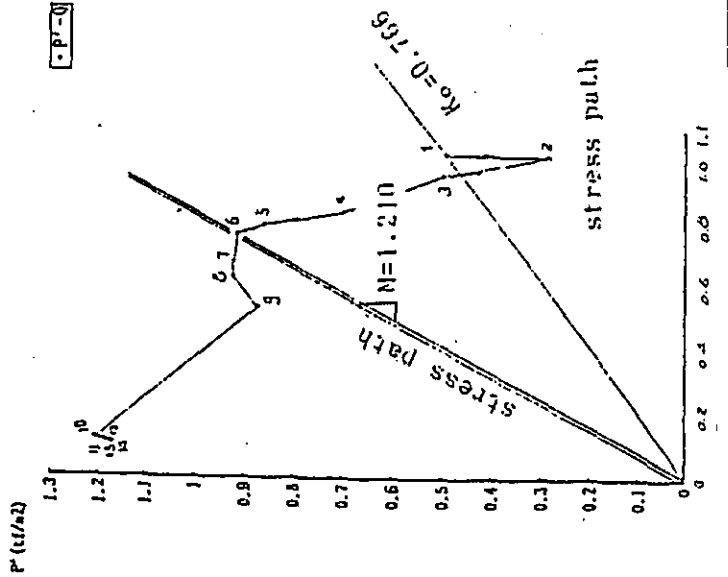


MEMO No. 305

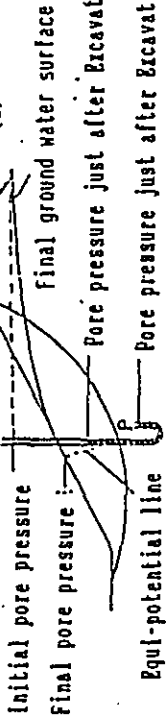
Pore.P. (t/m²)



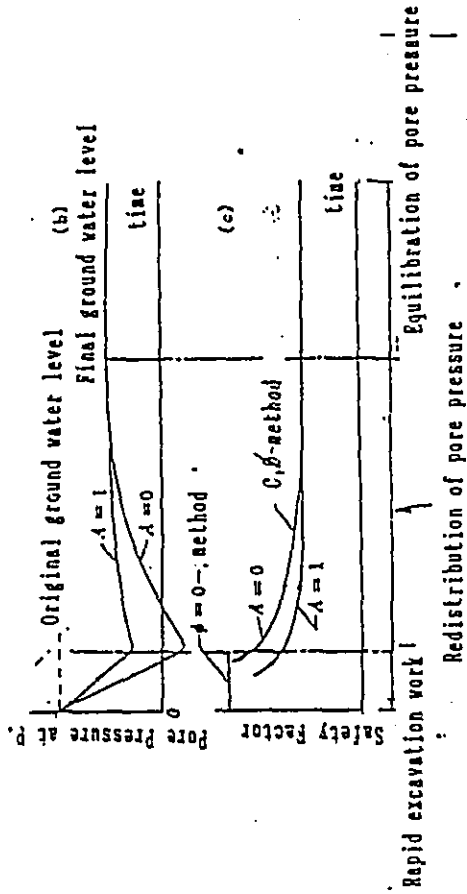
MEMO No. 305



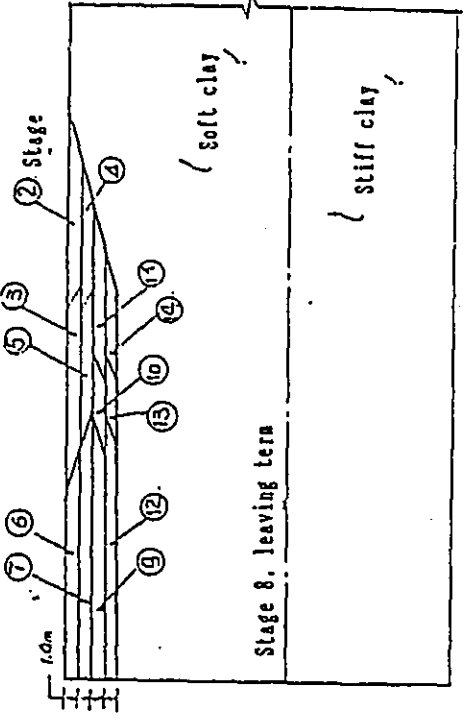
Original ground surface

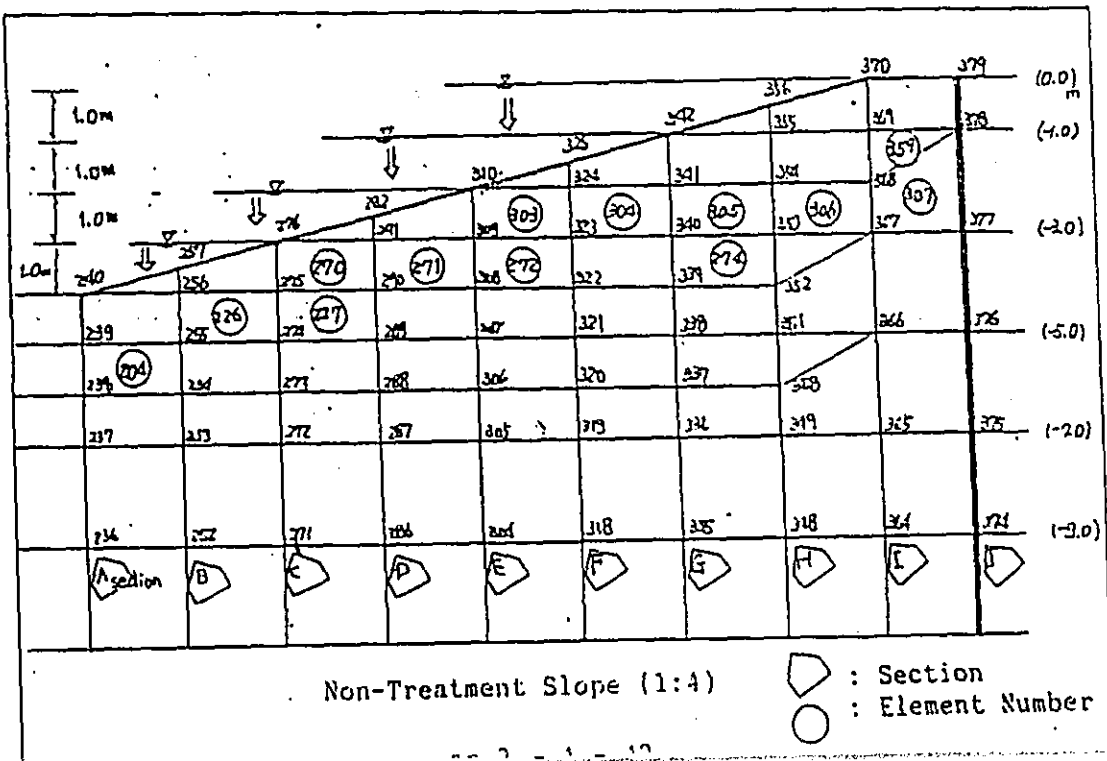
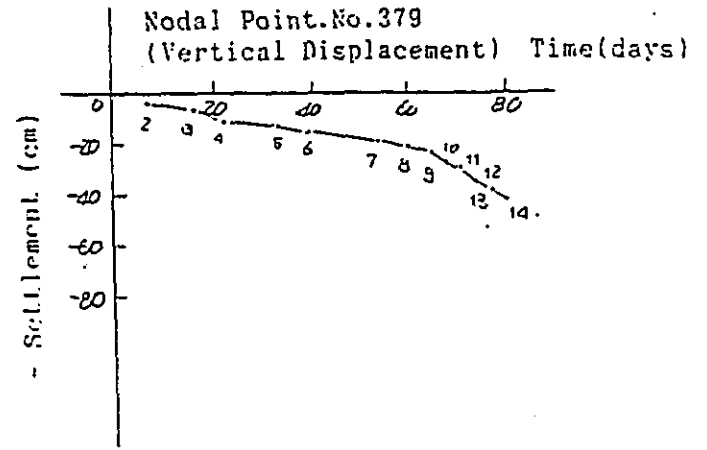
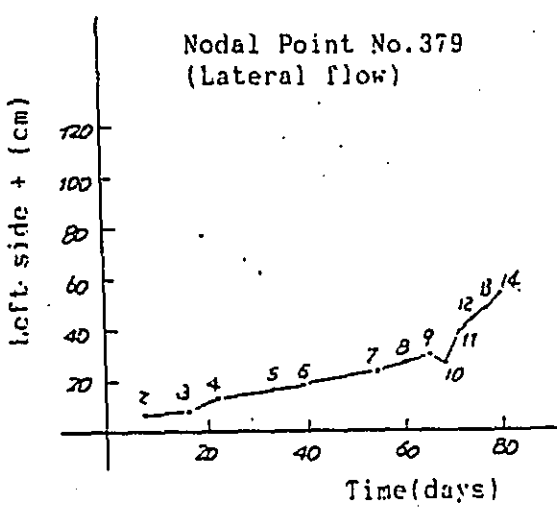
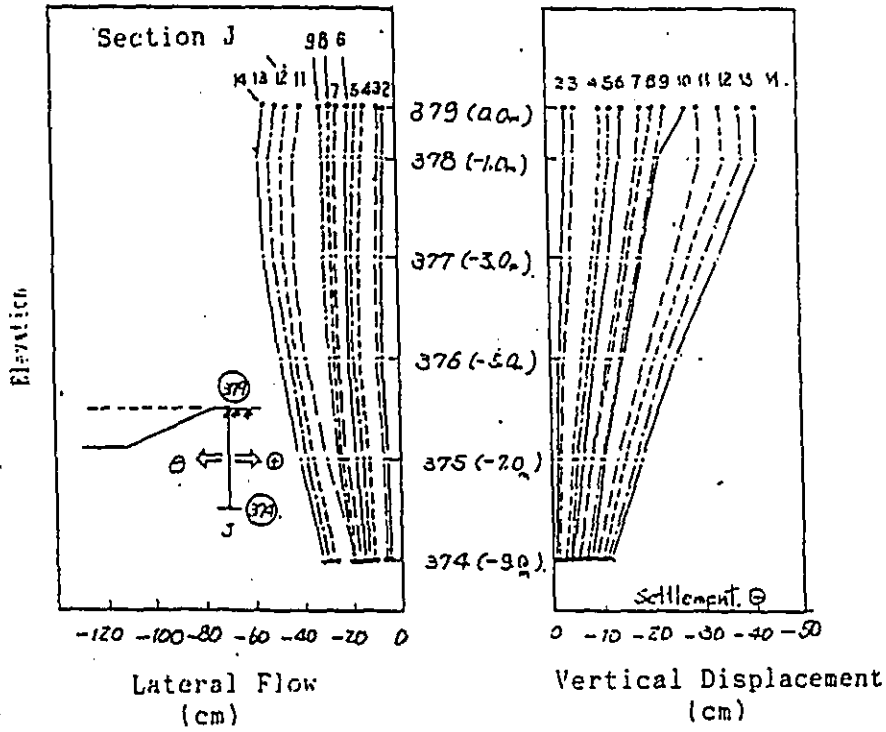


TIME-Pore.P.

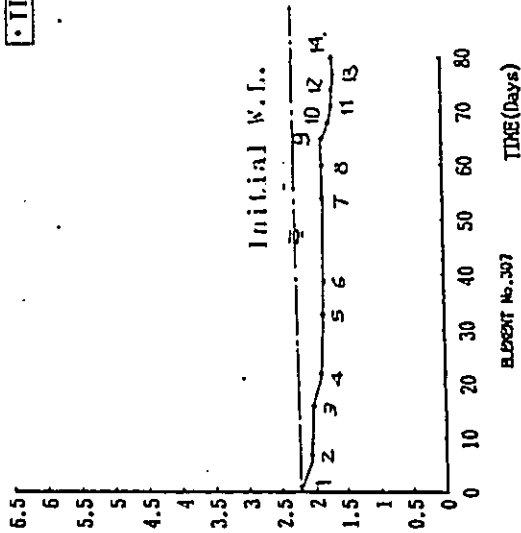


Slip Failure of Excavated Slope (Bishop-Bjerrum)



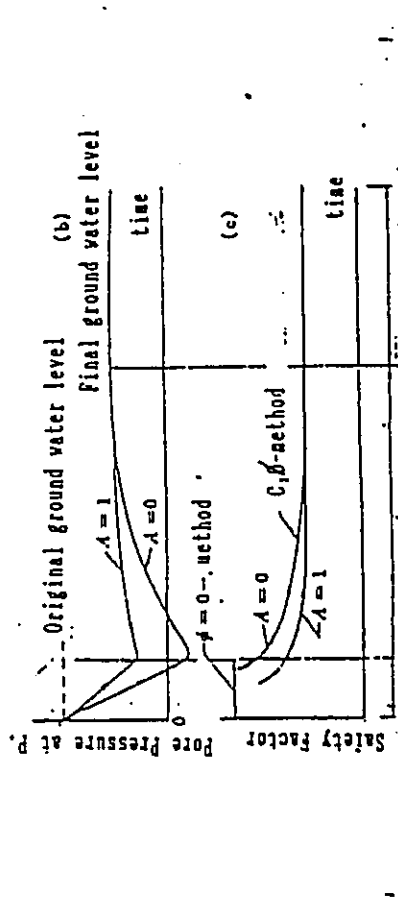
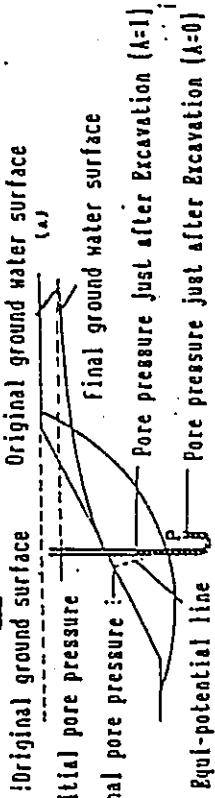
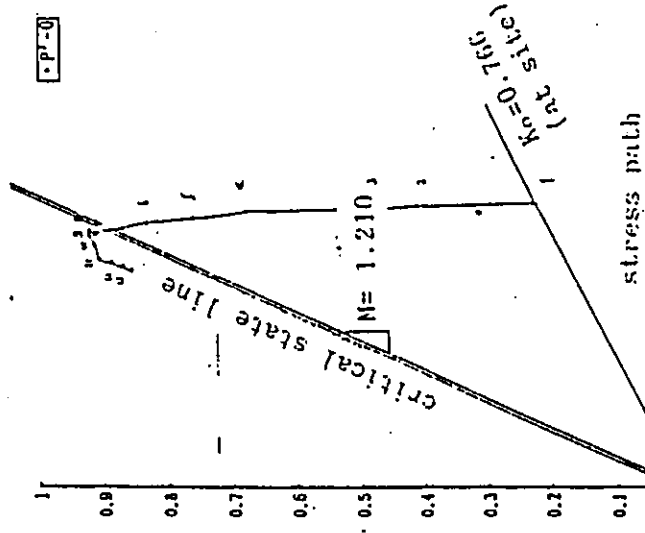


Pore.P. (tf/m²)

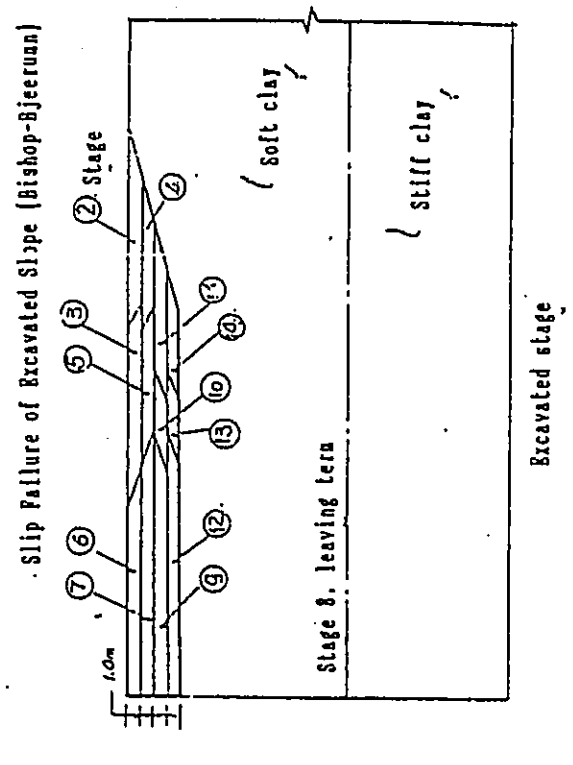


ELEMENT No. 307

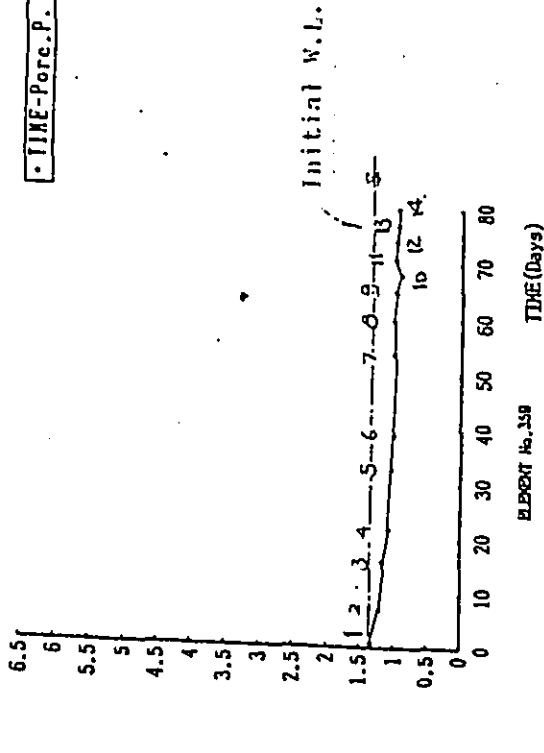
P (tf/m²)



Rapid excavation work
 Redistribution of pore pressure
 Equipotential of pore pressure

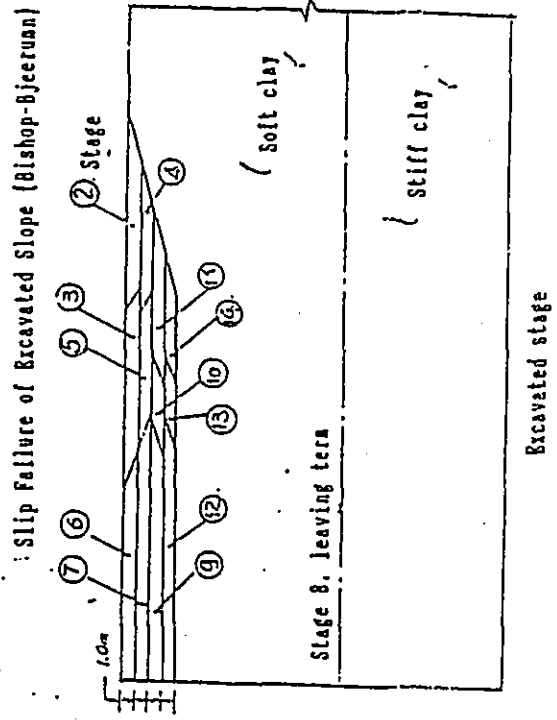
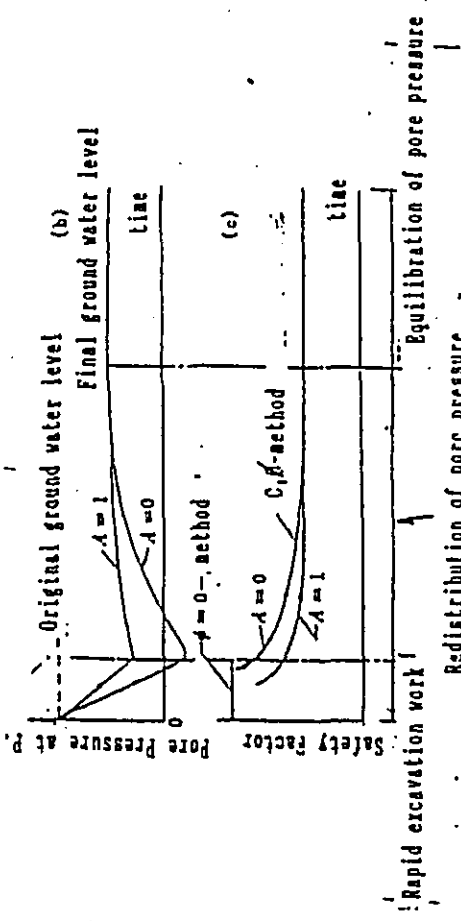
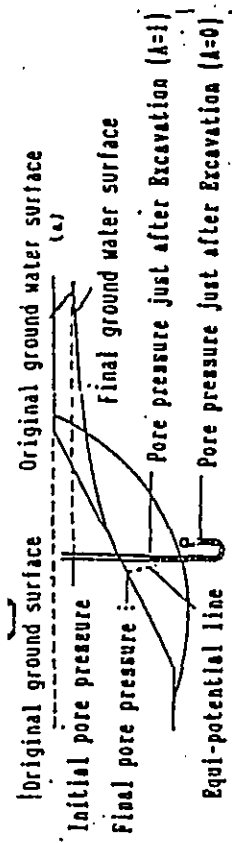
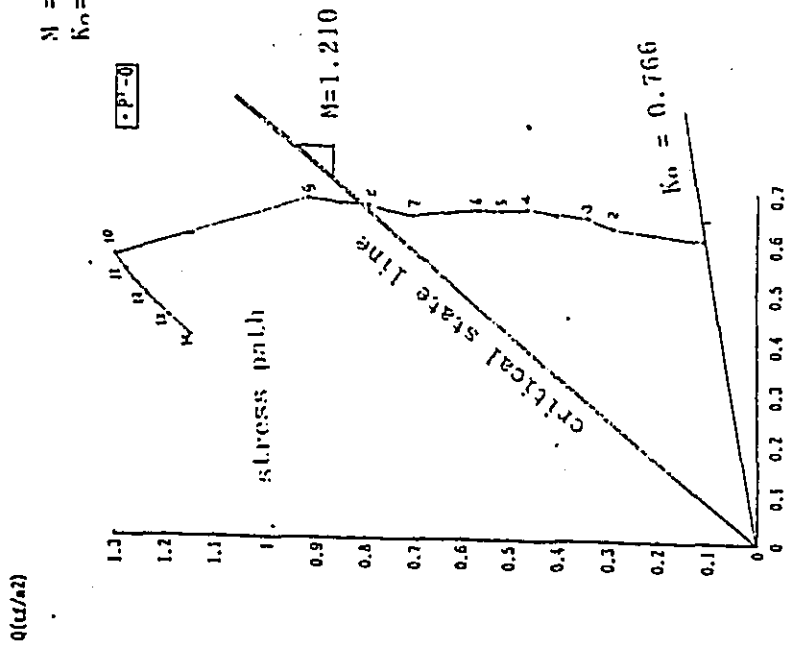


TIME-Pore.P.



$M = 1.210$
 $K_0 = 0.766$

P-P=0



EVIDENTIAL STUDY ON FORECASTING OCCURRENCE OF SLOPE FAILURE

Michitaka SAITO

Abstract

This paper describes an outline of three types of the procedure on forecasting occurrence of slope failure, that is to say, rough estimation based on steady-state strain rate in the secondary creep range, close estimation through calculation or graphical analysis using substituted logarithmic formula and final precise estimation based on linearity on a semi-logarithmic graph assuming temporary rupture life. Considered from several case studies it can be said that the method of forecasting failure time based on creep-rupture characteristics is effective and reliable.

1. INTRODUCTION

Method of forecasting occurrence of slope failure based on creep-rupture characteristics of soil was published in series in the previous Proceedings of the International Conferences on Soil Mechanics and Foundation Engineering. I would like to explain the progress of development of the method, present trend of studying creep-rupture characteristics and evidential evaluation of the method with case studies on actual slope failure.

The word "forecasting" seems to have various phases and will be taken as different meanings according to person, object or occasion.

In some cases, it means to select those slopes which may cause failure or intolerable movement in near future, although they seem to be stable at present. Our present knowledge, however, is not sufficient to give this judgment, and forcing such judgment will be often blamed for one-sided prejudice. It must be evaluated with actual case studies whether the judgment was right or not.

Sometimes the word "forecasting" is used as synonym to express "the degree of danger of slopes to failure"; it means possibility of occurrence of numerous slope failures within some limited region. In this case, it will be expressed with some conditions such as amount and intensity of rainfall or snow melting.

In most cases, however, "forecasting" means occurrence of slide or failure for a specific slope. It contains those of the spot or range, the type and the time of rapid movement of landslide or slope failure; and so hereafter we may make a point of limiting the meaning of forecasting to that of failure time.

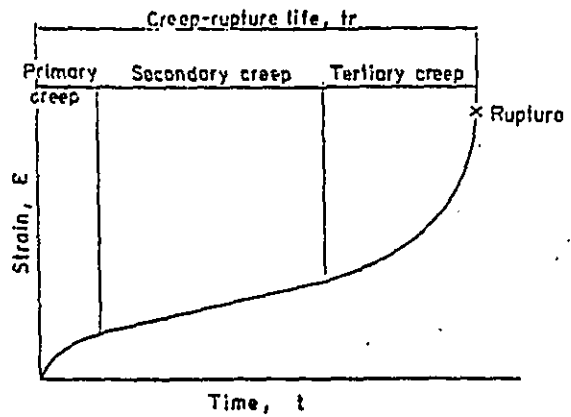
2. DEVELOPMENT OF THE METHOD OF FORECASTING THE TIME OF INITIATION OF INTOLERABLE MOVEMENT OF UNSTABLE SLOPES

2-1 Process to Develop Forecasting Methods.

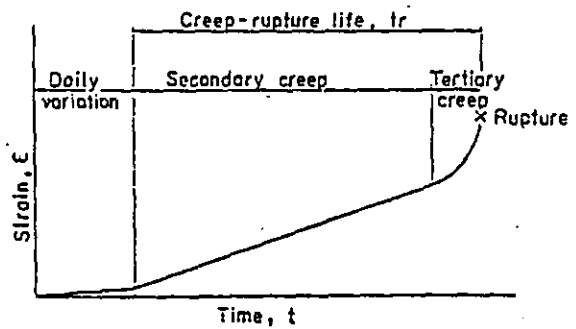
In order to develop forecasting method, it is necessary to find effective factors. Attribution

Approaches for studying rheological properties of materials			
Names	Micromechanistic solid-state physics	Macroanalytical phenomenological	Ad Hoc testing simulated service test
Level	Basic science	Applied science or engineering	Practical approach
Engineering utilization of each approach		Future	
		Present	
		Post	

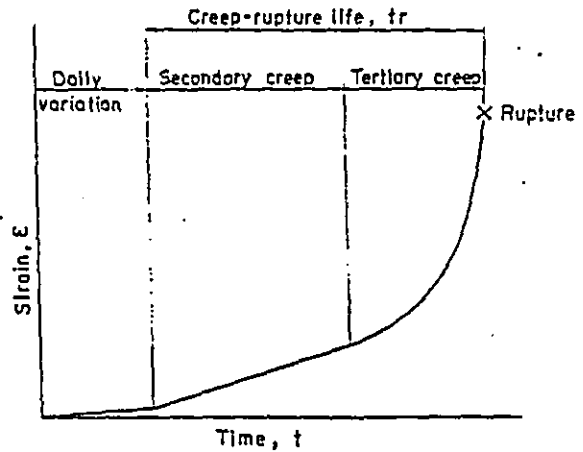
Fig. 1 Three approaches for studying rheological properties (Lazan, 1962)



(a) Creep rupture test on test piece



(b) Model test of slope failure



(c) Actual slope failure

Fig. 2 Typical expression of various creep-rupture curves

indispensable to effective factors for the purpose of forecasting are requested as that the factor will always appear before failure, that the level of factor is measured quantitatively and that the time length to failure after its appearance is not too short. And, moreover, it is desirable to the factor that its measurement is rather easy and decision can be done without confusion.

Forecasting factors may be divided into several groups;—the first group can be named as direct factor, such as horizontal or vertical displacement, inclination, or strain of surfaces of slopes.—the second one as semi-direct factor, such as stress in the ground, pore-water pressure, rainfall, snow melting or shear strength of soil, as directly connected to the mechanism of the movement.—and the third one as indirect factor, such as temperature, geoelectric potential, acoustic emission, animal behavior, etc., as accompanied with, or influenced by movement of the ground.

Various types of approaches can usually be classified under the following three heading (Lazan, 1962).

- (1) solid-state or micromechanistic approach as basic science,
- (2) macroanalytical or phenomenological approach as engineering science, and
- (3) ad hoc testing or simulation service test as practical approach.

Fig. 1 shows correlation of these three approaches and the changing pattern of emphasis with time. The first one is the most desirable, but it does not yet provide an engineering tool for calculating the properties of engineering materials. The third one is a completely different type of approach against the first one. The result of this approach is directly applicable to the specific problem of interest, but has many serious disadvantages such as for long-term phenomena or not extendable to problems in different regime. Contrary to those approaches, the second one is considered most practical and successful to analyse behavior of engineering materials. Recognition of this classification is very much useful to find effective forecasting factors.

2-2 Development of Forecasting Method Based on Creep-Rupture Phenomena of Soils.

A shortcut to find forecasting factors is to carry out slope failure tests and thereby to see what factors are most sensitive or can show earlier changes. But the range of failure modes reproducible experimentally represents only a part of natural failure, and not all the results are applicable to actual failures.

In case of creep rupture test with soil specimens, for example, application of stress leads first to a period of transient creep, during which strain rate increases suddenly at first and then decreases continuously with time, followed by creep with steady-state strain rate, and then it turns to accelerating stage, finally leading to failure. These three stages are usually termed as primary, secondary and tertiary, as shown in Fig. 2(a).

In case of model tests of slope failure with artificial rainfall, however, there is no sudden increase of stress; therefore the primary creep does not appear, but the secondary creep can be seen, directly followed to daily variation of creep, and the tertiary creep range is rather small as shown in Fig. 2(b).

Actual slope failure is similar to a case of model test with no primary creep range, but the tertiary creep range is very large, especially regarding to total strain and strain rate, as seen in Fig. 2(c): therefore a model slope test is not used as substitute for actual slope failure. Nevertheless, it is sure that they will offer valuable tools for selection of forecasting factors. It can be said that these facts just show the merits and demerits as fatality of ad hoc testing aforementioned.

Through full-scale slope failure tests by artificial rainfall at Nou Experiment Station of Japanese National Railways (JNR) in 1949, it was found that strain measurement of slope surfaces is the most effective as forecasting factor (Saito & Uezawa, 1961; Saito, 1965). It was turned to creep-rupture tests in laboratories as phenomenological approach (Saito & Uezawa,

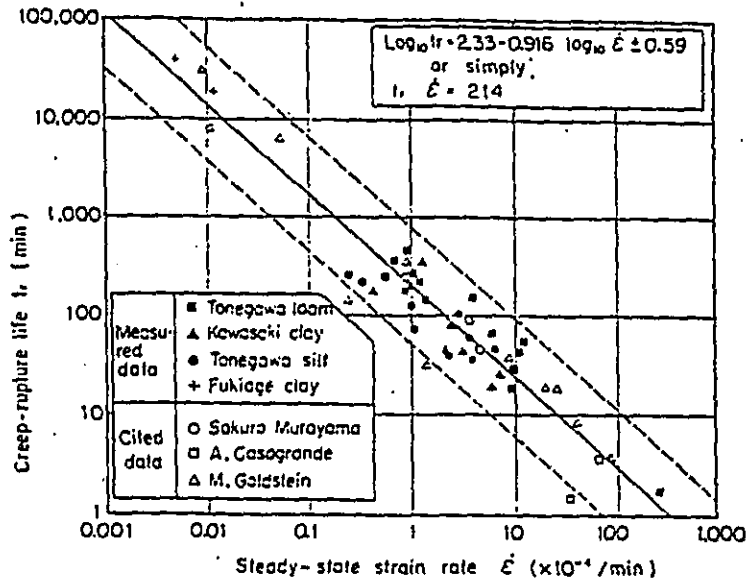


Fig. 3 Forecasting diagram using the relation between steady-state strain rate and creep-rupture life

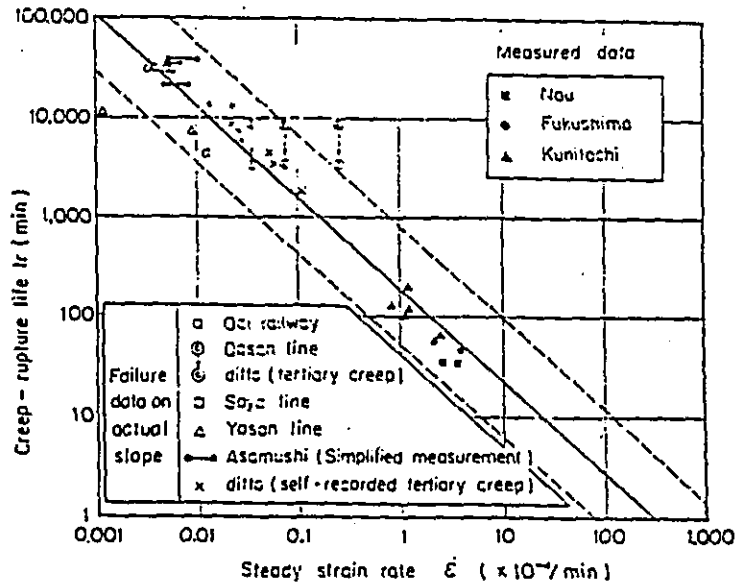


Fig. 4 Validity of forecasting diagram using data of slope failure tests and actual slope failures

1961). The results are shown in the forecasting diagram indicating inversely proportional relationship between steady-state strain rate and creep-rupture life as shown in Fig. 3. This relationship was examined with actual slope failure records (Saito, 1965), and verified effective to forecast the rupture life as shown in Fig. 4. It was found, furthermore, through the case study at Asamushi Landslide that the inversely proportional relationship can be extended to the tertiary creep range with some modification (Saito, 1969), that is called as graphical analysis and explained with the direction of arrows in Fig. 5. Actual application of

or simply expressed

$$t_r \cdot \dot{\epsilon} = 214.$$

where

t_r : creep-rupture life, in min.,

$\dot{\epsilon}$: steady-state strain rate, in $\times 10^{-4}$ per min.

In the tertiary creep range, a following logarithmic formula is applicable as an empirical one

$$\epsilon - \epsilon_0 = A \log \frac{t_r - t_0}{t_r - t},$$

or

$$d\epsilon = 1A \log \frac{t_r - t_0}{t_r - t},$$

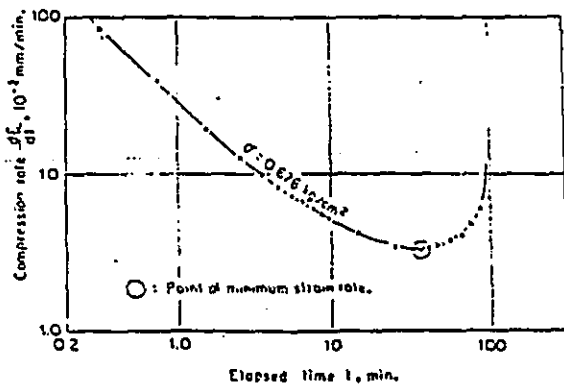
where

t_r : creep-rupture life left before failure.

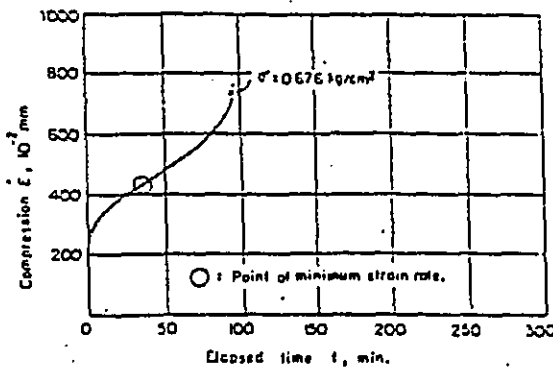
t_0 : reference time.

ϵ : strain at optional time.

ϵ_0 : strain at t_0 .

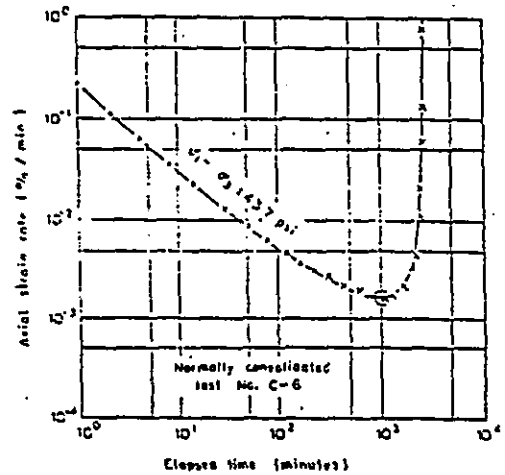


(a) log compression rate versus log elapsed time

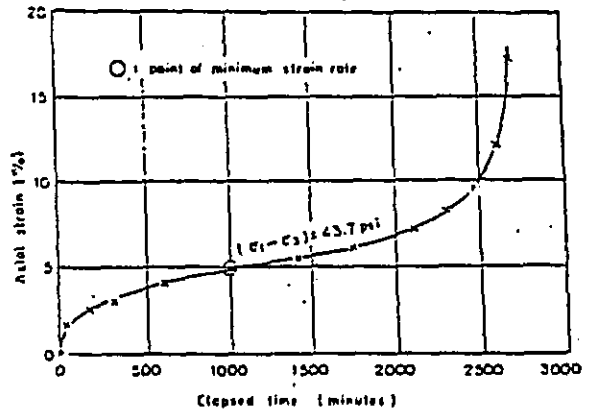


(b) Compression versus elapsed time

Fig. 7 Different expression of a creep-rupture curve published by Murayama & Shibata (1956)



(c) log axial strain rate versus log elapsed time



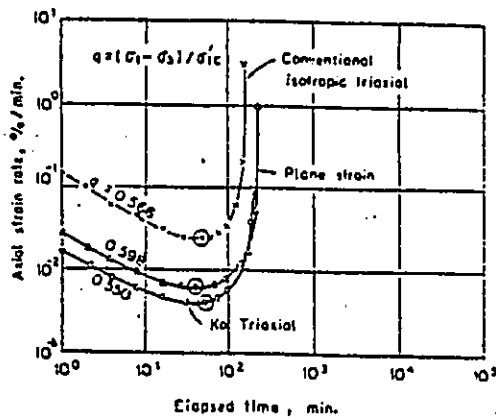
(d) Axial strain versus elapsed time

Fig. 8 Different expression of a creep-rupture curve published by Finn & Sneed (1973)

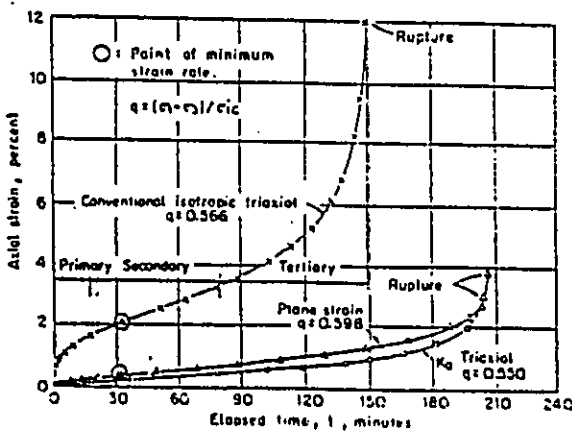
$$\Delta l = \epsilon \cdot l : \text{relative displacement.}$$

Rupture life before failure is obtained with the empirical logarithmic formula by calculating, by graphical analysis or by plotting on semi-logarithmic graph applied with measured values.

It is, therefore, advisable that the time of initiation of slope failure is roughly estimated with steady-state strain rate in the secondary creep range, and closely estimated using substituted logarithmic formula in the tertiary creep range. Besides, the estimation method in the secondary creep range may be used for forecasting in the tertiary creep range as a rough estimation, but warning should be paid to be in danger side within one hour before failure.

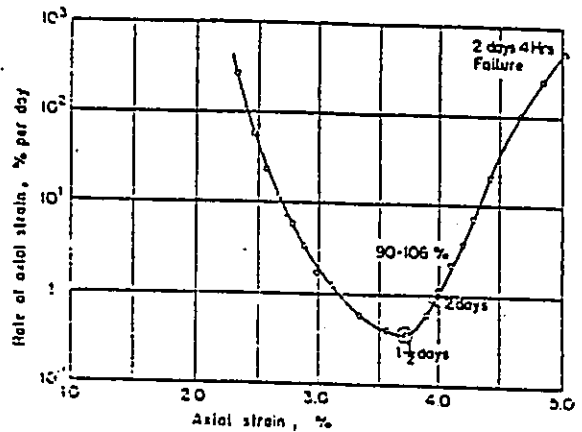


(a) log axial strain rate versus log elapsed time

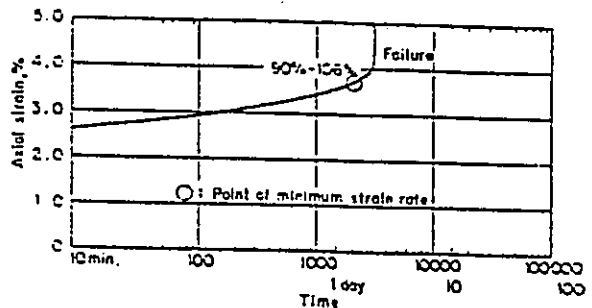


(b) Axial strain versus elapsed time

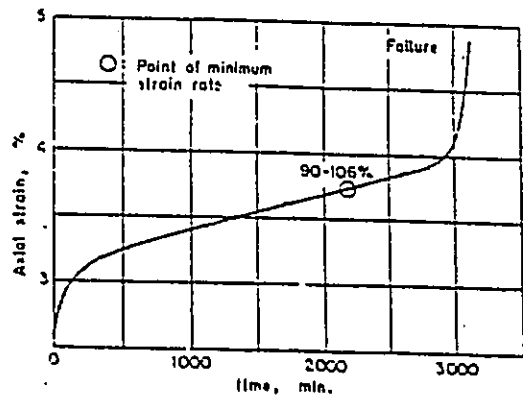
Fig. 9 Different expression of creep-rupture curve published by Campanella & Vaid (1974)



(c) log rate of axial strain versus axial strain



(b) Axial strain versus log time



(c) Axial strain versus time

Fig. 10 Different expression of a creep-rupture curve published by Bishop (1966)

2-3: Compilation of Experimental Data on Creep-Rupture Tests.

There can be found fairly many papers that deal with creep-rupture tests on specimens of soil or rock, and also found many opinions on interpretation and treatment of the test results.

First of all, there is a noteworthy opinion that the secondary creep range does not exist even where strain rate is considered constant, that is to say, strain rate continuously decreases and thereafter increases until rupture. These circumstances are clearly perceived, if strain rate and elapsed time are plotted on a full-logarithmic graph as shown by Murayama & Shibata (1961, 1965), Finn & Snead (1973) and Campanella & Vaid (1974), or if axial strain rate and axial strain are used as with the similar manner, such as presented by Bishop (1966) as seen in Fig. 7~10, respectively. This expression is quite correct as far as full-logarithmic scale is used. But, this is a kind of magic of presentation, because each equal increment on the coordinate scale does not mean the same length.

Logarithmic expression is to display the smaller parts extremely large and to demonstrate the larger parts extremely small. Therefore, in case of full-logarithmic coordinates of strain rate and elapsed time, the difference of strain rates within the range of a cycle near minimum strain rate is fairly small; nevertheless, a cycle of elapsed time near minimum strain rate means substantially very long time, by reason of long progress after initiation of creep: the last point of a cycle of elapsed time is enough ten times to the initial point of the cycle. The point of minimum strain rate is situated toward right-hand side on the logarithmic time axis; therefore, variation in creep rate on the time axis is small around this point, and thus, the apparent constant secondary creep rate computed from the strain-time plot with ordinary scale is essentially the same as the minimum creep rate as admitted by Campanella & Vaid (1974). The secondary creep range is, therefore, granted to exist actually.

The next problem is the definition of failure. In case of clay specimen, it is possible often to see shear crack develop shortly after the reversal of slope in the time curve takes place. Time to failure in creep-rupture test is, therefore, sometimes defined as the point of initiation of acceleration, that is to say, the point of the minimum strain rate as asserted by Casagrande

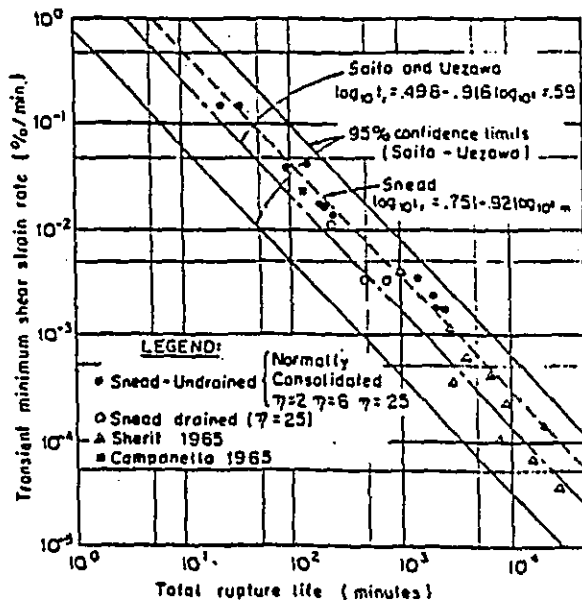


Fig.11 Relation between transient minimum shear strain rate and total rupture life published by Finn & Snead (1973)

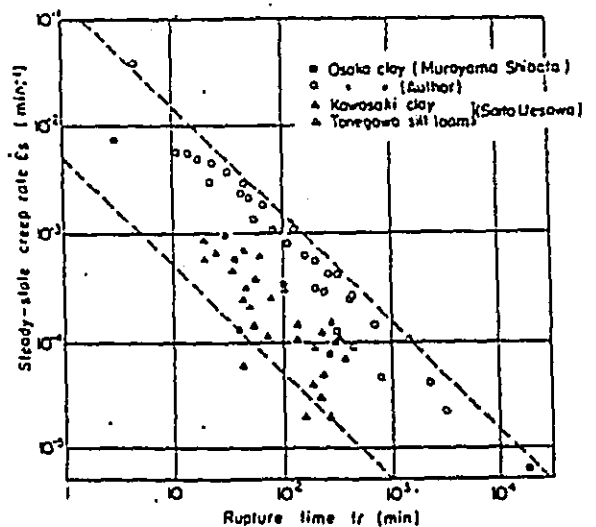


Fig.12 Relation between steady-state creep rate and rupture time published by Kurihara (1972)

& Wilson (1951), Singh & Mitchell (1969) and Finn & Snead (1973). But, this opinion seems to be rather strange and is not approved by all means. The reason is that this opinion has been derived from creep-rupture phenomena of metals, which is very dangerous and becomes out of use according to increase of strain rate, such as jet engines under high temperature and high pressure. On the contrary, in case of soil, usually there remains fairly long time and large movement before failure after passing the point of minimum strain rate as seen in Figs. 7~10. There is no reason why this tertiary creep range is abandoned as failure zone. In case of soil, therefore, failure should be defined with the final and macroscopic state of separation.

If we look round our surroundings, there can be found many useful contributions in recent papers. Fig. 11 shows the relation between transient minimum strain rate and total rupture life published by Finn & Snead (1973). Fig. 12 shows the relation between steady-state creep rate and rupture time published by Kurihara (1972). Fig. 13 shows the relation between minimum creep rate and time to failure published by Sekiguchi (1977). Fig. 14 shows the relation between strain rate and time to failure obtained on rocks published by Morlier (1964).

Upon admitting those consideration before mentioned, minimum strain rate is not considered to be very different from steady-state strain rate, so we may deal with both strain rate data in the same meaning. Fig. 15 shows the compilation of results from all creep-rupture tests in various publications. Most plots are situated within the range of 95 % confidence limits proposed by Saito & Uesawa (1961). Hereupon, Morlier's data are obtained with rocks. It is interesting that potassium is plotted within the range but chalk is found fairly below the range. On the other hand, aluminum alloys are found far above the soil range, but parallel to this range. As a result, it is concluded that creep-rupture life is longer for ductile material such as metals, and shorter for brittle material such as rocks

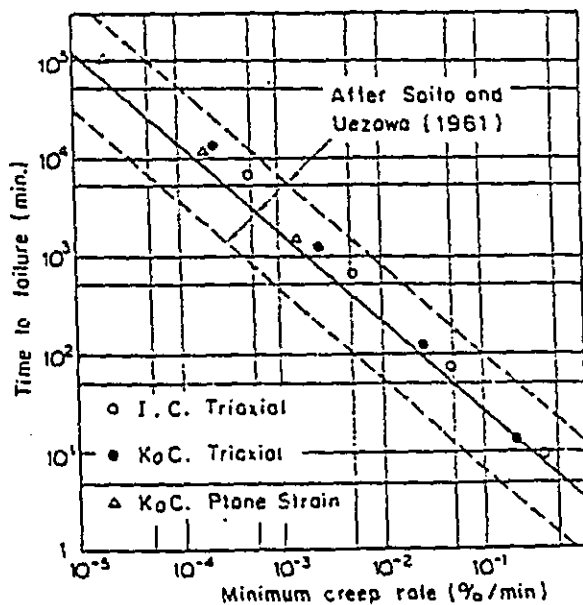


Fig.13 Relation between time to failure and minimum creep rate published by Sekiguchi (1977)

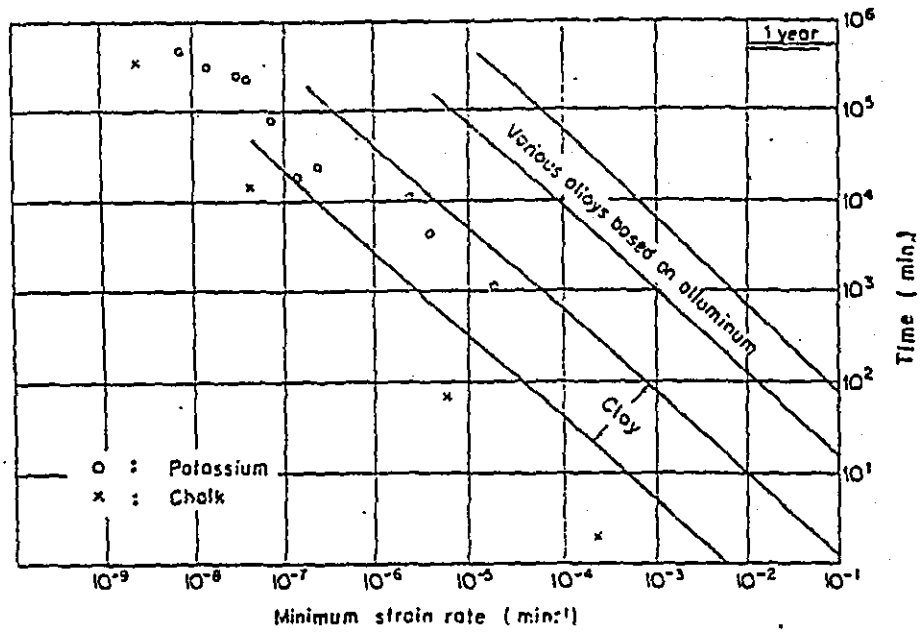


Fig.14 Relation between strain rate and rupture time published by Morlier (1964)

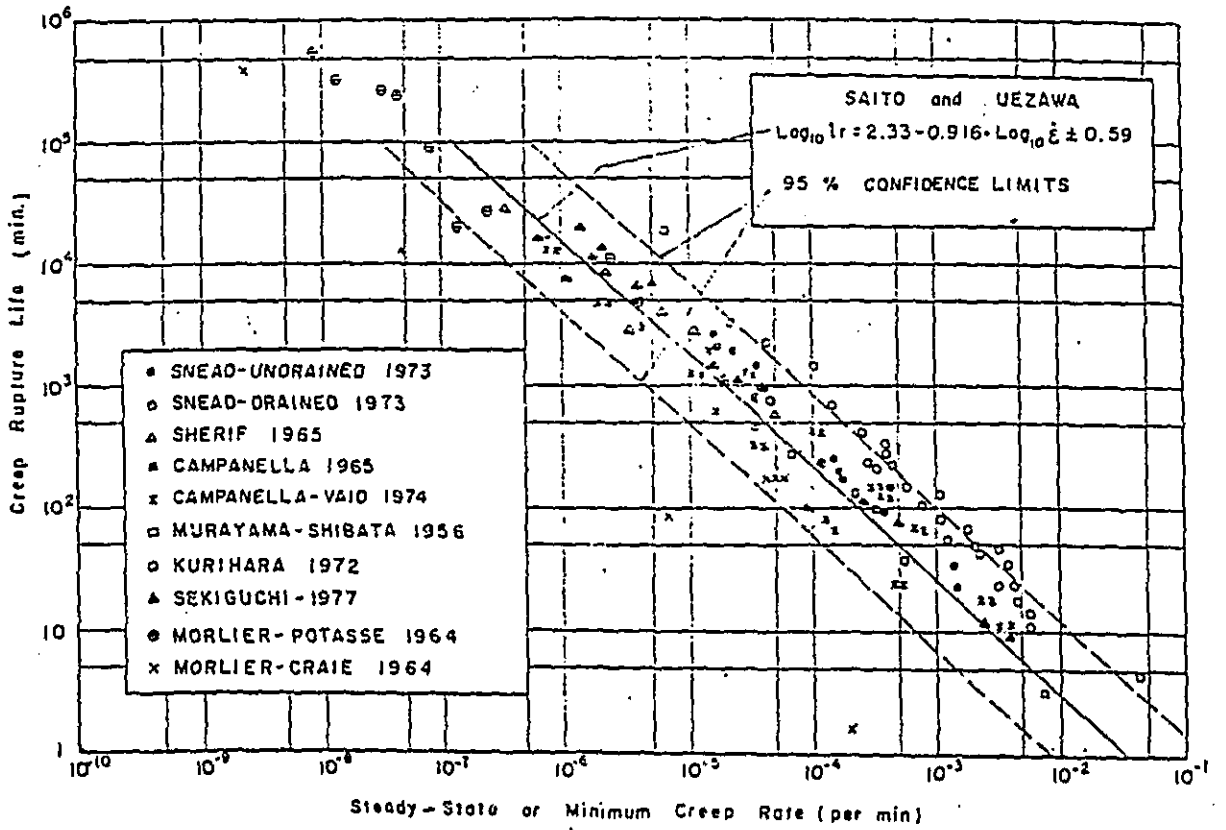


Fig.15 Compiled relationship between creep rate and creep-rupture life

3 RHEOLOGICAL INTERPRETATION FOR CREEP-RUPTURE OF SOIL.

Recently, rate process theory has come to gain ground to explain creep phenomena of soil, and it is afraid that such illusion would be impressed that all creep phenomena including creep-rupture characteristics could be explained with this theory.

It may be well just so in the primary and secondary creep range, but there are many problems that can not be explained with this rate process theory in the tertiary creep range. Exactly speaking, it should be said that no creep theory is formed at present to be applicable to the tertiary creep range.

First of all, such a proposition is very questionable that soil fails soon after creep movement has attained at a definite quantity as asserted by Murayama & Shibata (1951, 1956) and Vyalov, Maslov & Karaulova (1977). Essentially, properties of material are divided in two categories; that is to say, structure-insensitive and structure-sensitive properties. The former is caused by additive contribution of material constitution such as atoms, molecules or particles to the properties, for instance, elastic coefficient, Poisson's ratio, specific gravity or coefficient of thermal expansion. The latter is not caused by additive contribution of material constitution, but caused by strong control of such defects as dislocations, cavities or fissures fairly large enough compared to the size of material constitution, for instance, strength, plasticity or permeability.

Originally deformation is of structure-insensitive properties, and failure strength is of structure-sensitive properties. If rupture is defined according to deformation, the limit of deformation will be even in a way, but it cannot exist that rupture will cause at the same deformation, if it means final and macroscopic state of separation.

Next, there are very few examples of strain-time curves in the tertiary creep range. It should be expressed with a formula relating strain or displacement and time. As a creep formula in the tertiary creep range, it is requested that quantity of strain or displacement becomes infinite at a limited time. If such a creep formula that strain or displacement is finite at a limited time is used, rupture must be defined with deformation; it is too much willful and far from reality.

The experimental formula by Singh & Mitchell (1969),

$$\epsilon = A e^{\alpha D} \left(\frac{t_1}{t} \right)^m,$$

and also the formula by Vyalov, Maslov & Karaulova (1977),

$$\gamma = \gamma_0 + \frac{\tau}{\tau_0 [1 - n(\tau)]} \left[(t + 1)^{1-n(\tau)} - 1 \right],$$

are not suitable to make forecast close to failure, because they do not give infinite strain or displacement within limited time.

Contrary to these formulas, my experimental formula, i. e.

$$\epsilon - \epsilon_0 = A \log \frac{t_r - t_0}{t_r - t},$$

or

$$\epsilon = \frac{A}{t_r - t},$$

offers infinite strain and strain rate at a limited time, and can describe the form of creep curve close to the real displacement until the time of rupture. Therefore, this formula can be successfully applied to forecast the time of rupture.

4 CASE STUDIES OF ACTUAL SLOPE INSTABILITY.

4-1 Landslides Failed after Long Creep Movement.

a) Takabayama Landslide on the Iiyama Line, JNR (Saito & Yamada, 1973)

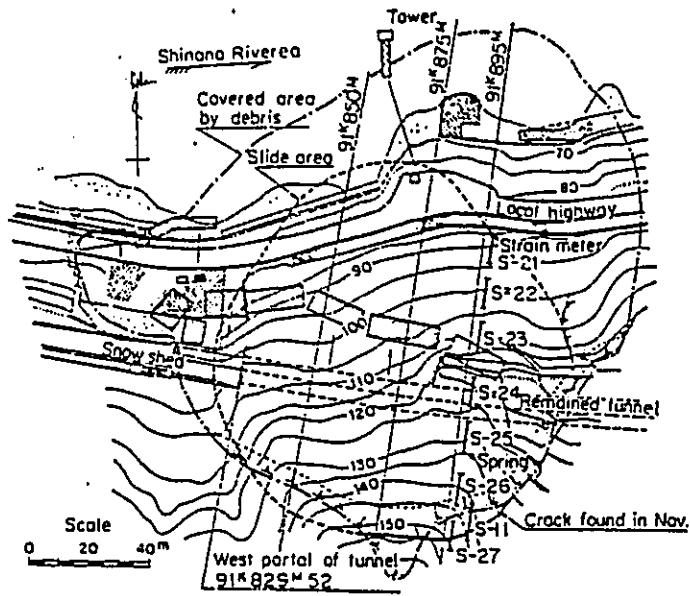


Fig.16 Plan of Takabayama Landslide

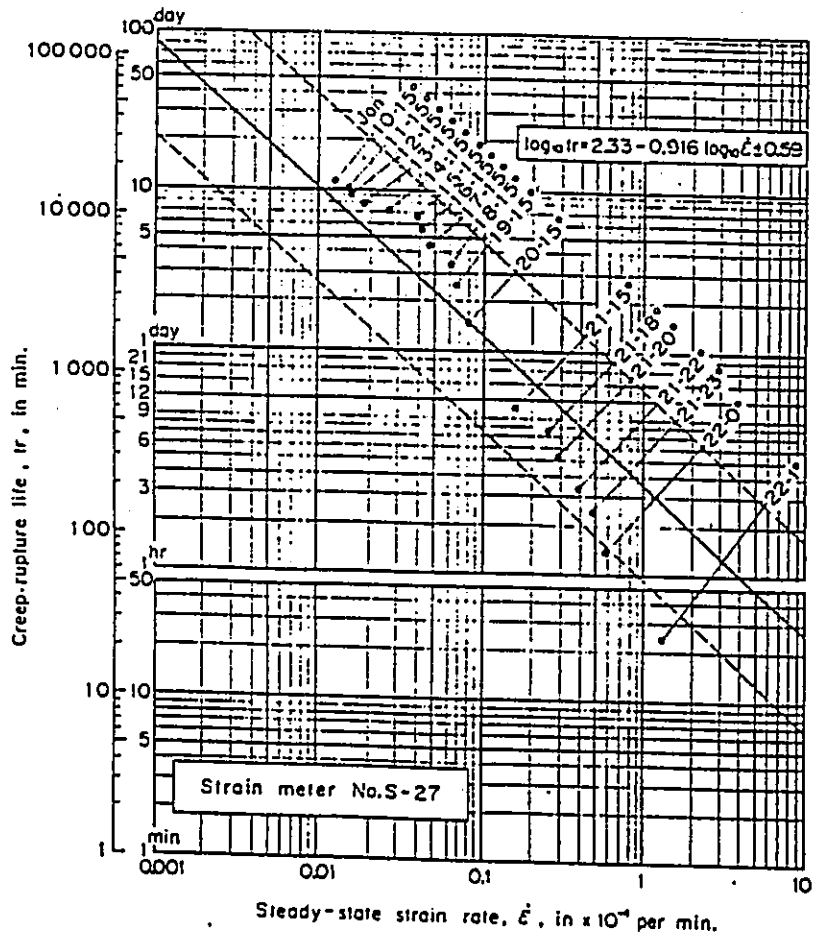


Fig.17 Reliability of forecasting failure time based on forecasting diagram in case of using transient strain rate, Takabayama Landslide

At the Moscow Conference in 1973, I reported Takabayama Landslide occurred in January, 1970, but I would like to explain again an outline of the accident, because forecasting of failure time was announced in advance to failure and it resulted in good coincidence with the actual failure time.

Takabayama Tunnel is located on the Iiyama Line, JNR. In April of 1969, unusual dislocation was found on the tunnel, and thereafter careful observation was performed continuously. In November, a long tension crack was found on the slope above the central part of the tunnel, and extensometers were set up across the crack in order to measure the relative movements. In the middle of December, heavy snowfall destroyed the measuring devices on the ground, then the extensometers of remote recording type were reset, buried in the ground and observations were resumed on 31st of December, 1969.

Forecasting of failure time was made with two ways; estimation with transient strain rate and graphical analysis for substituted logarithmic curve in the tertiary creep range. The methods are shown in Fig. 17 and 18, respectively. Public announcement for failure was made by the authority at 5 p.m. of the 21st that the slope would fail at the coming midnight or before dawn. The estimation of failure time was revised every hour. The final announcement was made at the midnight that the failure would occur at 1:30 on the 22nd, according to the

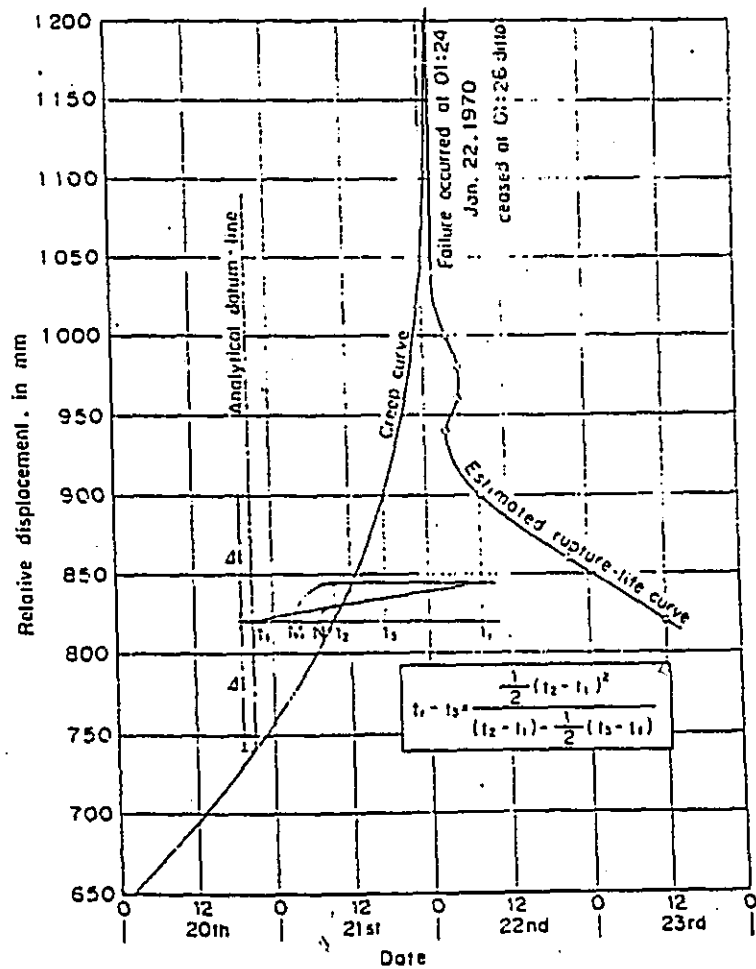


Fig.18 Forecasting failure time by means of graphical analysis in the tertiary creep range, Takabayama Landslide

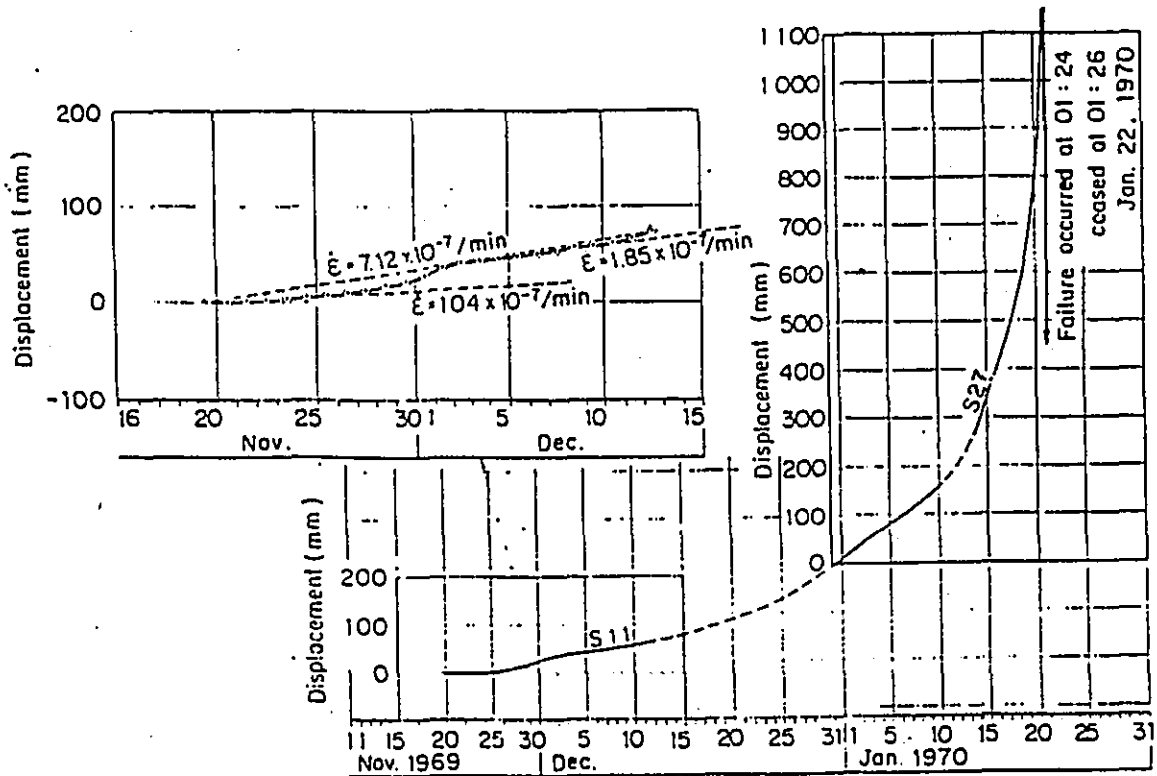


Fig.19 Relative displacement curve interrupted but connected under acceptable supposition, Takabayama Landslide

analysis in the tertiary creep range. After all, the slope above Takabayama Tunnel began to fail at 1:24 on the 22nd, and it ceased to move after two minutes. The difference between estimated and actual failure time is only 6 minutes. It was said that there was nothing else than a miracle.

Fig. 19 shows a curve of displacement which was made by connecting two curves obtained before and after snowfall in December under acceptable supposition. From three strain rates calculated on the curve obtained before snowfall, the failure time might be estimated as 30-60 days after the 13th of December, i. e. between the 10th of January and the 10th of February.

b) Agoyama Landslide in Fukui City (Watari, 1973)

About 5 km to the northwest of Fukui City, there occurred Agoyama Landslide in December 1972, which is a site of old landslide about 200 m wide, 80 m high and 180 m in slope length. This movement was caused by removing earth as borrow-pit at the foot of the slope. Bedrocks are composed of tuffaceous sandstone of Tertiary Period, and sliding surface is supposed on a fine grained layer of sandstone.

A long continued crack was found on a hillside of Agoyama in Oct. 4th of 1972, and observation was started at the 7th of the month after setting up measuring instruments. At first the movement was about 10 mm per day, but then the movement gradually increased and reached to 20mm per day at the end of October, and 100 mm per day after 20th of November. Analysis of forecasting failure time was carried out at Tokyo about 400 km apart from the site, and the result of analysis was informed to the person in charge of the site by telephone.

Graphical analysis in the tertiary creep range is shown in Fig. 21, and the failure time was guessed at about the late of November. But the supposition was disturbed with irregular

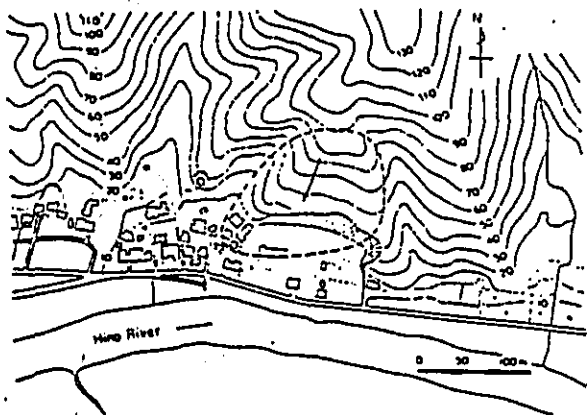


Fig.20 Plan of Agoyama Landslide

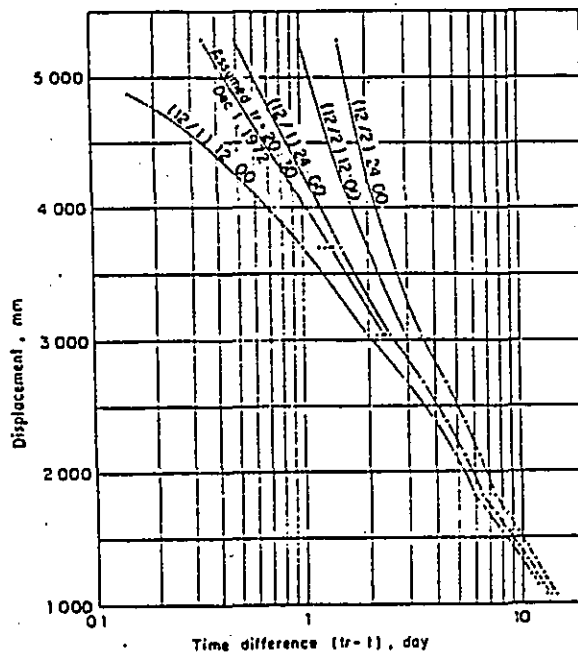


Fig.22 Forecasting failure time based on linearity on semi-logarithmic coordinates, Agoyama Landslide

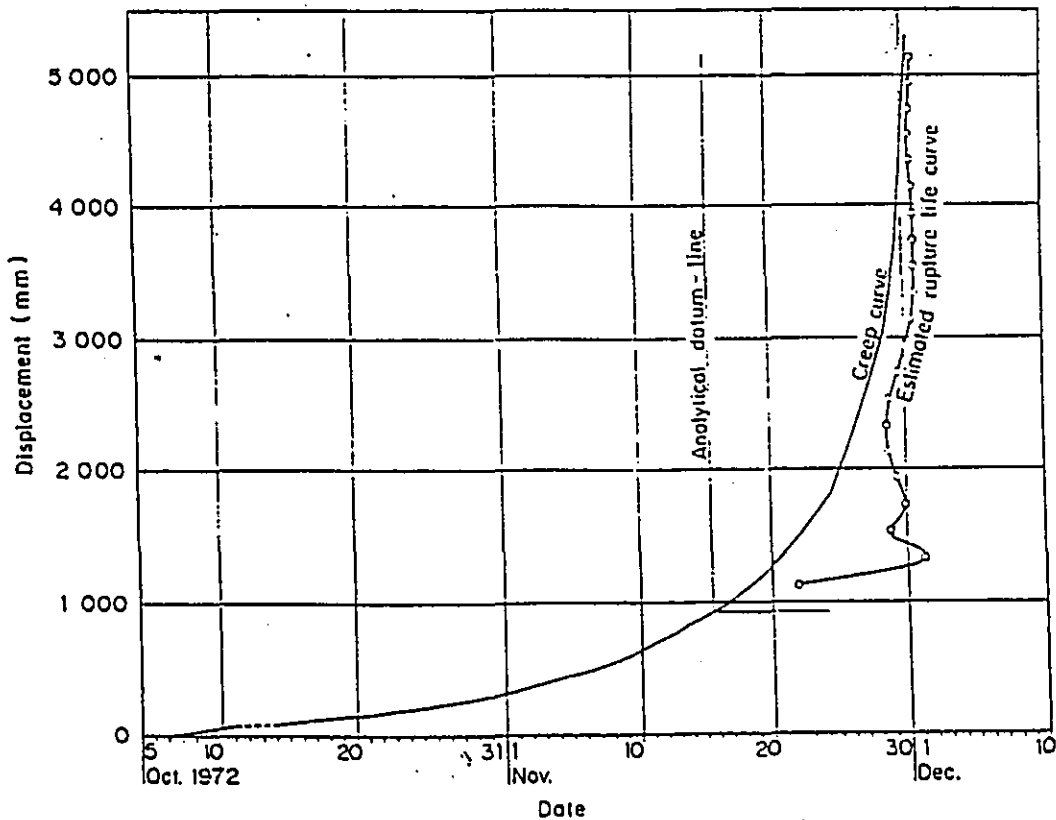


Fig.21 Creep curve and forecasting failure time by means of graphical analysis, Agoyama Landslide

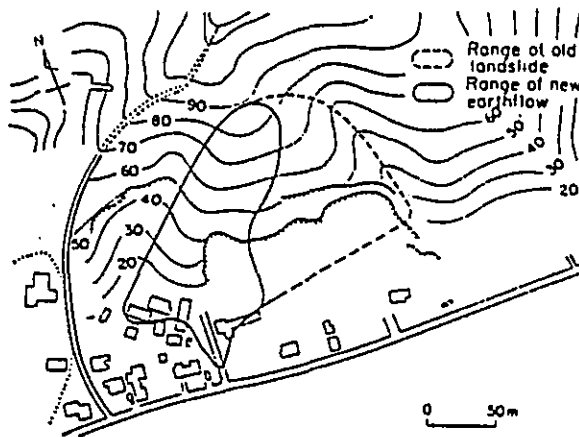


Fig. 23 Finally failed area of Agoyama Landslide

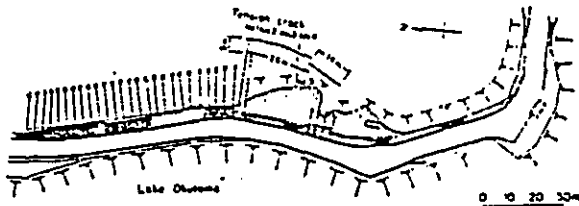


Fig. 24 Plan of damaged area along Tama Lakeside Road

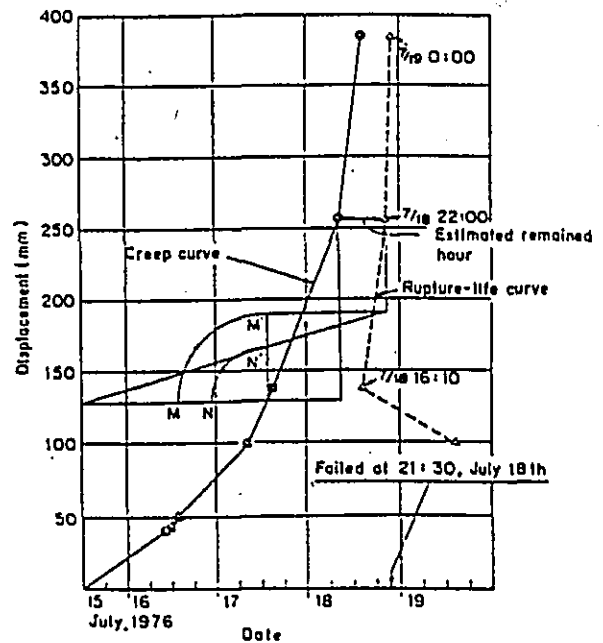


Fig. 25 Forecasting failure time by means of graphical analysis, slope failure along Tama Lakeside Road

movement at the final stage; then, the method of semi-logarithmic representation to pursue linearity of creep curve was used together with graphical analysis, as shown in Fig. 22. The linearity of creep curve on semi-logarithmic graph was not attained easily, showing irregular bending. Last forecasting of failure time was decided as 20:30 of the 1st of December in the evening of the very day; actual failure time was 1:30 of the 2nd of December. Later it was made clear that this discrepancy was caused by the reason that movement of total mass was stopped at the final stage and only one third of the mass failed at all, as seen in Fig. 23.

c) Collapse of a steep slope at Tama Lakeside Road (Hasegawa & Kiuchi, 1977)

A slope failure with volume of 9,500 m³ occurred at Tama Lakeside Road, about 70 km west of Tokyo on July, 1976. Bedrocks are mainly composed of Jurassic slates, partly containing sandstone, splitted by shearing and altered to clay formation. The slope in question is about 70 m in slope length, and 0.6 : 1 in inclination.

Signs of instability of the slope were found in July 13th of 1976. Measuring points were set up at 5 spots across a tension crack at the upper part of the slope. Observations of the distance variation between measuring points were begun on 14th of the month.

Graphical analysis in the tertiary creep range is shown in Fig. 25. At 10:00 of 18th, failure time was suggested as after 12 hours, and actual failure occurred at 21:30 of the day; the difference is just half an hour, resulting good forecasting.

I found the fact in a paper published in a technical magazine, that this forecasting was made according to my method, though I had no relations with this work of forecasting.

d) Yunotai Landslide on the Esashi Line, JNR (Saruta & Ishibashi, 1976)

In April of 1975, a landslide with the volume of 40,000 m³ occurred between Yunotai and

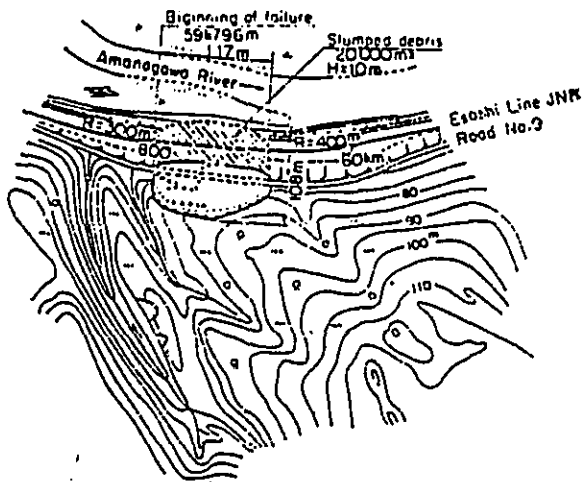


Fig. 26 Plan of Yunotani Landslide

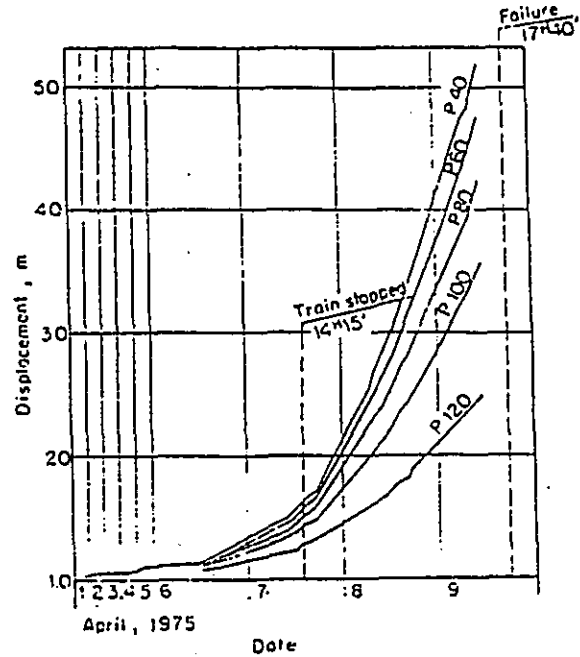


Fig. 27 Progress of displacements of road, Yunotani Landslide

Miyakoshi on the Esashi Line, JNR. Railroad was covered with soil mass, about 10 m high, 117 m long and 20,000 m³ of volume, and railway traffic was interrupted for 19 days. Bedrocks are composed of mudstone of Miocene Epoch, Tertiary Period and the site is considered as an old landslide area.

In March 21st, a cave-in of road surface above the railroad was found; then, many cracks appeared over both road surface and railroad roadbed. In April 7th, the slope came to cover the railroad and railway track moved laterally as much as 300 mm, and at last on 17:40 of 9th the slope fell down with loud and terrible sound. Movements of observation points on the road surface are shown in Fig. 27.

The creep curves show that they were in the secondary creep range before April 6th, and then it entered rapidly in the tertiary creep range. By the noon of the 8th, failure time was supposed as within 11th day, but on 10:45 of 9th day, when the last observation was done, failure time was estimated as 18:10 of the 9th; contrary to this forecasting, actual failure occurred on 17:40 of the 9th, 30 minutes earlier than estimation.

In this case, also I had no relation with their work of forecasting, as the same with mentioned before.

4-2 Landslides That Finally Ceased without Failure after Rapid Movement.

e) Landslide at Kashiwara Interchange on Nishimeihan Expressway (Tokunō & Tatsumi, 1971)

Late in April of 1969, signs of instability came out at buildings of a hospital standing on flat area of a hillside, and then fears were made clear with many cracks all over the area. Similar cracks were found on the main lines, rampways and retaining walls of Nishimeihan Expressway. Covering these instable areas, the range of the landslide became clear gradually, with the width of about 250 m and slope length of 250 m, and this site was considered as old landslide area, revived at this time.

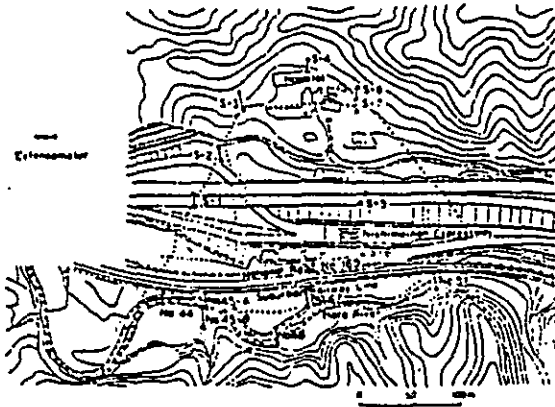


Fig. 28 Plan of Landslide at Kashiwara Interchange

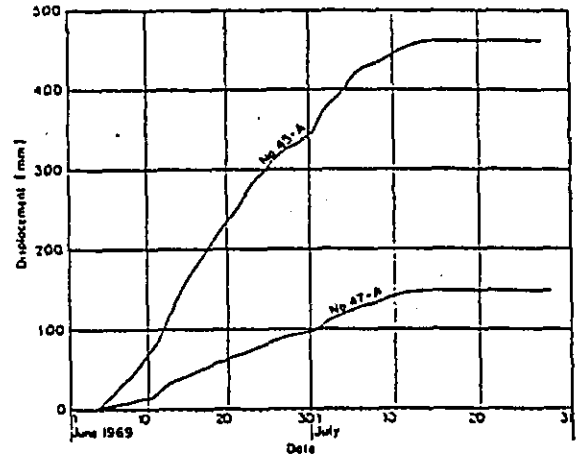


Fig. 29 Progress of displacements of suburban railway line, Landslide at Kashiwara Interchange

Investigations and observations were set to work at the last of May. The range of the landslide was extended over national highway and suburban railway line situated below the expressway, and sliding movement became gradually larger, such as 470 mm for 40 days from June 4th to July 16th, and 24 mm per day in June 13th as the maximum daily displacement, measured with extensometer No. 45-A.

Rapid movement continued for fairly long duration, as shown in Fig. 29; and then movement gradually decreased. Horizontal drillings for dewatering were carried out since the last of June, and the movement ceased July 10th, accompanied with the effects of dewatering.

Let us calculate the maximum strain rate. The span length of extensometer No. 45-A is 15.540 m, so strain rate corresponding to the movement 24 mm per day is calculated as 1.07×10^{-6} per min. This value is not so large, but cannot be ignored. If this rate would continue invariably, the slope would fail in 9.5 days based on my method. Considered from the fact the strain rate did not become larger than this value, this landslide is supposed to be such a type of slide as that would finally cease without failure.

f) Iwadonoyama Landslide at Ohtsuki on Central Expressway (Harada, 1972)

The site of Iwadonoyama Landslide experienced slope failure twice during construction. Bedrocks are composed of alternate of tuff, lapilli tuff, tuff breccia and tuffaceous sandstone of Miocene Epoch, with dykes of andesite, and dip of bedding is against slope. The site is a cut slope of 32 degrees. It was in February 17th of 1972, that several lines of cracks were found around the area, and in March 2nd the range of about 60 m in width and 90 m in slope length was perceived as sliding area, with increase of cracks. Observations with invar-wire extensometers were set to work in Feb. 24th. After that, additional extensometers were supplemented according to expanding of sliding area, and remote-recording type extensometers were also set over the upper or lower end cracks, prepared for emergent situation.

As shown in Fig. 31, displacements increased rapidly since 21st of March, and on 26th transient strain-rate attained to 6.14×10^{-4} per min. On the other hand, such a serious situation was anticipated that failure would occur in a day and a half according to graphical analysis in the tertiary creep range. But after that, against our anxiety, strain rate did not increase beyond the value, and came to cease without failure.

As seen in this case, there are such a many examples that a slope does not fail but cease to move, even if considerably accelerating strain rate is seen in the tertiary creep range. In such a case, it is extremely difficult to forecast with our present knowledge whether such a

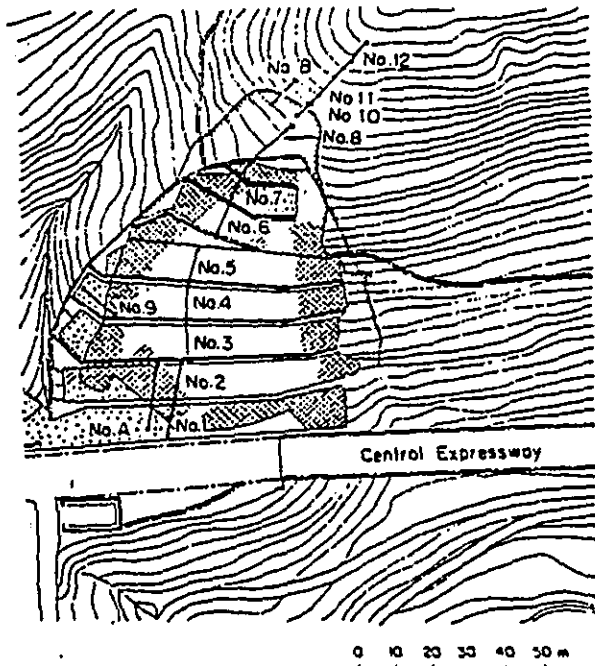


Fig.30 Plan of Iwadonoyama Landslide

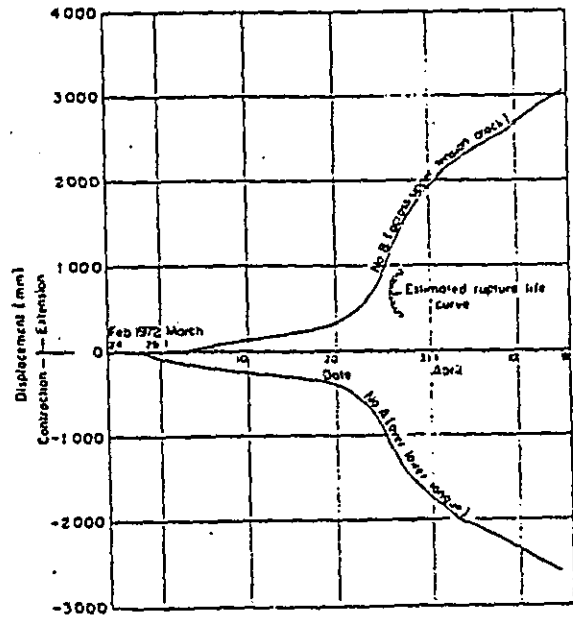


Fig.31 Progress of relative displacements crossing over upper or lower end cracks, Iwadonoyama Landslide

slope would fail presumably or not.

4-3 Split-Type Failure

g) Failure of a vertical cut in clay, Welland, Canada (Kwan, 1971)

Several years ago Mr. D. kwan of St. Lawrence Seaway Authority wrote to me that failure time estimated with my method did not coincide with actual one in a field test of vertical cut failure which he carried out for realignment of Welland Canal. In this case, I suppose, my method of forecasting failure time from steady-state strain rate cannot be applied because its type of failure is not sliding, but splitting and overturning separated by deep tension crack, and slip plane came out only near the toe of the vertical slope.

In this case, however, graphical analysis in the tertiary creep range can be applied to his test results and shows good astringency to the failure time as can be seen in Fig. 32.

4-4 Slope Failure Directly Caused by Rainfall.

h) Hiketa Landslide on the Kūtoku Line, JNR (Sakurai, 1974; Yano, 1976)

Hiketa Landslide is about 50 m wide, 80 m in slope length and supported with retaining wall at the foot. Owing to a typhoon in 1972, a tension crack about 60 m long and 50 cm wide, came out along the upper verge; so geological investigation was carried out and instrumentation such as extensometers and alarm fences were set up for guard over the area. Bedrocks are composed of sandstone of Mesozoic Era, fairly weathered and decomposed.

A typhoon in July of 1974 brought heavy rainfall such as 378 mm of total rainfall by the 7th day and 70 mm per hour of maximum rainfall intensity, and finally the slope failed down at 1:10 of th 7th.

Before failure occurred, an alarm bell in a lookout hut began to ring and guardmen, who were standing by in the hut, at once hurried on their ways of 6 km on foot, under a torrential rain. When they arrived at the distance of 150 m to the site, they stared the slope just failing

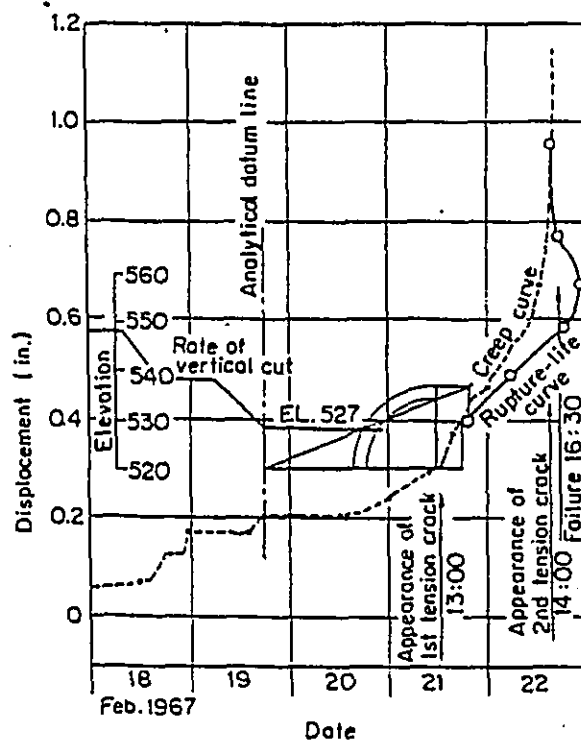


Fig.32 Graphical analysis for forecasting failure time, Welland, Canada

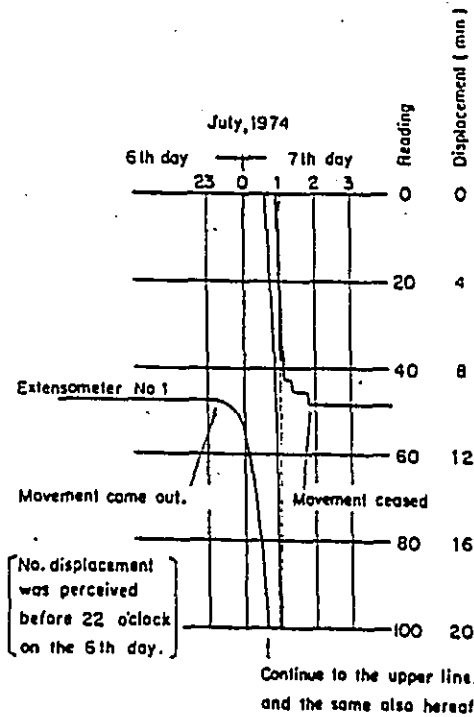


Fig.33 Progress of displacement, Hiketa Landslide

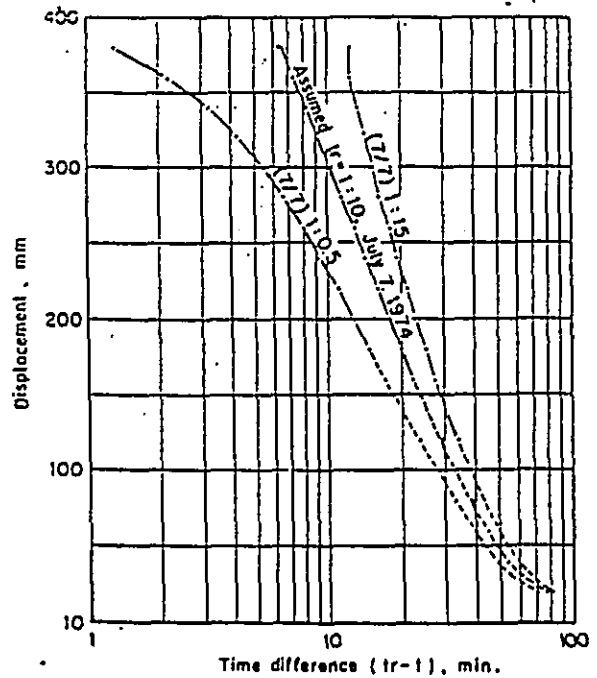


Fig.34 Forecasting failure time based on linearity on semi-logarithmic coordinates, Hiketa Landslide

under illuminating equipments. If they had arrived there one or two minutes earlier, or if the slope failure had occurred one or two minutes later, all the guardmen would have been endangered to be buried under huge moved debris.

A record of an extensometer is shown in Fig. 33. It is supposed that mechanism of sliding movement in case of slope failure caused by rainfall is not the same with that of usual landslide, because the condition of circumstances are changing every moment. Neither forecasting method using transient strain rate nor graphical analysis in the tertiary creep range is adaptable to this case.

However, the experimental formula in the tertiary creep range

$$\epsilon - \epsilon_0 = A \log \frac{t_r - t_0}{t_r - t}$$

indicates the other forecasting method, that plots of measured values will form a straight line on a semi-logarithmic graph, measured value on normal scale and $(t_r - t)$ on log-scale, if rupture life t_r could be chosen adequately. The result of this method is shown as Fig. 34. From the process of choosing temporary rupture life, failure time is about 10 minutes past one o'clock of the 7th day. This estimation would have been very effective, if this procedure had been applied in this case. Thus, forecasting of failure time directly caused by rainfall is also applicable with semi-logarithmic representation.

5 FINAL REMARKS.

Considered from several case studies explained above, it can be said that the method of forecasting failure time based on creep-rupture characteristics, that is to say, rough estimation of failure time based on steady-state strain rate in the secondary creep range, close estimation through calculation or graphical analysis using substituted logarithmic formula and final precise estimation based on linearity on a semi-logarithmic graph assuming temporary rupture life, is effective and reliable. As for reliability, it can be indicated with unit of day, if forecasting is made before several days, and with the unit of hour, or even with order of 10 minutes, if on the previous day.

6 ACKNOWLEDGEMENT.

Most of field investigations of slope failure were carried out with no relation to me, but these data resulted immediately to demonstrate the reliability of the forecasting method. I appreciate it very much that I was provided such opportunities to make practical use of them.

I would like to express cordial gratitude to Prof. Dr. Techn. Sc. G. I. Ter-Stepanian, who kindly gave me an approval of reproducing this paper in "OYO Technical Report" of OYO Corporation.

REFERENCES:

- Bishop, A. W., 1966. The strength of soils as engineering materials, Sixth Rankine Lecture, Géotechnique, 16(2), pp. 89-130.
- Campanella, R. G. and Vaid, Y. P., 1974. Triaxial and plane strain creep rupture of an undisturbed clay, Canadian Geotechnical Journal, 11(1), pp. 1-10.
- Casagrande, A. and Wilson, S. D., 1951. Effect of rate of loading on the strength of clays and shales at constant water content, Géotechnique, 2(2), pp. 251-263.
- Finn, W. D. L. and Snead, D., 1973. Creep and creep rupture of an undisturbed sensitive clay, Proc. Eighth Int. Conf. on Soil Mech. and Found. Eng'g, Moscow, 1-1, pp. 135-142.
- Harada, S., 1972. Landslide at Iwadonoyama on Central Expressway and its repair work (in Japanese), Construction, 10(8), pp. 30-37.
- Hasegawa, H. and Kiuchi, A., 1977. On forecasting slope failure along Tama Lakeside Road (in Japanese), Soils and Foundations, 25(3) pp. 83-86.
- Kurihara, N., 1972. Experimental study on creep rupture of clays (in Japanese), Proc. Japan Soc. Civil. Eng'rs, 202, pp. 59-71.

- Kwan, D., 1971. Observations of the failure of a vertical cut in clay at Welland, Ontario, *Canadian Geotech. Jour.*, 8(2), pp. 283-298.
- Lazan, B. J., 1962. Stress-strain-time relations for idealized materials, *Symposium on Stress-Strain-Time-Temperature Relationships in Materials*, ASTM, STP 325, pp. 3-18.
- Morlier, P., 1964. Étude expérimentale de la déformation des roches, *Revue de l'Institut Français du Pétrole*, 19(10), pp. 1113-1147, 19(11), pp. 1183-1217.
- Murayama, S. and Shibata, T., 1956. On the rheological characters of clay (in Japanese), *Trans. Japan Soc. Civ. Eng'rs.*, 40, 31pp.
- Murayama, S. and Shibata, T., 1961. Rheological properties of clays, *Proc. Fifth Int. Conf. on Soil Mech. and Found. Eng'g.*, Paris, 1, pp. 269-273.
- Saito, M. and Uezawa, H., 1961. Failure of soil due to creep, *Proc. Fifth Int. Conf. on Soil Mech. and Found. Eng'g.*, Paris, 1, pp. 315-318.
- Saito, M., 1965. Forecasting the time of occurrence of a slope failure, *Proc. Sixth Int. Conf. on Soil Mech. and Found. Eng'g.*, Montreal, 2, pp. 537-541.
- Saito, M., 1968. Research on forecasting the time of occurrence of slope failure (in Japanese), *Railway Technical Research Report*, 626, JNR, 53pp.
- Saito, M., 1969. Forecasting time of slope failure by tertiary creep, *Proc. Seventh Int. Conf. on Soil Mech. and Found. Eng'g.*, Mexico City, 2, pp. 677-683.
- Saito, M., 1970. Estimation of the rupture life of soil based on the shape of the creep curve, *Proc. Fifth Int. Cong. on Rheology*, Kyoto, 2, pp. 559-567.
- Saito, M. and Yamada, G., 1973. Forecasting and result in case of landslide at Takabayama, *Proc. Eighth Int. Conf. on Soil Mech. and Found. Eng'g.*, Moscow, 4-3, pp. 325-327.
- Sakurai, T., 1974. Landslide disaster on the Japanese National Rational Railways, *News (in Japanese)*, *Landslides*, 11(3), pp. 40-41.
- Saruta, T. and Ishibashi, M., 1976. Big slope failure in 20 days after beginning of movement (in Japanese), *Railway Civil Engineering*, 12(6), pp. 47-50.
- Sekiguchi, H., 1977. Rheological characteristics of clay, *Proc. Ninth Int. Conf. on Soil Mech. and Found. Eng'g.*, Tokyo, 1, pp. 289-292.
- Singh, A. and Mitchell, J. K., 1969. Creep potential and creep rupture of soils, *Proc. Seventh Int. Conf. on Soil Mech. and Found. Eng'g.*, Mexico City, 1, pp. 379-384.
- Tokunō, M. and Tatsumi, T., 1971. Landslide at Nishimeihan Expressway and its treatment (in Japanese), *Civil Engineering Execution*, 12(3), pp. 21-32, 12(4), pp. 17-27.
- Vyalov, S. S., Maslov, N. N. and Karaulova, Z. M., 1977. Laws of soil creep and long-term strength, *Proc. Ninth Int. Conf. on Soil Mech. and Found. Eng'g.*, Tokyo, 1, pp. 337-340.
- Watari, M., 1973. Landslide movement at Agoyama, Fukui Pref. (in Japanese), *Executive Technique*, 6(7), pp. 109-112.
- Yano, Y., 1976. I witnessed a big slope failure (in Japanese), *Railway Civil Engineering*, 18(6), pp. 75-76.

Additional Remark

This paper was originally contributed to "PROBLEMS OF GEOMECHANICS", as the Transactions of the Department of Geomechanics published by the Armenian Academy of Sciences, Yerevan, USSR, in December of 1977, in compliance with the request of Prof. G. I. Ter-Stepanian of the Academy.

This paper, therefore, should be regarded as a reproduction of the article in the Transactions, after the volume containing this paper would have been published.

Appendix 4-1 Sekiguchi-Ohta Model (Elasto-viscoplastic model)

1. Ohta Constitutive Model

Ohta (1967) introduced the yield function of clay and elasto-plastic strain according to the normality rule. He assumed that volume change of soil element under consolidation and shearing depends on the mean effective stress and the octahedral shear stress, γ_{oct} , is defined by the invariants of the effective stress components.

The octahedral shear stress is expressed by the following equation.

$$\gamma_{oct} = \frac{1}{3} \sqrt{(\sigma_1' - \sigma_2')^2 + (\sigma_2' - \sigma_3')^2 + (\sigma_3' - \sigma_1')^2} \quad \dots(1)$$

Where, σ_1' , σ_2' and σ_3' are principal stresses and under the triaxial compression condition ($\sigma_1' \geq \sigma_2' = \sigma_3'$), γ_{oct} is expressed by the following equation.

$$\gamma_{oct} = \frac{2}{3} (\sigma_1' - \sigma_3') \dots \dots \dots (2)$$

On this basis, dilatancy is defined as volume changes which occur under loading with P being held constant as follows.

$$\frac{-\Delta e}{1 + e_0} = \Delta \epsilon_v = \mu \Delta \left(\frac{\gamma_{oct}}{\rho} \right) \dots \dots \dots (3)$$

Where, P : Effective mean stress

μ : Constant value

On the other hand, the e-log P relation is expressed by the equation,

$$\Delta e = -\lambda \frac{\Delta \rho}{\rho} \dots \dots \dots (4)$$

Where, e : Void ratio

$-\lambda$: Gradient of e-log P relation

Δe : Volume change, given by the equation.

$$\Delta e = -\lambda \frac{\Delta \rho}{\rho} - \mu (1 + e_0) \Delta \left(\frac{\gamma_{oct}}{\rho} \right) \dots \dots \dots (5)$$

Then, integrating equation (5) under e_0 and P_0 at the normal consolidation line on $\gamma_{oct} = 0$ plane, the state boundary surface equation in the γ_{oct} - P - e plane is given by the following equation.

$$e - e_0 + \lambda \log \frac{\rho}{\rho_0} + \mu (1 + e_0) \frac{\gamma_{oct}}{\rho} = 0 \quad \dots\dots\dots (6)$$

It is noted that the yield surface is given by projecting the cross line of equation (6) and the elastic wall on the γ_{oct} - P plane.

The elastic wall equation is defined by

$$\Delta e = -\kappa \frac{\Delta \rho}{\rho} \quad \text{or} \quad e - e_0 + \kappa \log \frac{\rho}{\rho_0} = 0 \quad \dots\dots\dots (7)$$

In this way, the yield surface equation is finally obtained as,

$$\frac{\gamma_{oct}}{\rho} + \frac{(\lambda - \kappa)}{(1 + e_0) \mu} \log \frac{\rho}{\rho_0} = 0 \quad \dots\dots (8)$$

Comparing equation (8) and Roscoe's yield surface equation, the following relation can be obtained

$$M = \frac{3}{\sqrt{2}} \frac{(\lambda - \kappa)}{(1 + e_0) \mu} \quad \dots\dots (9)$$

On this basis, it is judged that Ohta's theory is substantially the same as Roscoe's theory.

Further, Sekiguchi and Ohta (1977) extended the Ohta model and introduced the inviscid and viscid constitutive relation for anisotropically and normally consolidated clay:

This model is known as the " Sekiguchi Ohta Model ".

2. Sekiguchi-Ohta Model

Sekiguchi and Ohta proposed a new constitutive law taking the effect of time and stress-induced anisotropy into consideration.

This model is known as the " Sekiguchi-Ohta Model ".

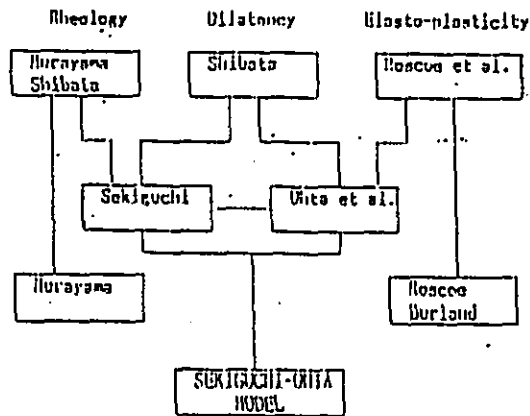


Fig. AP-1

(1) Volume creep equation

Sekiguchi and Ohta proposed a volumetric creep equation by the use of the new stress parameter, η^* , in the equation,

$$V = \frac{\lambda}{1 + e_0} \ln\left(\frac{P}{P_0}\right) + D \cdot \eta^* - \alpha \cdot \ln\left(\frac{V}{V_0}\right) \quad \dots\dots\dots (10)$$

- Where,
- λ : Compression index
 - e_0 : Initial void ratio
 - P_0 : Initial effective stress
 - P : Effective stress
 - η^* : New stress parameter, given by

$$\eta^* = \sqrt{\frac{3}{2} (\eta_{ij} - \eta_{ij0})(\eta_{ij} - \eta_{ij0})} \quad \dots\dots\dots (11)$$

D : Coefficient of dilatancy

(2) Scalar function

Sekiguchi et al. (1977) solved equation (11) and introduced a scalar function as the viscoplastic potential in the equation,

$$F \equiv \alpha \cdot l \cdot (1 + (V_0 t / \alpha) \cdot \exp(f / \alpha)) = v^r \quad \dots\dots\dots (12)$$

Where, f is a scalar function defined by,

$$f = \frac{\lambda - \kappa}{1 + e_0} \ln \left(\frac{p}{p_0} \right) + D \cdot \eta^r \quad \dots\dots\dots (13)$$

It is noted that V_p in equation (12) plays as a so-called strain-hardening parameter.

In this way, the strain rate effect of Ko-consolidated clay can be expressed using the volumetric creep equation and the scalar function.

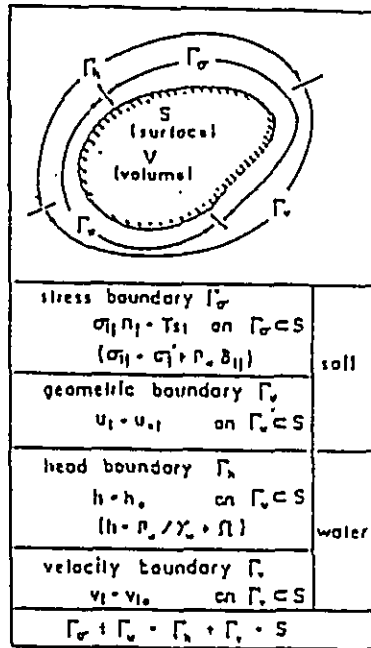
Figure AP-2 shows the summary of the elasto-viscoplastic model by Sekiguchi and Ohta.

volumetric strain of clays		continuum mechanics	
consolidation	dilatancy	non-linear elasticity	
$\dot{\epsilon}_v^e = \frac{\lambda - \mu}{1 + e_0} \cdot \frac{\dot{p}'}{p'}$	$\dot{\epsilon}_v^e = 0$	elastic (recoverable)	elastic - limit (yield condition) $\ln \ln \frac{p'}{p_0} \cdot v_{ij}' - \epsilon_v^p = 0$
$\dot{\epsilon}_v^p = \frac{\lambda - \mu}{1 + e_0} \cdot \frac{\dot{p}'}{p'}$	$\dot{\epsilon}_v^p = D \dot{\eta}^r$	plastic (irreversible)	
$E_v^{vp} = \alpha \ln [1 + \frac{V_0 t}{\alpha} \cdot \exp(\frac{f}{\alpha})] = F$ $f = \frac{\lambda - \mu}{1 + e_0} \cdot \ln \frac{p'}{p_0} + D \eta^r$		viscous (time-dependent)	flow rule $\dot{\epsilon}_{ij}^p = E \cdot \frac{\partial f}{\partial \sigma_{ij}} \cdot \dot{\epsilon}_{ij}^{vp} = 11 \cdot \frac{\partial F}{\partial \sigma_{ij}}$

AP-2 Summary of Elasto-plastic/Elasto-viscoplastic Constitutive Model Proposed by Sekiguchi and Ohta (1977)

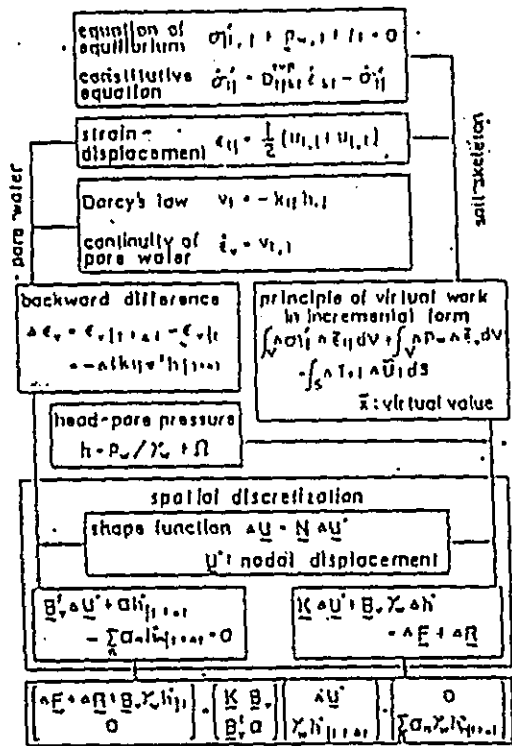
Appendix 4-2 Modeling of Soil Mass

Most of the boundary value problems in soil engineering require two kinds of boundary condition to be applied on the soil skeleton and the pore water flow as shown in the following figure.

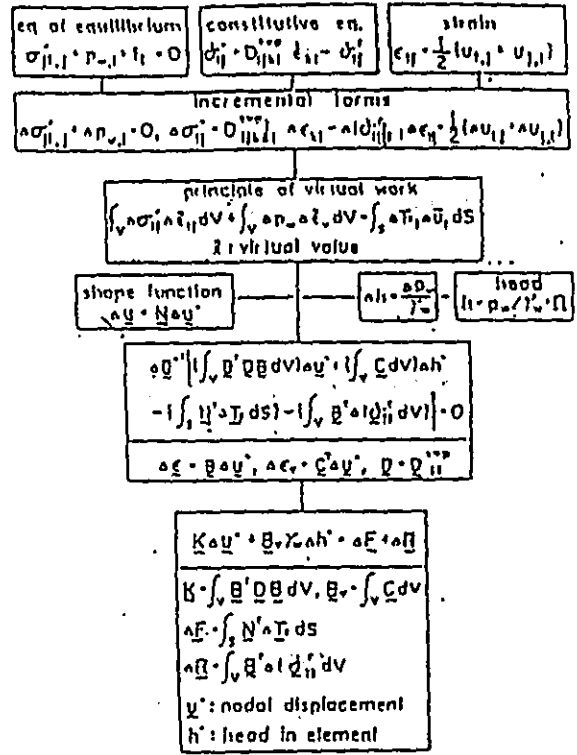


AP-3 Boundary Conditions of a Coupling Problem

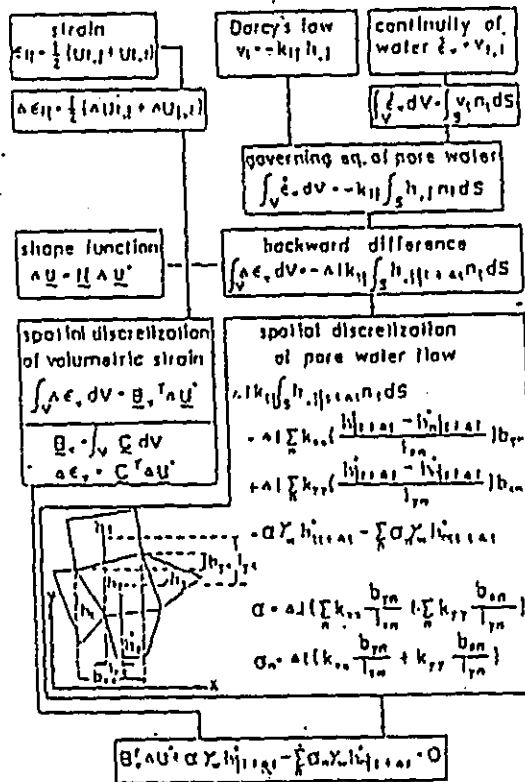
The governing equations of coupling problems of the soil skeleton (regarded as the elasto-viscoplastic material) and pore water (regarded as the incompressible fluid) are summarized in Figs. AP-4, AP-5 and AP-6 which indicate the discretization of the soil skeleton and pore water respectively. The theoretical framework of the elasto-viscoplastic constitutive model proposed by Sekiguchi and Ohta is as follows.



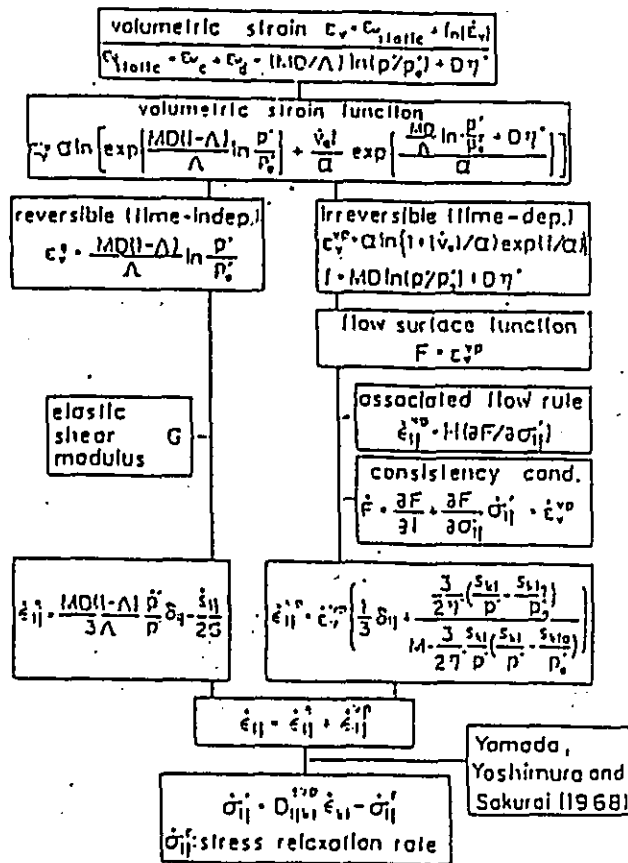
AP-4 Finite Element Formulation of DACSAR



AP-5 Discretization of Soil Skeleton



AP-6 Discretization of Pore Water Flow



AP-7 Theoretical Framework of the Elasto-Viscoplastic Constitutive Model Proposed by Sekiguchi and Ohta

The rigidity matrix of the elasto-viscoplastic constitutive model used for the Finite Element Method is mathematically described in Fig. AP-8.

$$\begin{aligned}
& \dot{\sigma}_{ij} = D_{ijkl} \dot{\epsilon}_{kl} - \dot{\sigma}_{ij} \\
& \dot{\sigma}_{ij} = \frac{\Delta \sigma_{ij}}{\Delta t} \quad D_{ijkl} = (1-\theta) D_{ijkl}^{t+\Delta t} + \theta D_{ijkl}^{t+\Delta t} \\
& \dot{\epsilon}_{ij} = \frac{\Delta \epsilon_{ij}}{\Delta t} \quad \dot{\sigma}_{ij} = (1-\theta) \dot{\sigma}_{ij}^{t+\Delta t} + \theta \dot{\sigma}_{ij}^{t+\Delta t} \\
& \text{plane strain } \dot{\epsilon}_{ij} \text{ - Eulerian } \theta = 0
\end{aligned}$$

$$\begin{aligned}
\Delta \sigma_{ij} &= D_{ijkl} \Delta \epsilon_{kl} - \Delta \sigma_{ij} \\
\Delta \sigma_{ij} &= \begin{pmatrix} \Delta \sigma_{11} \\ \Delta \sigma_{22} \\ \Delta \sigma_{33} \\ \Delta \sigma_{12} \\ \Delta \sigma_{13} \\ \Delta \sigma_{23} \end{pmatrix} \quad \Delta \epsilon_{ij} = \begin{pmatrix} \Delta \epsilon_{11} \\ \Delta \epsilon_{22} \\ \Delta \epsilon_{33} \\ \Delta \epsilon_{12} \\ \Delta \epsilon_{13} \\ \Delta \epsilon_{23} \end{pmatrix} \quad \dot{\sigma}_{ij} = \frac{C_{ij}}{C_i} \begin{pmatrix} \dot{\sigma}_{11} \\ \dot{\sigma}_{22} \\ \dot{\sigma}_{33} \\ \dot{\sigma}_{12} \\ \dot{\sigma}_{13} \\ \dot{\sigma}_{23} \end{pmatrix} \\
D_{ijkl} &= \begin{pmatrix} L+2G & L & 0 \\ L & L+2G & 0 \\ 0 & 0 & G \end{pmatrix} - \frac{C_{ij}}{C_i} \begin{pmatrix} A_{11}^i & A_{12}^i & A_{13}^i \\ A_{21}^i & A_{22}^i & A_{23}^i \\ A_{31}^i & A_{32}^i & A_{33}^i \end{pmatrix} \\
L &= \frac{3E}{1+\nu} \frac{\Lambda}{MOH-\Lambda} n^* \quad G = \frac{3H-2\nu}{2(1+\nu)} \frac{\Lambda}{MOH-\Lambda} n^* \\
A_{ij} &= L f_{ijk} \delta_{ij} + 2G f_{ij} \quad (i,j = x,y,z) \quad f_{kk} = f_{xx} + f_{yy} + f_{zz} \\
C_1 &= [L f_{11}^2 + 2G(f_{12}^2 + f_{13}^2 + f_{23}^2)] C_2 + f_{11} \\
C_2 &= [-\exp(-c^2/a)] \quad C_3 = \exp[(1-cT)/a] \\
f_{ij} &= \frac{Q}{3n^*} \left[(1-\frac{1}{2}\eta) \eta_{ij} (\eta_{11} - \eta_{11}) \right] \delta_{ij} + \frac{1}{2} \frac{Q}{n^*} (\eta_{ij} - \eta_{ij}) \\
\eta_{ij} &= \sigma_{ij} / n^* - \delta_{ij} \quad \eta_{11} = \sigma_{11} / n^* - \delta_{11} \quad (MOH) \frac{D}{n^*} = 0 \eta^* \\
\eta_{11} (\eta_{11} - \eta_{11}) &= \eta_{22} (\eta_{22} - \eta_{22}) + \eta_{33} (\eta_{33} - \eta_{33}) + 2\eta_{12} (\eta_{12} - \eta_{12}) \\
&\quad + \eta_{13} (\eta_{13} - \eta_{13}) \\
\eta^* &= \sqrt{13/2} (\eta_{11} - \eta_{11}) \eta_{11} \quad (i,j = x,y,z)
\end{aligned}$$

AP-8 Rigidity Matrix of the Elasto-Viscoplastic Constitutive Model proposed by Sekiguchi and Ohta

The discretization of continuum is carried out by the Finite Element Method using the Sekiguchi - Ohta Model as mentioned in the preceding.

Appendix 4-3 Estimation of Ko Value

The following five methods are studied regarding the presumptive equation to estimate the coefficient of earth pressure at rest (Ko) under a pre-consolidated condition

- ① Jaky's method (1944) : $K_o = 1 - \sin \phi'$
- ② Brooker & Ireland's methods (1965) : $K_o = 0.95 - \sin \phi'$
- ③ Fraser's method (1957) : $K_o = 0.9 \cdot (1 - \sin \phi')$
- ④ Kezdi's method (1962) : $K_o = (1 + 2 \sin \phi' / 3) (1 - \sin \phi') (1 + \sin \phi')$
- ⑤ Alpan's method (1967) : $K_o = 0.19 + 0.233 \log I_n$

① Ko value for Bangkok Clay

The data on Bangkok Clay are quoted from the master's thesis, "Determination of Ko Value by Hydraulic Fracture Method" by Wan Weng Tung, 1975, Asian Institute of Technology. Laboratory tests and in situ tests were performed on Bangkok Clay and Rangsit Clay in Nong Ngoo Hao and verification was carried out over the presumptive equations of the above five methods. The results are shown in Fig. AP-9 to Fig. AP-14. As a result, Alpan's equation is considered to be the most applicable compared with the others.

② Ko value of Kibushi clay

The data on Kibushi Clay are quoted from the doctoral thesis "Study on Lateral Flow of Soft Clay Foundation in Embankments" by Otohiko SUZUKI, August, 1986.

Uniform triaxial compression tests, Ko-note triaxial compression tests and plane shear tests were performed on Kibushi Clay and the following data were obtained. Although the values obtained from Alpan's equation are somewhat higher than the values from equations 2-4, there is no significant difference between them.

AP-9 Ko Values from Presumptive Equations

Method	Uniform triaxial Compression test	Ko-note triaxial Compression test	Plane shear test
①	0.523	0.597	0.590
②	0.518	0.542	0.540
③	0.470	0.537	0.531
④	0.467	0.540	0.533
⑤	0.545	0.545	0.545

AP-10 Comparison between Estimated Ko Values and
measured Ko Values

Method	Ko-note Triaxial Compression Test	Ko Value of Plane Shear Test
①	$0.597 / 0.508 = 1.175$	$0.590 / 0.511 = 1.155$
②	$0.542 / 0.508 = 1.067$	$0.540 / 0.511 = 1.056$
③	$0.537 / 0.508 = 1.057$	$0.531 / 0.511 = 1.039$
④	$0.540 / 0.508 = 1.063$	$0.533 / 0.511 = 1.043$
⑤	$0.545 / 0.508 = 1.073$	$0.545 / 0.511 = 1.067$

Judging from the results shown above, Alpan's equation seems applicable to Bangkok Clay. Therefore, this presumptive equation is applied in estimating the Ko values.

AP-11 Estimated Ko Values by Experiential Equation (1)

Bangkok Clay at Rangsit										
Depth (m)	Ip (%)	$\bar{\phi}$ (°)	Ko Predicted					Ko Measured		References
			ALPANI	BRONKOP IRELAND	FRASER	JAKY	KEZDI	Field	Laboratory	
1.2	42.6 ± 2.4	27.3 ± 0.5	0.57 ± 0.01	0.57 ± 0.01	0.56 ± 0.01	0.62 ± 0.01	0.56 ± 0.01		0.59	GULACHOL (1970)
1.75	42.6 ± 2.4	27.3 ± 0.5	0.57 ± 0.01	0.57 ± 0.01	0.57 ± 0.01	0.62 ± 0.01	0.56 ± 0.01		0.55	GULACHOL (1970)
2.5	45.8 ± 3.0	27.1 ± 0.5	0.58 ± 0.01	0.56 ± 0.01	0.56 ± 0.01	0.61 ± 0.01	0.56 ± 0.01		0.58	GULACHOL (1970)
4.0	48.1 ± 2.1	27.7 ± 0.5	0.58 ± 0.01	0.56 ± 0.01	0.56 ± 0.01	0.63 ± 0.01	0.57 ± 0.01	0.77 ± 0.05	0.56	GULACHOL (1970) WANG (1971)
7.0	50.7 ± 2.3	27.9	0.59 ± 0.01	0.57	0.56	0.62	0.56		0.60 ± 0.01	WANG (1969)
8.5	34.0 ± 7.5	25.0	0.56 ± 0.01	0.53	0.52	0.58	0.52	0.55 ± 0.03	0.50	WANG (1960)
9.0	35 ± 2.9	20 ± 2	0.56 ± 0.01	0.51 ± 0.03	0.59 ± 0.03	0.61 ± 0.03	0.51 ± 0.03		0.72	AHMAD (1970)

AP-12 Estimated Ko Values by Experiential Equation (2)

Bangkok Clay at Nang Ngao Hwa										
Depth (m)	Ip (%)	$\bar{\phi}$ (°)	Ko Predicted					Ko measured	References	
			ALPANI	BRONKOP IRELAND	FRASER	JAKY	KEZDI	Laboratory		
1.3	65 ± 2	23	0.61 ± 0.01	0.56	0.55	0.61	0.56	0.70 ± 0.02		WANG (1974) CHANG (1974)
1.75	82 ± 4	25.6 ± 0.2	0.63 ± 0.01	0.52	0.51	0.57	0.51	0.65 ± 0.02		WANG (1974) CHANG (1974)
4.0	73	21.4	0.62	0.59	0.57	0.60	0.58	0.60		CHANG (1971)
5.7	75.3 ± 0.1	27.7 ± 0.1	0.63	0.49	0.48	0.54	0.48	0.63		CHAIYADHUMA (1974)
7.7	67.1 ± 0.1	26.1 ± 0.3	0.62	0.48	0.48	0.53	0.47	0.62		CHAIYADHUMA (1974)
10.0	70		0.53					0.65 ± 0.08		LIU (1974)

Notes: $\bar{\phi}$ shown in the table are obtained from $\overline{C K_u U}$ tests, except for

* - - - C A D tests

** - - - $\overline{C I U}$ tests

AP-13 Ko Values Obtained by Laboratory Tests
(Nong Ngoo Hao)

Bangkok Clay at Nong Ngoo Hao				
Depth (m)	K _o	Size of Specimen	Method of Determination	Investigators
1.3	0.74 ± 0.01	1.4 f x 2.8	CHANG's Method	WANG (1974)
2.65	0.65 ± 0.01	1.4 f x 2.8	CHANG's Method	WANG (1974)
2.5	0.65 [±]	1.4 f x 2.8	Controlled Stress Triaxial Test	HWANG (1975)
4.0	0.60 [±]	1.4 f x 2.8	CHANG's Method	CHANG (1973)
5.5	0.65 [±]	1.4 f x 2.8	Controlled Stress Triaxial Test	CHAUDRY (1975)
5.7	0.63 [±]	1.4 f x 2.8	POULOS and DAVISS's Method	CHAIYADUNA (1974)
7.2	0.67 [±]	1.4 f x 2.8	POULOS and DAVISS's Method	CHAIYADUNA (1974)
10.0	0.65 ± 0.08	1.4 f x 2.8	CHANG's Method	LIU (1974)

AP-14 Ko Values Obtained by In-situ Tests
and Laboratory Tests (Rangsit Clay)

Field Test Results			Laboratory Test Results		
Depth (m)	K _o	Method of Determination	Depth (m)	K _o	Method of Determination
4.0	0.72 ± 0.05	BJERRUM and ANDERSEN	4.0	0.56	BISHOP and HENKEL
4.0	0.67 ± 0.00	WILKES	4.5	0.63 ± 0.05	Laboratory Hydraulic Frac.
6.0	0.64 ± 0.05	BJERRUM and ANDERSEN	6.25	0.56 ± 0.06	Laboratory Hydraulic Frac.
6.0	0.61 ± 0.03	WILKES	7.0	0.60 ± 0.01	BISHOP and HENKEL
8.0	0.55 ± 0.09	BJERRUM and ANDERSEN	8.0	0.57 ± 0.03	Laboratory Hydraulic Frac.
8.0	0.53 ± 0.03	WILKES	8.5	0.59	BISHOP and HENKEL

JICA